Characterisation of the anti-Gal response to *Leishmania* infection, and its possible exploitation for the diagnosis of cutaneous leishmaniasis

Thesis submitted in accordance with the requirements of the University of Liverpool for the degree of Doctor in Philosophy

by

Victoria Macleod Austin

September 2019

Acknowledgements

Thank you to my supervisor, Alvaro, and my lab group, all members past and present. It has been a privilege to work with you and learn from you. Thank you.

To my friends[1] I have unlimited gratitude for your tolerance over the last four years. I owe you a holiday to make up for all the ones I missed.

Above all, this thesis belongs to my family. Without your support, advice and endless patience I would have given up long ago. Finally, to Granny, who didn't see this completed. Your home was a sanctuary and respite whenever I needed one. I hope I've made you proud.

[1] Specifically, Raadhika Shinh and Nathan Thorpe.

Characterisation of the anti-Gal response to *Leishmania* infection for the diagnosis of cutaneous leishmaniasis

By Victoria M. Austin

Abstract

The most abundant natural IgG antibody in healthy humans is known as anti-Gal. These antibodies are continually generated in response to antigenic αGalactosyl residues expressed by gastrointestinal microbiota. However, during the course of several parasitic infections, including leishmaniasis, the levels of serum anti-Gal are greatly increased mainly due to the expression of αGalactosylated glycoconjugates by these parasites.

The surface glycocalyx of *Leishmania* parasites consists of a complex mix of glycoconjugates, with varied roles in cell invasion and protection from host immune responses. Most abundant amongst these is a family of glycoinositolphospholipids (GIPLs), the glycan components of which vary between *Leishmania* species. Type-II GIPLs are abundantly expressed by *L. major* parasites and contain terminal αGalactosyl residues that are recognised by serum from infected patients. Since the oligosaccharidic portion of the main *L. major* GIPLs terminate with the linear sequences Galα(1,3)Gal$_f$β(1,4)-R (GIPL-2) or Galα(1,6)Galα(1,3)Gal$_f$β(1,4)-R (GIPL-3), which differs to the main epitope (Galα(1,3)Galβ(1,4)GlcNAcβ1-R) recognised by normal anti-Gal antibodies, I hypothesised that the specificity of the anti-Gal produced during a course of a *Leishmania* infection will be different to that of normal anti-Gal.

In this thesis, I set out to characterise the human anti-Gal response that is triggered during *Leishmania* infection, aiming to exploit this knowledge for the development of a novel diagnostic test. The utility of native GIPLs extracted from both *L. major* and *L. tropica* cells as diagnostic antigens was assessed first through a combination of Thin Layer Chromatography (TLC) immuno- and lectin-staining, mass spectrometry analysis, and chemiluminescent ELISA (CL-ELISA). GIPLs extracted from *L. major* promastigotes were strongly recognised by sera from *L. major*-positive patients, but not from *L. tropica*-positive patients, or that from healthy controls. In addition, it was confirmed that *L. tropica* does not express αGalactosylated GIPLs, suggesting that this residue must be decorating an uncharacterised glycoconjugate.

To determine the specificity of the *Leishmania* spp. anti-Gal, a bespoke panel of neoglycoproteins (NGPs) was used to investigate anti-Gal produced in response to leishmaniasis infection in three patient cohorts. These sample collections encompassed the spectrum of the leishmaniases, from systemic visceral disease to localised cutaneous lesions. Antibody detection in *Leishmania* patients has potential in screening of suspect cases, but also in monitoring response to treatment. NGPs with Galα(1,3)Gal*f*β-R and Galα(1,6)Galα(1,3)Gal*f*β-R terminating glycans were the best discriminators of *L. major* infections and also showed potential in the diagnosis

of American cutaneous leishmaniasis caused by *L. braziliensis*. In addition, the presence of a terminal β-galactofuranose residue in these NGPs dramatically improved their recognition in CL-ELISA, and their value in the diagnosis of Old World CL. Combining these two glycotopes maximises antibody detection, through capture of two anti-Gal populations.

Fluorescent microscopy analysis confirmed *L. major* cells express αGalactosylated epitopes throughout the parasite lifecycle, whilst in *L. tropica* the same epitope was only detected in promastigote cells. While the nature of this epitope remains unknown, future work should focus on the analysis of *L. tropica* glycoconjugates.

Results in this thesis are discussed in relation to the variability of αGalactosyl epitopes recognised by sera from patients with different *Leishmania* infections, and their possible exploitation in the development of novel disease biomarkers.

Declaration

I hereby certify that this dissertation constitutes my own product, that where the language of others is set forth, quotation marks so indicate, and that appropriate credit is given where I have used the language, ideas, expressions or writings of another.

I declare that the dissertation describes original work that has not previously been presented for the award of any other degree of any institution

Signed

List of Abbreviations

Anti-Gal	Anti-αGalactosyl Antibody
AUC	Area Under the Curve
BSA	Bovine Serum Albumin
CBAG	Coffee bean αGalactosidase
CE	Cell Equivalent
CE/well	Cell Equivalent per well
CL	Cutaneous Leishmaniasis
CL-ELISA	Chemiluminescent Enzyme Linked Immunosorbent Assay
CRP	C-Reactive Protein
CV	Column Volume
Da	Dalton
DAPI	4', 6-diamidino-2-phenylindole
EIS-MS	Electrospray Ionization Mass Spectrometry
EIS-MS/MS	Electrospray Ionization Tandem Mass Spectrometry
FT	Flow Through
Gal	Galactose
Galf	Galactofuranose
Galp	Galactopyranose
GIPL	Glycoinositolphospholipid
GlcNAc	N-Acetylglucosamine
GPI	Glycosylphosphatidylinositol
Hex	Hexose
HP-TLC	High Performance Thin Layer Chromatography
HRP	Horse Radish Peroxidase
IB4	Isolectin B4
IgG	Immunoglobulin G
IgM	Immunoglobulin M
ITS1 PCR	Internal Transcribed Spacer 1 Polymerase Chain Reaction
kDa	Kilodalton
KSA	the Kingdom of Saudi Arabia
LPG	Lipophosphoglycan
Man	Mannose
MCL	Mucocutaneous Leishmaniasis
NGP	Neoglycoprotein
NTD	Neglected Tropical Disease
PAHO	Pan American Health Organization
PBS-T	Phosphate-Buffered saline Tween 20
PBS-TB	Phosphate-Buffered Saline Tween 20 + BSA
PIBMA	Poly(isobutyl methacrylate)
qPCR	Quantitative Polymerase Chain Reaction
RDT	Rapid Diagnostic Test
RFLP	Restriction length fragment polymorphism
RLU	Relative Luminescence Unit
ROC Curve	Receiver Operating Characteristic curve
SDS-PAGE	Sodium Dodecyl Sulphate-Polyacrylamide Gel Electrophoresis

TBS-S	Tris-Buffered Saline + salts
TLC	Thin Layer Chromatography
U/well	Units per well
UK	United Kingdom
UTEP	University of Texas, El Paso
VL	Visceral Leishmaniasis
WHO	World Health Organisation
αGal	αGalactosyl

Contents

List of Figures

Chapter Four. Specificity of *Leishmania* anti-Gal in Old and New World leishmaniasis

Chapter Five. Detection and partial characterisation of surface αGalactosylated antigens from *Leishmania* spp.

List of Tables

Chapter Five. Detection and partial characterisation of surface αGalactosylated antigens from *Leishmania* spp.

Chapter Seven. Supplementary Tables

Chapter One
Introduction

1.1 Leishmaniasis

The leishmaniases are a diverse group of diseases caused by the parasitic protozoa *Leishmania. Leishmania* infection in humans have a long history; reports in Syria date back to the 17th century, and *L. donovani* DNA has been identified in mummified Egyptian remains dating to between 1500-2500 BCE [1,2].

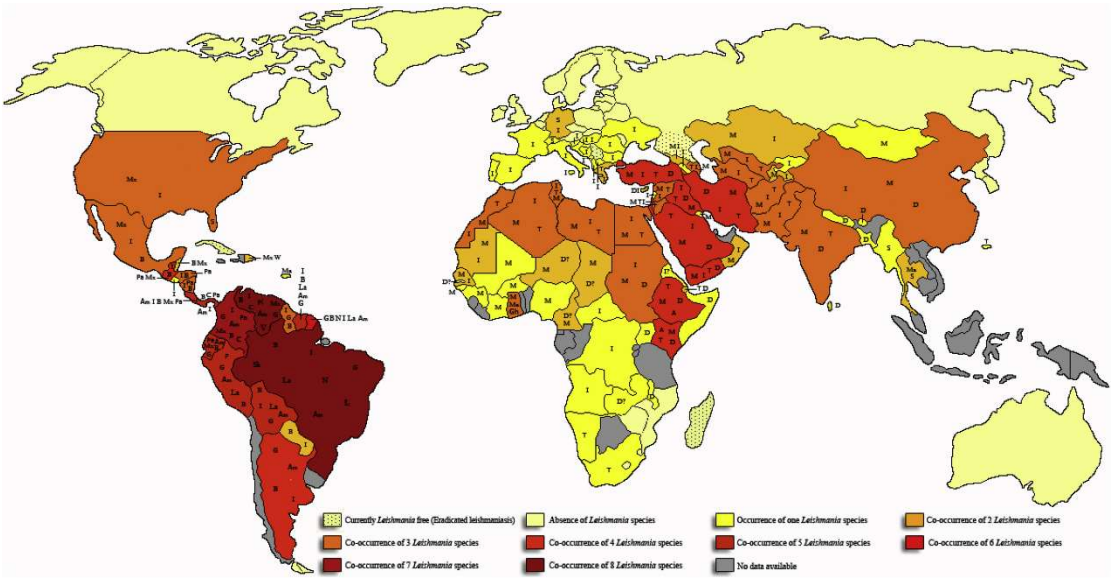

Figure 1.1. Co-endemicities of human pathogenic *Leishmania* species globally. Colours indicate the number of species endemic within each country, from pale yellow (complete absence of *Leishmania* spp.) to dark red (eight species of *Leishmania*). Grey regions indicate the absence of data. Dots represent countries where leishmaniasis has been eradicated. Abbreviations for species name are as follows: A: *L. aethiopica*; Am: *L. amazonensis*; B: *L. braziliensis*; C: *L. colombiensis*; D: *L. donovani*; G: *L. guyanensis*; Gh: 'Ghana strain'; I: *L. infantum*; La: *L. lainsoni*; L: *L. lindenbergi*; M: *L. major*; Ma: *L. martiniquensis*; Mx: *L. mexicana*; N: *L. naiffi*; Pa: *L. panamensis*; P: *L. peruviana*; S: *L. 'siamensis'*; Sh: *L. shawi*; T: *L. tropica*; V: *L. venezuelensis* and W: *L. waltoni*. The species with question marks need to be confirmed by further genotyping. Taken from Akhoundi *et al*. (2017).

Leishmaniasis has wide distribution across the Americas, Europe, North Africa and the Middle East, with the majority of disease focused disproportionately on the poorest in society (Figure 1.1) [4,5]. Like many neglected tropical diseases (NTDs) the burden of leishmaniasis is difficult to estimate; despite many advances in diagnosis and reporting, new cases are chronically under reported. Studies put the number of new infections each year between 0.9 and 1.6 million although this figure likely misses a considerable proportion of cases [6]. The disease has spread dramatically in the last 20 years due to a complex interplay of environmental and human factors,

including deforestation, urbanisation and conflict [7–9]. Changes in human behaviour that bring naive populations into contact with the disease can cause resurgence of infections or new areas of endemicity, as seen with CL in Syria since 1998, and the repeated outbreaks of VL in Sudan [10–14].

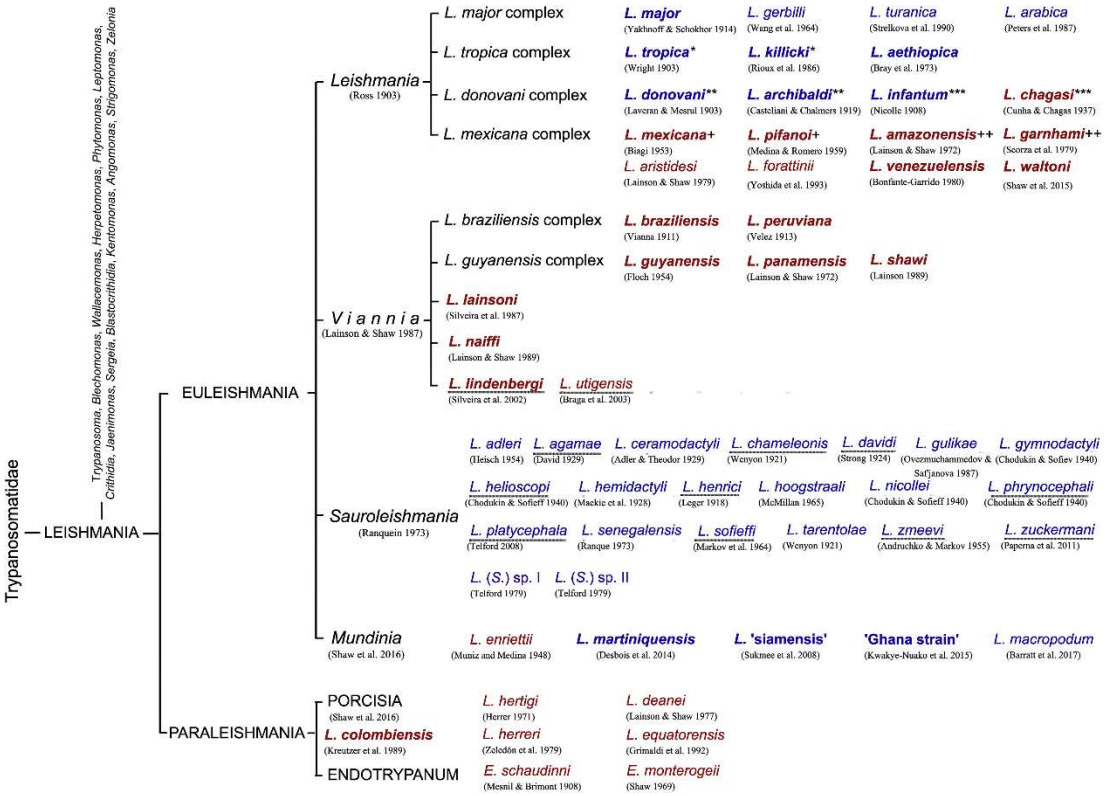

Figure 1.2. Taxonomy of *Leishmania* species, both Old World (blue text) and New World (red text). * and + indicate synonymous species, and names in bold are human pathogens. Underlined species have no final classification. Taken from Akhoundi *et al.* (2017).

There are 20 *Leishmania* species and species complexes that cause disease in humans (Figure 1.1,[3,15]). The parasite has a digenetic lifecycle (detailed in Figure 1.2), alternating between the intracellular amastigote form in the mammalian host and extracellular, flagellated promastigote forms in female phlebotomine sandflies, the insect vector. Within the sandfly there are several developmental stages before the transmissible metacyclic promastigotes are produced [16]. Historically, the human-infecting *Leishmania* spp. were divided into two subgenera based on the location of parasite development within the sandfly, with parasites in the subgenera *Viannia* developing in the hindgut initially before migrating to the fore- and midgut, and those in the *Leishmania* subgenera developing entirely in the fore- and midgut

(Figure 1.2, Figure 1.3) [17]. Molecular classification groups a further three species, capable of infecting humans, into the Mundinia subgenera [3,18,19].

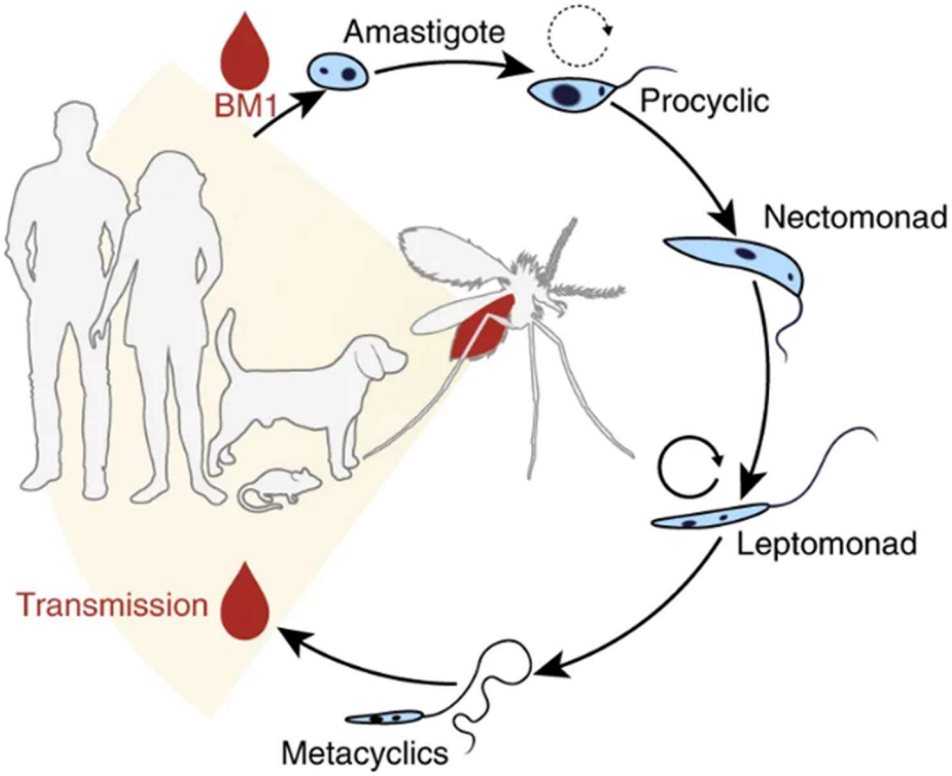

Figure 1.3. Life cycle of *Leishmania* parasites within the human and sandfly hosts. The human host becomes infected through the injection of motile promastigotes into the skin by an infected sandfly. The intracellular amastigote forms multiply within human cells and are ingested by a sandfly as it feeds. The parasites flagellate and multiply extracellularly within the sandfly, passing through several distinct forms. The metacyclics are injected with saliva as the sandfly feeds on a mammalian host. BM1 = the first bloodmeal. Circular arrows at procyclic and leptomonad indicate multiplicative stages of development. Adapted from Serafim *et al*. (2018).

1.2 *Leishmania* Transmission

The vast majority of *Leishmania* transmission for all species is through the bite of an infected female sandfly (Figure 1.3) [21]. There are an estimated 400 sandfly species, although less than 50 are medically important [22]. The leishmaniases can be categorised based on the type of transmission; zoonotic or anthroponotic (Figure 1.4). Zoonotic transmission generally involves a single reservoir species but may incorporate multiple minor or incidental hosts depending on local geography and

biodiversity [23]. Anthroponotic transmission requires no reservoir hosts to maintain transmission.

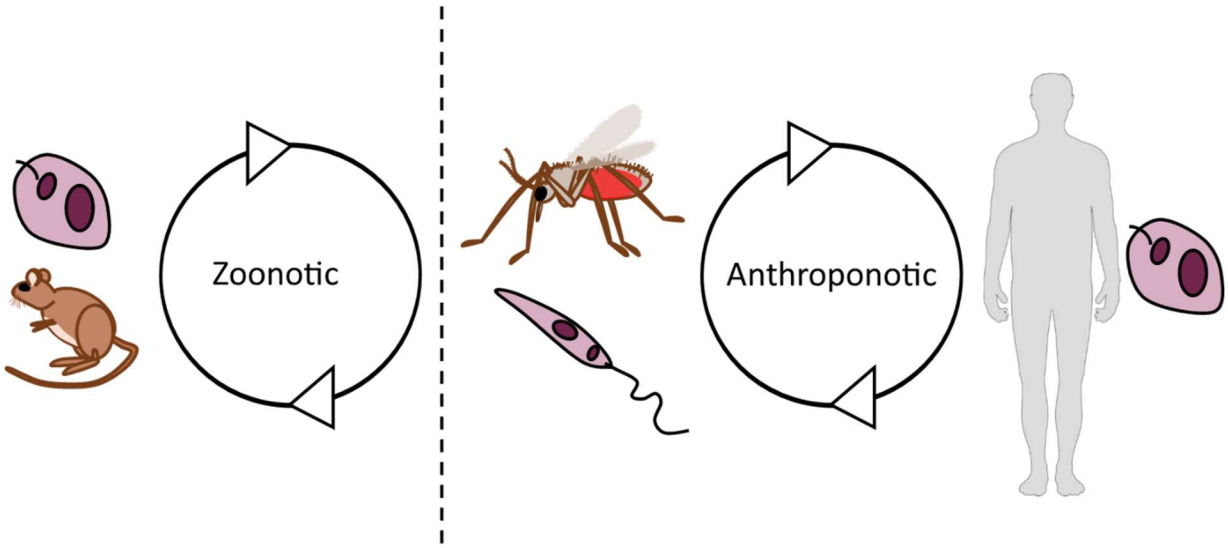

Figure 1.4. Vector-borne *Leishmania* transmission cycles. Human leishmaniasis transmitted through insect bite can be the result of either zoonotic infection, involving many types of mammalian hosts (rodents and dogs in particular), or anthroponotic, independent of animal reservoirs. Sandflies bite infected hosts and take up amastigotes in the bloodmeal, which develop into transmissible promastigotes within the gut. (Human figure from Servier Medical Art).

1.3 Leishmaniasis Disease Types

Leishmania infection is classified according to the clinical presentation of disease, which is determined by a number of factors including the parasite species or strain [24], sandfly factors [25–28] and the host immune response [29–31].

1.3.1 Visceral leishmaniasis

The most severe form of the disease is visceral leishmaniasis (VL), which affects the internal organs including the liver, spleen and pancreas [32,33]. Infection with viscerotropic *Leishmania* species frequently results in asymptomatic infection (estimated 10 asymptomatic cases for each symptomatic), and the complex determinants of visceralisation are not well understood [34]. In those that do develop overt disease, mortality approaches 100% without treatment [35,36]. VL is predominately caused by the *L. donovani-L. infantum* complex although there are some instances of VL resulting from *L. tropica* in the Middle East and *L. amazonensis* in the Americas [37,38]. While VL has historically affected predominantly children, in

some regions the disease focus has shifted to adults, associated with an increase in HIV infection and immunosuppressant therapy used in organ transplantation [15]. VL outbreaks can be extremely dangerous, particularly in vulnerable and unstable populations. Epidemics in South Sudan have resulted in tens of thousands of cases, and are linked with the continued civil unrest and associated human migration [39].

1.3.2 Tegumentary leishmaniasis

In 2017, 87 of the 200 countries and territories reporting to the WHO were endemic for CL, with 95% of new cases reported in Iraq, Afghanistan, Algeria, Brazil, Colombia, the Syrian Arab Republic and Iran [40]. Tegumentary leishmaniasis can take several clinical forms (Figure 1.5).

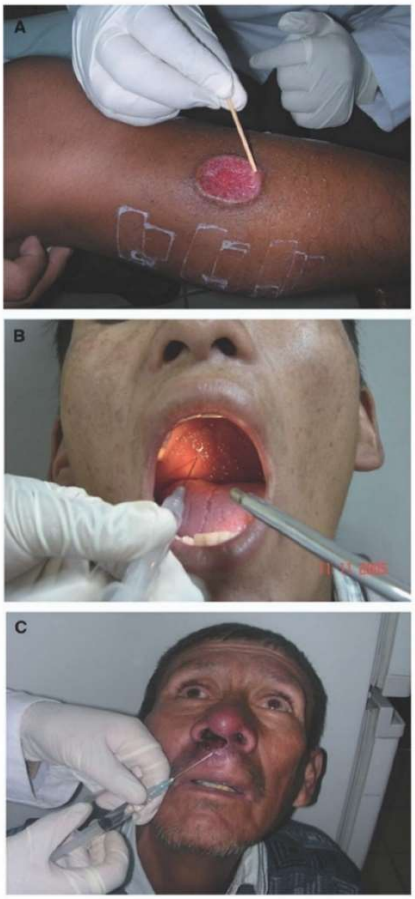

Figure 1.5. Diversity of tegumentary leishmaniasis disease. Uncomplicated cutaneous lesions (A) typically form at the infectious insect bite. Disease can progress to severe and disfiguring mucocutaneous leishmaniasis (B and C). All images taken in Bolivia [41].

Typically characterised by localised ulceration at the site of infection, cutaneous leishmaniasis (CL) can take several months to manifest symptoms (Figure 1.5A) [42,43].

Symptoms are usually limited to the skin, although parasites can migrate to the lymph nodes [44]. CL lesion appearance depends on a complex interplay between various factors, including host immune response [45,46], parasite species [37,47–49] and the presence of other infections, such as HIV [50–52]. Most lesions are localised to areas of the body that are uncovered, such as hands and feet, or the face i.e. where a sandfly can bite [42,53,54]. In some species, typically limited to the Americas, the disease can progress into severe disfiguration of mucosal membranes, termed mucocutaneous leishmaniasis (MCL; Figure 1.5B+C) [55,56]. MCL never self-heals and tissue damage occurs as the disease advances, which can require reconstructive surgery once the infection has been treated. In the Middle East and Africa, MCL can occur, although it is much rarer than in the New World and is associated with immune suppression and HIV co-infection [55,57–59].

Uncomplicated CL lesions are frequently painless, although discomfort can occur when lesions become secondarily infected with bacterial or fungal pathogens [60]. The effect of secondary infections on healing is unclear; some reports link infection to reduced healing and increased scarring, while others see no effect [60,61]. Typically CL is a sporadic disease in areas of endemicity, although epidemics are noted in groups of naïve people, such as during military deployment, or settlement by refugees and/or internally displaced people [13,62–66]

While usually not fatal, both CL and MCL can have a significant negative impact on a patient's mental health due to the highly visible and sometimes extensive nature of the tissue damage, and resulting scars (Figure 1.6) [67–69]. The negative impact on an individual correlates with size/visibility of the lesion [70,71]. Children are often kept out of school and isolated from others during active infection, and adults report ostracisation from the community [69,72]. Young women in particular seem to report fears of lowered marriage prospects; a significant concern in patriarchal societies that equate female beauty with human worth [67,72–74]. Much of the stigma is linked with a lack of education surrounding the mode of transmission, with people avoiding patients through fear of contracting the illness. Educational schemes

designed to alleviate the fear and stigmatisation focus on changing attitudes in school age children, as well as wider cultural change [75].

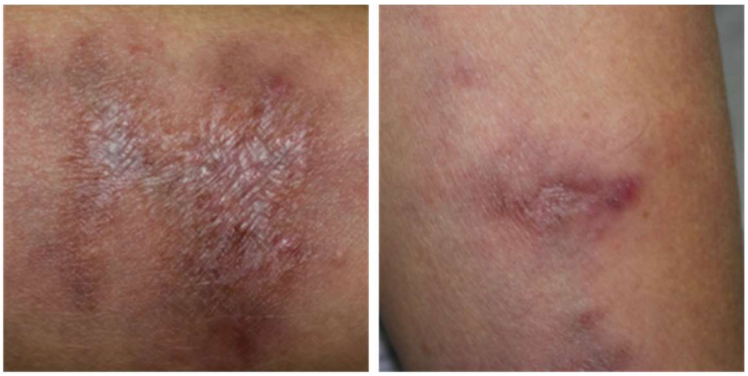

Figure 1.6. Examples of the scars left by cutaneous leishmaniasis, likely caused by *L. major* infection. Images taken of healed patients in 2017, at the Al-Ahsa leishmaniasis clinic, Saudi Arabia. Credit: Dr L. Haines.

1.4 Leishmaniasis in the Old World

CL is widespread throughout the Middle East, Asia and northern Africa, with four main etiological species; *L. major*, *L. tropica*, *L. aethopica* and *L. infantum* (Figure 1.7B) [3,6]. VL has a more restricted distribution, with the vast majority of cases limited to Bangladesh, China, Ethiopia, India, Kenya, Nepal, Somalia, South Sudan and Sudan, and outbreaks in East Africa are frequent and deadly (Figure 1.7D) [6,14].

1.4.1 Leishmaniasis in the Kingdom of Saudi Arabia

While VL outbreaks are low level, sporadic and restricted to a single district (Jazan), CL is a significant public health problem in the Kingdom of Saudi Arabia (KSA) [54,76,77]. Zoonotic CL is caused by *L. major* and transmitted by *Ph. papatasi*, with several reservoir rodent species including *Psammomys obesus* and *Meriones libycus* [78,79]. *L. tropica*, which has a more limited distribution within KSA, causes anthroponotic CL and is transmitted by *Ph. sergenti* [76,78–80]. There is variation in lesion number, treatment requirements and duration of infection between parasite species. *L. major* infections are frequently self-curing (>50%), with multiple, painless lesions that resolve without treatment [49]. In contrast, *L. tropica* infections are associated with fewer lesions which can persist for many years and result in extensive scarring

[42,75,76,81]. 17 countries, including the Kingdom of Saudi Arabia, are co-endemic for both *L. major* and *L. tropica* [5].

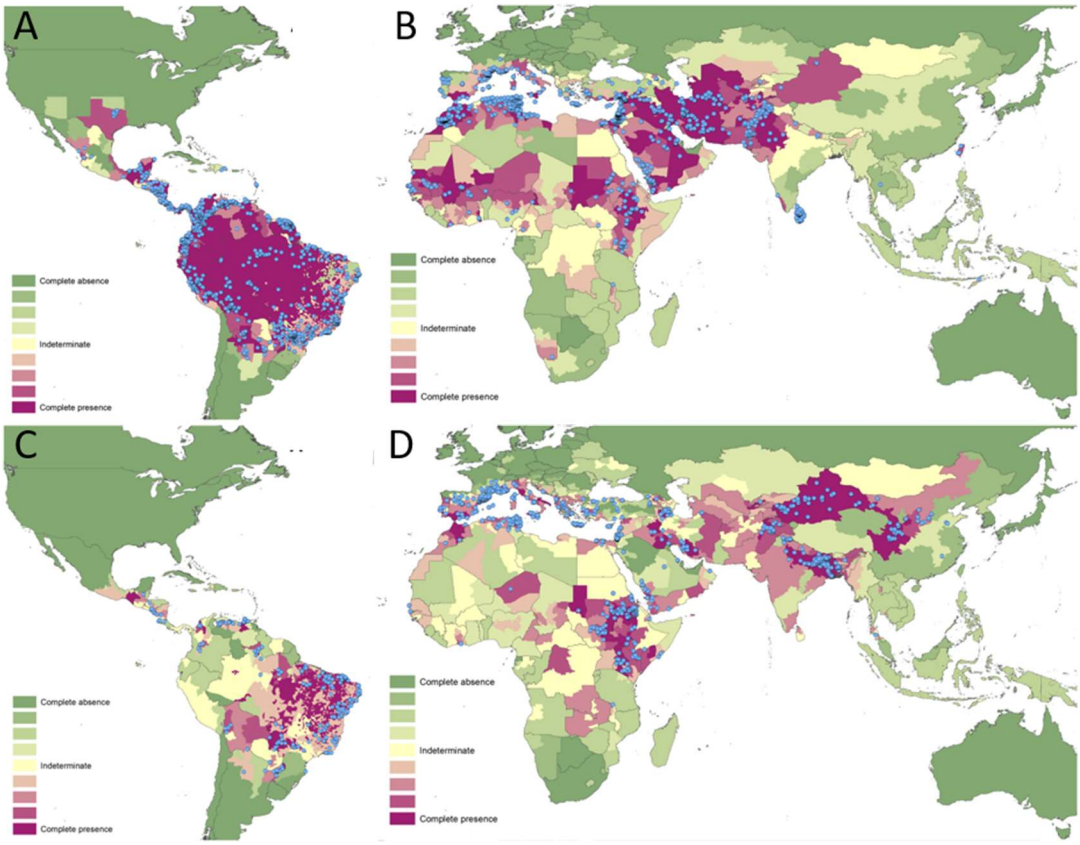

Figure 1.7. Global Distribution of the Leishmaniases. Blue points indicate occurrence points or centroids of occurrences. Colour indicates the evidence consensus for presence of disease within each country, from green (100% consensus of absence) to purple (100% consensus of presence). Left Panels (A + C) show New World and Right Panels (B + D) show Old World countries. Top Panels (A + B) depict CL incidence, and Bottom Panels (C + D) VL incidence. (Adapted from Pigott *et al*. (2014)).

Visceralisation of typically dermatropic species, which is sometimes observed in *L. tropica* infection, is not reported in KSA [81]. *L. tropica* and *L. major* lesions are typically categorised as wet and dry respectively, however there is sufficient variation in appearance that presentation alone is not diagnostic [82,83]. Within KSA there is a reliance on clinical presentation and patient history for diagnosis, despite the low specificity of this approach [76]. Anti-leishmanial drug treatment is performed in two steps: the first one consists of the topical application of fusidic acid in combination with oral azoles to reduce secondary infections. This resolves the infection in 30% of *L. major* infections [84]. If re-epithelization is not achieved,

patients undergo 1-2 courses of intralesional antimonial injections (Pentostam™). Interestingly, a recent report suggests that the presence and type of secondary infections tend to modulate the treatment outcome in patients infected with *L. major*, but not with *L. tropica* [84]. In this study, 60% of *L. tropica* infections were unresponsive to two injections of SSG. National programmes in KSA have been successful in reducing numbers of CL cases, although the zoonotic nature of *L. major* transmission requires continued monitoring and control [85–87].

1.4.2 Leishmaniasis in Spain

The zoonotic species *L. infantum* is hypoendemic in Spain, with domestic dogs as the main reservoir host [88]. VL is the most common disease type, and, in adults, is associated with HIV coinfection, although non-HIV infected patients are also at risk [51,89–92]. An outbreak of leishmaniasis in Madrid, between 2009-12 was, unusually, linked to hares as a reservoir host, and decreases in human cases was in part due to rabbit and hare culls [93–96].

1.5 Leishmaniasis in the New World

Leishmania infection in the Americas reaches from Texas in North America to Argentina in South America, covering at least 18 countries (Figure 1.7A+C) [97]. Tegumentary leishmaniasis is caused by several species of both the *Viannia* and *Leishmania* subgenera [3,98]. In 2017, 3.9% of all cases were MCL, of which 90% were reported in Bolivia, Brazil, Colombia, Paraguay and Peru [97]. Zoonotic VL, caused by *L. infantum* (syn. *L. chagasi*), results in several thousand cases reported annually, although this is certainly an underestimate [6,36]. Where living standards improve, cases of VL have fallen, however the changing epidemiology of VL, from rural to urban settings, indicates that VL transmission in cities may become more of a concern [6,99]. Response to treatment of leishmaniasis in New World countries differs between both species and strain of infecting parasites [100].

1.5.1 Leishmaniasis in Bolivia

In 2017, four tegumentary-causing species were reported in Bolivia*; L. amazonensis*, *L. braziliensis*, *L. guyanensis*, and *L. lainsoni*. Of the over 2000 reported cases of

tegumentary leishmaniasis in 2017, 10% were MCL, which is the highest ratio of CL:MCL cases in Latin America, and is attributed to prevalence of *L. braziliensis* in the country [41,101]. Bolivia has one of the highest incidences of CL in the Americas, due in part to the large percentage of forest (70% of the country) and the associated sylvatic transmission risk [102]. VL is comparatively much less common and is caused by *L. infantum*. *Leishmania* spp. have been detected in several animal species including rodents, domestic dogs, skunks and porcupines, but incrimination as reservoirs requires further study [41].

1.6 Leishmaniasis Control

Zoonotic outbreaks can occur when human activity encroaches on animal reservoir populations, with human infection incidental alongside the established transmission cycle [35]. Where the primary host species is known, trapping of animals, and destruction of burrows and food sources can be effective methods of reducing overlap between human and animal habitats [103]. However, this can be costly and requires repeated intervention to maintain control. Often the relationship between vector and reservoir host is unknown, preventing adequate removal of either [23,104]. Canine reservoirs are a major risk factor for *L. infantum* infection, and interruption of contact between dogs and sandfly bites can reduce incidence of associated human VL, although efficacy of canine culls is debated [33,104–106]. Reports of reduced incidence following treatment of seropositive dogs is tempered by noted resurgence of disease following treatment in endemic areas [104,107].

Reduction of contact between humans and vector species is effective at preventing infection, but not practical for many at-risk populations, such as agricultural workers who work outside with exposed skin. Indoor residual spraying (IRS), such as national programmes with DDT in India or pyrethroids in Nepal to control *P. argentipes*, can have some impact on indoor biting sandflies, although resistance and poor quality control limits efficacy [108–111]. When sandflies bite out of doors, IRS is less effective than when employed against endophagic species, requiring a good understanding of the transmission setting for each locality [23]. Focused spraying and

distribution of barriers (i.e. insecticide treated bed nets) to transmission "hot spots" may have an impact on transmission, particularly in anthroponotic cycles, and in the control of VL [112–114]. Truly effective control strategies are unclear, with most randomly controlled trials too small to give strong evidence for or against intervention [115].

Leishmanization (vaccination with live *Leishmania*) is one of the oldest known methods of leishmaniasis control that is still in use today [116]. Historically, the deliberate exposure of infants' skin to biting sandflies resulted in an infection early in life, and protects against subsequent lesions. It was typically the buttocks that were exposed, leading to a scar that was hidden from view. Modern attempts to use a live *Leishmania* vaccine have variable levels of protection [116–118]. The importance of sandfly saliva in transmission success is possibly one reason for the reduced efficacy of artificial inoculation, although the age and virulence of the culture used is also likely a major determinant [117]. There is currently no available vaccine against human leishmaniasis, despite many varied approaches which have been extensively reviewed [118–121]. Recent advances include a partially protective vaccine against *L. major* infection, based on antigenic *Leishmania* glycans (discussed in further detail in section 1.11.4) [122].

Effective control of leishmaniasis is most probably through a combined approach; case detection, treatment and educational programmes in at-risk human populations, control/treatment of reservoirs and reduction of vector numbers [33,75,104,112,123].

1.7 Treatment of leishmaniasis

While mortality from VL infection approaches 100% without intervention, it is not always necessary to treat CL; a decision is made based on lesion number and location, as well as the parasite species [68,98]. Response to treatment varies between *Leishmania* species, although trial data is conflicting and reflects the complex nature of leishmaniasis [98,124–126].

Pentavalent antimonials have been the front line drug of choice since the 1940s, and are still used where resistance is not reported, mostly outside of the Indian sub-continent [127,128]. Intralesional injection of antimonials have cure rates of over 75%, although cure requires multiple injections over several weeks and adverse reactions are frequent [129]. Intramuscular injection is recommended as a second line treatment for Old World CL, when lesions are present in high numbers or in particularly problematic places, for example, joints [130]. However, systemic antimonials are almost always required in the treatment of New World CL, due to the risk of mucosal involvement. Pentamidine is used in the treatment of *L. guyanensis*, for which antimonials are ineffective [131]. The antifungal Amphotericin B has been in use for decades, and typically a single dose of the liposomal amphotericin B (AmBisome, Gilead, USA) can cure VL, although the cost can be prohibitive [132–134]. Oral drugs are preferable to parenteral methods, but again, options are limited. Miltefosine is effective in the treatment of VL, although has associated gastrointestinal adverse effects, and is not always superior to standard antimonials, as is the case in American CL caused by *L. braziliensis* [135,136]. Further restrictions apply to its use in childbearing women due to the teratogenic risks [137]. However, utility in treating unresponsive MCL can justify recommendation as a second line treatment in the Americas [138]. Oral treatment with azole drugs can also be effective across the spectrum of tegumentary leishmania, although there is considerable heterogeneity between trials and clinical settings [98]. Topical paromomycin for *L. major* and *L. tropica* has demonstrated high cure rates alone and in combination with gentamicin, but has limited availability currently and some trials report no improvement *vs* placebo controls after several weeks [125,126,139,140]. In spite of WHO guidelines for treatment, drug concentrations and duration of treatment can vary between heath care providers, giving an inconsistent approach to chemotherapy across regions [141].

Non-chemical treatments may also be efficacious in treatment of lesions, and avoid the complication of resistance faced by chemotherapeutic methods [128]. Cryotherapy

can be useful in treating uncomplicated lesions, even in species with reduced drug sensitivity, such as *L. tropica*, and has only mild reported side effects [142,143]. While cryosurgery by liquid nitrogen can be very expensive and therefore unsuited to low-resource countries, the cheaper alternative of carbon dioxide slush has been used with some success in Yemen, however it must be noted there was no control comparison group in this study so true benefit is unclear [144]. Photodynamic therapy is another alternative to chemotherapy, although one that is unlikely to find widespread use in low resource settings [145]. Thermotherapy is more widely used. A single application of localised heat (50°C) was demonstrably effective in the treatment of CL, in several settings including *L. tropica* in Afghanistan [146] and *L. donovani* CL in Sri Lanka [147]. Adverse effects are relatively low when compared to systemic treatments such as pentavalent antimonials, and so thermotherapy is typically tolerated, although it may not be a suitable treatment in areas where the risk of mucosal involvement is high [148]. Self-treatment with non-biomedical chemicals and traditional methods is sometimes used, and these can vary from battery acid and bleach to veterinary products and insecticides [149–151].

1.8 Current status of *Leishmania* diagnostics

CL diagnosis is typically based on epidemiology, clinical features, and laboratory tests, but can be difficult due to the lack of specificity in clinical symptoms, as CL lesions can resemble many other skin conditions [100,152–156]. Further complications arise due to the diversity in lesion appearance, which can vary widely depending on duration of infection, presence of secondary infections and host responses (Figure 1.8) [157]. For both VL and CL local procedures vary, depending on available infrastructure and expertise, but fall into three main categories: parasitological, molecular and serological.

Parasitological diagnosis depends on either *in vitro* culture from patient samples or direct staining of tissues to visualise amastigotes. It is considered the gold standard due to high specificity, although sensitivity is low (50-70%), particularly when amastigotes are scanty, such as in chronic cutaneous leishmaniasis [158]. A high level

of histopathological expertise is required, and, as all *Leishmania* species are morphologically very similar, species cannot be determined. Establishment of parasite culture from lesions aspirates is limited by the need to control bacterial/fungal contaminants, a heavy dependence on lab infrastructure, and the lengthy period required for cell growth (>10 days) [158]. Both methods also depend on tissue collection, which can be invasive, painful, and even fatal if performed inexpertly, particularly for VL (bone marrow or splenic aspirates) [32,159].

Figure 1.8. Diversity in the appearance of cutaneous lesions caused by *L. major* infection. Each image is of a different patient and was taken at the Al-Ahsa leishmaniasis clinic, Saudi Arabia in 2017. Credit: Dr L. Haines

Molecular detection of parasite DNA has many advantages over parasitological methods, including the ability to differentiate between *Leishmania* species and higher sensitivity, especially for chronic CL or cases with similarly low parasitaemia [83,160–162]. The method of sample collection for PCR can be invasive, although in CL, punch biopsies can be replaced with lesion scrapings, which have equal diagnostic value [163]. However, as with parasite culture, high quality DNA detection usually depends on appropriate laboratory facilities, and consumables and equipment are

expensive, limiting applications in low-resource settings. The development of a loop-mediated isothermal amplification (LAMP) assay for the detection of multiple *Leishmania* species, Loopamp™ Leishmania Detection Kit (Loopamp™), has considerable advantages over traditional molecular methods, in that it requires no cold chain (reagents are dried), a single temperature (no thermocycling), and samples can be collected through swabs rather than invasive methods [164]. As a novel protocol, Loopamp™, requires validation in more endemic regions, but is potentially an important tool in the diagnosis of both VL and CL [165,166]. An alternative method, direct-boil LAMP, further simplifies the protocol and shows encouraging results, however, it has a much lower detection limit than conventional LAMP, and remains unvalidated in clinical settings [167,168].

Serological diagnostic approaches have been highly successful in the diagnosis of VL, particularly with the recombinant leishmanial antigen K39 or a direct agglutination test (DAT) [169–172]. Antibody detection is less widely used for CL diagnosis, due in part to lower humoral response and associated low sensitivity. However, several ELISA methods have shown promise in antibody detection, for both New World [173,174] and Old World CL [175,176]. Recently, an immunochromatic point of care test has become available; the CL Detect™ Rapid Test (InBios International Inc., USA), which detects amastigote peroxidoxin antigen, shed by amastigotes of *Leishmania.* This RDT has mixed performance, with low sensitivity in cohorts from Suriname, Sri Lanka and Afghanistan [177–180]*,* but reportedly high sensitivity in Tunisia (de Silva et al. 2017 cites conference communications by Ben Salah et al., ASTMH 2012 Atlanta/2014 New Orleans). Vink *et al*. (2018) show that combining Loopamp™ and CL Detect™ to screen patients in Afghanistan maximised the potential of both tests, and minimised false negative cases.

1.9 The case for improved leishmaniasis diagnostics

Under-reporting of *Leishmania* infection is rife, in large part because the burden of disease falls on the poorest and most isolated communities, and the stigma associated with infection further hinders access to healthcare [4,43]. A rapid diagnostic

test (RDT) that could be used in rural communities could increase uptake of diagnostic tests by bringing the test to the patient, rather than requiring long distance travel to specialist health centres [181]. RDTs are simple medical devices (often cassettes or dipsticks) that require minimal training, allowing preliminary screening of suspected cases at community level. A cost effectiveness study comparing combinations of a CL RDT (CL Detect™), a molecular testing kit (Loopamp™) and the gold standard microscopy determined that initial screen with the RDT in a rural clinic, followed by LAMP/microscopy of negative suspects at the central reference clinic, was a cost-effective and robust diagnostic protocol [181]. Further benefits to a low-tech RDT would be during intense human displacement, as seen in recent decades [182]. Human migration and resulting imported cases are becoming increasingly important for the control and monitoring of CL in the Middle East and North Africa [13,78]. Vast numbers of displaced Syrian refugees are linked to changing patterns of *Leishmania* incidence, in Lebanon [62,183], Jordan [184], Iran [185], Turkey [186–188], and Northern Europe [189,190]. While diagnosis to species level is not always necessary when the local disease dynamics are known, imported and newly emerging infections demand a more in-depth screening process. Active case surveillance is essential in the changing climate of leishmaniasis burden globally, but requires accurate, cheap diagnostic tests that can be used in low-resource settings [76]. Health care for economically deprived people requires minimal investment in infrastructure and human expertise. This rules out most molecular and parasitological diagnostic methods, and requires something more akin to the RDT format used in malaria detection [62,67].

1.10 Glycan Diversity

Monosaccharides, the building blocks of more complex glycans, are carbohydrates that cannot be hydrolysed into simpler forms, and, when attached to each other through glycosidic linkages are typically found in ring form. The pyranose form (denoted *p* as in Gal*p* for galactopyranose) has a six-ring structure, whereas the furanose form gives a five-ring structure (Gal*f*). This work is primarily concerned with hexoses (sugars with six carbons), although hexosamines (hexoses with an

amino group at the 2-position, such as GlcNAc) are incorporated into several of the structures discussed (Figure 1.9).

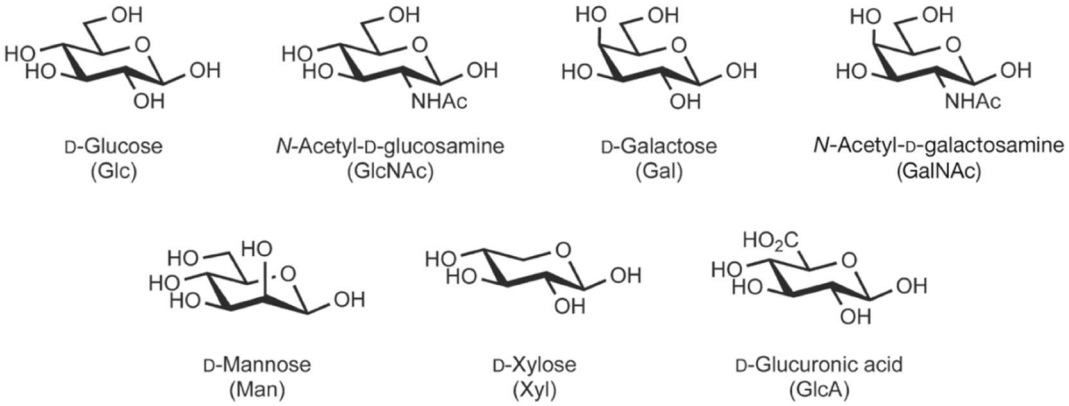

Figure 1.9. Common monosaccharides found in vertebrates. Monosaccharides found in *Leishmania* spp. GIPLs include Galactose, Mannose and N-Acetylglucosamine. Adapted from Essentials of Glycobiology, 2nd Ed.

The carbons in a hexose are numbered 1-6, so a glycosidic bond described as Gal(1,4)Man, indicates a bond between C-1 of the galactose and C-4 of the mannose. The configuration of the hydroxyl group at C-1 determines if the glycan is α or β (Figure 1.10). This determines the biological and structural function of the glycan, neatly demonstrated by the human immunogenic αGal*p* and the non-immunogenic βGal*p*, which are otherwise identical in structure.

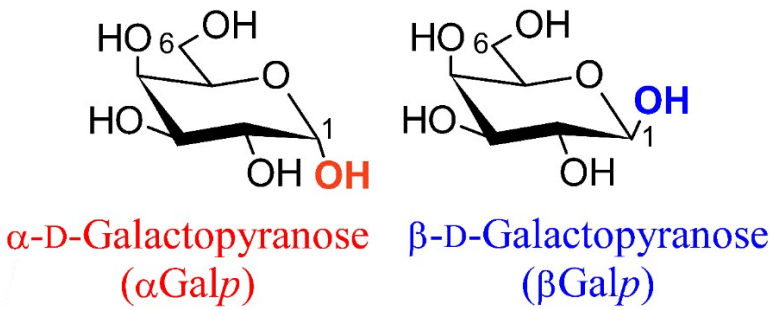

Figure 1.10. α and β configurations of galactopyranose monosaccharides. Immunogenicity of galactopyranose is determined by its α or β configuration. If the hydroxyl group on C-1 is axial (α), the residue is immunogenic. If the hydroxyl group is equatorial (β), then the galactose is not immunogenic**.**

1.11 Human anti-αGalactosyl antibodies (anti-Gal)

Anti-Gal is a natural human antibody (i.e. produced continually without inducement by a vaccine) that constitutes 1-5% of circulating IgG in healthy adults, with lower

levels in young children [191–193]. The high titre of natural anti-Gal in healthy humans is likely due to continual antigenic stimulation by gut microbiota, as it has been shown to bind to several bacterial species, including *E. coli* and *Klebsiella,* which are commonly found in the human gut, and clearance of gram negative bacteria in baboons has a corresponding reduction in circulating anti-Gal IgG [194,195]. Interestingly, individuals on a meat-free diet have lower anti-Gal titres than those who are not vegetarian [196]. Natural anti-Gal specifically binds the trisaccharide Galα(1,3)Galβ(1,4)GlcNAcβ-R. Binding of anti-Gal is determined largely by the terminal, non-reducing αGalactosyl (αGal) residue, however, overall specificity is driven by the subsequent glycans in the chain [197–199]. The Galβ(1,4)GlcNAc linkage is an important feature, likely due to the relative rigidity of the linkage, as compared to the more flexible Galα(1,3)Gal portion, allowing a consistent antibody recognition [200]. This αGal epitope is present on cells of New World primates and other mammals, but not human or Old World primates, because the glycosylation enzyme required (α1,3galactosyl-transferase, α1,3GT) was lost in these latter groups through a mutation >20 million years ago [201–203]. Individuals synthesising αGal epitopes would be unable to produce anti-Gal antibodies without generating an autoimmune response. The loss of the enzyme and subsequent synthesis of the polyclonal anti-Gal is likely to have given a significant evolutionary advantage [203]. Galili (2018) hypothesises that a hyperepidemic may have eliminated ancient primate species that had functional α1,3GT.

The relationship between anti-Gal and blood type has been described in detail [204–206]. B antigens (Galα1-3[Fucα1-2]Galβ1-4GlcNAc-R) have a similar structure to αGal (Galα(1,3)Galβ(1,4)GlcNAc-R), and are recognised by anti-Gal from sera of A- and O-Type patients. B Type-Individuals produce less anti-Gal than other blood types, and the frequency of this blood type correlates positively with the incidence of certain αGalactosylated pathogens, while a non-αGal-containing virus, Dengue, had no relationship [207]. αGal epitopes are a major barrier to xenotransplantation, for instance in the use of porcine organs in humans. Hyperacute rejection of grafts can occur within hours due to the presence of αGal epitopes on porcine cells [208].

Rejection can be overcome temporarily through depletion of anti-Gal from sera, or the use of organs from α1,3GT-KO pigs [209,210].

Due to its ubiquity in humans, anti-Gal has been the focus of many studies for exploitation in a variety of clinical settings. A recent study showed the conjugation of αGal to a therapeutic antibody increased immune response against cancer cells, through recruitment of anti-Gal [211]. Anti-Gal can also be exploited in improving immunogenicity of influenza vaccines, and against HIV glycoproteins in α1,3GT-KO mice [212,213]. Cancer immunotherapy using intratumoral injection of αGalactosylated glycolipids to generate a protective anti-tumour response in humans may have promise, following a Phase I Clinical Trial demonstrating safety [214–216]. Whalen *et al*. (2012) suggest utility in this approach as a vaccine against recurrence of tumours, following resection of tissue. Injection of αGal lipids into a tumour, 3-4 weeks prior to surgical removal, could induce continued protection against tumour antigens [214].

1.11.1 Anti-Gal during a leishmaniasis infection

It has been known for more than three decades that the titres of antibodies recognising αGal terminating residues are increased, compared to healthy controls, in both CL and VL infections [217–220]. Inoculation of α1,3GT-KO mice with *L. major* promastigotes results in high titres of IgG anti-Gal [221]. During VL infection, levels increase throughout the initial course of disease, with high values seen in over 70% of patients at 0.5 months after onset of symptoms [218]. These antibodies, the main subject of this thesis, present a viable candidate for a biomarker of *Leishmania*, if a specific capture antigen can be identified (discussed in the Chapters 4 and 5).

1.11.2 αGal epitopes in *Leishmania* parasites

The surface of *Leishmania* parasites is covered in a vast number of glycoconjugates. This glycocalyx is made up mainly of glycosylphosphatidylinositol (GPI)-linked proteins, proetophosphoglycans (PPG), lipophosphoglycan (LPG) and glycoinositolphopholipids (GIPLs) (Figure 1.11) [222–225]. The nature of this surface coat changes throughout the parasite lifecycle, becoming thinner during the amastigote stage due to a down-regulation in LPG expression [226]. Furthermore, the

exact composition is species-specific. LPG expression varies, in both the length and composition of glycan side chains as well as copy number per cell [222,227,228]. GIPLs are the most abundant glycoconjugates present (an estimated 10^7 copies per cell), with likely important roles in mediating parasite:host interactions [229–232]. These low molecular weight glycolipids are categorised according to the structure of their glycan and lipid components (Type-I, Type-II or Hybrid). While the number of GIPLs

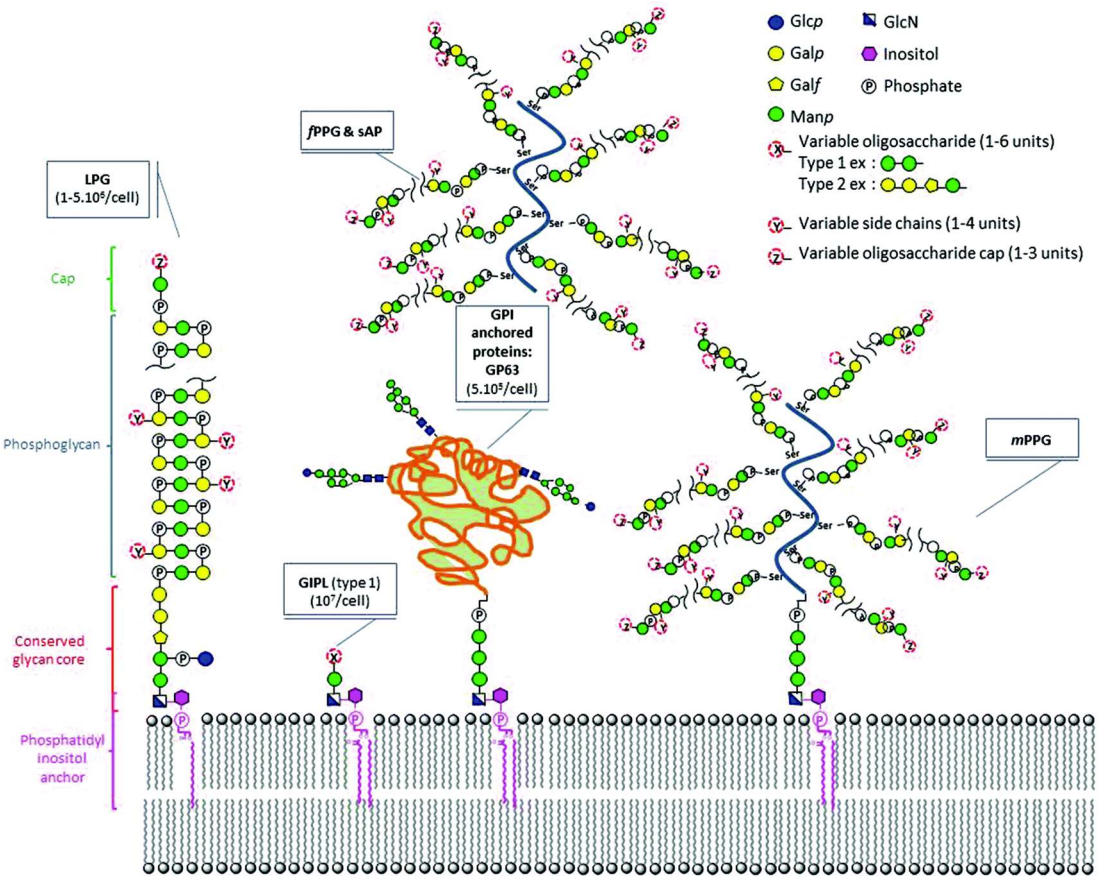

Figure 1.11. Details of the promastigote *Leishmania* surface glycocalyx. Major glycoconjugate components of *Leishmania* promastigote surface. GPI anchored (LPG, lipophosphoglycan; GIPLs, glycoinositolphospholipids, and proteins e.g. gp63), and secreted (proteins e.g. sAP, secreted phosphoglycan; PPG, proteophosphoglycan). There is variation in glycan core between GIPLs, LPG and GPI-anchored proteins, and in the PI anchor [233]. Downregulation of LPG expression in amastigotes exposes low molecular weight GIPLs, which are invariant throughout the life cycle [226]. Adapted from Cabezas *et al*. (2015).

is invariant throughout the *Leishmania* lifecycle, the presence of each type depends on the parasite species (Figure 1.12) [230,235,236].

The majority of the GIPLs present in *L. mexicana*, *L. major* and *L. braziliensis* parasites are Type-II, and contain a terminal galactose residue [230,231,237]. Anti-Gal recognises the major GIPLs found on the surface of *L. major* which contain the immunogenic αGal residues, but the epitope on *L. tropica* remains unknown [230,238,239]. Despite this apparent lack of αGal, anti-Gal antibodies are raised during

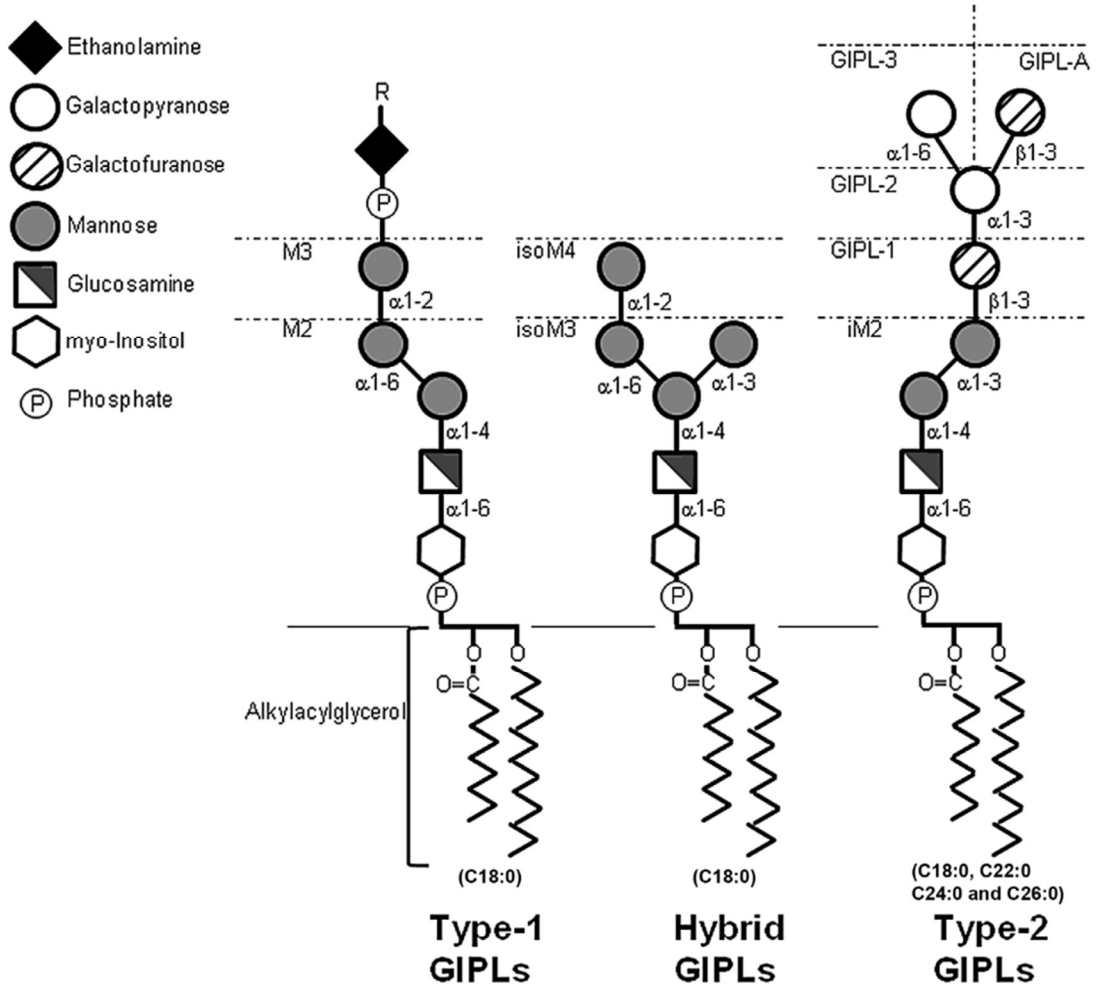

Figure 1.12. Structure of the three *major* classes of GIPL found on the surface of *Leishmania* parasites. The Type-II GIPL series contain the immunogenic terminal αGal residues. This type contains an R-Manα1- substitution on the 3rd carbon of the proximal mannose ring. Type-I GIPLs are mannosylated and are characterised by the R-Manα1-addition at the 6th carbon of the proximal mannose ring. Hybrid GIPLs contain features of both Type-I and Type-II GIPLs, with R-Manα1- substitutions on both the 3rd and the 6th carbons of the mannose ring. Adapted from Assis *et al*. (2012).

infection with *L. tropica*, as with *L. major* [217]. Other *Leishmania* species, including *L. infantum* and *L. tropica,* have structurally different GIPLs; largely Type-I GIPLs. Assis

et al. (2012) discusses the mannose-rich glycans detected in GIPL extract from *L. infantum* promastigotes, with 82% of the glycan composition derived from mannose residues, compared to around 30% in *L. braziliensis*.

1.11.3 Anti-Gal antibodies in Chagas disease and malaria

Over 5 million people are estimated to be infected with *Trypanosoma cruzi*, the aetiological agent of Chagas disease [240]. The majority of transmission is through the insect vector, triatomine bugs, although transfusion of infected blood [241,242], transplacental transmission from mother to child [243,244] and ingestion of contaminated food contribute to the burden of disease globally [245]. Chagas disease has two stages beginning with the acute phase with generally mild or no symptoms that lasts up to two months [246]. Between 30-40% of infected individuals will subsequently develop the chronic phase, which has much higher morbidity and mortality due to heart and digestive complications [247].

T. cruzi parasites have a dense glycocalyx, largely made up of GPI anchored mucin-like glycoproteins (Figure 1.13A) [248]. These mucins coat the entire surface of the bloodstream trypomastigote stage, including the flagellum, with around 2 x 10^6 copies per cell. Each mucin can be heavily *O*-glycosylated with glycans that have a terminal αGal residue at the non-reducing end (Figure 1.13B) [222,248–250]. High anti-Gal titres, recognising these immunogenic mucins, have been reported in patients infected with several *Trypanosoma* species, including *T. cruzi* and *T. rangeli* [229,251–253]. Chagasic anti-Gal are likely to be an important immunological method of protection against *T. cruzi*, with these antibodies directly lysing parasites, and inducing complement-mediated clearance [253–257]. The high levels of anti-Gal are seen in the acute and chronic phase of Chagas, returning to normal once the patient is cured; this trait has been exploited as a marker for effective cure following chemotherapeutic treatment [253,258,259]. Natural anti-Gal recognises *T. cruzi* mucins, but to a lesser degree than anti-Gal from patients with chronic Chagas infection [254,260]. Chagasic anti-Gal has broad affinity for αGal-terminating structures (Galα(1,2/3/6)Gal and Galα(1,3)Gal*f*), whereas natural anti-Gal has a much more

limited range of recognition, driven by its higher specificity for the subterminal units as well as the terminal, non-reducing αGal residue [200].

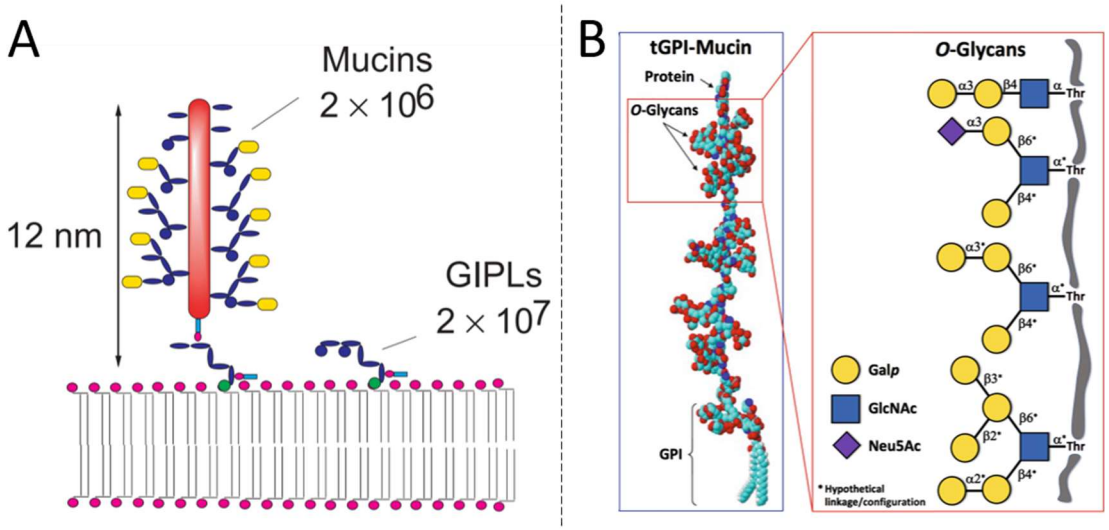

Figure 1.13. The main components of the surface glycocalyx of *T. cruzi* parasites. A. Major GPI components of *T. cruzi* trypomastigote surface; mucins number 2 x 10^6 copies/cell, while the much smaller GIPLs are the most abundant. Red components are protein, blue are saccharides and yellow ovals denote sialic residues. Adapted from Ferguson *et al*. (1999). B. Detailed structure of *T. cruzi* trypomastigotes mucins. Left panel: The heavily *O*-galactosylated protein core. Right. The glycan side chains have abundant αGal terminal residues that are recognised by Chagasic anti-Gal. Adapted from Ortega-Rodriguez *et al*. (2019).

Anti-Gal titres are also increased in patients with *P. falciparum*, and individuals living in *P. falciparum*-endemic regions [262]. IgM anti-Gal is linked to protection from clinical malaria in children [263]. A study of serum from 112 *P. vivax*-infected people found titres of anti-Gal were significantly higher than in non-malarial controls but to date no study has investigated the presence of αGal in *P. vivax* cells [263]. αGal has been identified on *P. falciparum* cells, both in asexual and sporozoite stages, by indirect methods [264,265]. Curiously, no α1,3GT orthologue gene has been yet identified in *P. falciparum*, leading to the hypothesis that the detected αGal may be vector-derived [266,267]. Natural anti-Gal, produced through antigenic stimulation by gut microbiota, has been linked to protection from *P. falciparum* infection [265]. Theoretically, this could be exploited in the generation of an anti-malaria probiotic to induce anti-Gal and therefore protect against *Plasmodium* infection [268].

1.11.4 Anti-Gal vaccines against parasitic infection

The presence of αGal on *Plasmodium*, *Leishmania* and *T. cruzi* cells alludes to the possibility of anti-Gal based vaccines for these pathogens [269,270]. Yilmaz *et al*. (2014) demonstrate that α1,3GT-KO mice are protected from *P. berghei* and *P. yoelii* infection after inoculation with a synthetic αGalactosyl-terminating glycan, conjugated to bovine serum albumin (αGal-BSA). This protective effect was largely driven by IgM antibodies and was limited to the dermis; immunisation had no impact on sporozoites injected intravenously, rather than intradermally or through mosquito bite. Additionally, for immunised mice that did get infected, disease was just as severe as in the controls. As fluorescent labelling of sporozoites confirmed the presence of αGal in *P. falciparum*, as well as *P. berghei* and *P. yoelii*, there are potential application in the human malaria species.

No therapeutic or prophylactic vaccine exists for Chagas disease, but Portillo *et al*. (2019) demonstrate promising results in mice, exploiting the immunogenic *T. cruzi* mucin glycans. α1,3GT-KO mice immunised with a synthetic Galα(1,3)Galβ(1,4)GlcNAc conjugated to human serum albumin were protected from a lethal *T. cruzi* challenge for up to 31 days (the experimental end point). Parasite load was reduced >90% in all tissues/organs tested, and weight loss reduced and then reversed in the immunised groups, compared to the non-immunised control mice. Antibodies from the immunised mice lysed a higher proportion of *T. cruzi* trypomastigotes than naïve mouse sera in *in vitro* assays [271].

A similar approach was used to evaluate the protective potential of three synthetic disaccharides, Galα(1,3)Galα-BSA, Galα(1,4)Galβ-BSA, and Galα(1,6)Galβ-BSA, against *L. major* infection in the same mouse model [122]. Immunisation with Galα(1,6)Galβ-BSA (with and without an adjuvant) resulted in significantly smaller lesions, alongside weight gain following challenge, an indicator of general health (the non-immunised mice consistently lose weight after *L. major* challenge). As with Chagas anti-Gal, anti-Gal from the immunised mice lyse *L. major* metacyclics *in*

vitro. Both Yilmaz *et al*. (2014) and Iniguez *et al*. (2017) observe a high titre of IgG1 and IgG3 in response to immunisation with the synthetic αGal.

Taken together, these three studies demonstrate both the importance of αGal epitopes in generating an immune response, and the protective potential of anti-Gal against parasitic infection.

1.12 Objectives of this work

Diagnostic tools for cutaneous leishmaniasis are currently limited to methods requiring expertise and laboratory infrastructure, which is antithetical to the rising burden of CL in refugee and migrant communities who lack access to healthcare. Therefore, the overall objective of this thesis was to assess whether human anti-gal antibodies developed during a leishmaniasis infection can be exploited as biomarkers in the diagnosis of CL.

1.13 Aims

1. Assess the utility of parasite glycolipids in diagnostic development, through TLC and ELISAs (Chapter Three).
2. Determine the anti-Gal specificities in patient sera with Old and New World leishmaniasis, using synthetic neoglycoproteins (NGPs) (Chapter Four).
3. Identify anti-Gal epitopes on *L. tropica* and *L. major* cells throughout life stages (Chapter Five).

Chapter Two
Methods

2.1 Cell Culture Methods

2.1.1 *Leishmania* Cell Culture

L. major (Friedlin strain; MHOM/IL/81/Friedlin) and *L. tropica* (LV357 strain; MHOM/IR/60/LV357) were cultured in Medium 199 (M199) with Hanks' Balanced Salts (Gibco, 22350029), supplemented with Penicillin-Streptomycin (Life Technologies, 15140-122), 1.5% BME vitamins (Sigma, B6891) and 10% heat-inactivated Foetal Bovine Serum (Hyclone, SV30160). Flasks were seeded at low density and passaged at 48-72 hours as needed. Cultures were maintained at 27°C in non-filter flasks and discarded after 15 passages.

2.1.2 Large scale *Leishmania* spp. cell culture

L. major and *L. tropica* promastigote cultures were grown to log phase (density ~1 x 10^7 cells/mL) in large volumes (>500 mL). The culture was harvested in volumes of around 200 mL, and washed twice with ice cold, sterile PBS, counted using a Neubauer haemocytometer and pelleted at maximum speed to remove the supernatant. A final high-speed centrifugation step ensured maximal liquid removal. Parasite pellets were stored at -80°C until used. The cells were collected in batches to minimise the length of time each step took and therefore reduce the risk of degradation during the collection. Counts were performed after two washes to give as accurate an estimate of the number of cells collected as possible, as a percentage of cells are lost with each wash. A sample of each batch was kept at this point and stored for PCR confirmation of species purity (Section 2.1.3). The final wash was performed at maximum speed, and ensures minimal loss of cells, but damages the cells to such a degree that counts at this stage are impossible. There is a degree of inaccuracy in this way of counting cells, so although counts were done on 100-200 cells, and in duplicate, cell equivalents are estimates only, and should be considered as such.

2.1.3 Identification of *Leishmania* spp. by PCR of parasite ITS1 region

Confirmation of *Leishmania* species in culture was performed on each batch of parasite cells, prior to extraction of glycolipids or use in other assays. A PCR method based on that developed by Schonian *et al*. (2003) exploits the polymorphisms in fragment length of the ribosomal internal transcribed spacer locus (*ITS1*), after

treatment of extracted parasite DNA with *Hae*III restriction enzyme. Genomic DNA was extracted using DNeasy Blood & Tissue Kit (Qiagen, 69504). PCR reactions contained 5 µL 10x PCR buffer, 1 µL genomic DNA, 1.5 µL each forward and reverse primers, 1 µL dNTPs, 1 µL Taq DNA Polymerase and 39 µL nuclease free water. PCR conditions were one cycle at 95°C for 40 seconds, 35 cycles of 95°C for 40 seconds, 53°C for 40 seconds and 72°C for 50 seconds, followed by cooling to 4°C for storage. Restriction digests were performed according to the manufacturers protocol for *Hae*III digestion (New England Biolabs, R0108S). 43 µL of PCR product was incubated with 5 µL NEB Buffer 2 and 2 µL *Hae*III for 2 hours at 37°C. Digests were then run on 2% agarose gels with SYBR Safe DNA Gel Stain and the species confirmed based on banding pattern (compared to [272]).

2.1.4 Human monocyte THP-1 cell culture

THP-1 monocytes (kindly donated by H. Price, Keele; original source [273]), were cultured at low density in RPMI (ThermoFisher, 21875), supplemented with 10% HI-FBS (Hyclone, SV30160) and 100 U/mL Penicillin-Streptomycin (Life Technologies, 15140-122). When cultures approached a density of 1 x 10^6 cells/mL, cells were washed and resuspended in fresh media to a density of 2-5 x 10^5 cells/mL. Cultures were discarded every four weeks and fresh aliquots thawed.

2.1.5 Infection of THP-1 cells with *Leishmania* spp.

THP-1 cells were differentiated at densities between 2.5-3 x 10^5 cells/mL. Phorbol 12-myristate 13-acetate (PMA; Merck, P8139), stock solution dissolved in DMSO, was added to a final concentration of 25 ng/mL and incubated at 37°C for 48 hours. Non-adherent cells were removed, by gentle washing with serum-free RPMI pre-warmed to 37°C, three times. The adherent cells were supplied with complete RPMI with 10% HI-FBS were rested overnight at 37°C.

Leishmania procyclic promastigote cultures were collected in late log phase, washed and resuspended in RPMI media before counting. Parasites were incubated with THP-1 cells at a ratio of 10 parasites per THP-1 cell, for 4 hours at 37°C. Non-internalised parasites were removed with gentle washing with pre-warmed

incomplete RPMI, and the infected THP-1 cells incubated for 72 hours at 37°C, with daily media changes. After 72 hours (peak of amastigote yields and minimal loss of THP-1 cells) the cells were processed for other applications i.e. immunostaining.

2.1.6 Amastigote extraction from infected THP-1 cells

THP-1 cells were differentiated into 6 well plates, and infected (as described Section 2.1.5). Each parasite species was added to wells in triplicate. After 72 hours the infection was confirmed through Giemsa stain. One well for each species (*L. major* or *L. tropica*) was washed gently with PBS twice, and fixed with methanol for 10 minutes on ice. The methanol was removed, and Giemsa solution added for ten minutes at room temperature. The stain was rinsed off with distilled H_2O and wells allowed to dry. Parasites were counted using an eye-piece objective, as 1) a percentage of infected THP-1 cells, and 2) number of parasites per cell. The remaining unstained wells were then harvested; adherent THP-1 were treated with 0.25% trypsin for 3 minutes at 37°C and collected in 15 mL Falcon tubes. The cells were pelleted at 100 x *g* for 5 minutes and washed once with incomplete RPMI. The pellet was resuspended in a small volume of incomplete media supplemented with 0.05% SDS and gently agitated by hand for 30 seconds to release amastigotes. A large volume (10X the current volume) of incomplete media was added, and the cells pelleted at 3000 x *g* for 5 minutes. The supernatant was collected and transferred to a plate, and the pellet washed a further time. The pellet was resuspended in incomplete media and transferred to a plate and rested at 37°C for 1 hour to allow cells to settle and viability confirmed (intact cell bodies, normal morphology). The amastigotes were then gently aspirated from the plate, spun at low speed to pellet and transferred to slides for staining, as described below.

2.1.7 Immunostaining of fixed *Leishmania* promastigote cells using IB4-AF488 lectin

Leishmania procyclic promastigotes were cultured to stationary phase (days 5-7) i.e. until metacyclic promastigotes were visualised. 2-3 mL culture (~2 x 10^7 cells/mL) was washed and resuspended in serum-free M199 and returned to the incubator for 2 hours. 1 mL culture was washed 3 times with ice cold TBS (1900 x *g* for 5 mins,

4°C). On the final wash, the supernatant was removed, and the pellet resuspended in a small volume. 50 µL of the suspension was transferred to a poly-L-lysine slides and allowed to settle for 30-60 minutes in a humidity chamber. The remaining liquid was removed after this time and the slides transferred to 100% ice-cold methanol and incubated on ice for 10 minutes. The slides were then washed twice in TBS before blocking overnight in 0.22 µM-filtered 2% BSA-TBS-S (TBS supplemented with salts – $CaCl_2$, $MgCl_2$, $MnCl_2$, each at 1 mM). Staining with IB4 lectin was done for 2 hours at room temperature, in the dark. The lectin solution was resuspended in TBS-S, and for inhibition experiments, 0.5 M galactose was added and the solution preincubated for one hour at RT, prior to application to the slide. Slides were washed in TBS three times for five minutes each, to remove excess lectin. 200 µL DAPI at 200 ng/mL was added to each slide for 3 minutes at room temperature, in the dark, before washing as before. Slides were mounted in VectaShield™ and coverslip edges sealed with clear nail varnish. Slides were stored at 4°C in the dark until imaged using a Zeiss Confocal LSM 880/Axio Observer Z1 microscope. Confocal imaging facilities were funded by a Wellcome Trust Multi-User Equipment Grant (104936/Z/14/Z).

2.2 Antibody Purification methods

2.2.1 Purification of IgG from sera using a Protein G Column

1 mL Pierce Protein G Chromatography Cartridge (ThermoFisher, 89926) was equilibrated with 10 column volumes (CV) Binding Buffer (50 mM sodium acetate, pH 5.0), flow rate of 1 mL/minute. Pooled *L. major* sera was diluted 1:1 in binding buffer (total volume 1 mL), centrifuged at 10,000 x *g* for 20 minutes, and applied to the column at a rate of 1 mL/minute. A sample of the diluted sera was kept for binding quantification. The column was incubated for 1 hour at room temperature, before washing with 10 CV binding buffer. 1 mL fractions of the washes were kept and assayed for absorbance. Elution of the bound antibody was only performed once absorbance of the fractions was zero. 5 CV elution buffer (0.1 M glycine, pH 2.5) was applied to the column, and fractions collected in tubes containing 1 M Tris (pH 9) for immediate neutralisation. The purified IgG was then applied to a second column of NHS-activated Agarose conjugated to Dextra-BSA.

2.2.2 Elaboration of an αGalactosyl column for anti-Gal purification

Activated agarose contains N-hydroxy succinimide (NHS) ester functional groups that form amide linkages with the primary amine groups on proteins, such as BSA. A quantity of Pierce NHS-Activated Agarose Dry Resin (ThermoFisher, 26196) was added to a spin column and incubated with 500 µg of the synthetic glycan Galα(1,3)Galβ(1,4)GlcNAcβ-BSA (Dextra Laboratories Ltd, NGP0334; hereafter called Dextra-BSA), diluted in 100 µL coupling/wash buffer (0.1 M sodium phosphate, 0.15 NaCl, pH 7.2), to give a final volume of 250 µL hydrated resin. The resin was mixed end-over-end at room temperature for one hour. Flow through (FT) was collected and retained for analysis of binding efficiency. The column was washed with 2 CV of coupling/wash buffer, before addition of quenching buffer (1 M Tris, pH 7.4), to block remaining active sites. The column was mixed end-over-end for 20 minutes at room temperature, then washed with 5 CV of coupling/wash buffer, until absorbance approached zero.

2.2.3 Affinity purification of anti-Gal antibodies by affinity chromatography

IgG from *L. major* infected patient sera, acquired through Protein G chromatography (Section 2.2.1) was diluted 1:10 in PBS, and 500 µL applied to the column. The column was incubated overnight at 4°C with end-over-end mixing. The FT was collected for monitoring binding efficiency, and the column washed with 5 CV of PBS. The bound antibody was eluted with 0.1 M glycine and immediately neutralised with 1 M Tris (pH 9). The final fractions were dialysed into PBS, concentrated and assayed from protein content.

2.2.4 Anti-Gal purification using αGalactosyl coated nitrocellulose membrane

50 µg Dextra-BSA was diluted in 100 µL in PBS and applied to a strip of nitrocellulose (7 mm x 30 mm). The strip was dried for approximately one hour at room temperature, before washing three times with PBS (1 mL each time). The strip was then incubated with 1% BSA-PBS for 1 hour at room temperature under gentle

agitation, gently washed three times with PBS, then incubated overnight at 4°C in pooled sera from *L. major* positive patients. The serum was diluted 1:10 in PBS, to a total volume of 1 mL (50 µL kept for protein quantification). Following the incubation, the unbound serum was collected and stored at -20°C for binding assessment. The membrane was washed well with PBS, before the bound antibody was eluted with 50 mM citric acid (pH 2.8). The elution was performed three times, each elution immediately neutralised with 1 M Tris (pH 9). The membrane was washed with PBS, and each wash kept for protein analysis to ensure no unbound antibody remained. The final elution was pooled, dialysed into PBS and assayed for protein content. The membrane strip was stored at 4°C, in PBS with 0.05% sodium azide for further use.

2.2.5 Anti-Gal quantification after purification

Protein quantification was done through BCA assay, according to the manufacturers protocol (Pierce BCA Protein Assay Kit; ThermoFisher, 23225). 25 µL of sample was pipetted into each well of a clear 96-well plate, and 200 µL of working reagent added. The plate was incubated at 37°C for 30 minutes, cooled to room temperature and the absorbance measured at 562 nm. Where necessary, the Pierce 660nm Protein Assay (ThermoFisher Scientific, 22660) was used as an alternative, according to the manufacturer protocol. 10 µL of each sample was added to the wells of a clear 96-well plate, with 150 µL of Protein Assay Reagent. Following agitation for 60 seconds, the plate was incubated at room temperature for 5 minutes and the absorbance at 660 nm read. The concentration was calculated from a standard curve generated from Bovine Gamma Globulin (ThermoFisher, 23212) standards, ranging from 2 mg/mL to 20 µg/mL (the working range of the BCA assay is 20-2000 µg/mL, and 50-2000 µg/mL for the 660nm).

2.2.6 SDS-PAGE and Western blotting analysis of purified anti-Gal fractions

Membrane elution fractions of antibodies were fractionated by SDS-PAGE using two 12.5% gels. The gels were run for 90 mins at 120V. One gel was then washed under distilled water three times for 15 minutes each and incubated overnight with

Coomassie protein stain. The proteins from the second gel were transferred to nitrocellulose membrane at 90V for 30 minutes, on ice in Tris-Glycine buffer containing 20% methanol. The membrane was incubated with Ponceau Red (Sigma, P7170) stain to reversibly visualise the transferred bands, then washed gently to remove the stain before incubation in 5% skim milk for 1 hour. The membrane was washed vigorously with PBS-0.05% Tween 20 (PBS-T) three times for 5 minutes, then incubated in goat anti-human IgG secondary antibody with HRP conjugation (Abcam, ab6858) at 1:50,000 overnight at 4°C. The membrane was washed several times and developed with SuperSignal™ West Dura Extended Duration Substrate (ThermoFisher, 34076) and exposed to Kodak Carestream® BioMax® light film (Merck, Z370371). Film was processed with AFP Imaging Corp X-Ray developer using RG X-Ray Developer and Fixer solutions.

2.2.7 Coffee bean α-Galactosidase enzyme treatment of Dextra-BSA

0.5 µg Dextra-BSA was incubated overnight at 27°C with either 0.1 U coffee bean α-galactosidase (CBAG; New England BioLabs, P0747S) or the equivalent volume of 0.1 M potassium phosphate buffer (pH 6.5). The digested product was fractionated on a 12.5% SDS-PAGE gel and then transferred to nitrocellulose as described above. After transfer, the membrane was incubated with Ponceau Red, washed and incubated in 5% goat serum-TBS (Sigma, G9023) overnight, 4°C. The membrane was washed with TBS-T three times for 5 minutes, then sequentially incubated with 1) 0.2 µg/mL eluted antibody (15 mL total volume) and 2) goat anti-human IgG-HRP (Abcam, ab6858) 1:100,000 (15 mL total volume). Each incubation was for 1 hour at room temperature and followed by three TBS-T washes. The membrane was developed with SuperSignal™ West Dura Extended Duration Substrate (ThermoFisher, 34076) and exposed to Kodak Carestream® BioMax® light film (Merck, Z370371). Film was processed with AFP Imaging Corp X-Ray developer using RG X-Ray Developer and Fixer solutions.

2.2.8 Dot blot with enzyme treated Dextra-BSA and eluted antibody

0.1 µg Dextra-BSA was incubated overnight at 27°C with either 0.1 U CBAG (treated) or equivalent volume of 0.1 M potassium phosphate buffer (pH 6.5) (mock-treated).

Treated and mock-treated Dextra-BSA was dotted on a small nitrocellulose strip, alongside 0.1 µg of BSA. The strip was dried, washed gently in PBS then sequentially incubated with 1) 1% BSA-PBS, 2) 1 ug/mL eluted antibody (1 mL total volume) and 3) goat anti-human IgG-HRP (Abcam, ab6858) 1:50000 (1mL total volume). Each incubation was for 1 hour at room temperature and followed by three PBS washes. The membrane was developed with SuperSignal™ West Pico PLUS Chemiluminescent Substrate (ThermoFisher, 34579), 100 µL total volume, and exposed to Kodak Carestream® BioMax® light film (Merck, Z370371) for 90 seconds. Film was processed with AFP Imaging Corp X-Ray developer using RG X-Ray Developer and Fixer solutions.

2.3 Glycolipid Analysis Methods

2.3.1 Extraction of *Leishmania* spp. GIPLs

Glycolipids were extracted from *L. major* and *L. tropica* parasite pellets (as collected in Section 2.1.2) under sonication, through sequential treatment of the parasite pellet with chloroform:methanol (1:1, by volume) to remove phospholipids and chloroform:methanol:water (10:10:3, by volume) to extract the polar glycolipids. The C:M:H_2O fraction was dried under N_2 and partitioned with equal volumes n-butanol and H_2O. The lower phase was washed with water-saturated butanol twice, and both phases dried under N_2 and resuspended in chloroform:methanol:water (10:10:3, by volume).

2.3.2 High Performance Thin Layer Chromatography (HPTLC) separation of *Leishmania* lipids

The fractions were applied to aluminium-backed silica HPTLC plates in volumes equivalent to 2 x 10^8 cells. The fractions are dotted onto marked lanes of 7 mm width and dried. Plates were developed sequentially in two separate solvent systems; A) chloroform:methanol:0.2% KCl-H_2O (5:5:1.5, by volume) and B) butanol:pyridine:0.2% KCl-H_2O (9:6:4, by volume), and dried overnight. To ensure solvent evaporation plates were additionally gently dried with a hairdryer or in an oven at 30°C. Samples are duplicated on each plate, allowing one half to be chemically stained, and the remaining half processed for lectin/immunostaining.

2.3.3 Orcinol staining of *L. major* and *L. tropica* glycolipids fractionated on HPTLC

The plate was clipped to a glass support and sprayed with the orcinol/H_2SO_4 (180 mg orcinol in 83% ethanol, 11% H_2SO_4, 6% H_2O) solution using a fine aerosoliser. Porcine ganglioside mixture (Avanti Polar Lipids, 860053) was used as a standard for band migration (applied in a lane adjacent to the *Leishmania* extracts prior to HPTLC separation). The plate and glass were heated to 120°C in an oven for 5 minutes, until the bands were visible. Longer heating results in darker stain; the optimal resolution is achieved when the stain is pink in colour. The plate was cooled and any excess stain was removed by sandwiching the plate between pieces of filter paper.

2.3.4 Immunostaining of glycolipids from *Leishmania* spp.

Chromatographed TLC plates were dipped in 100% hexane for 30 seconds and transferred immediately to a solution of 0.2% poly(isobutylmethacrylate) (Merck, 181544) in hexane for 90 seconds, and air dried. PIBMA-fixed plates were blocked with of 5% BSA-PBS-T for 30 minutes at room temperature. The plate was gently washed in PBS-T before serial incubation in 1) human sera (1:500), 2) goat anti-Human IgG (1:1000; Sigma, I2136), 3) donkey anti-Goat biotin (1:2000; ThermoFisher, PA128663) and 4) streptavidin-HRP conjugate (1:2000; Invitrogen, SNN4004), between washes with PBS-T. Binding was visualised through incubation with SuperSignal™ West Pico PLUS Chemiluminescent Substrate (ThermoFisher) (1 ml solution per 5 cm^2 plate) and the plate exposed to Kodak Carestream® BioMax® light film (Merck, Z370371). Film was processed with AFP Imaging Corp X-Ray developer using RG X-Ray Developer and Fixer solutions.

2.3.5 Lectin staining of αGalactosylated lipids from *Leishmania* spp.

As in section 2.3.4, TLC plates were fixed with 0.2% PIBMA in hexane. The fixed plate was incubated in Carbo-Free block buffer (Vector Labs), washed gently in PBS-T and incubated overnight with 20 µg IB4-HRP in 50 mL PBS with 0.1 mM salts ($MgCl_2$, $MnCl_2$, $CaCl_2$) at 4°C, under very gentle agitation. The plate was gently washed three times with PBS-T. Bands were visualised through incubation with SuperSignal™ West Pico

PLUS Chemiluminescent Substrate (ThermoFisher) (1 ml solution per 5 cm^2 plate, applied to a glass support and the TLC plate inverted into the solution). The plate was then exposed to Kodak Carestream® BioMax® light film (Merck, Z370371). Film was processed with AFP Imaging Corp X-Ray developer using RG X-Ray Developer and Fixer solutions.

2.3.6 Octyl-Sepharose purification of *L. major* and *L. tropica* GIPLs

1.4 x 10^9 cell equivalents (CE) of the butanol phases of glycolipid extracts were dried under N_2 and resuspended in 100 µL 0.1 mM ammonium acetate, through repeated vortexing and sonication. This was applied to a 0.5 mL Octyl-Sepharose column (Sigma Aldrich, O0511). The vial was washed with a further 100 µL 0.1 M ammonium acetate buffer, and this was again applied to the column. The 200 µL buffer was allowed to enter the resin bed, before the column was capped at both ends and incubated at room temperature for one hour. FT was collected, and the column washed with 1 mL 5% 1-propanol-0.1 M ammonium acetate. Fractions were collected in volumes of 250 µL. The bound glycolipids were eluted from the column with increasing concentrations of 1-propanol in 0.1 M ammonium acetate (10, 20, 30 and 40%). Fractions were collected as before. The column was washed and regenerated with 10 CV of 0.1 M ammonium acetate buffer. Fractions were checked for glycan contents through spotting on TLC plates and staining with orcinol/H_2SO_4 as described above (Section 2.3.3). Small aliquots of positive fractions are applied to TLC plates and chromatographed as above (Section 2.3.2), to confirm presence and migration of GIPL species.

2.3.7 Extraction of glycolipids from silica and identification by orcinol staining

Two controls were included on each plate; 10 µg of porcine ganglioside mixture (Avanti Polar Lipids, 860053), as a standard for the migration from the point of origin to the solvent front, and a duplicate of each sample, to allow marking an extraction of the location of each band of interest. Control lanes were placed on one side of the plate with a gap of 2 cm between the controls and the samples. After the plates were chromatographed (Section 2.3.2) and air dried to remove all solvents, the plate was

placed in a tank saturated with iodine vapour. Iodine (reversibly) stains many lipid compounds and gave visual confirmation that the plate has run consistently; i.e. bands are at the same height in all lanes.

After the iodine dissolved off the plate, the section of the plate containing the controls was cut off using a razor blade. This portion of the TLC plate is stained using orcinol/H_2SO_4 (Section 2.3.3). The bands of interest were identified from the orcinol stained controls and the distance of migration was measured. Using a pencil, the band location was marked in the unstained plate, and a clean scalpel was used to scrape the silica containing the band into a vial. This silica was then treated with three washes of chloroform:methanol:H_2O (10:10:3, by volume) to extract the glycolipids from the silica, with sonication and high-speed centrifugation between each wash. The solvent was dried under N_2 to dryness, before the extract was resuspended in a small volume of chloroform:methanol:H_2O (10:10:3, by volume). A small volume of this sample (equivalent of 1-2 x 10^8) was applied to a new plate, alongside the original sample, chromatographed as described above (Section 2.3.3) and stained with orcinol to detect glycolipids migration.

2.3.8 Electrospray ionisation mass spectrometry (ESI-MS) and ESI-MS/MS analysis of *L. major* and *L. tropica* glycolipids

Glycolipid extract and individual bands were dried under nitrogen flow with gentle heat and resuspended in 70% 1-propanol 5 mM ammonium acetate, followed by high speed centrifugation for 15 minutes to ensure supernatant was clear of precipitate. Samples were run on LTQ Orbitrap XL MS in positive and negative mode, by Dougie Lamont at the University of Dundee.

2.3.9 CL-ELISA detection of reactivity of serum samples against native *Leishmania* spp. glycolipid samples

A sample of glycolipid extract (Section 2.3.1) in chloroform:methanol:water (10:10:3, by volume) was dried under N_2 and resuspended, through sonication and vortexing, in PBS. White lipid-binding 96-well plates (ThermoFisher, 9502887) were coated with glycolipid extract (concentration determined through titration experiments) in 50 mM

carbonate:bicarbonate buffer (pH 9.6), 75 µL/well, and allowed to dry overnight at 37°C. Plates were blocked with 200 µL/well 1% BSA-PBS, followed by serial incubation with primary antibody (concentration determined through titration) and goat anti-human IgG HRP conjugate antibody (1:8000; Abcam, ab6858). The signal was developed with SuperSignal™ ELISA Pico Chemiluminescent Substrate (ThermoFisher, 37070). All volumes (except the blocking step) were in 50 µL, and plates were shaken for 1 minute at a gentle speed to ensure complete coating of the base of the well with each step. Each plate contained two *Leishmania*-negative controls - pooled sera from North America and Saudi Arabia, and a primary antibody negative control i.e. incubated with diluting buffer only in place of the primary antibody. All samples were run in triplicate. Luminescence were read at excitation 425nm using a FLUOstar OMEGA plate reader.

To determine glycan specificity, after antigen fixation and drying overnight, CBAG (Sigma, G8507) was added to wells in 0.1 M potassium phosphate buffer (pH 6.5), and plates were covered and incubated overnight at 27°C. Enzyme (mock) controls were treated with potassium phosphate buffer without enzyme under identical conditions. The plates were then washed prior to blocking and the ELISA then continued as described above.

2.4 Neoglycoprotein ELISA methods

2.4.1 Neoglycoprotein (NGP) Synthesis for use in CL-ELISA

The synthesis of all non-commercial NGPs used in this study was performed in the lab of Dr Katja Michael (University of Texas at El Paso, UTEP). The general method is described in detail by Ashmus *et al*. (2013) but briefly, chemically synthesised glycans were conjugated to maleimide-activated BSA through a thioether linkage. BSA was chosen for its ease of use in immobilising on microtiter plates for CL-ELISA analysis, low or no recognition by human serum, the multiple binding sites per BSA molecule and its high solubility in aqueous solutions [260,274].

The first set of NGPs (KM1-KM17) were synthesised in 2013, with a second panel synthesised in 2015 (new KM3, KM24), and a third (KM27-KM30, BME), to give a

total of 15 structures (Table 2.1, Figure 2.14). Due to minor variation in conjugation efficiency, the average number of glycans per BSA molecule ranges from 20-25. Lyophilised NGPs were reconstituted in distilled H_2O by gentle pipette mixing, with no vortex or sonication. After protein concentration quantification by BCA (Pierce BCA Protein Assay Kit, Thermo Scientific, 23225; protocol according to manufacturer's instructions), samples were adjusted to a standard concentration, aliquoted into small volumes and frozen at -80°C.

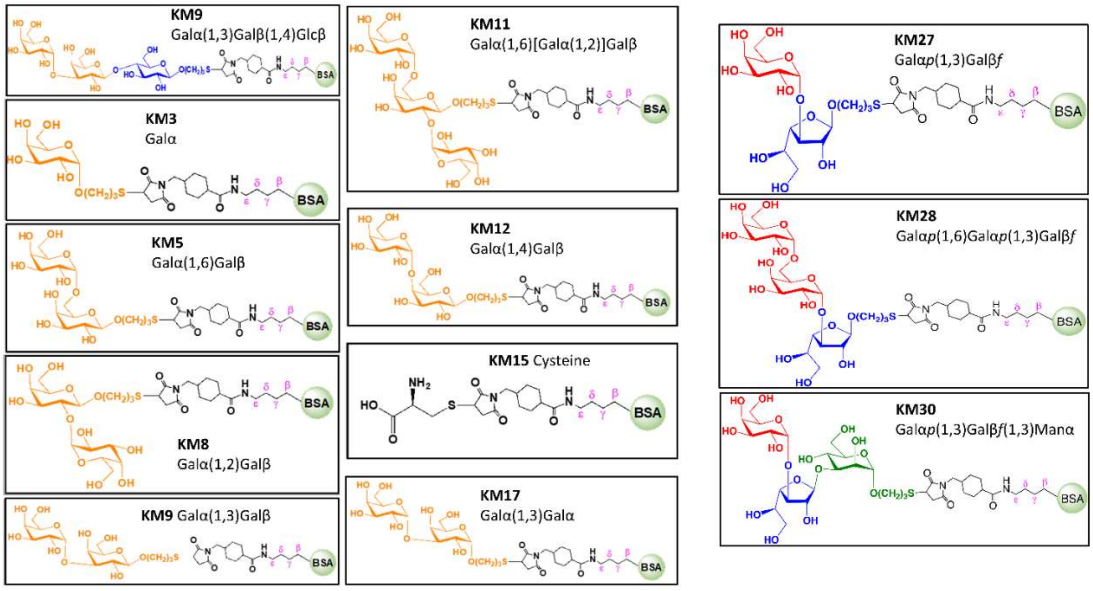

Figure 2.1. Structures of non-commercial NGPs synthesised in Dr K Michael's laboratory. Linear structure detailed in Table 2.1. Chemically synthesised glycans were conjugated to maleimide-activated bovine serum albumin (BSA) through a thioether linkage.

Table 2.1. Non-commercial neoglycoproteins (NGPs) used to assess levels of anti-Gal in human serum samples. ID refers to the code used to refer to each structure throughout this thesis. The glycan portion varies for each structure. R corresponds to the linker-BSA. All NGPs have at least one terminal αGal residue, except two controls KM15 (cysteine) and BME (β-mercaptoethanol). The NGPs were synthesised in batches; KM1-17 in Panel 1, KM24 in Panel 2, and KM27-BME in Panel 3.

Panel	ID	Structure of Terminal Glycan
1	KM1	Galα(1,3)Galβ(1,4)Glcβ-R
	KM3	Galα-R
	KM5	Galα(1,6)Galβ-R
	KM8	Galα(1,2)Galβ-R
	KM9	Galα(1,3)Galβ-R
	KM11	Galα(1,6)[Galα(1,2)]Galβ-R
	KM12	Galα(1,4)Galβ-R
	KM17	Galα(1,3)Galα-R
	KM15	Cysteine-R
2*	KM24	Galα(1,3)Galβ(1,4)GlcNAcα-R
3	KM27	Galα(1,3)Galβ-R
	KM28	Galα(1,6)Galα(1,3)Galβ-R
	KM30	Galα(1,3)Galβ(1,3)Manα-R
	BME	2-ME-R

* Panel 2 also included KM3

2.4.2 CL-ELISA assays to determine with αGal-NGPs

Levels of *Leishmania* anti-Gal IgG antibodies in human sera was determined as previously described [217,275]. The antibodies and concentrations varied between assays (see Table 2.2 for details) but the overall steps remained the same. Briefly, white 96-well plates (Nunc) were coated with the appropriate NGP in 0.2 M carbonate:bicarbonate buffer (pH 9.6) at 4°C, overnight, at concentrations determined through titration experiments. The plates were blocked with 200 µL/well 1% BSA-PBS (PBS-B), and serially incubated with antibodies; all incubations were performed at 37°C for one hour. Plates were washed between incubations, three times with PBS-T. The luminescence was developed with SuperSignal™ ELISA Pico Chemiluminescent Substrate (ThermoFisher, 37070) diluted 1:1:8 in 0.2 M carbonate-bicarbonate buffer. Controls for each NGP/sera pool combination were included in duplicate on each plate; Antigen Negative, Primary Negative, Secondary Negative, and HRP Negative. The average RLU was taken for these controls and

subtracted from the average of the unknown sample replicates to control for non-specific/background signal from the reagents.

To determine if a single, polyclonal antibody was responsible for binding to the αGal-NGPs, wells were coated with pairs of NGPs at the same concentrations as in solo experiments. CL-ELISA protocol was followed as described above.

Table 2.2. CL-ELISA Conditions for each NGP Panel as described in this thesis.

Reagent		CL-ELISA Type				
		KSA Sera		Bolivian Sera		Spanish Sera
		NGP Panel 1	NGP Panel 3	NGP Panel 2	NGP Panel 3	NGP Panel 3
NGP		250 ng/well	KM27/30/BME 50 ng/well KM28 12.5 ng/well	125 ng/well	KM27/30/BME 50 ng/well KM28 12.5 ng/well	125 ng/well
Antibody	1°	1:100	1:800	1:100	1:800	1:100
	2°	Goat anti-Human IgG (Fc Specific) Sigma cat# I2136 1:1000	Goat anti-Human IgG (H+L) Biotin conjugate Thermo Fisher Scientific cat# 31770 1:10,000	Goat anti-Human IgG (Fc Specific) Sigma cat# I2136 1:1000	Goat anti-Human IgG (H+L) Biotin conjugate Thermo Fisher Scientific cat# 31770 1:10,000	Goat anti-Human IgG (Fc Specific) Sigma cat# I2136 1:1000
	3°	Donkey anti-Goat IgG Biotin conjugate ThermoFisher Scientific cat# PA128663 1:1000	Pierce™ High Sensitivity NeutrAvidin™-HRP Thermo Fisher Scientific cat# 31030 1:5000	Donkey anti-Goat IgG Biotin conjugate ThermoFisher Scientific cat# PA128663 1:1000	Pierce™ High Sensitivity NeutrAvidin™-HRP Thermo Fisher Scientific cat# 31030 1:5000	Donkey anti-Goat IgG Biotin conjugate ThermoFisher Scientific cat# PA128663 1:1000
	4°	HRP-Streptavidin Invitrogen cat# SNN4004 1:2000	N/A	HRP-Streptavidin Invitrogen cat# SNN4004 1:2000	N/A	HRP-Streptavidin Invitrogen cat# SNN4004 1:2000

2.4.3 Specificity of αGal-NGPs after CBAG treatment

Optimisation of the appropriate conditions for the use of CBAG in the CL-ELISA was carried out for a single NGP (KM30), using a checker-board titration of enzyme *vs* serum concentration. Plates were coated with NGP as described previously at a concentration of 50 ng/well. After overnight incubation, wells were blocked with PBS-B. The required amount of CBAG (Sigma, 8507) was removed to a centrifuge tube and spun at 13000 x *g* for 10 mins, 4°C to discard the ammonium sulphate buffer. The pellet was then resuspended in 0.1 M potassium phosphate buffer (pH 6.5) and applied to the plate in a serial dilution from 0.1 U/well to 0.013 U/well. Some wells had no enzyme and only buffer added. The ELISA was carried out as previously described (Section 2.4.2), using *L. major* positive pooled sera. The serum was diluted in PBS and titrated down the plate from 1:100 to 1:800. In a separate experiment, NGP was titrated against enzyme concentration. Plates were coated with NGP in a serial dilution from 50 ng/well to 12.5 ng/well, and the enzyme

titrated from 0.1-0.025 U/well, with the primary antibody constant at 1:800 in all wells.

2.4.4 Glycan inhibition of purified anti-Gal antibodies

CL-ELISA was conducted as described with one modification. Sera samples were pre-incubated in PBS-T with 1% BSA (PBS-TB) buffer containing either 0.1 M or 0.5 M inhibitory sugars (detailed in legends for individual experiments), for one hour at 37°C, before addition to the plate. Reduction in binding was calculated relative to controls, where the serum was incubated with PBS-TB alone, under the same conditions. Results were expressed as percentage of antibody titre bound, relative to control (the control is set at 100%)

2.4.5 C-Reactive Protein (CRP) assay

To assess any correlation between CRP concentration and infection status, a subset of samples was randomly selected for testing with the Eurolyser CRP test kit (Eurolyser, ST0102; machine and reagents were donated by Dr E. Adams). The protocol was carried out according to the manufacturer's instructions. 5 µL serum were added to the supplied ERS cuvette, the cap replaced, and the cuvette inserted into the Eurolyser CUBE machine. The machine then initiates an automated protocol to detect the levels of CRP in the sample, giving values in µg/mL.

2.5 Statistical Analysis

All analysis was conducted using SPSS 24, and figures produced in GraphPad v5.

2.5.1 One-Way ANOVA

For CL-ELISA data, Log_{10} transformation corrected positive skew and the absence of outliers was assessed in boxplots. Normal distributions confirmed through plotting histograms and as assessed by Shapiro-Wilk's test ($p > 0.05$). For variables that did not violate the assumption of homogeneity of variance as assessed by Levene's test for equality of variances ($p > 0.05$), one-way ANOVA on the transformed values was followed with Tukey-Kramer post hoc tests to identify if any variables showed a

significant difference between groups. For the NGPs that did violate this assumption ($p < 0.05$), a Welch ANOVA followed by Games-Howell post hoc tests were used.

2.5.2 Kruskal Wallis H Test

For CL-ELISA data that could not be normalised through transformation, Kruskal Wallis H test was used to compare differences between group means. Normality was assessed through histograms and Shapiro Wilks normality score (normal if $p = > 0.05$). Outliers were detected through boxplots, and extreme values that could not be justified for inclusion were removed (Table 2.3). Post-hoc comparisons were used to determine where differences lay, either by planned contracts using Mann Whitney non-parametric tests or all pairwise comparisons. Mean ranks were used when the distributions of groups were dissimilar, otherwise group medians were used.

Table 2.3. Outliers from the KSA 2017 cohort that were removed from analysis.

Outlier	Analysis	Reason
H47 T0	Titres against KM30	Replicates all lower than background for this antigen only
A26 T0	All	All replicates lower than background signal
H71 T0	Titres against KM27	Replicates all lower than background for this antigen only

2.5.3 Repeated Measures ANOVA

Histograms and Shapiro Wilk test of normality showed moderate non-normal distribution for all NGPs, which was corrected to approximately normal on Log_{10} transformation. Mauchly's test of sphericity was used to confirm that the assumption of sphericity had not been violated ($p > 0.05$). Where the assumption was violated, the Greenhouse and Geisser (1959) correction was used. Planned contrasts were used for specific comparisons between groups, or all pairwise comparisons were conducted as needed. Bonferroni correction was used for multiple comparisons [277].

2.5.4 Correlation curves

Variables were checked for linearity and normality, based on scatterplots and non-significant Shapiro-Wilk scores ($p > 0.05$) and any variable that violated these assumptions were corrected through Log_{10} transformation. Data were plotted to confirm the absence of outliers.

2.5.5 Binary Logistic Regression

To ascertain diagnostic potential of the NGPs for the patient samples, binary logistic regression was performed, followed by ROC curve generation. Data were coded as either positive (1) or negative (0), to give a binary disease outcome. Linearity of the continuous variables with respect to the logit of the dependent variable was assessed via the Box-Tidwell (1962) procedure. A Bonferroni correction was applied to correct for multiple comparisons [277]. Based on this assessment, all continuous independent variables were found to be linearly related to the logit of the dependent variable. The absence of outliers was confirmed based on standardized residuals (values accepted with a range of ±2.5 SD); no values were excluded from the model.

2.5.6 Paired Sample T Test

Paired Sample T Test was used for comparison of titres between active and cured samples from the same patient. After calculating the mean difference, one sample (LCC1, difference between active and cured titre = 293 RLU) was excluded as being an extreme outlier in the BME set. The differences between active and cured samples were all normally distributed as determined through Shapiro-Wilks test of normality ($p > 0.05$). No extreme outliers were detected in mean difference scores for VL patients, although KM27 showed a significant deviation from normality, as denoted by Shapiro-Wilk score of normality ($p = 0.04$). Paired sample T-test is fairly robust to deviations from normality, and the violation of normality was driven by a single value (LV3, difference between active and cured titre = -1787 RLU). The Paired Sample T-Test was performed both with and without this value and gave the same result, so the decision was made to perform the test without transformation or outlier removal.

2.6 Cohort Descriptions

All patient samples were collected by collaborators. The Saudi Arabian samples were collected chiefly by Dr Waleed Al-Salem, Mr Yasser Al-Raey, and the Saudi Ministry of Health, in collaboration with other colleagues at LSTM. Molecular analysis of the samples was performed by Dr Waleed Al-Salem and Mr Yasser Al-Raey. The Bolivian samples were collected by the laboratory team of Dr Albert Picado from ISGlobal, Barcelona. Molecular analysis was performed by this team. The Spanish samples were donated to LSTM by Dr Javier Moreno Javier Moreno of the Instituto de Salud Carlos III. Molecular analysis was also performed by this team.

2.6.1 Characteristics of patient cohorts from Saudi Arabia

This cohort of archived samples from 2013 was collected from 5 CL endemic regions in Al-Ahsa, KSA, and has been described in detail elsewhere (Table 2.4) [275]. Three sample types were collected;

1) Active *L. major* infection (n = 17) (confirmed through dermatological examination and microscopy)
2) Cured infections (determined through re-epithelisation of the lesion)
3) Heterologous controls – individuals with non-CL dermatological conditions, such as eczema (confirmed negative by *ITS1*-PCR RFLP).

Leishmaniasis was treated as directed by KSA Ministry of Health guidelines. Serum and parasite isolates were collected from each patient. Gender, lesion number, nationality and age were recorded (blood type was not recorded).

A second collection in 2017 was conducted at two sites, one in Al-Ahsa, and one in Asir (Table 2.5). Individuals with suspected CL were referred to the clinic and diagnosed by dermatological examination. Lesion aspirates were taken for culture and microscopy confirmation of parasites, as were swabs for *ITS*1-PCR RFLP identification of *Leishmania* species. Serum samples were also collected at the same time. Where possible, patient samples were collected before any treatment had commenced. Where secondary infection was present (fungal or bacterial), antibiotics or antifungals were prescribed first, before assignation of either intralesional or intramuscular sodium stibogluconate (Pentostam®). Where patients

returned to the clinic for subsequent treatment, additional samples were collected. Blood type, gender, lesion number, nationality and age were recorded.

Table 2.4. Details of patient samples in the 2013 collection from KSA.

Characteristics	*L. major* (n = 17)	Cured (n = 31)	Heterologous (n = 29)
Gender	Male = 17	Male = 21 Missing = 10	Male = 15 Female = 2 Missing = 12
Age [†]	29 (18 - 60)	Missing = 31	33 (23 - 50) Missing = 16
Province	Al Ahsa = 13 Central = 2 Medinah = 2	Al Ahsa = 18	Al Ahsa = 17 Missing = 12
Lesion Number	1-5 = 11 6-11 = 5 12+ = 1	N/A	N/A
Lesion Appearance	Papular = 7 Nodular = 3 Ulcerated/Nodular = 7	N/A	N/A
Curative period	N/A	1 month = 14 4-6 months = 2 1-2 years = 2 Missing = 13	N/A
Nationality	Saudi = 3 Indian = 4 Egypt = 1 Pakistani = 4 Missing = 5	Saudi = 1 Indian = 11 Syrian = 1 Nepali = 5 Missing = 13	Saudi = 18 Bangladesh = 1 Missing = 10

[†] Median age with range in brackets.
N/A Criteria not applicable to sample type

Table 2.5. Details of patient samples in the 2017 collection from KSA.

Characteristics	*L. major* (n = 56) *	*L. tropica* (n = 15)
Gender	Male = 54 Female = 1 Missing = 1	Male = 7 Female = 8
Age †	33 (16 - 67)	20 (10-58)
Province	Al Ahsa = 54 Asir = 1 Missing = 1	Asir = 15
Lesion Number	1-5 = 42 6-11 = 10 12+ = 3 Missing = 1	1 = 13 2-5 = 2
Appearance of Lesion	Nodular = 13 Nodular/Ulcer = 8 Papular = 11 • Scar = 3 Ulcerative = 14 Missing = 4 Mixed = 3 ◊	Nodular = 2 Nodular/Ulcer = 5 Papular = 3 Scar = 4 Ulcerative =1
Nationality	Bangladesh = 5 Egypt = 13 Filipino = 3 India = 17 Nepal = 5 Pakistan = 4 Saudi = 4 Other = 5 □	Bangladesh = 1 Saudi = 14
Blood Type	A = 17 B = 14 AB = 4 O = 14 Missing = 7	A = 7 AB = 1 O = 7

* 1st visit (n = 56), 2nd visit (n = 33), 3rd visit (n= 15)

† Median age with range in brackets

• Papular + one other lesion type (n =4)

◊ Three or more lesion types

□ Yemen/Lebanon/Bedouin-Saudi (n= 1), Sudan (n = 2)

2.6.2 Characteristics of patient cohorts from Bolivia

Patient samples were collected by Dr Albert Picado (ISGlobal) and their detailed methods are described elsewhere (Table 2.6; Publication pending, 2019). Between September 2014 and November 2015, patients with suspected CL or ML/MCL infection in Cochabamba city were invited to participate in the study. Consent was obtained, demographic information collected, and clinical samples obtained (smears/lesion aspirates and blood samples). Diagnosis was confirmed via culture of lesion aspirates and microscopic examination of Giemsa-stained lesion smears. Patients were categorised based on lesion location i.e. cutaneous or mucosal (no molecular species ID was performed).

Table 2.6. Details of patient samples in the collection from Bolivia.

Disease Type	CL (n = 32)	ML/MCL (n = 16 (4) †)	Controls (n = 36)
Chagas Co-infection	Yes = 4 Missing = 1	Yes = 6	Yes = 13
Initial Infection •	Yes = 22	Yes = 0	N/A
Lesion number	1 = 19 2 = 5 3 = 4 4-5 = 4	1-4 = 4 Missing = 16	1 = 19 2 = 6 3-6 = 2 Missing = 9

† Patients with Mucosal and Cutaneous lesions in brackets.
• No lesions prior to this occurrence

2.6.3 Characteristics of patient cohorts from Spain

Archived samples from an outbreak of leishmaniasis in Fuenlabrada, Madrid (2010-2012) were kindly donated by Dr Javier Moreno (Table 2.7) [93]. Diagnosis was based initially on clinical symptoms, with immunofluorescent antibody titre (IFAT), cellular assays (IL-2 and cell proliferation), and/or PCR confirmation. Cure was determined when parasite DNA was undetectable by qPCR. Control samples were collected from blood bank donations by healthy individuals from the endemic region, who were serologically negative and had no prior history of leishmaniasis. Individuals with prior exposure to leishmaniasis gave positive cellular assay results (IL-2 and cell proliferation), but negative serology and qPCR results, and were termed asymptomatic samples. Patients were treated according to local protocols.

Individuals provided informed consent under the ethics applications (APR 12-65 and APR 14-64), approved by the Human Research Ethics Committee of the Hospital Universitario de Fuenlabrada, which covers the blood bank and hospital samples.

Table 2.7. Details of patient samples in the collection from Spain, *L. infantum* infection.

Type	Asymptomatic (n = 30)	Endemic Controls (n = 30)	Visceral •		Cutaneous ◊	
			Active (n = 20)	Cured (n = 37)	Active (n = 25)	Cured (n = 30)
Age †	40 (18 - 66)	35 (18 - 57) ¥	41 (34 -76) §	42 (19-93) ¥	49 (21-82)	57 (25 -85) ¤
Gender	Male = 25	Male = 15	Male = 11*	Male = 26	Male = 14	Male = 13*
Time since active sample (months) □	N/A	N/A		1-3 = 7 4-6 = 9 7-9 = 3		1-3 = 3 4-6 = 10 7-9 = 1 10-12 = 5

Paired samples collected for • 15 or ◊19 patients
† Median with range in brackets
Data missing for *1, ¤2, ¥3, or §4 patients
□ Data missing for 18 (VL) or 11 (CL) patients

Chapter Three
Identification and characterisation of immunogenic glycolipids from *Leishmania* spp.

3.1 Introduction

Antibodies against αGal epitopes have been implicated in protection from parasitic diseases, including malaria and Chagas [265,271]. The surface glycoconjugates of *T. cruzi* parasites have important roles in the production of anti-Gal, which is highly specific for the *O*-linked glycans decorating the mucins that coat much of cell surface [254]. Similarly, glycoconjugates of *Leishmania* species have demonstrable immunogenicity, and the highly abundant glycoinositolphospholipids (GIPLs) of *L. major* are strongly recognised by sera from individuals with leishmaniasis [219,279]. The likely epitope on these glycolipids are the αGal-terminating oligosaccharides that are only found on certain GIPL types; GIPL-2 and GIPL-3 of the Type-II GIPL family, which are expressed in all stages of *L. major* cells [230,235,239,280]. Unlike *L. major*, αGal residues have not been identified in GIPLs extracted from *L. tropica*; instead the only components so far characterised so far are the Type-I mannosylated GIPLs [230]. However antibodies in serum from patients with *L. tropica* infection recognise an αGal epitope at comparable levels to *L. major* serum in CL-ELISA analysis, indicating that there must be an as yet-unknown αGalactosylated glycoconjugate expressed by this species [217]. If the glycan structure of this epitope is significantly different from the αGal epitopes of *L. major* cells, this could be exploited in the development of biomarkers of infection for both species, based on the native glycolipid composition of each. The known antigenicity of *L. major* GIPLs suggests that revisiting the immunogenicity and structural features of the glycolipid components of *L. tropica* promastigotes are a sensible starting point for investigation.

To evaluate the potential of glycolipids extracted from *Leishmania* parasites as diagnostic antigens, I have first purified antigenic material from cultured promastigote cells and confirmed their recognition by lectin and human serum. Mass spectrometry allowed confirmation of the expected glycolipid profiles for *L. major* and *L. tropica*, although the structural composition of the *L. tropica* extract was not possible to determine. Using ELISA, *L. major* extracts proved to be antigenic

against human sera and are discussed in the context of the potential development of a novel CL diagnostic.

3.2 Results

3.2.1 Recognition of *Leishmania* glycolipids by IB4 lectin

In order to characterise GIPLs, total glycolipids from *L. tropica* and *L. major* promastigotes were purified using sequential extraction with organic solvents (according to methods detailed in [239]) and then fractionated on HPTLC (as described in Section 2.3). The chromatographed glycolipid samples showed a pattern consistent with that previously published [239]. The glycolipid families are separated by their relative polarities (depending on glycan composition) and hydrophobicity (fatty acid species) (Figure 3.1A). Thus, GIPLs containing the same glycan core tend to resolve on TLC plates as multiple bands due to the heterogeneity of their fatty acids and hydrophobicity of the solvent system used.

IB4 lectin has broad specificity for glycans with terminal αGalactopyranose, but does not bind to βGal-terminating glycans [281–283]. As expected, based on published structural work, IB4 did not recognised *L. major* GIPL-1 as its oligosaccharide core is capped by a βGalactofuranose residue [230,237]. *L. major* GIPL-2 and -3, containing terminating glycans with Galα1-3Gal*f*- and Galα1-6Gal*p*-, respectively, were well recognised by lectin on HPTLC plates (Figure 3.1B). On the other hand, no bands were recognised in the *L. tropica* samples, supporting previous structural work showing that no αGal-containing GIPLs are made by procyclic promastigotes in this species (Figure 3.1B).

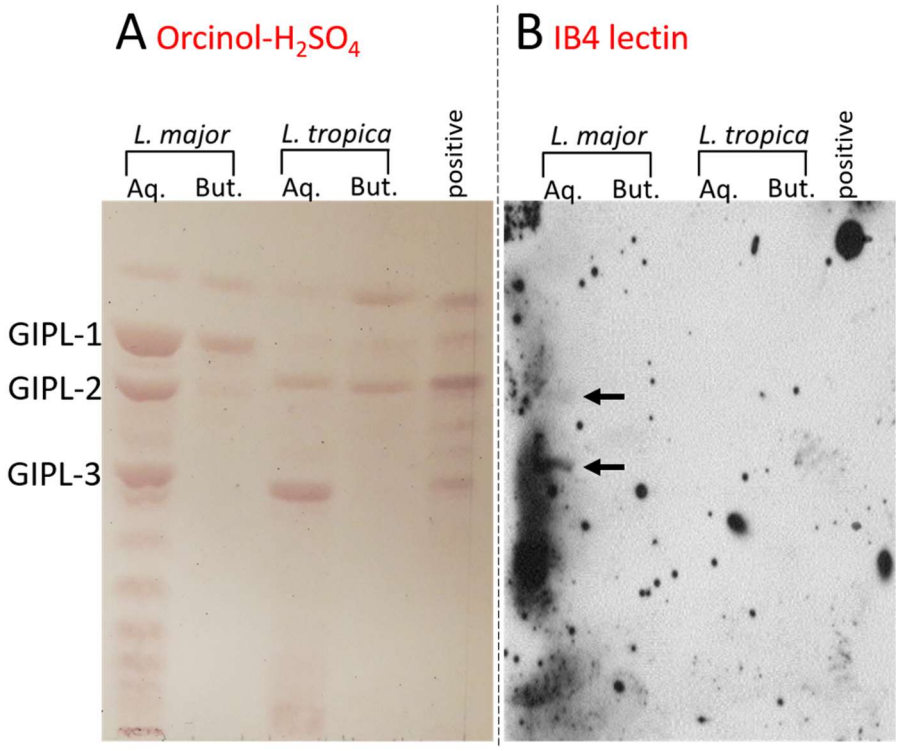

Figure 3.1. HPTLC analysis of *Leishmania* spp. glycolipids with IB4 lectin. *Leishmania* glycolipids were extracted with organic solvents as described in (Chapter 2, Section 2.3.1). Samples equivalent to ~2 x 10^8 (*L. major*) and ~4 x 10^8 (*L. tropica*) cells were fractioned on HPTLC plates using chloroform:methanol:0.2% KCl-H_2O (10:10:3, by volume), and butanol:pyridine:0.2% KCl-H_2O (9:6:4, by volume) organic solvent systems and either stained with orcinol-H_2SO_4 (A) or IB4-HRP (B). In (A) commercial porcine gangliosides (20 µg/lane) were used as positive control for orcinol staining. In (B) αGalactosylated Dextra-BSA (1 µg; upper right) and BSA alone (1 µg; not shown) were used as positive and negative controls, respectively.

In order to corroborate the identity of the GIPLs species, parasite glycolipid extracts were analysed by positive ion ESI-MS and ESI-MS/MS (Chapter 2, Section 2.3.8). *L. major* GIPL-1-3 were easily detected as multiple $[M+H^+]^+$ species, with GIPL-2 being the most abundant of all with a *m/z* of 1663 (Figure 3.2B). This mass is consistent with a glycan core composed of Hex_4-HexN-PI as indicated by the MS/MS fragmentation spectrum (Figure 3.2B) and in agreement with a previous work [284]. However, this paper reports a main GIPL-2 species of *m/z* 1607 indicating that our detected species contains fatty acids bigger by four carbon units (56 Da). Unfortunately, it was not possible to corroborate the PI lipid structure in negative ion mode, which would have indicated the types and possible positions of the two fatty acid chains. Nevertheless, the masses are consisting with the reported GIPL-2 structure Galα(1-3)Gal*f*β(1-3)Manα(1-6)Manα(1-4)GlcNα1-alkyl-acyl-phosphatydil

inositol, with a great fatty acid heterogeneity as depicted in Figure 3.2C. Furthermore, consistent with this structure, less abundant species like GIPL-1 and GIPL-3 seem to contain the same lipid composition (Figure 3.2B and C), but differ in the glycan core with respect to GIPL-2; i.e. whilst GIPL-1 (of *m/z* 1501) is shorter by one hexose (one galactose residue of mass 162), GIPL-3 (of *m/z* 1825) contains a glycan core with an extra galactose residue (Figure 3.2C and E). Unfortunately, I was unable to identify by mass spectrometry the GIPL species extracted from *L. tropica* promastigote cells.

Table 3.1. Predicted and experimental masses of *L. major* GIPLs, based on EIS-MS analysis (Figure 3.2B+C). Glycolipid extract from *L. major* promastigotes was analysed by positive ion ESI-MS. Experimental values reported in Figure 3.2. Predicted values and suggested glycan structures and fatty acid compositions calculated from [238]. Hex = Hexose. HexN = Hexosamine.

GIPL Species	Predicted $[M+H^+]^+$	Experimental Value $[M+H^+]^+$	Suggested Glycan Structure	Suggested Fatty Acid Composition (alkyl marked ')
Unknown	-	1319	Unknown	Unknown
	-	1343		Unknown
	-	1481		Unknown
1	1418	-	Hex_3-HexN	18:0' 12:0
	1446	-		18:0' 14:0
	1502	1501		24:0' 12:0
	-	1529		Unknown
2	1580	-	Hex_4-HexN	18:0' 12:0
	1608	1607		18:0' 14:0
	1636	1635		18:0' 16:0 or 22:0' 12:0
	-	1649		Unknown
	1664	1663		24:0' 12:0
	-	1677		Unknown
	1692	1691		24:0' 14:0 or 26:0' 12:0
	1720	1719		24:0' 16:0 or 26:0' 14:0
3	1798	1797	Hex_5-HexN	18:0' 16:0 or 22:0' 12:0
	1826	1825		24:0' 12:0
	1854	1853		24:0' 14:0 or 26:0' 12:0

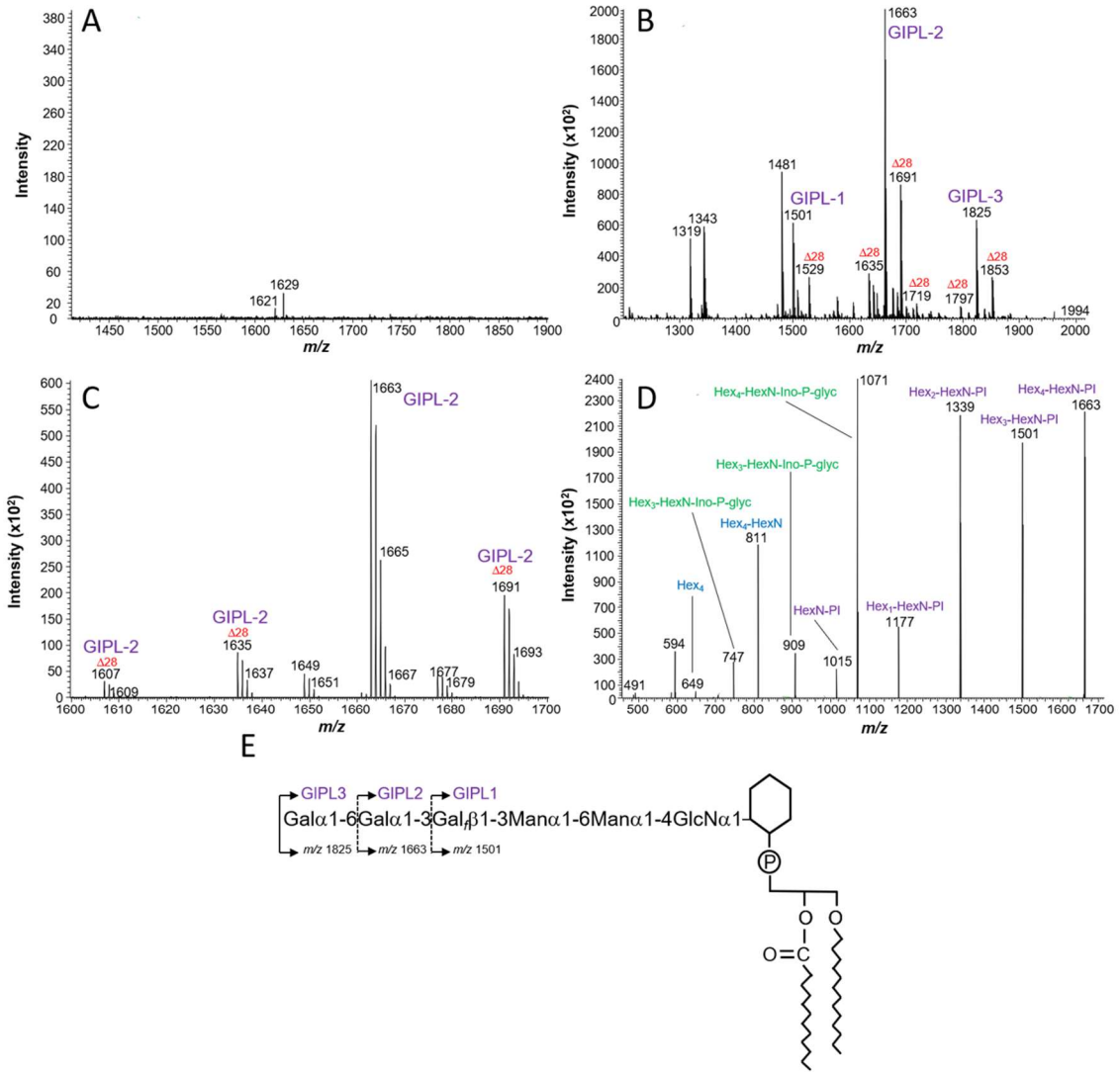

Figure 3.2. Positive ion EIS-MS and EIS-MS/MS analysis of glycolipid extracts from *L. major* promastigotes. *L. major* GIPLs were extracted with organic solvents and enriched after butanol/water partition (as described in Section 2.3.1). Whole butanol extracts were then processed for EIS-MS analysis in positive ion mode. GIPL species are summarised in Table 3.1. A. ESI-MS of a blank sample consisting only of organic solvents; no contaminating peaks were detected. B. EIS-MS of whole butanol extract. Δ28 indicates variation in fatty acid composition (the identity of *m/z* ions 1319, 1343 and 1481 was not determined, but they are likely to be related to GIPL-1). C. Analysis of GIPL-2 species showing a high variability in fatty acids composition. D. Positive mode EIS-MS/MS fragmentation spectrum of main GIPL-2 species at *m/z* 1663. The spectrum revealed at least three types of fragmentation patterns: a series of abundant ions (at *m/z* 1501, 1339, 1177, 1015; indicated in purple) showed that the main fragmentation pattern occurred from the non-reducing end, as indicated by losses of one Hex (162 Da); the second most abundant series of fragments (*m/z* 1071, 909, and 747; indicated in green) showed a group of ions lacking both fatty acids from the glycerol moiety and reduced glycan cores; and the least abundant series (*m/z* 811 and 649; indicated in blue) corresponds to fragments of the glycan core (no lipid attached); glycan fragments are summarised in Table 3.2. E. Proposed GIPL structures based on the analyses done in this thesis and previous published work [284].

Table 3.2. Composition of fragments identified by EIS-MS/MS analysis of GIPL-2 (*m/z* 1663) (Figure 3.2D). Fragmentation of m/z 1663 resulted in three fragmentation patterns, indicated by Series A, B or C. Series A (blue text in Figure 3.2D) are fragments of the glycan core, with no attached lipid. Series B (green text in Figure 3.2D) show ions lacking fatty acid chains, with reduced glycan core. Series C (purple text in Figure 3.2D) are ions with the fatty acid components intact, with loss of hexoses from the non-reducing end.

Peak	Series	Experimental Mass $[M+H^+]^+$	Suggested Composition
1	A	649	Hex_4
2	A	811	Hex_4-HexN
3	B	747	Hex_2-HexN-Ino-P-glyc
4	B	909	Hex_3-HexN-Ino-P-glyc
5	B	1071	Hex_4-HexN-Ino-P-glyc
6	C	1015	HexN-PI
7	C	1177	Hex-HexN-PI
8	C	1339	Hex_2-HexN-PI
9	C	1501	Hex_3-HexN-PI
10	C	1663	Hex_4-HexN-PI

3.2.2 *Leishmania* spp. glycolipids recognition by human serum

Having identified putative glycolipid species containing terminal αGal (Figure 3.1), I then tested the antigenicity of the same *Leishmania* glycolipids on HPTLC-immunostaining. It was found that only a pool of sera from *L. major* patients reacted against all *L. major* GIPL species (Figures 3.3 and 3.4). GIPL-2 and GIPL-3 are Gal*p*α-terminating, but GIPL-1 is Gal*f*β. The presence of all three bands confirms the immunogenic nature of both galactosyl configurations. This pattern is different to the one obtained with IB4, with only the two bands with αGal-terminal glycan recognised by the lectin (GIPL-2 and -3). Interestingly, *L. major* sera also recognises a single band in *L. tropica* glycolipid extract, which IB4 did not. This is therefore unlikely to be αGal-binding and is probably instead cross-reactivity against a shared structure. The identity of this glycolipid species remains to be determined.

Both *L. tropica* sera and healthy sera pools showed no recognition of any glycolipid component from either parasite species (Figure 3.4). While this was expected for healthy sera (having no immune-priming against *Leishmania* antigens), it was surprising that serum from *L. tropica* did not recognise any of the *L. major* GIPLs, not even the αGalactosylated (GIPL-2 and -3). Neither increasing the sample amount nor changing conditions of the antibody incubations revealed any bands.

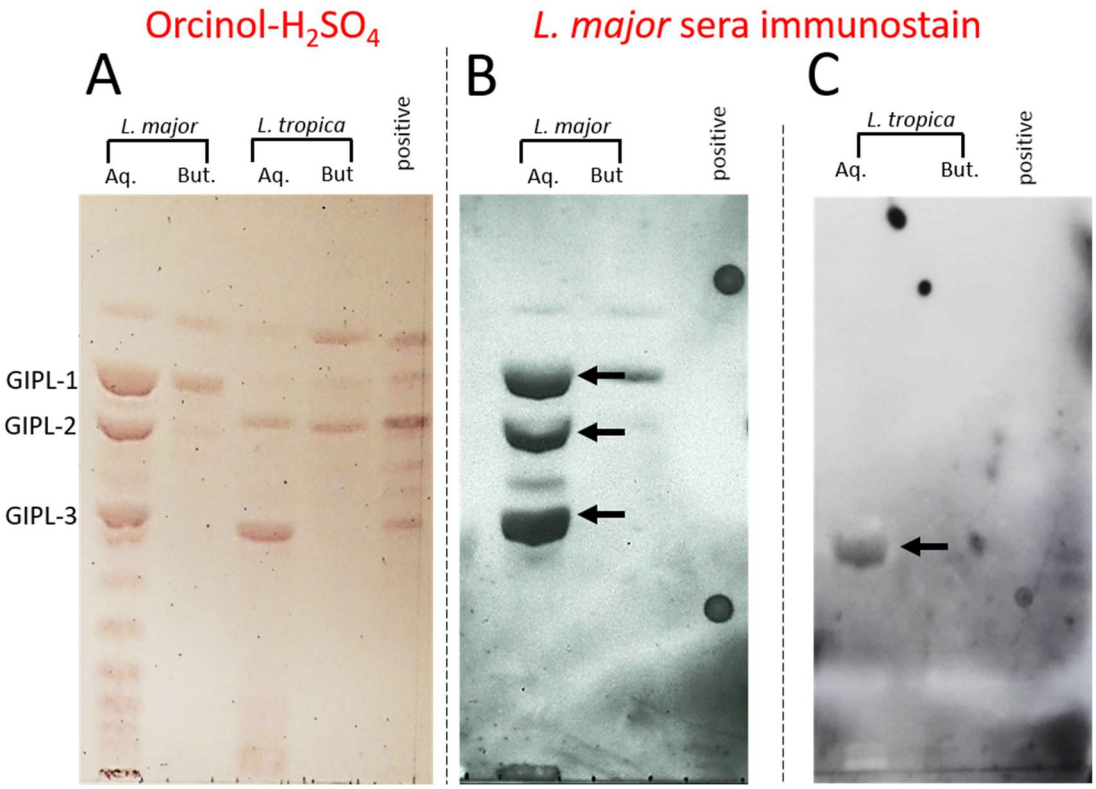

Figure 3.3. HPTLC immunostaining of *Leishmania* spp. glycolipid extract with pooled sera from *L. major*-infected individuals. Lipid extracts from either *L. major* (~2 x 10^8 cells) or *L. tropica* (~4 x 10^8 cells) were fractionated on HPTLC using chloroform:methanol:0.2% KCl-H_2O (10:10:3, by volume), and butanol:pyridine:0.2% KCl-H_2O (9:6:4, by volume) solvent systems and then either stained with orcinol-H_2SO_4 (A) or processed for immunostaining with a pool of sera from *L. major* (B and C). Arrows indicate glycolipids recognised by sera. In (A) commercial porcine gangliosides (20 µg/lane) were used as positive control for orcinol staining. In (B) and (C), α-galactosylated Dextra-BSA (1 µg; dots in upper and lower right) and BSA alone (1 µg; not shown) were used as positive and negative controls, respectively.

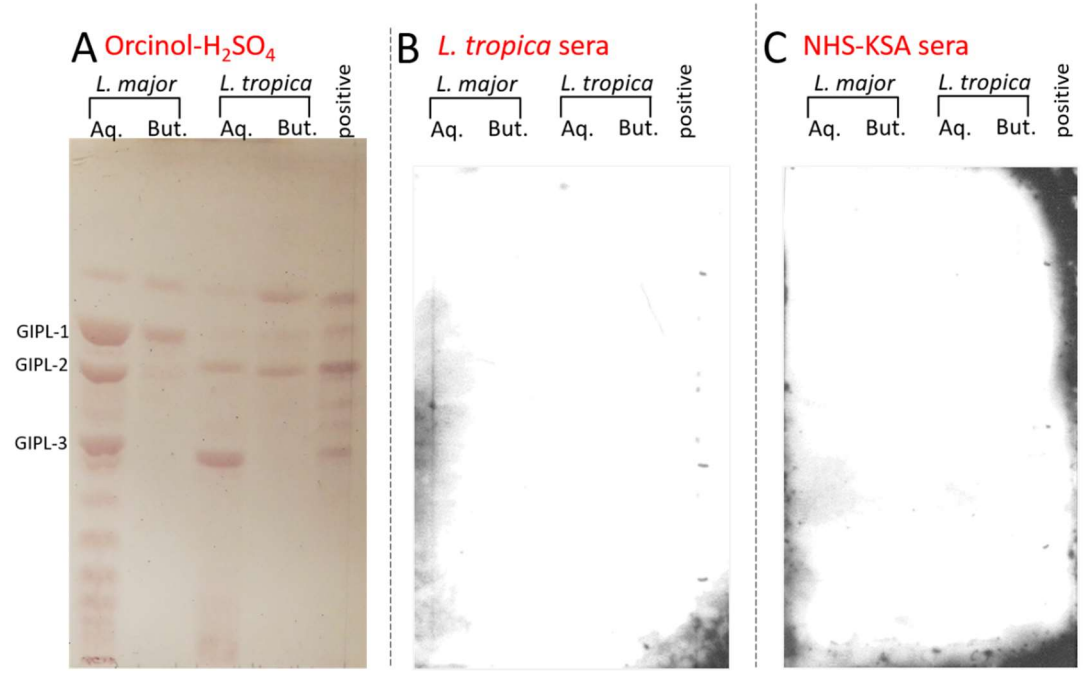

Figure 3.4. HPTLC immunostaining of *Leishmania* spp. glycolipid extract with pooled sera from *L. tropica*-infected individuals or healthy controls. Lipid extracts from either *L. major* (~2 x 10^8 cells) or *L. tropica* (~4 x 10^8 cells) were fractionated on HPTLC using chloroform:methanol:0.2% KCl-H_2O (10:10:3, by volume), and butanol:pyridine:0.2% KCl-H_2O (9:6:4, by volume) solvent systems and then either stained with orcinol-H_2SO_4 (A) or processed for immunostaining with a pool of sera from *L. tropica* (B) or sera from healthy individuals from KSA (C).In (A) commercial porcine gangliosides (20 µg/lane) were used as positive control for orcinol staining. In (B) and (C), α-galactosylated Dextra-BSA (1 µg; dots in upper and lower right) and BSA alone (1 µg; not shown) were used as positive and negative controls, respectively**.**

3.2.4 CL-ELISA optimisation with *L. major* GIPL extract

The results of the TLC immunostaining strongly indicated that the main *L. major* GIPLs were exclusively recognised by sera from *L. major* patients but not from those infected with *L. tropica* parasites (Figure 3.3). Therefore, I reasoned that an ELISA assay using fractions enriched with *L. major* GIPLs as antigens will be more informative in terms of specificity and could lead the way to develop this as a specific *L. major* diagnostic assay.

The first step was to develop glycolipid CL-ELISA protocol, using *L. major* glycolipid extract. Optimisation of block steps, antigen immobilisation, wash steps, and buffers was conducted, and conditions selected were used for all subsequent assays (Section 2.3.9). Cross-titration of *L. major* glycolipid extract against pooled sera

allowed the selection of conditions that showed the differential levels of recognition between *L. major* infected sera and healthy KSA control sera (Figure 3.5). All further assays were conducted with sera at 1:400 dilution, as this gave a clear distinction between control and patient sera.

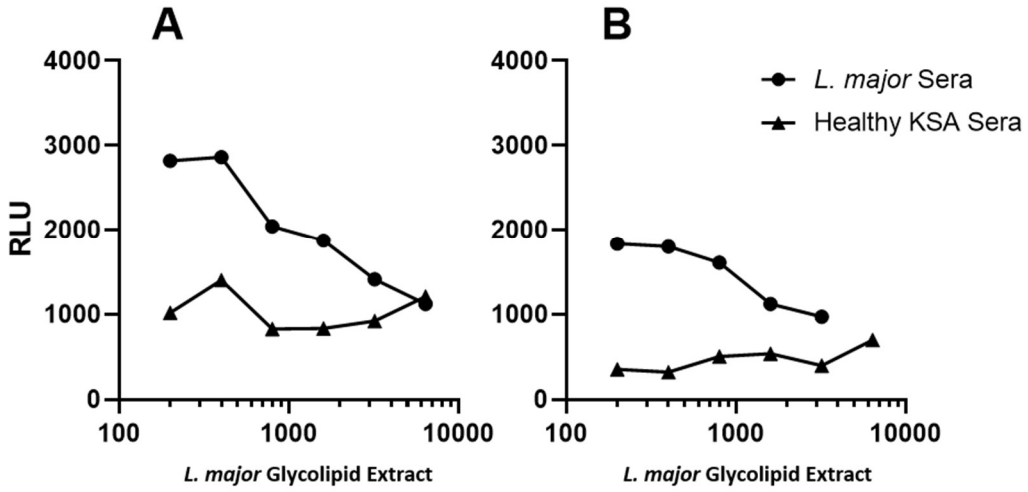

Figure 3.5. Recognition of *L. major* glycolipids by pooled serum samples from individuals with active *L. major* infection, or from healthy controls from the endemic region. *L. major* glycolipid extract was serially diluted in PBS 1:1 (starting from 5 x 10^6 CE/well). Serum pools are at 1:200 (A) or 1:400 (B) and detected with anti-IgG-HRP antibody at 1:5000. RLU = relative luminescence units**.**

3.2.5 *L. major* glycolipids are only recognised by sera from *L. major*-infected individuals

Further optimisation with extract concentration showed a sigmoidal curve of *L. major* antibody binding with changing glycolipid concentration (Figure 3.6A). Healthy sera and *L. tropica* sera show slight decreases in binding with reduced concentration of *L. major* glycolipids, but there is no clear distinction between these two pools. From the 1:1600 dilution point (approximately 6.25 x 10^5 CE/well) the three pools, *L. major*, *L. tropica* and healthy KSA are indistinguishable from each other.

Binding to *L. tropica* extract was reduced for all sera types, as compared to *L. major* extract, despite the coating concentration being approximately equivalent for both extracts (Figure 3.6B). It should be noted that the quantification method used to ascertain glycolipid amount, i.e. counting cells using a haemocytometer, is

inherently inaccurate and a second quantification method using mass spectrometry analysis is currently underway. These results are pending, but will inform my interpretation of the titration results if they indicate a significant variation from the counts. However, these ELISAs indicate that there is no noteworthy recognition of *L. tropica* glycolipids. The lack of binding by *L. major* sera, which is enriched for anti-Gal of various specificities (Chapter 4), indicates that if there are αGal epitopes in the glycolipids extracted from *L. tropica* cells, they are at very low levels so as to be indistinguishable from background signal.

Sera from healthy individuals from KSA, and those with *L. tropica* infection show very little recognition of either glycolipid extract. This result demonstrates the specificity of antibodies produced during *L. major* infection. However, this glycolipid extract contains a variety of glycan epitopes, and the role of anti-Gal in this assay is unclear, so confirmation of specificity with coffee bean αGalactosidase (CBAG) treatment is necessary.

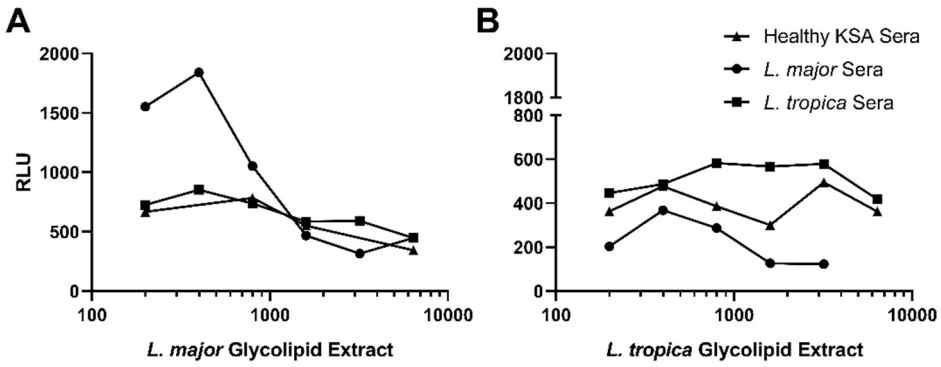

Figure 3.6. Recognition of *L. major* or *L. tropica* glycolipids by pooled serum samples from individuals with active *L. major* or *L. tropica* infection, or from healthy controls from the endemic region. Glycolipid extract from *L. major* (A) or *L. tropica* (B) promastigotes was serially diluted 1:1 (starting from 5 x 10^6 CE/well). Pooled serum was diluted 1:400 and detected with anti-IgG-HRP antibody at 1:5000. RLU = relative luminescence units**.**

3.2.7 Determining specificity of anti-Gal binding using CBAG enzyme

To determine the degree of recognition of αGal epitopes by anti-Gal in the different pools of sera, plates were coated with purified glycolipids and treated with CBAG to cleave terminal αGalactosyl residues of any glycosidic linkages (Figure 3.7) [285,286].

Addition of the enzyme should reduce or abolish binding of anti-Gal through removal of these residues. In this assay, there was a clear increase in signal when enzyme was added to the wells. However, this was true of all wells, including controls where glycolipid coating was absent. When RLU was normalised to healthy KSA sera (e.g. $\frac{L.\ major\ RLU}{KSA\ pool\ RLU}$) the reduction in binding could be calculated.

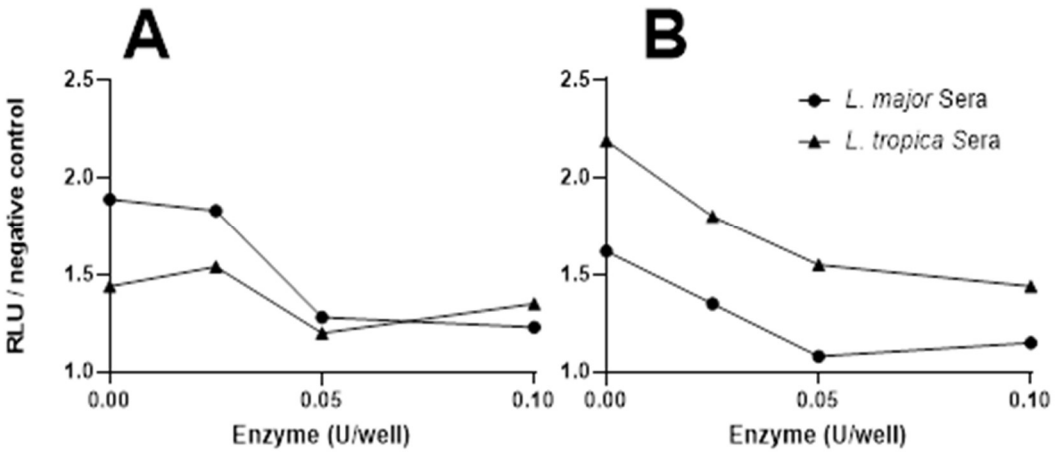

Figure 3.7. Reduction in recognition of CBAG-treated *Leishmania* spp. glycolipid extract by pooled sera from patients with active *L. major* or *L. tropica* infection. Plates were coated with glycolipid extract (5 x 10^6 CE/well) from *L. major* promastigotes (A) and *L. tropica* promastigotes (B) before incubation with CBAG (enzyme concentration between 0.025 0.1 U/well). Negative controls with no enzyme added were treated with buffer only. Relative luminescence units (RLU) is plotted normalised to recognition of the extracts by pooled sera from healthy KSA controls**.**

Treatment of *L. major* glycolipids with CBAG reduces recognition by *L. major* sera, but only marginally by *L. tropica* sera. This extent of reduction increases with higher enzyme concentration (Figure 3.7A, Table 3.2). There is still a degree of recognition by antibodies at the highest enzyme concentration for both sera types, which is likely a combination of 1) incomplete digestion leaving some glycans intact and 2) recognition of non-αGal binding sites by sera.

When comparing these results with the TLC plates (Figure 3.3), the residual binding can be explained, at least in part, through the approximately equivalent recognition of GIPL-1 (Gal*f*β-R) and GIPL-2/-3 (Galα-R); removal of the αGal sites leaves a significant amount of immunogenic Gal*f*β-terminating glycolipids that are capable of

binding serum antibodies. Additionally, cleavage of the final αGal exposes the next glycan in the structure; for GIPL-2, this is a Gal*f*β, which as discussed is also immunogenic in *L. major* sera. Therefore, when removing binding sites, CBAG reveals others.

Treatment of *L. tropica* glycolipid also showed a reduction in recognition, to a similar degree for both sera types. This would indicate that the enzyme is removing binding sites for antibodies, an unexpected result based on the TLC immuno- and lectin-overlays, where recognition was not detected. The overall level of binding to *L. tropica* glycolipids in the CL-ELISA was considerably lower than when *L. major* glycolipids were the coating antigen, therefore, this is in actuality a very small reduction in real terms. If αGal epitopes are present in *L. tropica* glycolipids, the TLC immuno-overlay with HRP conjugated lectin/antibody may not be sensitive enough to detect them, if they are at very low levels. Alternatively, the CL-ELISA conditions may be optimised to the extent that I am detecting low affinity binding, that is not "real" anti-Gal.

Table 3.3. CBAG treatment of *Leishmania* spp. glycolipids reduces recognition by serum pools. Results are expressed as percentages, relative to the untreated control wells (Control set at 100%).

Glycolipid Extract	Sera pool	Enzyme (U /well)		
		0.025	0.05	0.1
L. major	*L. major*	97%	68%	65%
	L. tropica	107%	83%	94%
L. tropica	*L. major*	83%	67%	71%
	L. tropica	82%	71%	66%

To validate this result, various *L. major* sera pools were tested against *L. major* glycolipid extract treated with CBAG at 0.1 U/well (Figure 3.8).

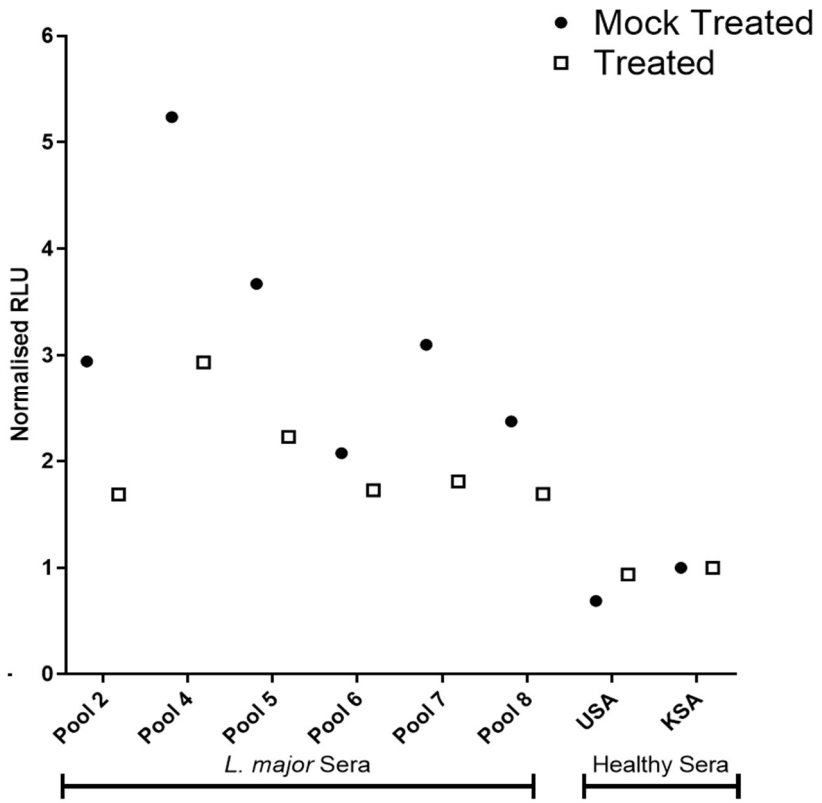

Figure 3.8. CBAG enzyme treatment reduced recognition of *L. major* glycolipids, by pooled sera from *L. major*-infected patients. Plates were coated with glycolipid extract (5 x 10^6 CE/well) before incubation with CBAG (enzyme concentration 0.1 U/well). Negative controls with no enzyme added were treated with buffer only (Mock Treated). Sera was diluted 1:400. Relative luminescence units (RLU) is plotted normalised to recognition of the extracts by pooled sera from healthy KSA controls**.**

As noted in the previous assay, addition of enzyme caused an increase in signal, relative to the mock-treated i.e. buffer-only controls. Normalised results indicate a clear reduction in binding however, although the extent of the reduction varies between pools (Figure 3.8). No reduction in recognition was detected in healthy pools, further emphasising the absence of *Leishmania*-binding anti-Gal in healthy sera.

In summary, these experiments show evidence of the potential utility in exploiting the anti-Gal recognition of *L. major* glycolipids as biomarkers of infection.

Furthermore, anti-Gal from sera of *L. major*-infected patients does not appear to recognise *L. tropica* glycolipids at any noteworthy level.

3.3 Discussion

The main aim of this Chapter was to identify *Leishmania* glycoconjugates containing terminal αGal residues. Until now, the only αGalactosylated glycoconjugates from any *Leishmania* species have been the Type-II GIPL-2 and GIPL-3, both of which are recognised by anti-Gal from *L. major*-infected individuals. However, despite reported anti-Gal in serum from patients with *L. tropica* that recognised a trisaccharide Galα(1,3)Galβ(1,4)GlcNAcβ-R, no epitope has been incriminated in *L. tropica* cells [217]. Therefore, I have attempted to identify galactosylated glycolipids in *L. tropica*, using TLC and ELISA.

TLC separation of glycolipid extract from *L. major* sera allowed the confirmation of the reported immunogenicity of GIPL-2 and GIPL-3 against serum from patients with *L. major* infection. No binding of healthy serum pools was detected against any glycolipid, either in TLC or ELISA formats. Anti-Gal produced during Chagas disease is highly specific for *T. cruzi* glycans, whereas natural anti-Gal from healthy adults has much lower reactivity [254,274]. This trend is confirmed in *L. major* infection, with antibodies recognising *L. major* glycolipids not circulating in healthy sera. This is essential for the development of a biomarker that is based on native *L. major* glycolipids; the antigen must be specific to *Leishmania* infection and not also a feature of other pathogens that could generate an immune response and cause false positives.

CL-ELISAs using whole glycolipid extract contains multiple glycolipid species, and likely contamination by membrane phospholipid species and other hydrophobic lipid molecules that are not completely removed by the organic solvent extraction steps. Therefore, recognition of this extract is not mediated solely by anti-Gal, but likely by a combination of several antibody populations. Treatment with CBAG has been shown to effectively remove immunogenic epitopes from porcine tissues, and

in seroconversion from blood type O to type B through terminal α-gal cleavage [285,287,288]. Treatment of *L. major* glycolipids with this same enzyme reduced recognition by *L. major* sera but did not completely abolish it. Anti-Gal in sera from *L. major* infected patients was a significant proportion of the binding detected in these assays.

L. tropica glycolipids showed surprisingly little reactivity against *L. tropica* sera, despite loading TLC plates with twice the amount required for detection of *L. major* glycolipids with *L. major* serum. Interestingly, *L. major* sera did bind a single glycolipid species in from *L. tropica* glycolipid extract. I was unable to identify this band through mass spectrometry, but the lesser reactivity against this band as compared to the *L. major* GIPL-2 and GIPL-3, and the absence of recognition by IB4 lectin, suggest it is unlikely to be a Galα-terminating structure. However, this is not definite; the epitope could be present but at much lower levels than in *L. major* cells, and as I have only tested material from promastigotes, I cannot rule out expression of αGal in *L. tropica* amastigotes. In CL-ELISA assays, *L. tropica* serum recognition of the *L. tropica* lipid extract was minimal, and indistinguishable from binding by healthy serum. Treatment of *L. tropica* glycolipid extract with CBAG enzyme reduced binding of *L. tropica* sera marginally (~30%), which would be an indication that the enzyme is removing an αGal and therefore reducing antibody recognition. However, as the starting levels of reactivity were low it's unclear if this is an artefact of the assay, or truly an indication of an αGal epitope. One option for further investigation to quantify the specific recognition of anti-Gal would be a CBAG inhibition assay. Sera would first be incubated with either enzyme-treated or mock-treated glycolipid extracts immobilised on a support/membrane, so that any anti-Gal antibodies would bind to available αGal sites. Levels of unbound antibody would be higher in samples exposed to enzyme treated glycolipids, due to fewer available binding sites. The unbound antibody for all samples could then be incubated with a synthetic αGal-containing molecule (i.e. αGal conjugated to BSA) in an CL-ELISA format, and the differences in binding detected. Greater inhibition indicates a higher number of αGal-terminating glycoconjugates in the glycolipid extract.

All of these experiments presented in this chapter have utilised glycolipid extract from cultured promastigotes, due to the logistical challenges of generating the large cell numbers (>10^{10}) required to obtain sufficient material. *L. major* GIPLs do not change in their galactosylation profile throughout the life cycle, but other glycoconjugates of all species do change in abundance, reflecting the different environments of each life stage. The *L. tropica* GIPL profile has not been quantified throughout the life cycle, and so it is possible that the galactosylation does change between the insect and human stages. Therefore, a true understanding of *L. tropica* glycoconjugates requires further investigation using the full repertoire of developmental stages.

To conclude, the reduction in antibody binding of *L. tropica* sera to *L. tropica* glycolipid extract after CBAG treatment hints at the presence of an αGal epitope present at very low levels. However, it looks unlikely that any αGal epitope in such diminutive amounts could generate the anti-Gal response reported by Al Salem *et al*. (2014). The lack of similar reactivity in this study indicates that there is no similar glycotope in the glycolipid portion of *L. tropica* cells. Therefore, it is most probable that an alternative glycoconjugate is responsible for any anti-Gal recognition. To this end, preliminary results have detected low molecular weight glycoproteins recognised by IB4 (Liu, YC, and Acosta-Serrano, A, unpublished). In Chapter 5, I have explored the localisation of αGal through lectin staining of *L. tropica* promastigotes and amastigotes.

However, native *Leishmania* glycolipid extracts are not a viable candidate for a diagnostic marker. The TLC results here indicate that antibodies against αGal-containing glycolipids are not the only anti-*Leishmania* antibodies circulating in *L. major* infected patients, which, in an ELISA, bind to the non-αGalactosylated lipids. Synthetic *Leishmania*-mimetic glycans are likely a better option to investigate the specific glycans mediating the immunogenicity of *L. major* parasites.

Chapter Four
Specificity of Leishmania anti-Gal in Old and New World leishmaniasis

4.1 Introduction

Anti-Gal profiles during parasitic infection have been described for a number of diseases including malaria, cutaneous leishmaniasis, and Chagas [217,265,289,290]. Antibodies recognising terminal αGal epitopes, in particular the canonical Galili glycan sequence (Galα(1,3)Galβ(1,4)GlcNAcα-R), are thought to have a role in protection against an array of fungal, microbial and parasitic invaders [291]. The increased titres of anti-Gal detected during *Leishmania* infection has potential for exploitation as a biomarker of infection, due to the differences in galactosylation of surface molecules between *Leishmania* species [217,275,290]. The challenge has always been the identification of the correct αGalactosylated antigen(s), to discriminate the different populations of anti-Gal antibodies triggered during an infection with different *Leishmania* species. Historically, rabbit gangliosides which contain terminal αGalactosyl residues were used to assay levels of anti-Gal antibodies in human serum [262]. However, they are limited, as most of the oligosaccharidic structures end with a Galα(1,3)-R sequence hence preventing the detection of epitopes with other αGal linkages (i.e. 1,2/4/6) [292]. More recently, neoglycoproteins (NGPs) consisting of BSA molecules chemically modified with glycans have become commercially available. For example, in this thesis I was used one such NGP, from Dextra Laboratories Ltd., that contains glycans made only of the canonical Galili's epitope (i.e. Galα(1-3)Galβ(1-4)GlcNAc-R).

Native αGalactosylated glycolipids extracted from *L. major* and *L. tropica* promastigotes showed varying levels of success in discriminating between infected sera and controls (Chapter Three). However, there are challenges that preclude the use of extracted glycolipids as a diagnostic tool, including cost, reproducibility between batches of parasite extractions, and the facilities required for large-scale cell culture. A panel of synthetic NGP antigens that mimics recognition by the anti-Gal response during a *Leishmania* infection has potential application in diagnostic test development. Some of these NGPs, synthesised in the lab of Dr Katja Michael at the University of Texas, El Paso (UTEP), were effectively used to analyse the specificity of Chagasic anti-Gal (Table 4.1) [260,274]. The panel encompasses an array of

αGal terminating mono-, di- and trisaccharides chemically conjugated to BSA, with various configurations of the bonds between residues. While the αGal terminal residue is the immunogenic portion, the presentation of the epitope will depend on the whole glycan, and the shape and configuration will determine binding affinity and other biophysical properties of the ligand-antibody complex. The rationale behind the glycan structures in Panel 1 was twofold; some glycans correspond to epitopes described in the literature as of likely importance in mediating *Trypanosoma cruzi*-antibody binding, such as the Galα(1,3)Galβ disaccharide, whereas others have similar structures to those described but with slight alterations to capture a diversity of antibodies. Panel 3 was synthesised to specifically mimic the epitopes identified on *L. major* GIPL-2 and GIPL-3.

Table 4.1. Non-commercial NGPs used to assess levels of anti-Gal in human serum samples. ID refers to the code used to refer to each structure throughout this thesis. The glycan portion varies for each structure. R corresponds to the linker-BSA. All NGPs have at least one terminal αGal residue, except two controls KM15 (cysteine) and BME (β-mercaptoethanol). The NGPs were synthesised in batches; KM1-17 in Panel 1, KM3 and KM24 in Panel 2, and KM27-BME in Panel 3**.**

Panel	ID	Structure of Terminal Glycan
1	KM1	Galα(1,3)Galβ(1,4)Glcβ-R
	KM3	Galα-R
	KM5	Galα(1,6)Galβ-R
	KM8	Galα(1,2)Galβ-R
	KM9	Galα(1,3)Galβ-R
	KM11	Galα(1,6)[Galα(1,2)]Galβ-R
	KM12	Galα(1,4)Galβ-R
	KM17	Galα(1,3)Galα-R
	KM15	Cysteine-R
2*	KM24	Galα(1,3)Galβ(1,4)GlcNAcα-R
3	KM27	Galα(1,3)Gal*f*β-R
	KM28	Galα(1,6)Galα(1,3)Gal*f*β-R
	KM30	Galα(1,3)Gal*f*β(1,3)Manα-R
	BME	2-ME-R
* Panel 2 also included KM3		

In this Chapter, I have used this bespoke panel of synthetic NGPs to study anti-Gal profiles during both Old and New World *Leishmania*-infected sera. I demonstrate a comprehensive screening of samples from patients from three geographically

distinct regions. These αGal NGPs have most potential in identification of *L. major* sera, although further development may allow application in diagnosis of American tegumentary leishmaniasis caused by *L. braziliensis*. As treatment response varies between parasite species, the ability to determine the infecting species will inform the correct chemotherapy assignation [100,130]. For instance, *L. tropica* is comparatively resistant to SSG injection in Saudi Arabia whereas *L. major* is typically responsive [84]. Treatment of *L. braziliensis* is typically intramuscular pentavalent antimonials which has varying success, but is ineffective against *L. guyanensis* [293]. Both of these species are co-endemic in Bolivia.

4.2 Results

4.2.1 Anti-Gal analysis in patients with Old World cutaneous leishmaniasis in Saudi Arabia

For the analysis of anti-Gal antibodies from Old World CL patients, two cohorts of sera were collected from the Kingdom of Saudi Arabia, in 2013 and 2017 (Section 2.6.1). The two species of *Leishmania* circulating in KSA are *L. major* (zoonotic) and *L. tropica* (anthroponotic). In 2013, only serum samples from individuals infected with *L. major* were collected, whereas in the 2017 collection, alongside *L. major*-positive samples, 15 patients with *L. tropica* infection were obtained and confirmed through molecular identification.

4.2.1.1 Serum levels of anti-Gal antibodies are higher in active *L. major* infected samples, compared to cured and non-CL samples from the 2013 collection

The anti-Gal activity against nine NGPs (eight αGal-R-BSA and one control-BSA; Table 4.1 - Panel 1) was measured in a panel of serum samples from the 2013 collection. This cohort had three patient types: 1) active *L. major* infection, 2) cured infection (showing different degrees of lesion healing), and 3) heterologous non-CL controls (patients with an alternative skin pathology, but negative for CL).

Of the eight NGPs containing a terminal αGal residue, four (KM3, KM9, KM11 and KM17) showed significant difference between patient groups, as determined by either ANOVA or Welch ANOVA as appropriate (Supplementary Table 2). Post-hoc

comparisons, however, only showed significant between-group differences for three NGPs; KM3, KM17 and KM11 (Figure 4.1; Table 4.2). Although KM15 (negative control, cysteine-BSA) was not identified by ANOVA as showing different levels in infected vs. control patients, the overall levels of recognition to this control are a concern, as they are indistinguishable from the αGalactosylated NGPs (Figure 4.1). As a control, KM15 fails to show that recognition of these NGPs is αGal-specific, rather than, for example, cross-reactivity against the BSA component, or another artefact of the assay. Only one NGP, KM17 (Galα(1,3)Galα-R), had significant increased titres in both cured and active infection, when compared to the heterologous controls. In comparison to KM9 (Galα(1,3)Galβ-R, significantly different within groups by ANOVA $p < 0.05$), the switch of Galβ to Galα in the second position increases its discrimination potential. The two NGPs with Galα(1,2)Galβ or Galα(1,4)Galβ linkages had the lowest recognition by sera.

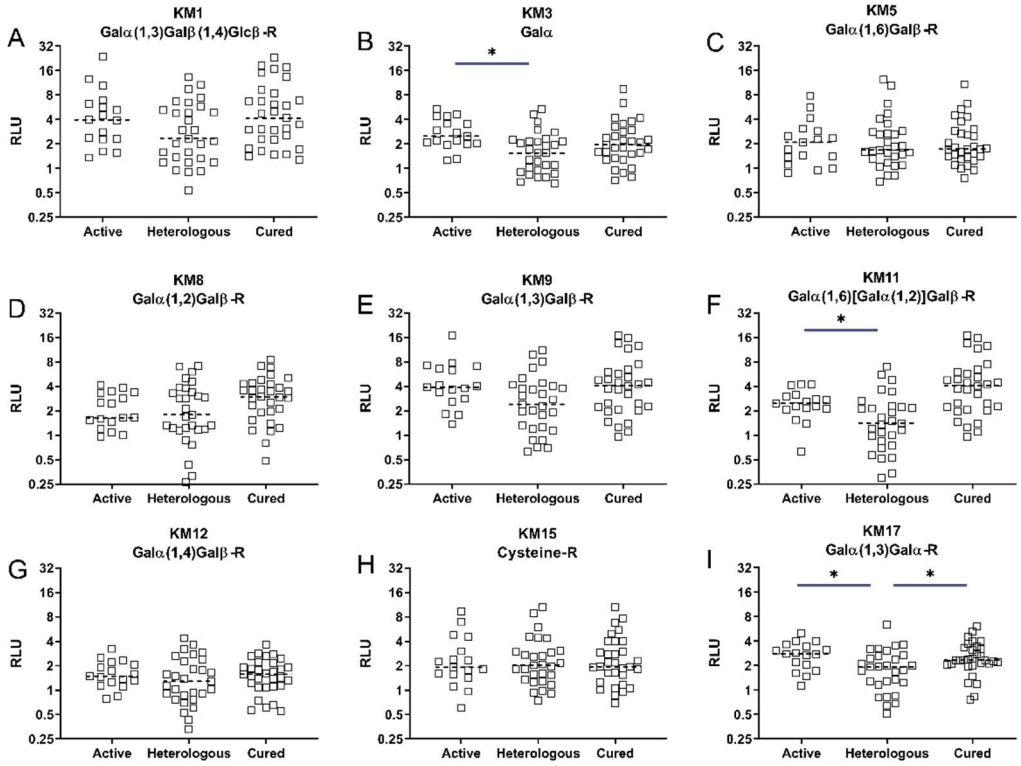

Figure 4.1. Anti-Gal titres in patient samples with active or cured *L. major* infection, or controls from the endemic region, against αGalactosylated NGPs. Individual sera were diluted 1:100 and recognition of 9 NGPs assessed through CL-ELISA. Relative luminescence units (RLU) are plotted as Log_2 transformed, normalised to the negative control (UK NHS). *L. major* active (n=17), cured (n=31) and Heterologous (n=29). * $p < 0.05$. Each panel shows data for one NGP. A = KM1, B = KM3, C = KM5, D = KM8, E = KM9, F = KM11, G = KM12, H = KM15, I = KM17.

Table 4.2. Differences in anti-Gal titres against three αGal NGPs (KM3, KM11, KM17) in samples from healthy controls, active infection (*L. major* from the 2013 KSA cohort) and cured individuals. Comparison of recognition of NGPs by active *L. major* patients (Active), cured CL patients (Cured) and control patients with non-CL lesions (Heterologous) against different NGPs, assessed through CL ELISA. Only significant comparisons are shown, all other post hoc tests had $p > 0.05$. Bonferroni corrected significance is reported for each difference. *= $p < 0.05$, ** = $p \leq 0.01$.

NGP	Group 1	Group 2	Mean Difference	Std. Error	*p* value	95% CI	
						Lower	Upper
KM3	Active	Heterologous	0.232	0.074	**	0.055	0.409
KM11	Active	Heterologous	0.220	0.081	*	0.024	0.416
KM17	Active	Heterologous	0.181	0.068	*	0.019	0.344
	Cured	Heterologous	0.145	0.058	*	0.007	0.282

4.2.1.2 Diagnostic potential of nine NGPs using 2013 *L. major* cohort

To ascertain the diagnostic potential of the eight αGal NGPs (Section 4.2.1.1), a binomial logistic regression was performed. The logistic regression model was statistically significant ($\chi^2(9) = 29.302$, $p < .001$), explaining 64.4% (Nagelkerke R^2) of the variance in infection status, and correctly classified 82.6% of cases. The ROC curve gave an area under the curve (AUC) of 0.909 (95% CI 0.825 to 0.992) (Figure 4.2). The sensitivity was 70.6%, specificity was 89.7%; in addition, the positive predictive value (PPV) was 80% and negative predictive value (NPV) was 83.9%. Of the ten predictor variables only one was statistically significant: KM3 (Supplementary Table 2). An increase in of one Log_{10}-transformed RLU in CL-ELISA with KM3 corresponds to a 33 times increased chance of being positive for *L. major*.

This analysis indicates the potential utility of αGal NGPs in discriminating between infected and uninfected patient samples. However, a combination of eight antigens has little real-world application, as any diagnostic requiring this many antigens would be complex to interpret and expensive to produce. Therefore, further refinement of the NGPs was warranted.

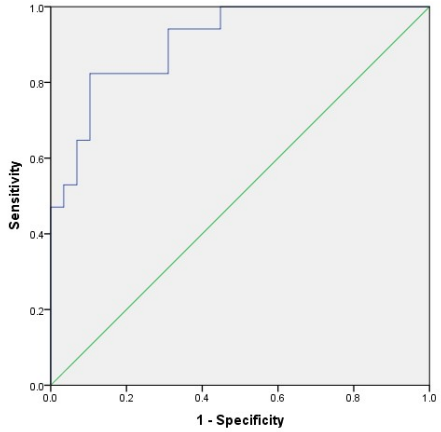

Figure 4.2. ROC for logistic regression analysis of the recognition of 9 NGPs by *L. major* and control sera (Figure 4.1). Antibody titres in serum samples from *L. major* positive individuals and non-CL heterologous controls were detected in CL-ELISA. Area under the curve (AUC) is .909. Curves above the Reference line (solid green) at 0.5 indicates the test is better than chance at predicting disease state.

4.2.1.3 Optimisation to improve detection of anti-Gal levels in pools of sera from patients with either active *L. major* or *L. tropica* infection, or from healthy controls

For assay optimisation, I used the cohort of serum samples collected from KSA in 2017 and screened with a new panel of 4 NGPs (Table 4.1, Panel 3). The updated panel more closely reflect the naturally occurring glycan structures on the surface of *L. major*, which, as shown in this thesis (Chapter 3) have some discriminating power between *L. major* and *L. tropica* sera in both CL-ELISA and TLC applications. Three NGPs have terminal αGal residues (KM27, KM28 and KM30), while the fourth was an updated control, capped with β-mercaptoethanol (BME) (See Table 4.1, and Section 2.4.1 for detailed structures).

Initially, anti-Gal levels in pooled serum samples were assessed. Both antigen concentration and serum dilution were titrated in each plate, to give a checkerboard titration for each combination of NGP and sera type (Figure 4.3). The updated control (BME) is an improvement compared to the previous iteration (KM15, cysteine-BSA) (Figure 4.3D); there is very little cross-reactivity with the sera pools, even at the highest antigen and sera concentrations. All other antigens have excellent differentials between *L. major* and both *L. tropica* and control sera. On the

other hand, the anti-Gal levels in *L. tropica* pools were indistinguishable from healthy controls at all dilutions.

The conditions for subsequent assays were selected based on the concentrations that maximised the differential between infected samples and controls and minimised the amount of sample required. For KM27, KM30 and BME this was 50 ng/well, and for KM28 this was 12.5 ng/well. All sera were used at 1:800.

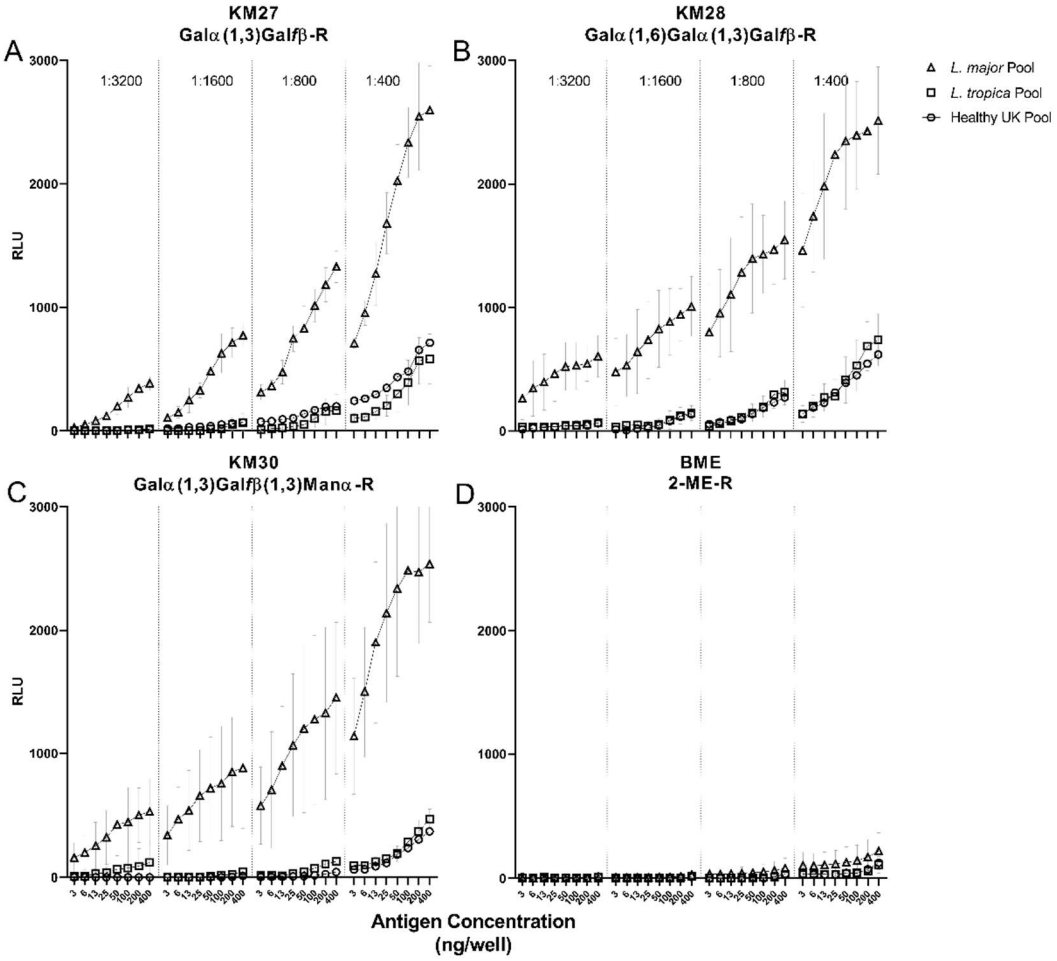

Figure 4.3. Titration of antigen (NGP) and pooled sera from control and CL patients, using CL-ELISA to assess recognition. CL-ELISA with checkerboard titration of each of four NGPs against pooled sera from either *L. major* (n=3) or *L. tropica* (n=3) infected patients or healthy UK controls (n=1). Quartiles of each panel indicate sera dilution; sera pools were titrated from 1:400 to 1:3200. Antigen coating was from 400 ng/well to 3.125 ng/well. A = KM27, B = KM28, C = KM30, D = BME. RLU = relative luminescence units.

4.2.1.4 Anti-Gal detection in pools of sera samples from the 2017 collection

Pools of sera from the 2017 collection were screened using the conditions selected through the titration assay (Section 4.2.1.3) in CL-ELISA. Using a small number of pooled serum samples (created based on shared patient characteristics, such as lesion number, nationality and gender), four NGPs were screened. Pools were from *L. major* (n = 7) or *L. tropica* (n = 6) infected patients, or healthy controls from KSA and UK (n = 10). Due to the small sample size it was difficult to assess normality of distributions, so a Kruskal Wallis H test was conducted with post-hoc comparisons, to determine if there were significant differences between anti-Gal titres in different serum types (Supplementary Table 3 and 4).

L. major sera has significantly highly titres for the three galactosylated NGPs (KM27, KM28 and KM30), compared to all other serum types (Figure 4.4). No other significant differences were observed, i.e. *L. tropica* and all healthy controls have similar antibody titres (Table 4.3). Anti-Gal titres vary within the groups, but the trend is consistent, indicating that anti-Gal levels are increased, independent of gender, nationality and lesion number.

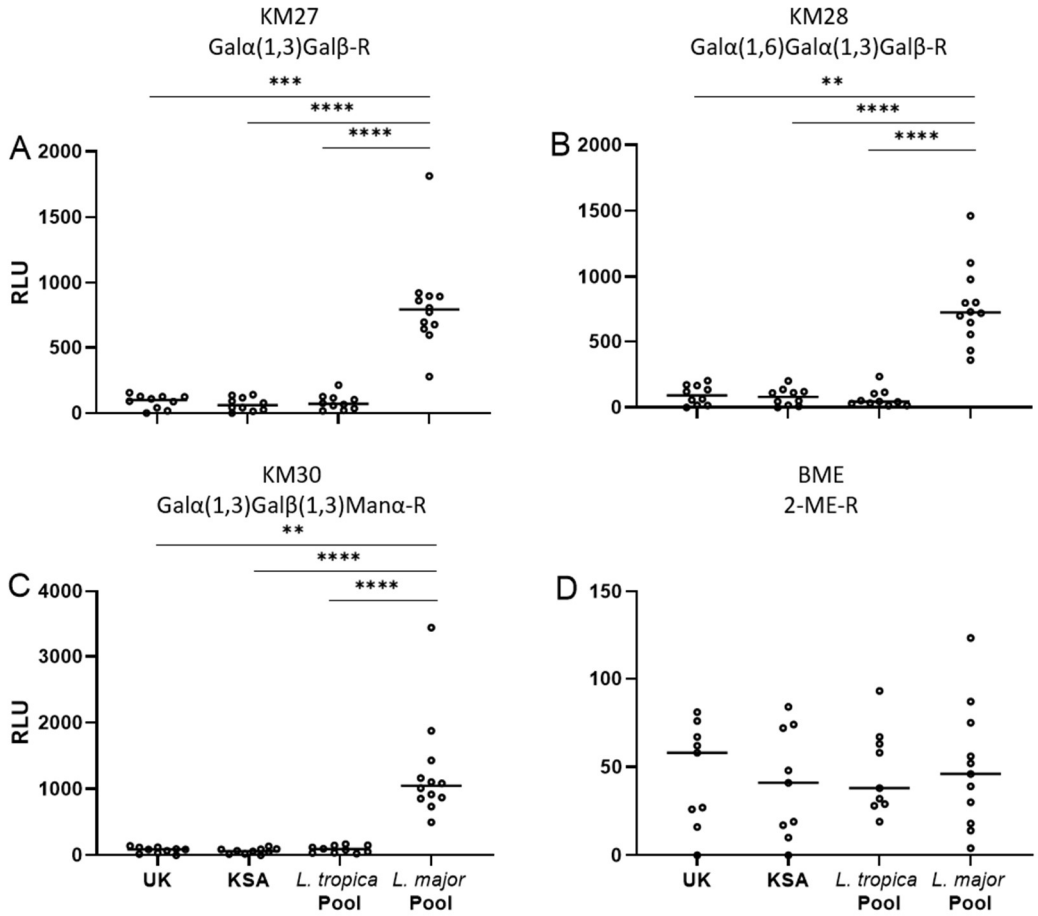

Figure 4.4. Anti-Gal levels detected by CL-ELISA in pooled sera samples from the 2017 collection. Pooled sera samples from healthy controls (UK or KSA patients), or active infection (*L. tropica* and *L. major*) were diluted 1:800. Each panel corresponds to a single antigen. A = KM27, B = KM28, C = KM30, D = BME. ** = $p \leq 0.01$, *** = $p \leq 0.001$, **** = $p < 0.0005$.

Table 4.3. Differences in anti-Gal titres in pooled sera from healthy controls (UK or KSA patients) or active infection (*L. tropica* and *L. major* from the 2017 cohort). Differences (Diff.) were calculated from CL-ELISA data, subtracting the mean rank score of Group 2 from that of Group 1. Mean ranks are listed in Supplementary Table 4. Bonferroni corrected significance is reported for each difference. ** = $p \leq 0.01$, *** = $p \leq 0.001$, **** = $p < 0.0005$, ns = $p > 0.05$.

Group One	Group Two	KM27		KM28		KM30	
		Diff.	*p* value	Diff.	*p* value	Diff.	*p* value
L. major	*L. tropica*	21.35	****	22.9	****	18.5	****
	UK	19.25	***	18.95	**	20.9	**
	KSA	22.4	****	21.15	****	23.6	****
L. tropica	UK	-2.1	ns	-3.95	ns	2.4	ns
	KSA	1.05	ns	-1.75	ns	5.1	ns
UK	KSA	3.15	ns	2.2	ns	2.7	ns

4.2.1.5 Anti-Gal detection with an updated panel of NGPs is increased in active *L. major* infection, but not *L. tropica*

As CL-ELISA using pooled samples indicated that serum anti-Gal titres recognising αGal NGPs are significantly increased during active *L. major* infection, a more in-depth screen was carried out using individual patient samples from additional groups. The samples were from either active infection with *L. tropica* (n = 15), or *L. major* (n = 56) samples from 2017, or *L. major* from 2013 (n =24), cured (previous CL infection; n = 25), or heterologous control (non-CL dermatological pathologies; n = 25). For the *L. major* 2017 group, where some patients visited the clinic on multiple occasions, only the first visit was included. A Kruskal-Wallis H test identified that there were differences in anti-Gal between the different patient groups, for each of the four new NGPs (Supplementary Table 5 and 6). Post-hoc tests identified where significant differences lie (Figure 4.5; Table 4.4).

RLU for all samples against BME are very low relative to the galactosylated NGPs (<200 RLU), however, one pair-wise comparison was significant; *L. major* samples from 2017 (mean rank = 85.17), and heterologous controls (mean rank = 56.40) ($p < 0.05$). Inspection of the data shows that the difference between these groups is minor, but this perhaps indicates a trend that could become clearer with an increased samples size in the heterologous controls (n = 25).

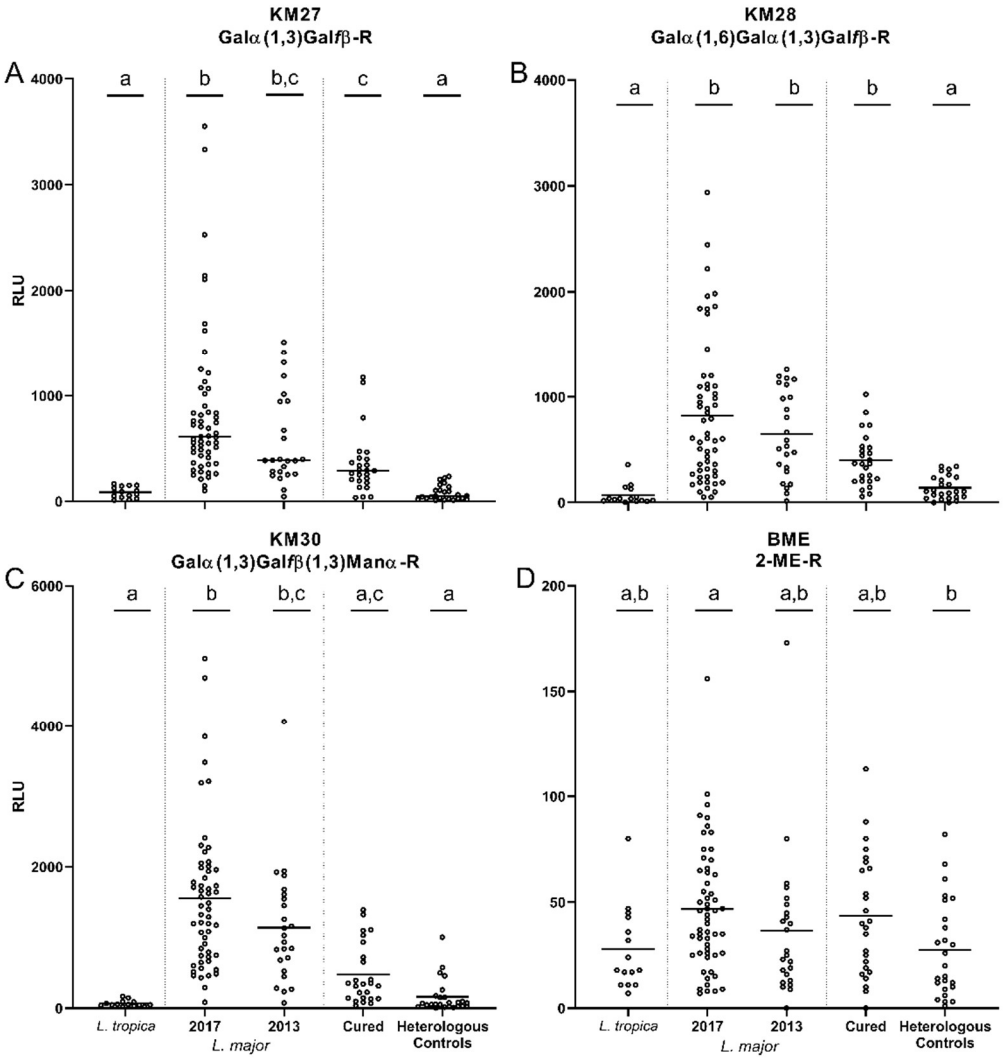

Figure 4.5. Anti-Gal levels detected by CL-ELISA in individual sera samples from the 2013 and 2017 cohorts, using four NGPs. Antibody titres are plotted as relative luminescence units (RLU), for individual patient serum samples from active *L. major* infection (either 2017 or 2013 collection cohorts), active *L. tropica* infection, post-infection (Cured) and heterologous (non-CL controls). Each panel corresponds to one NGP - A = KM27, B = KM28, C = KM30, D = BME. Lower case letters above data indicate mean ranks that do not differ significantly**.**

As for the activity against the remaining three αGal NGPs (KM27, KM28 and KM30), despite a lower median for the 2013 samples, titres in *L. major*-positive sera did not differ across the cohorts ($p > 0.05$). All NGPs gave higher mean ranks during *L. major* infection. Most interestingly, both KM27 and KM30, the Galα(1,3) terminating structures had significantly higher titres in *L. major* 2017 patients, than in both cured and heterologous control patients. This was not the case for the Galα(1,6)

terminating KM28, where the mean ranks for cured patients were not different to active *L. major* patients. *L. tropica* and heterologous controls show no difference, indicating these patients have similarly low levels of circulating anti-Gal.

In summary, of the 11 αGal NGPs screened against these two cohorts of Old World CL patients, those with Galα(1,6)Gal and Galα(1,3)Gal detected higher anti-Gal in *L. major* sera than in controls. Galα(1,3)Galβ recognition was improved further when the βGal was furanose (as in KM27 and KM30), rather than pyranose (as in KM1 and KM9), more closely mimicking the combination of pyranose and furanose glycans in *L. major* GIPLs.

Table 4.4. Comparison of anti-Gal levels for individual patient serum samples from active *L. major* infection (either 2017 or 2013 collection cohorts), active *L. tropica* infection, post-infection (Cured) and heterologous (non-CL controls) against four NGPs (KM27, KM28, KM30 and BME). Differences (Diff.) are calculated subtracting Group Two mean rank score from Group One. Mean ranks are reported in Supplementary Table 6. Bonferroni corrected significance is reported for each difference. * = p ≤ 0.05. ** = p ≤ 0.01, *** = p ≤ 0.001, **** = p < 0.0005, ns = p > 0.05**.**

Group One	Group Two	KM27		KM28		KM30		BME	
		Diff.	*p*	Diff.	*p*	Diff.	*p*	Diff.	*p*
L. major 2017	*L. major* 2013	14.98	ns	4.04	ns	14.10	ns	18.94	ns
	L. tropica	76.90	****	74.89	****	82.54	****	28.77	ns
	Heterologous	79.68	****	59.13	****	75.09	****	30.53	*
	Cured	36.12	**	21.33	ns	45.37	****	4.61	ns
L. major 2013	*L. tropica*	61.92	****	70.85	****	68.44	****	9.83	ns
	Heterologous	64.70	****	55.09	****	60.99	****	11.59	ns
	Cured	21.14	ns	17.29	ns	31.27	ns	-14.33	ns
Cured	*L. tropica*	40.78	*	53.56	***	37.17	ns	24.16	ns
	Heterologous	43.56	**	37.80	ns	29.72	ns	25.92	ns
Heterologous	*L. tropica*	-2.78	ns	15.76	ns	7.45	ns	-1.76	ns

4.2.1.6 Three αGal NGPs have diagnostic potential for *L. major* but not *L. tropica* infection in KSA

To assess the discriminatory power of anti-Gal titres in patient sera (comparing patients with *L. major* or *L. tropica* infection to negative control samples) that bind each of the four NGPs (KM27, KM28, KM30 and BME), I first used Frey's method (1998) to calculate a cut off value for end-point ELISA data, below which a reading is deemed "negative" and above which, "positive". Each CL-ELISA plate contained two

negative controls (two pools of sera from healthy individuals), so for the equation given below, $\bar{X}$ is the mean of the two control readings, SD is the standard deviation of the mean and f equals 7.733, giving the confidence interval at the 95% level (Equation 4.1). For the data presented in Figure 4.5, I scored each individual sample as positive or negative for leishmaniasis (Supplementary Table 7). I performed this analysis twice, with different "true negatives". The first true negative group only included patients with no prior history of leishmaniasis (heterologous only) and, the second included heterologous controls and those with cured CL infection combined. The latter group is likely to be more representative of a true population, as, in an endemic region, individuals with past infection may still have specific antibodies at detectable levels, which could confound attempts to diagnose only active cases.

Equation 4.1. Equation to calculate the cut-off value between positive and negative scores, using ELISA data [294].

$$cutoff = \bar{X} + SDf$$

The data for *L. major* (2013 and 2017 cohorts) and *L. tropica* patients and the two sets of controls were analysed using binomial logistic regression (Supplementary Tables 8-13). If the logistic regression model was significant for an individual NGP, a secondary analysis was conducted combining the data for all the significant NGPs. Finally, ROC curves were generated to compare AUC values for *L. major* (Figure 4.6, Table 4.6) and *L. tropica* (Figure 4.7, Table 4.7) to assess utility of each NGP as a potential diagnostic.

For *L. major* infection the regression models were significant for all NGPS, whether considering the "true negative" group as only heterologous controls, or both heterologous and cured combined (Table 4.8). AUC values for αGalactosylated NGPs indicate an exceptional level (based on criteria from Scott *et al*. (2013)) of discrimination between positive and negative samples, even when patients with cured samples are included in the "true negative" group, with AUC of 0.8-0.9 for each individually, >0.9 for all NGPs combined (Table 4.9). AUC values were ≥0.9 for each curve, when including only heterologous controls.

Sensitivity (the ability to accurately detect a positive test) and specificity (accuracy of negative results) for each NGP is summarised in Table 4.5. Reassuringly, BME was universally useless as a biomarker, correctly categorising zero samples as positive. Sensitivity was generally low for *L. tropica* infected samples (peaking with KM30 at 20%), although this is unsurprising given the non-significant difference between *L. tropica* and control groups as shown in Figure 4.5.

Table 4.5. Positive and negative test results calculated for *L. major* and *L. tropica* patient serum samples screened with four NGPs (KM27, KM28, KM30 and BME). Test Results were assigned positive (+) or negative (-) based on the cut-off values, calculated for each CL-ELISA plate. Active infection samples are either *L. tropica* or *L. major* (collected in 2013 and 2017). Negative samples are categorised as Heterologous (only heterologous controls) or Combined (cured and heterologous controls).

NGP	Test Result	Disease Present		Disease Absent	
		L. major	*L. tropica*	Heterologous	Combined
KM27	+	118	0	1	12
	-	11	15	27	41
KM28	+	120	2	3	17
	-	10	13	25	36
KM30	+	126	3	8	25
	-	3	12	20	28
BME	+	0	0	0	0
	-	129	15	28	53

Table 4.6. Sensitivity and specificity for each NGP (KM27, KM28, KM30 and BME) when predicting positive or negative status of serum samples. Calculations were performed using either heterologous controls only, or combined values for cured patients and heterologous controls as the "true negative" group**.**

NGP	**Sensitivity**		**Specificity**	
	L. major	*L. tropica*	Heterologous only	All Negative
KM27	91%	0%	96%	77%
KM28	92%	13%	89%	68%
KM30	98%	20%	71%	53%
BME	0%	0%	100%	100%

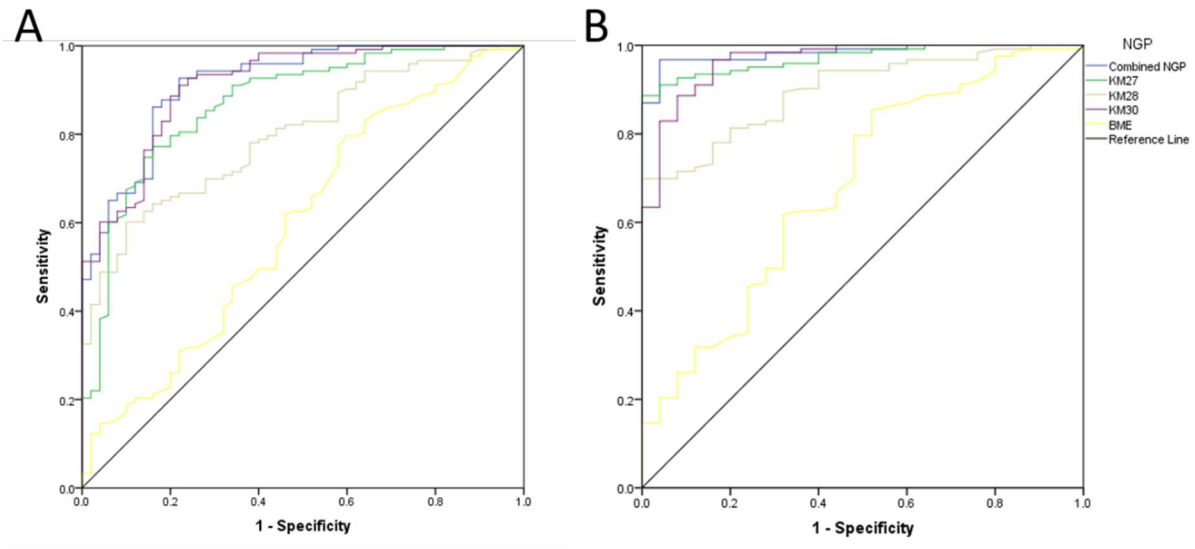

Figure 4.6. ROC curve analysis for four NGPs (KM27, KM28, KM30 and BME) for *L. major* infected samples. ROC curves were generated using a "true negative" group of either Combined values from cured and heterologous patients (A) or Heterologous control values only (B). AUC values for each curve are listed in Table 4.6. Curves above the Reference line (solid black) at 0.5 indicates the test is better than chance at predicting disease state**.**

Table 4.7. Area under curve (AUC) values for *L. major* ROC curves. ROC curves (Figure 4.6) were generated using Combined values from cured and heterologous patients or Heterologous control values only**.**

NGP	Combined (Figure 4.6A)			Heterologous (Figure 4.6B)		
	AUC	95% CI		AUC	95% CI	
		Lower	Upper		Lower	Upper
Combined	**0.916**	0.872	0.961	**0.983**	0.966	1.00
KM27	**0.870**	0.811	0.930	**0.971**	0.949	0.994
KM28	**0.798**	0.732	0.864	**0.898**	0.845	0.951
KM30	**0.913**	0.867	0.958	**0.966**	0.932	1.000
BME	**0.597**	0.501	0.692	**0.683**	0.565	0.801

ROC curves for *L. tropica* patient diagnostics showed a surprising level of discrimination, with AUC values of >0.8 when all NGPs were combined, although perhaps this was a product of the sample size (negative samples out number positives), maximising specificity (Figure 4.7).

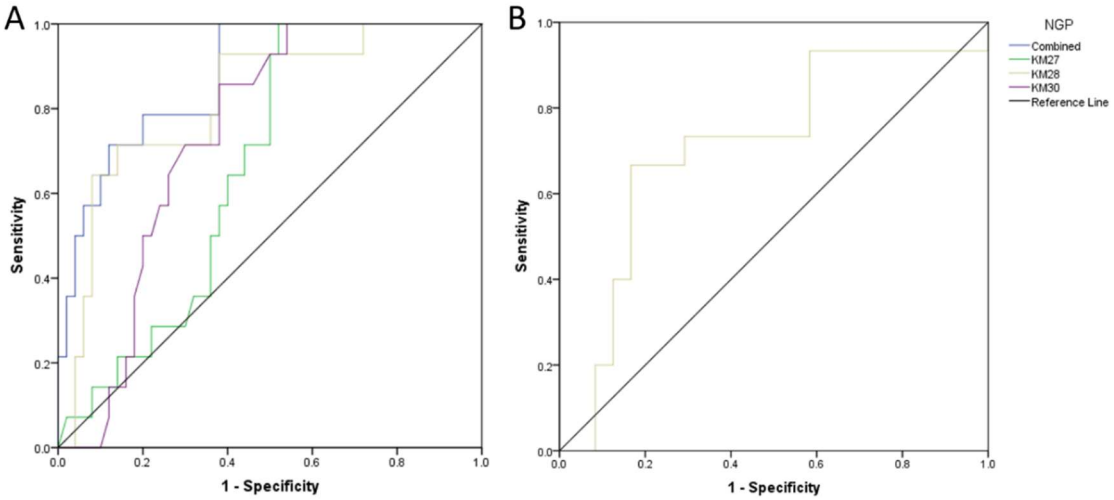

Figure 4.7. ROC curve analysis for four NGPs (KM27, KM28, KM30 and BME) for *L. tropica* patient samples. ROC curves were generated using either Combined values from cured and heterologous patients (A) or heterologous control values only (B). AUC values for each curve are listed in Table 4.7. Curves above the Reference line (solid black) at 0.5 indicates the test is better than chance at predicting disease state**.**

Table 4.8. Area under curve (AUC) values for *L. tropica* (2017 KSA Cohort) ROC curves (Figure 4.7). ROC curves (Figure 4.7) were generated using either Heterologous control values only (A), or Combined values from cured and heterologous patients (B).

NGP	Combined (Figure 4.7A)			Heterologous (Figure 4.7B)		
	AUC	95% CI		AUC	95% CI	
		Lower	Upper		Lower	Upper
Combined	**0.876**	0.783	0.969			
KM27	**0.663**	0.530	0.796			
KM28	**0.819**	0.696	0.941	**0.711**	0.536	0.886
KM30	**0.736**	0.617	0.856			

4.2.1.8 Serum levels of anti-Gal antibodies do not change during chemotherapeutic treatment of *L. major*-infected individuals

To determine how the serum levels of anti-Gal antibodies change in patients over the course of anti-leishmanial drug treatment, I used serum samples taken from some of the *L. major*-positive patients (KSA 2017) and measured their reactivity against the updated panel of NGPs (KM27, KM28, KM30, BME). These patients were treated with first with azoles and antibiotics, followed by antimonials, as described in (Section 2.6.1). To determine significance, a Repeated Measures One-Way ANOVA was performed to assess any change in titre over time. As this test cannot be used when there are missing values (i.e. when some patients visited the clinic

twice, and others three times), only the 15 patients with 3 recorded visits are included in the analysis (Figure 4.8).

There was a slight increase in anti-Gal titre against KM28 and KM30 across the time points. However, there was no significant change in mean titre for any of the four NGPs (Table 4.8). The time between first and last clinic visit is not long enough to detect a drop in antibody titre in response to parasite reduction.

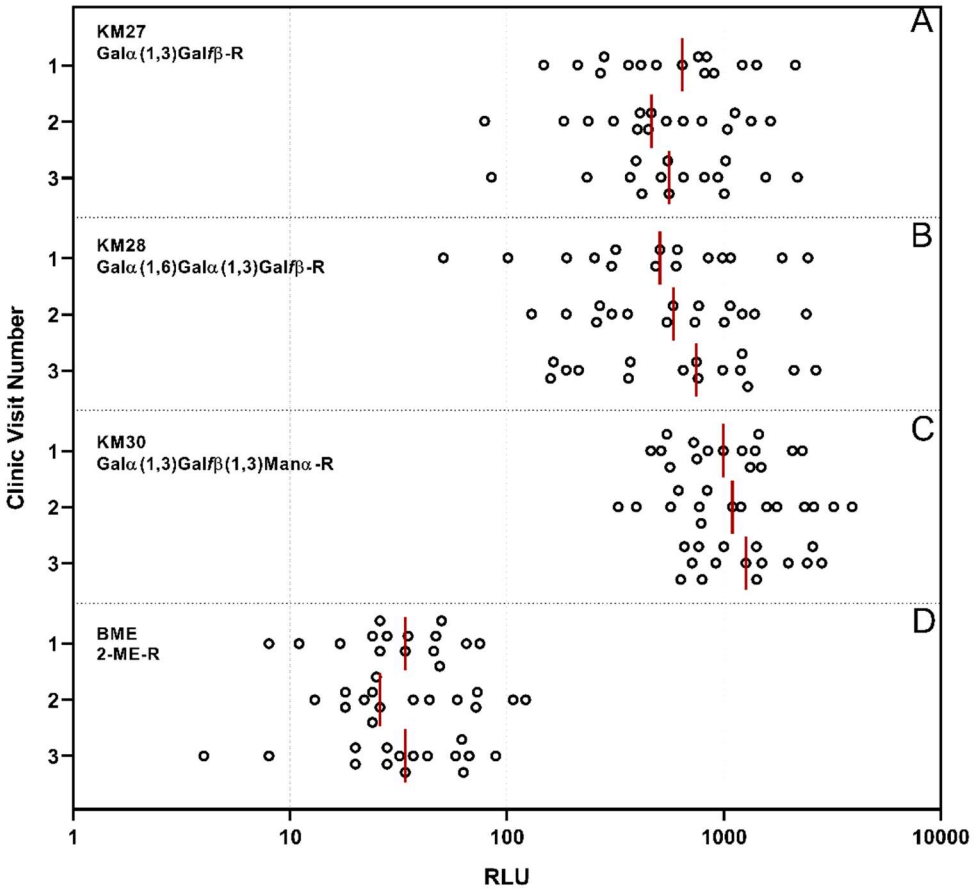

Figure 4.8. Anti-Gal titres in sera from *L. major* patients (n=15) during a course of drug treatment. The activity of individual serum samples from *L major*-infected patients that received 1-3 doses of anti-leishmanial drug treatment was screened against four NGPs (panels A-D). Results were plotted as Log_{10} RLU. Medians for each visit are marked as red lines. Repeated measures ANOVA showed no change in titres over time.

Table 4.9. Repeated Measures ANOVA results comparing anti-Gal titres in sera from *L. major* patients (n=15) during a course of drug treatment. Titres were detected in CL-ELISA analysis of serum samples taken at three separate clinic visits, for the treatment of *L. major* infection. ns = p > 0.05**.**

NGP	F Statistic [a]	*p* value
KM27	0.295	ns
KM28	1.324	ns
KM30	1.730	ns
BME	0.248	ns
[a] DF (2,28)		

4.2.1.9 Assessing polyclonality of anti-Gal titres in *L. major* sera samples

There is a possibility of cross-reactivity among the different anti-Gal populations in serum from CL-infected individuals (reflecting the complexity of the parasite glycan epitopes). I determined this by assaying the activity of serum from *L. major*-infected patients against NGPs (KM27, KM28 and KM30) under various conditions. First, CL-ELISA plates were coated with two antigens in the same well, to determine if several anti-Gal populations were present. Then I used an enzyme to cleave the terminal αGal residue from the NGP, to measure the associated reduction in binding. Finally, serum was incubated with various monosaccharides, to investigate if other glycans had inhibitory effect on anti-Gal recognition of NGPs.

For the dual antigen assays, a Repeated Measures One-Way ANOVA was conducted to determine if there were statistical differences in antibody titres binding antigens singly or in combination. *L. major* serum samples (n = 56; taken at the first clinic visit were used) were assayed by ELISA in plates coated with either KM27, KM28 or KM30 alone, or KM27+KM28, KM27+KM30 or KM28+KM30 in the same well (Figure 4.9). Antibody titres were significantly different between the different antigen coatings (F (1.798, 95.306) = 70.073, p < 0.0005, partial η2 = 0.569). Planned contrasts showed that mean titres increased in all combination wells (Table 4.9). This was least pronounced in the comparison of KM30 alone (mean = 3.11) and KM27+KM30 (mean = 3.16), however, even this comparison was deemed significant after Bonferroni correction for multiple comparisons (p = 0.018).

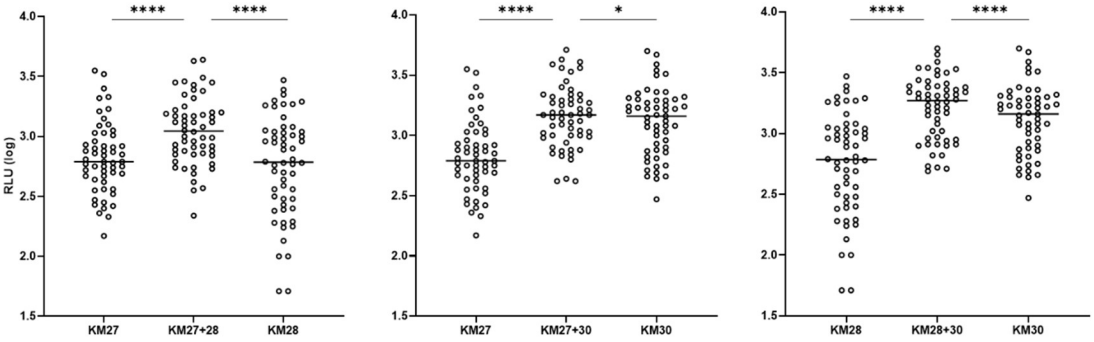

Figure 4.9. Anti-Gal titres in *L. major* patient samples (n = 56) with single or dual NGP antigens. Antibody titres detected in patient sera with active *L. major* infection, diluted 1:800. Wells were coated with NGPs alone or in combination, KM27 and KM30 at 50 ng/well, and KM28 at 12.5 ng/well. Data are presented as Log_{10} transformed relative luminescence units (RLU). Lines correspond to median. * = $p \leq 0.05$, **** = $p < 0.0005$**.**

Table 4.10. Comparison of anti-Gal titres detected using single or dual antigens (KM27, KM28 and KM30) in serum from *L. major*-positive samples. Planned contrasts were performed after One Way Repeated Measures ANOVA analysis of Log_{10}-transformed CL-ELISA data with single and dual antigen coatings (Figure 4.9). Difference is calculated between the mean of individual NGP (Group Two) and the mean of dual NGPs (Group One). * = $p \leq 0.05$, **** = $p < 0.0005$**.**

Group One	Group Two	Difference	CI		*p* value
			Lower	Upper	
KM27+KM28	KM27	0.217	0.174	0.261	****
	KM28	0.297	0.228	0.75	****
KM27+KM30	KM27	0.333	0.255	0.089	****
	KM30	0.047	0.006	0.579	*
KM28+KM30	KM28	0.466	0.353	0.066	****
	KM30	0.100	0.579	0.134	****

In order to demonstrate that the terminal αGal residues are essential for recognition of the NGP, coffee bean αGalactosidase (CBAG) was used to cleave all types of terminal αGal (Galα(1/4/6)) linkages. I immobilised KM30 (Galα(1,3)Galβ(1,3)Manα-BSA) onto ELISA plates and treated with increasing amount of CBAG. Despite titration of the primary antibody (from 1:100 to 1:800 dilutions), the coating NGP amount (12.5-50 ng/well) and the enzyme amount (0.0125-0.1 U/well) I was unable to reduce anti-Gal titres against KM30 by more than 18% (Figure 4.10). This is likely due to cross-reactivity against the truncated glycan; removal of the terminal αGal leaves Gal*f*β(1,3)Manα-BSA, which

demonstrates a high level of binding to patient sera. Due to this complication, I decided to use competitive glycan concentrations to confirm specificity.

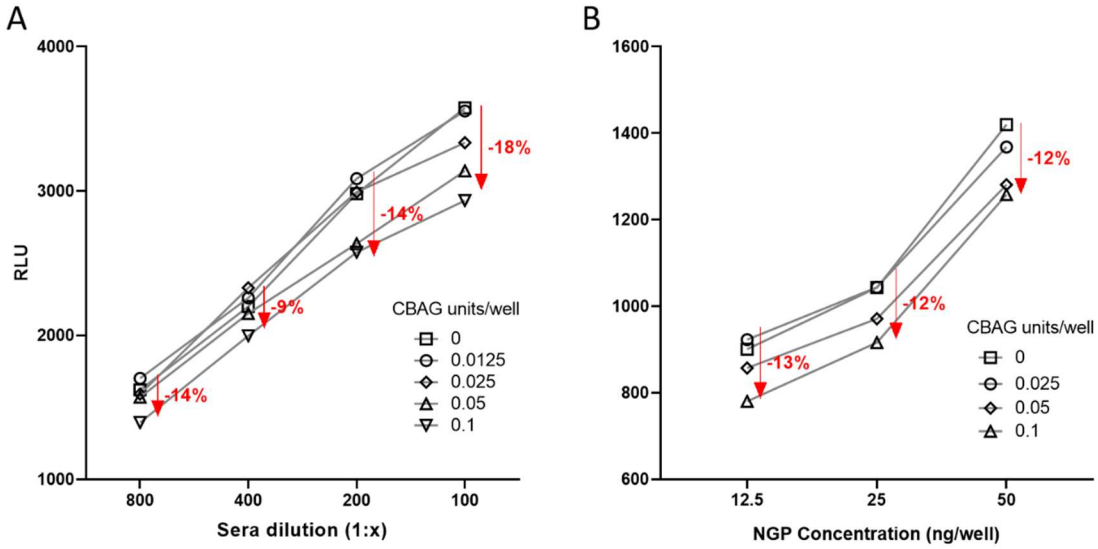

Figure 4.10. Anti-Gal titres in *L. major* positive patient samples from KSA (2017 cohort) against KM30 are reduced following CBAG treatment. Red arrows and percentages indicate reduction of titre between highest enzyme amount (0.1 U/well) and enzyme-negative controls (0 U/well). A. *L. major* positive sera was diluted between 1:100 and 1:800, and titrated against increasing amounts of CBAG enzyme. NGP coating was 50 ng/well. B. KM30 was titrated between 12.5-50 ng/well against increasing amounts of CBAG enzyme. Sera was diluted 1:800**.**

To assess the degree of recognition of NGPs determined by the configuration of the terminal galactosyl residue, pooled sera was incubated with monosaccharides at 0.1 M and 0.5 M concentrations before addition to the CL-ELISA plate (Figure 4.11). Glycans used were methyl-α-D-galactopyranose, methyl-β-D-galactopyranose, D-Galactose and D-Mannose. Inhibition was measured in relation to a glycan-free control.

Inhibition of all pools was greatest with αGal and D-Galactose, although β-Gal almost completely abolished binding at 0.5 M. Mannose was much less effective at inhibiting binding, except at 0.5 M for *L. tropica* sera, where binding was reduced to almost zero.

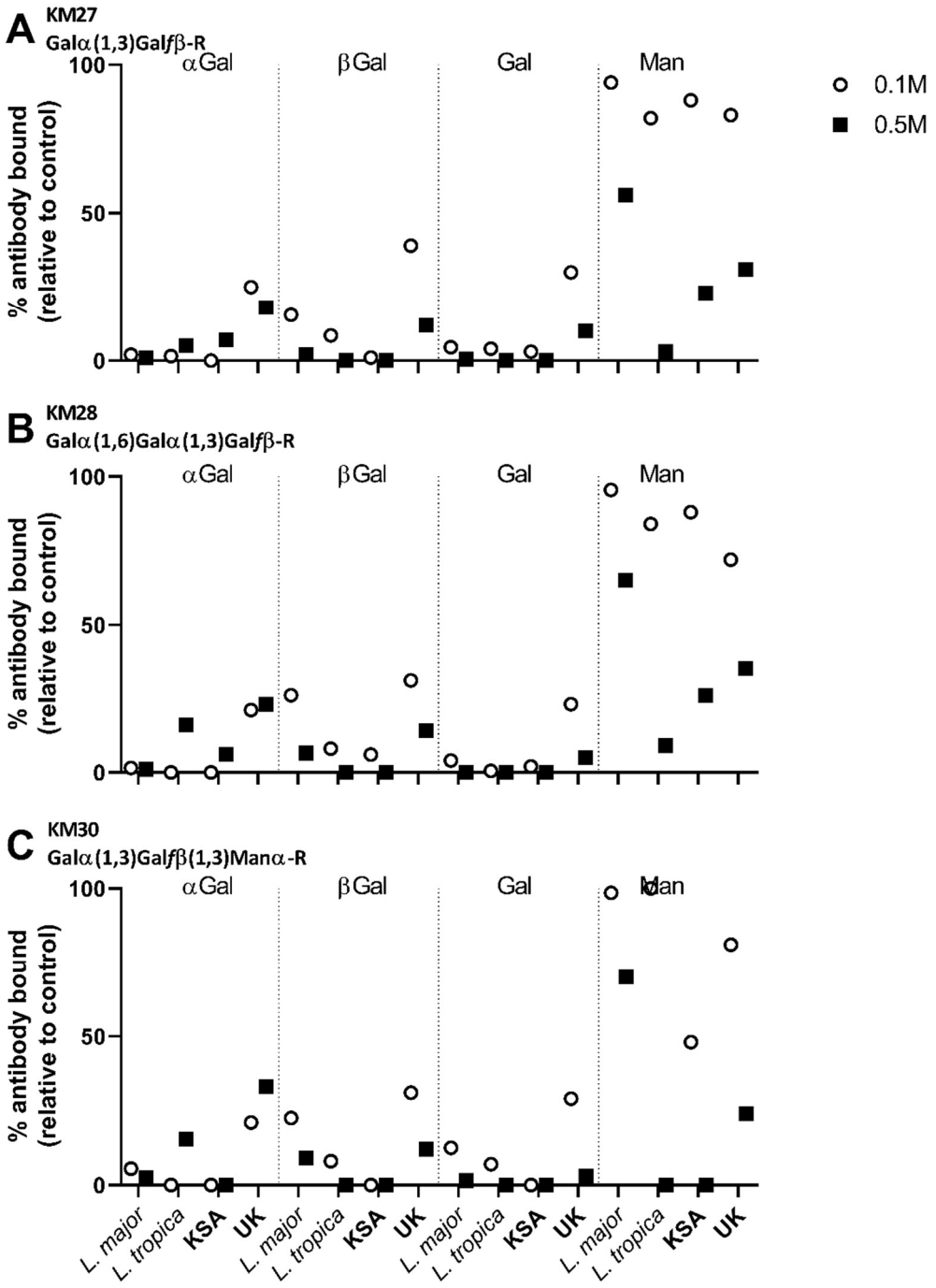

Figure 4.11. Anti-Gal recognition of three NGPs (KM27, KM28 and KM30) in the presence of inhibitory glycans, in pooled serum samples from active infection (*L. major* or *L. tropica*) and healthy controls (UK or KSA). Data are plotted as percentages, relative to a control, uninhibited control pools. Pooled serum was pre-incubated with specific glycans at either 0.1M (blue circle) or 0.5M (red square) concentration. *L. major* (n = 2), *L. tropica* (n = 2), UK (n =1), KSA (n=1). Top: KM27. Middle: KM28. Bottom: KM30**.**

Taken together, these assays demonstrate the diversity of anti-glycan antibodies produced during *L. major* infection. At least two populations are detected in the dual antigen assays (anti-Galα(1,6)-R and anti-Galα(1,3)-R). The inhibition of recognition of KM27/28/30 by *L. major* sera through pre-incubation with galactose verifies the importance of the terminal αGal-residue, although as both βGal and D-Mannose pre-incubation also inhibited recognition of the NGPs, this assay is detecting a degree of polyreactivity. Anti-Gal has been shown to be polyreactive and low affinity binding to structures other than αGal epitopes has been demonstrated [296].

4.2.1.10 Correlation of *L. major* anti-Gal titre with disease characteristics

Lesion number and parasite load vary widely between CL individuals, and it is possible that low parasite numbers could result in low anti-Gal titres, confounding diagnosis. C-Reactive Protein (CRP) is a plasma protein that is a well-studied marker of inflammation and tissue damage [297]. Understanding how host responses to infection correlate with anti-Gal levels may flag patient groups for which the test is less useful. If patients with low parasite burdens, such as in chronic CL, or very low markers of inflammation, have correspondingly low anti-Gal titres, these could result in false negatives.

4.2.1.10.1 Serum CRP levels are increased in CL infection

Kruskal Wallis H test showed the mean rank values for CRP levels in sera were significantly different across the three sera types (χ^2 (3) p = 0.03, Figure 4.12). Post-hoc comparisons identified the difference between *L. major* patients and Heterologous controls, but not in any other comparison (Supplementary Table 14, Table 4.10). It must be noted that the sample size for these comparisons is very small (n= 7 for cured patients, and n = 17 for heterologous).

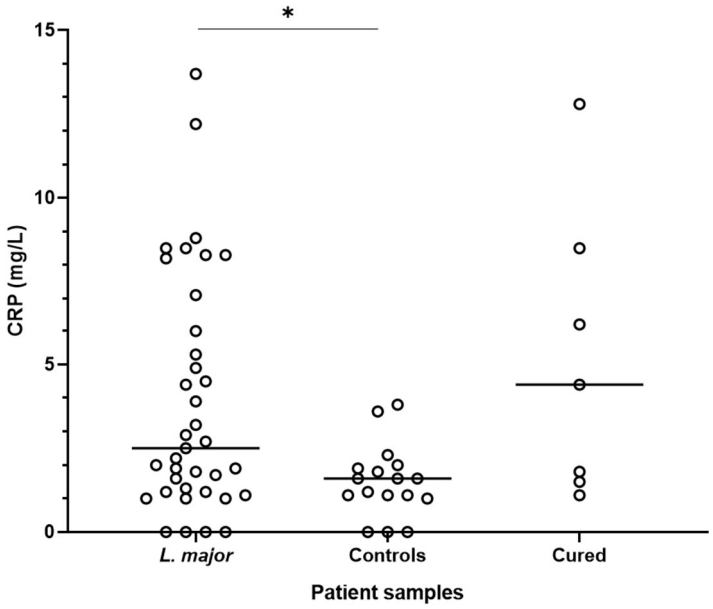

Figure 4.12. CRP levels in individual patient sera from KSA with either active L. major infection (2017 cohort), cured patients or healthy controls. CRP was measured, using the Eurolyser CRP test kit, in individual patient serum samples from active *L. major* infection (n = 37), Cured patients (n=7) and heterologous controls (n = 17). Lines are at the median. * = p ≤ 0.05**.**

Table 4.11. Differences in serum CRP levels in patients from KSA with active *L. major* infection (2017 cohort), cured patients and heterologous controls. Kruskal Wallis H results comparing differences (Diff) in mean ranks scores, calculated by subtracting the mean rank score of Group Two from that of Group One. Bonferroni corrected significance is reported for each difference (P). * = p ≤ 0.05.

Group One	Group Two	CRP	
		Diff.	*p* value
L. major 2017	Heterologous	12.51	*
	Cured	-5.18	ns
Heterologous	Cured	-17.69	ns

4.2.1.10.2 Anti-Gal titre is not dependent on parasite load or lesion number

Sera was taken at the same time as swabs from CL lesions during the 2017 collection. This was then used to detect parasite DNA using quantitative PCR (molecular tests performed by Yasser Al Raey, LSTM). Detected DNA is proportional to parasite load in the sample, allowing an approximate correlation of parasite

number to be calculated with other factors. Correlations were not carried out using data from *L. tropica* patients, due to the small sample size in this group (n=15).
For all NGPs, there is a small, positive correlation of *L. major* DNA load with anti-Gal titres, but this was only significant for CL-ELISA results with KM30 (Table 4.11). Detected DNA explains 14% of the variation in log_{10} antibody titre against KM30. Log_{10} CRP level had a positive moderate correlation with both antibodies recognising KM27 and KM28, and with the number of lesions but this was not significant (Table 4.11).

Table 4.12. Pearson Correlations for DNA load, lesion number and CRP levels, with antibody titres against each of four NGPs (KM27, KM28, KM30 and BME), in KSA patients with active *L. major* infection (2017 cohort). Correlation coefficients were calculated between anti-Gal titres for each NGP, serum CRP levels, the number of lesions and kDNA copy number calculated from qPCR analysis of lesion swabs. Positive values indicate a positive correlation, negative values indicate a negative correlation. * = $p < 0.05$

NGP	DNA	Lesion Number	CRP
KM27	0.271	0.082	0.313
KM28	0.259	-0.102	0.183
KM30	0.373*	0.008	-0.074
BME	0.114	-0.339*	-0.255
CRP	-.237	0.137	
Lesion Number	-0.161		

4.2.1.12 anti-Gal titres do not differ across blood types

Cross reactivity between anti-Gal and blood type antigens is widely reported, due to similarity in structure between glycans decorating type B blood cells and αGalactosylated glycoconjugates found on pathogens. This potential cross-reactivity could be detrimental to developing an anti-Gal diagnostic. A Kruskal-Wallis H test was used to determine if there were differences in antibody titre between patients with different blood type: A, B, O or AB. Mean rank titres were not statistically significantly different between blood types for all NGPs, indicating that blood type has no impact on levels of antibody recognising the three NGPs assessed (Table 4.12). This is potentially due to the inclusion of the galactofuranose in this panel, which closely reflects the natural glycochemistry of *L. major* GIPLs.

Table 4.13. Anti-Gal titres against three NGPs (KM27, KM38 and KM30) in serum samples from individuals with either A, B, AB, or O type blood. Kruskal Wallis H Test results comparing antibody titres between blood types. ns = $p > 0.05$.

NGP	χ^2	DF	*p* value
KM27	3.295	3	ns
KM28	4.436	3	ns
KM30	1.193	3	ns

4.2.2 Analysis of the anti-gal response in patients from other geographical locations.

Structural studies performed on surface glycoconjugates from *Leishmania* spp. isolated from different parts of the world have demonstrated that there is a degree of overlap in some of these molecules [230]. The similarity is not only restricted to the type of molecule (e.g. LPG and GIPLs) expressed by a given *Leishmania* species, but also on the type of sugar residues and how they may be displayed. This means that there is a potential for developing an antibody-based diagnostic to have a universal deployment, if a generic *Leishmania* antigen of oligosaccharidic nature could be found. On the other hand, travel between areas of endemicity could confound accurate diagnostics, if antigens are not included in the detection panel that are species specific. To this end, in addition to the Middle Eastern samples described above, I have screened a patient cohort with American leishmaniasis infection collected from Bolivia, and another cohort from Spain infected with *L. infantum*.

4.2.2.1 Anti-Gal titres in individual Bolivian sera are highest in ML/MCL patients

The Bolivian cohort were categorised by lesion location; either cutaneous lesions (CL; n = 32) or mucosal lesions (ML/MCL; n = 20). Control patients (n = 36) with a non-CL lesions were also sampled. PCR was not performed to identify the species, but based on epidemiological data, we can assume the majority (85%) are *L. braziliensis*. *L. braziliensis* has a similar GIPL profile to *L. major*, with predominantly Type-II, αGalactosylated GIPLs.

This cohort was screened initially with three NGPs (Figure 4.13). KM3 (Galα-BSA) was selected based on the results from the 2013 *L. major* cohort screen, which

indicated that KM3 was the most important of the nine NGPs screened, in *L. major* detection. A commercial NGP termed Dextra-BSA (Galα(1,3)Galβ(1,4)GlcNAcβ-BSA) which had been used to great effect by Al-Salem *et al*. (2014) to detect anti-Gal in Old World CL, was also used, alongside a "complimentary" structure, KM24 (Galα(1,3)Galβ(1,4)GlcNAcα-BSA). KM24 differed from Dextra-BSA only in that it contains an αGlcNAc configuration (instead of βGlcNAc). Anti-Gal titres against these glycans were measured in CL-ELISA for the three sera types (CL, ML/CL and Controls) alongside *L. major* positive controls and Chagas positive controls for reference. Kruskal Wallis H test followed by post-hoc comparisons was used to determine if anti-Gal titres differ between sera types (Supplementary Tables 15 and 16).

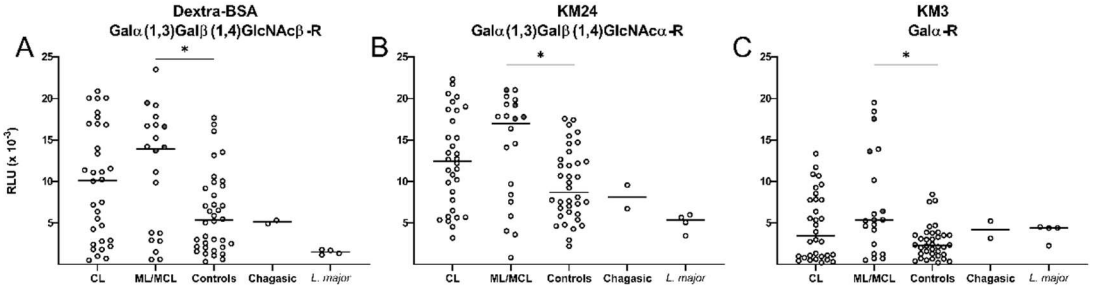

Figure 4.13. Anti-Gal activity in individual Bolivian patient sera with active tegumentary leishmaniasis (CL or ML/MCL lesions) or healthy controls against three αGalactosylated NGPs (Dextra-BSA, KM24, KM3). In the ML/MCL group, closed circles (n = 4) indicate patients with both mucosal and cutaneous lesions (MCL). Open circles indicate patients with only mucosal lesions (ML). Lines correspond to median. Comparisons were only performed between CL, ML/MCL and Controls, and not for Chagasic or *L. major* positive sera. Only significant differences are identified. A = Dextra-BSA, B = KM24, C = KM3. * = $p \leq 0.05$.

The levels of anti-Gal recognising each of the three NGPs was significantly increased in patients with mucosal lesions (ML/MCL) versus the negative controls (Figure 4.13, Table 4.13). Antibody titres did not differ between patients with mucosal tissue involvement (MCL/ML), compared to patients with only cutaneous lesions (CL), although it is interesting to note that the four patients with both mucosal and cutaneous lesions (MCL) showed titres above the median in all cases. A limitation of this cohort is that without parasite identification, there is likely a mix of species present within each of the two groups. *L. braziliensis* is known for its relatively high percentage of ML/MCL progression, but other species present in the region also

have this potential. Control patients show a large amount of variation in anti-Gal titres (Figure 4.13).

Seven patients had very low titres against both Dextra-BSA and KM24. There is no universal aspect of their patient history i.e. they are mix of primary and recurring infection, Chagas infection state and various lesion numbers. These seven patients do not demonstrate similarly low titres against KM3, indicating that different antibody populations are recognising the Galα monosaccharide.

Table 4.14. Anti-Gal titres against three NGPS (Dextra-BSA, KM24 and KM3) in Bolivian patient serum samples with either active *Leishmania* infection (CL or ML/MCL lesions), or from healthy Bolivian controls. Kruskal Wallis H results comparing differences in mean ranks scores. Differences (Diff.) were calculated subtracting the mean rank score of Group 2 from that of Group 1. Bonferroni corrected significance is reported for each difference (P). * = p ≤ 0.05, ns = p > 0.05**.**

Group One	Group Two	Dextra-BSA		KM24		KM3	
		Diff.	*p* value	Diff.	*p* value	Diff.	*p* value
CL	ML/MCL	-3.91	ns	-6.48	ns	-11	ns
	Control	13.4	ns	12.45	ns	9.17	ns
ML/MCL	Control	17.31	*	18.93	*	20.17	*

4.2.2.2 No cross-reactivity of anti-Gal titres in Bolivian patients with both leishmaniasis and Chagas disease is detected

In sera from chagasic patients, the anti-Gal antibody titres are reportedly 4- to 5-fold higher than in sera from healthy or bacteria-infected individuals [220,298]. Chagas seroconversion takes up to 5 years, indicating that patients deemed negative for Chagas through parasitological methods may still have detectable chagasic anti-Gal, which may cross react with leishmaniasis anti-Gal. There is little in the literature about specific antigen/antibody complexes that are responsible for cross-reactivity between these two parasite infections, however shared surface antigen families have been reported.

Despite previous reported cross-reactivity of leishmaniasis anti-Gal and chagasic anti-Gal, there was no difference in overall recognition of αGal epitopes (at least when using Dextra-BSA, KM24 and KM3) between patients positive for Chagas

infection and those who were negative (Table 4.14), independent of *Leishmania* infection status.

Table 4.15. Differences in anti-Gal titres serum samples from Bolivian individuals with and without Chagas disease. Mann Whitney U tests comparing anti-Gal titres in patients with (Ch^+) or without (Ch^-) Chagas infection, for either control patients or those where *Leishmania* was diagnosed. Mann Whitney U statistic for each test, with corrected test statistic (z). ns = $p > 0.05$.

NGP	Controls				CL/ML/MCL			
	U	z	*p* value	Diff (Ch^+-Ch^-)	U	z	*p* value	Diff (Ch^+-Ch^-)
Dextra-BSA	183	1.10	ns	4.04	209	0.10	ns	0.5
KM24	160	0.35	ns	1.27	187	-0.43	ns	-2.24
KM3	155	0.18	ns	0.66	190	-0.36	ns	-1.87

4.2.2.3 Anti-Gal titres in Bolivian serum using updated NGP panel are increased in active disease compared to healthy controls

KM27, KM28 and KM30 proved most successful in discriminating infected from control sera in the Middle Eastern samples. Therefore, I applied the same conditions used in (Section 4.2.1.5) to measure anti-Gal titres in the remaining Bolivian sera. This equated to 18 CL samples, 3 ML samples and 21 control samples. Due to the small sample number for ML patients, all infected sera results were grouped together for analysis (combined infected patients, n = 21).

Only anti-Gal titres against KM27 and KM30 were significantly increased in infected sera as compared to controls (Figure 4.14, Table 4.15). As before, the BME control showed minimal recognition by all sera types, with RLU <200 in all samples.

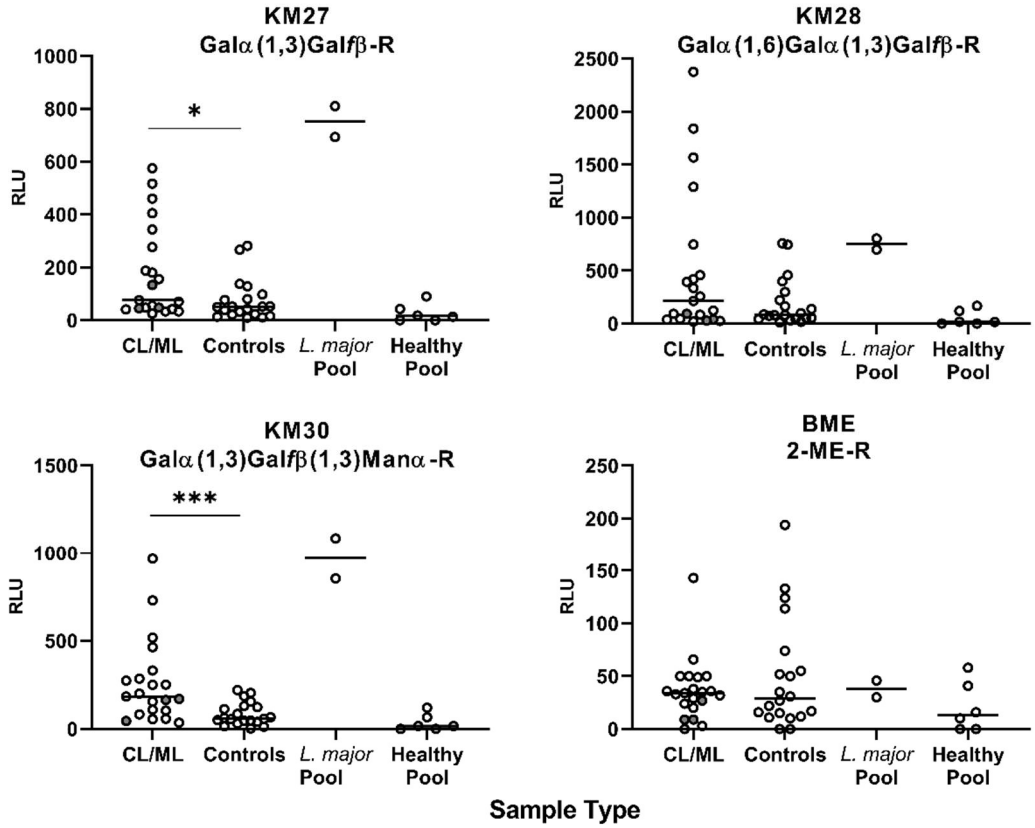

Figure 4.14. Anti-Gal activity in individual Bolivian patient sera with active tegumentary leishmaniasis (all lesion types) or healthy controls against three αGalactosylated NGP (KM27, KM28, KM30 and BME). In the CL/ML group, shaded circles indicate ML patients and open circles indicate CL patients. Only significant comparisons shown. *L. major* and Healthy pools shown for reference RLU values. * = $p \leq 0.05$, ** = $p \leq 0.01$, *** = $p \leq 0.001$.

Table 4.16. Anti-Gal titres against four NGPS (KM27, KM28, KM30 and BME) in Bolivian patient serum samples with active tegumentary *Leishmania* infection, or from healthy Bolivian controls. Mann Whitney U comparison (U) results for comparison of anti-Gal titres in Bolivian serum samples, between healthy controls and patients with tegumentary leishmaniasis (all lesion types). z - corrected test statistic. Diff. * = $p \leq 0.05$, *** = $p \leq 0.001$, ns = $p > 0.05$.

NGP	U	z	*p* value	Diff.
KM27	309.5	2.239	*	8.48
KM28	270.5	1.258	ns	4.76
KM30	347	3.183	***	12.04
BME	224.5	0.101	ns	0.38

4.2.2.4 Two panels of αGal NGPs have moderate diagnostic potential for Bolivian leishmaniasis

As before, the usefulness of anti-Gal titres to discriminate between infected and control patients was assessed through binomial logistic regression followed by ROC curve generation for each NGP individually (Supplementary Table 17 - 19). Significant NGPs were then combined for a secondary analysis.

The results indicate that none of the 7 NGPs in this small screen are useful at discriminating between disease (CL and ML/MCL patients combined, n = 52) or control samples (n =36) (Figure 4.15). The initial screen with Dextra-BSA, KM24 and KM3 had moderate discriminatory power (AUC = 0.6-0.7) (Figure 4.15, Table 4.16). KM3 was the least effective, but the reduction in AUC was very small. The combined model was still poorly discriminative. The second panel demonstrated some improvement, with the combined model having an AUC of 0.79. KM30 was most effective, with an AUC at almost identical levels to the combination model. The second panel screened a smaller number of samples, due to limited volume of serum remaining for many of the patients.

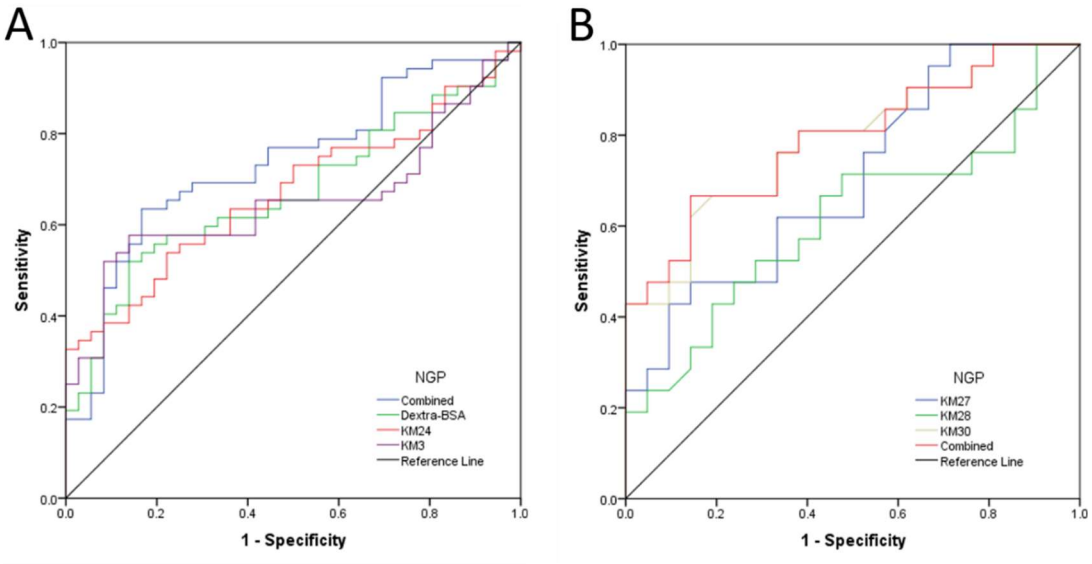

Figure 4.15. ROC curve analysis for Bolivian patient samples with tegumentary leishmaniasis. ROC curves were generated using all CL and ML patient samples combined. Panel A = initial NGP panel. Infected patients (n= 42), control patients (n = 36). Panel B = second NGP panel. Infected patients (n = 21), control patients (n = 21). AUC values for each curve are listed in Table 4.16. Curves above the Reference line (solid black) at 0.5 indicates the test is better than chance at predicting disease state.

Table 4.17. Area under curve (AUC) values for Bolivian patient ROC curves (Figure 4.15). A = initial NGP panel (Dextra-BSA, KM24 and KM3). B = second NGP panel (KM27, KM28 and KM30)**.**

	NGP	AUC	95% CI	
			Lower	Upper
A	**Combined**	0.735	0.630	0.840
	Dextra-BSA	0.669	0.557	0.781
	KM24	0.670	0.559	0.781
	KM3	0.652	0.537	0.768
B	**Combined**	0.791	0.655	0.928
	KM27	0.702	0.545	0.859
	KM28	0.613	0.439	0.788
	KM30	0.787	0.649	0.925

4.2.2.5 Anti-Gal levels are increased in serum samples from patients with active VL caused by *L. infantum* (Spanish cohort)

The Spanish cohort (*L. infantum* infections) was categorised by disease presentation; either visceral (VL) or cutaneous (CL) disease. Samples were collected from some patients following treatment (paired samples), with an additional set of samples without matched pairs (i.e. only active infection, or only cured samples). Control samples were also collected from both healthy individuals from the endemic region (endemic controls) and patients with positive *Leishmania* test, but no symptom of disease (asymptomatic).

Detection of anti-Gal titres in *L. infantum* sera was performed using the most successful panel from the KSA cohorts: KM27, KM28, KM30 and BME as control (Figure 4.16). Due to the paired nature of some of these samples, comparisons were only made between *L. infantum* samples (active or cured infection) and control groups. Mann Whitney U test demonstrated that anti-Gal titres in patients with *L. infantum* infection were significantly increased, compared to both endemic controls and asymptomatic cases, only when the disease was active and visceral (Supplementary Table 20 and Table 4.17). CL cases were indistinguishable from controls, except for active CL titres against KM30. Titres against both KM27 and KM30 were significantly higher in Cured VL cases, compared to healthy controls (but not asymptomatic cases). Of significant concern in this cohort, however, is the

apparent cross reactivity against the BME control in all *L. infantum* positive sera types, including to a limited extent the asymptomatic individuals. BME was in fact the most impressive antigen, performing better than the three galactosylated structures.

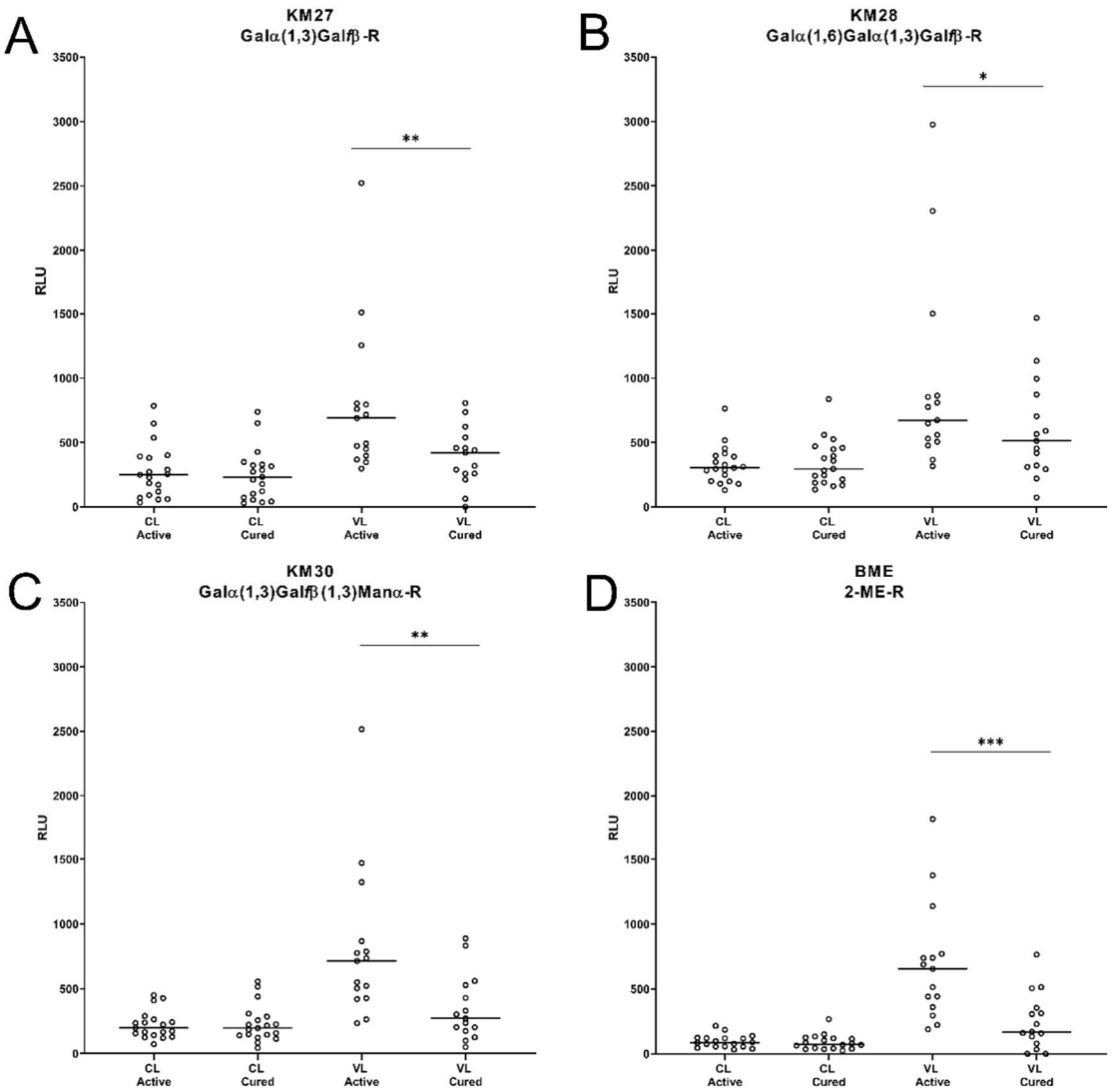

Figure 4.16. Anti-Gal titres in serum samples from infected with *L. infantum*, using a panel of four NGPs (KM27, KM28, KM30 and BME). Antibody titres are plotted as relative luminescence units (RLU), for individual patient serum samples from Asymptomatic (n = 30) or Endemic Controls (n = 30), or patients with *L. infantum* infection. Infected patients are grouped as cutaneous leishmaniasis, either active (Active CL; n = 25) or cured (Cured CL; n = 30), or visceral leishmaniasis, either active (VL Active; n = 20) or cured (VL Cured; n = 37). Each panel corresponds to one NGP - A = KM27, B = KM28, C = KM30, D = BME**.**

Table 4.17. Comparison of anti-Gal titres against four NGPs (KM27, KM28, KM30, BME) between controls groups (Endemic Controls or Asymptomatics) and patients with active of cured *L. infantum*. Mann Whitney U statistic for each test, with corrected test statistic (z). * = p ≤ 0.05, **** = p < 0.0005, ns = p > 0.05.

Group 1	Group 2	KM27				KM28				KM30				BME			
		Mean Rank Difference	U	Z	P	Mean Rank Difference	U	Z	P	Mean Rank Difference	U	Z	P	Mean Rank Difference	U	Z	P
Endemic Controls	CL Active	-9.42	246.5	-2.172	ns	-9.42	246.5	-2.172	ns	-13.05	197	-3.009	*	-22.62	66.5	-5.215	****
	CL Cured	-3.74	394	-0.828	ns	-5.6	366	-1.242	ns	-8.84	317.5	-1.959	ns	-21.16	132.5	-4.694	****
	VL Active	-21.25	555	5.05	****	-18.42	521	4.377	****	-22.67	572	5.386	****	-25	600	5.941	****
	VL Cured	-16.84	869	3.693	****	-11.4	761	2.359	ns	-18.04	872.5	3.736	****	-26.09	1007.5	5.404	****
	Asymptomatic	-3.7	394.5	-0.821	ns	-6.74	349	-1.493	ns	-6.9	346.5	-1.53	ns	3.66	505	0.813	ns
Asymptomatic	CL Active	-4.03	430	0.93	ns	0.4	369.5	-0.93	ns	-5.1	444.5	1.175	ns	-21.19	664	4.885	****
	CL Cured	0.8	438	-0.177	ns	1.6	426	-0.355	ns	-1.14	467	0.251	ns	-21.14	767	4.687	****
	VL Active	-18.42	521	4.377	****	-15.42	485	3.664	****	-20.38	544.5	4.842	****	-24.5	594	5.822	****
	VL Cured	-11.84	786.5	2.452	ns	-3.64	631	0.753	ns	-10.92	753	2.26	ns	-25.68	1000.5	5.317	****

4.2.2.6 Anti-Gal titres in decrease following cure of active VL

15 patients each with VL infection and 19 patients with CL infection had an additional sample taken after clinical cure. A Paired Sample T Test compared means before and after cure in these patients, to determine if anti-Gal titres changed during the test window (Table 18).

There was a significant reduction in antibody titre against all antigens, including the control BME antigen, in VL patients after cure (Figure 4.17). No difference was detected in CL patients. Again, a high level of cross-reactivity was observed against the BME control.

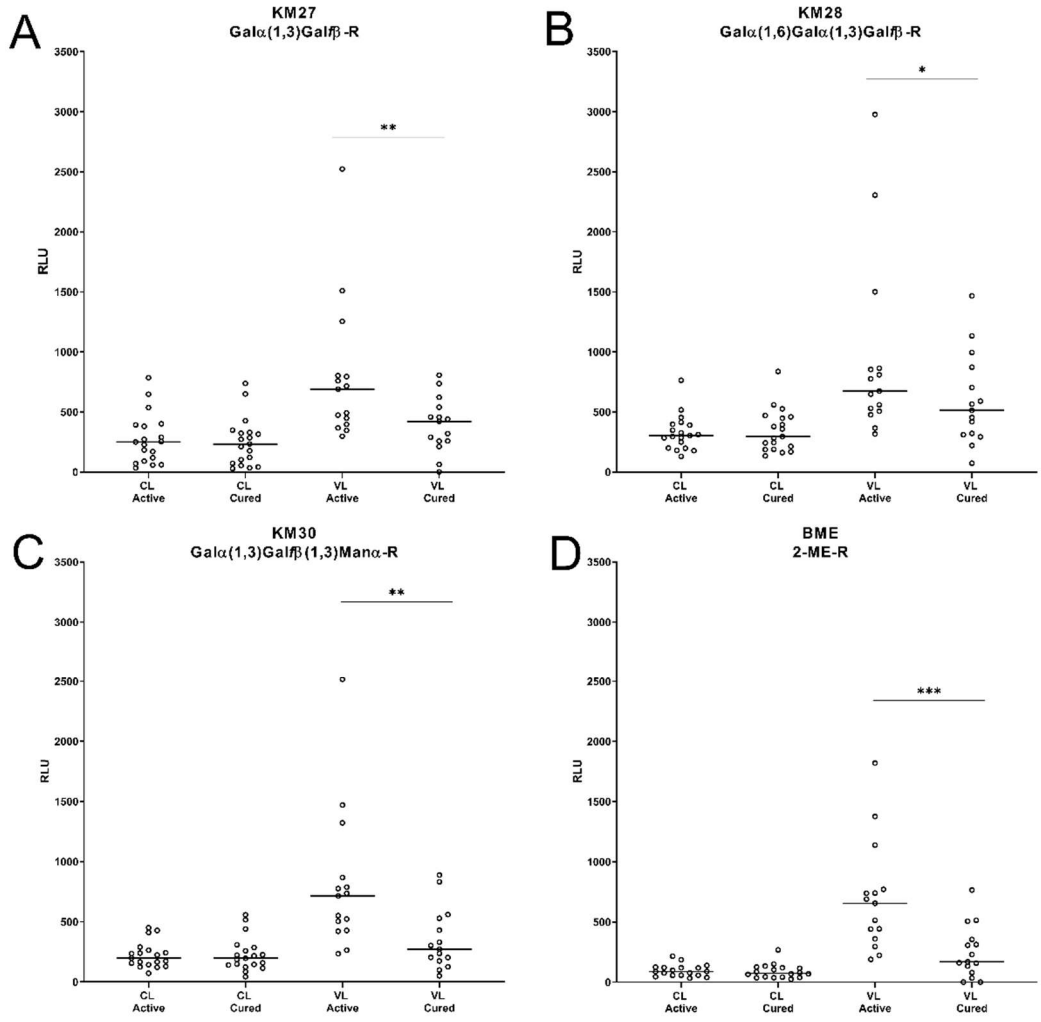

Figure 4.17. Anti-Gal levels detected in paired sera samples of *L. infantum* patients, using a panel of NGPs (KM27, KM28, KM30 and BME). Antibody titres are plotted as relative luminescence units (RLU), for matched pairs of patient serum samples patients with *L. infantum* infection. Pairs are plotted at active and cured infection states, for VL (n = 15) and CL (n = 19). Each panel corresponds to one NGP - A = KM27, B = KM28, C = KM30, D = BME. * = $p \leq 0.05$, ** = $p \leq 0.01$, *** = $p \leq 0.001$, ns = $p > 0.05$.

Table 4.19. Differences in anti-Gal titre before and after treatment in patients with *L. infantum* infection, against four NGPs (KM27, KM28, KM30 and BME). Paired Sample T-Test analysis of change in anti-Gal titre (Diff.), calculated from Active (A) RLU subtracted from Cured (C). One sample is excluded from CL BME analysis, due to its being an extreme outlier. Significance (P) of the test statistic (t) is reported as * = p ≤ 0.05, ** = p ≤ 0.01, *** = p ≤ 0.001, ns = p > 0.05**.**

Disease Type	NGP	Diff. (C-A)	95% CI of Diff.		t	DF	*p* value
			Lower	Upper			
CL	KM27	-24	-58	9	-1.5	18	ns
	KM28	17	-20	54	1.0	18	ns
	KM30	7	-20	35	0.6	18	ns
	BME ‼	-7	-28	13	-0.8	17	ns
VL	KM27	-400	-684	-117	-3.0	14	**
	KM28	-349	-646	-51	-2.5	14	*
	KM30	-458	-721	-196	-3.8	14	**
	BME	-449	-663	-234	-4.5	14	***

‼ n = 18

4.2.2.7 Glycan inhibition of anti-Gal in *L. infantum* infection

A glycan inhibition assay was performed to determine anti-Gal specificity. Pools of sera were preincubated with a range of inhibitory sugars, before assayed against immobilised NGPs on an ELISA plate. For active VL sera, inhibition was fairly uniform across all glycan treatments, indicating the binding to the NGPs may not be due to recognition of αGal residues only, unlike that seen in *L. major* infection (Section 4.1.2.5). BME binding was inhibited to same degree as the αGal-NGPs. No glycan reduced binding by more than 50%, even at 0.5 M concentration (Figure 4.18). Cured VL sera binding to the NGPs was slightly more inhibited, especially against KM28 (Galα(1,6)-R) by the three galactose monosaccharides tested.

The inhibition of VL antibody recognition by this broad range of glycans shows that the NGPs are not binding specific anti-Gal, and further work is required to understand the affinity of the antibodies produced during *L. infantum* infection.

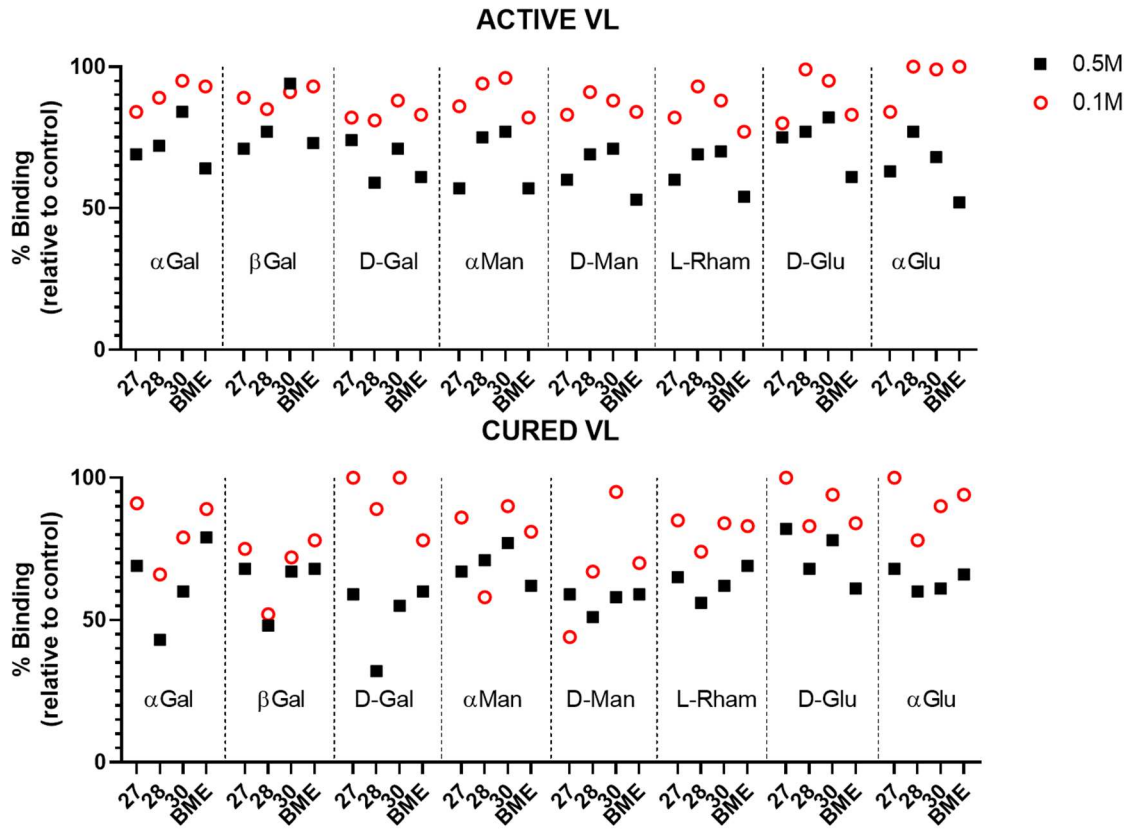

Figure 4.18. Glycan inhibition of anti-Gal recognition of KM30 in pooled *L. infantum* sera. Pooled serum from active (Top) or cured (bottom) VL patients was preincubated with one of eight glycans at either 0.1 M (open circles) or 0.5 M (filled squares). Left to Right: Methyl-D-α-galactopyranose (αGal), Methyl-D-β-galactopyranose (βGal), D-galactose, D-α-mannose (αMan), D-Mannose (Man), L-Rhamnose (L-Rham), D-Glucose (D-Glu) and α-Glucose (αGlu). Reduction was measured relative to an uninhibited control pool.

4.3 Discussion

Previous work has validated the use of synthetic, αGalactosylated NGPs in the detection of *Leishmania* anti-Gal in human sera [103,275,290]. Using a cohort of patients from KSA, Al-Salem and colleagues (2014) detected a significant increase in anti-Gal in patients with either active or cured *Leishmania* infection compared to uninfected patients. However, the synthetic epitope used was not suited to use in diagnostics when differentiating between *Leishmania* infection types, as *L. major* and *L. tropica* samples had similar titres. Any successful diagnostic test would need to accurately distinguish between parasite species. This is a pressing concern for the control of leishmaniasis in the Middle East. A rapid diagnostic test, capable of detecting species-specific antibodies would fill a gap in the current diagnostic tool kit, which relies heavily on dermatologist expertise and microscopy. Furthermore, a diagnostic

tool that detects antibodies in sera could have utility in monitoring response to treatment, as Al Salem *et al*. (2014) data indicates that, despite lesion healing, parasites could persist and continue to generate an antibody response.

The surface glycocalyx of the different *Leishmania* species is rich in immunogenic sugars. Since the specificity and titres of anti-Gal antibodies is likely to vary among *Leishmania* infections, in this Chapter I show the results from the screening and epitope characterisation of these antibodies from infected individuals from three geographically distinct regions, using a panel of non-commercial αGalactosylated NGPs (summarised in Table 4.19).

4.3.1.1 Anti-Gal antibodies as potential biomarkers of *Leishmania* infection?

Screening of the Old World CL samples from KSA have three patient types; active leishmaniasis infection (*L. major* or *L. tropica*), cured CL infection and heterologous non-CL individuals. This latter group is an important control, as these were individuals who presented at a clinic with a skin infection that was suspected to be CL, but subsequently determined to be an alternative skin pathology, such as eczema. Accurate diagnosis of CL is hampered by the overlap of symptoms between many dermatological conditions, and so this is the patient group at most risk of a false-positive diagnostic. Thirteen NGPs were used to screen these samples (Table 4.19). While comparison between the first and second set of assays is complicated by a number of changes to the method, the variation in the glycan component gives insight into the specificity of anti-Gal produced during *Leishmania* spp. infection.

Table 4.20. Summary of anti-Gal titres against fifteen NGPs used to screen sera from three geographically distinct cohorts of patients with leishmaniasis. +/++ = titres are increased in leishmaniasis patients compared to controls. - = no difference between infected and uninfected samples detected. nd = the NGP was not used to detect anti-Gal in these samples. NGPs are grouped based on the terminal glycan/glycosidic linkage. ID refers to the assigned code for each glycan. Dextra is the only commercially sourced NGP in this study, all others are synthesised by Dr Michaels, UTEP. Structure of Glycan is the glycan component of each NGP, where R is the linker-BSA component**.**

Terminal Glycan	ID	Structure of Glycan	Species			
			L. major	*L. tropica*	Bolivian*	*L. infantum*
Galα(1,6)	KM28	Galα(1,6)Gal*f*β	++	-	+	+◊
	KM11	Galα(1,6)[Galα(1,2)]Galβ	+	nd	nd	nd
	KM5	Galα(1,6)Galβ	-	nd	nd	nd
Galα(1,3)	KM17	Galα(1,3)Galα	+	nd	nd	nd
	KM27	Galα(1,3)Gal*f*β	++	-	+	+◊
	KM1	Galα(1,3)Galβ(1,4)Glcβ	-	nd	nd	nd
	KM30	Galα(1,3)Gal*f*β(1,3)Manα	++	-	+	+•
	KM9	Galα(1,3)Galβ	+	nd	nd	nd
	KM24	Galα(1,3)Galβ(1,4)GlcNAcα	nd	nd	+¥	nd
	Dextra	Galα(1,3)Galβ(1,4)GlcNAcβ	nd	nd	+¥	nd
Galα	KM3	Galα	+	nd	+¥	nd
Other	KM8	Galα(1,2)Galβ	-	nd	nd	nd
	KM12	Galα(1,4)Galβ	-	nd	nd	nd
	BME	2-ME	-	-	-	+◊
	KM15	Cysteine	-	-	nd	nd

* Species unconfirmed, majority likely *L. braziliensis*
◊ VL only
¥ Mucosal leishmaniasis only
• CL and VL infection

KM3 (the simplest structure tested, Galα-BSA) was surprisingly useful as a biomarker for *L. major* CL; I had expected the more complex structures to have more discriminatory power. It is possible that monosaccharide αGal is picking up an array of polyclonal anti-Gal antibodies, which are at greater abundance in *L. major* infection than in control sera, and could bind at low affinity to this glycan. Of the three NGPs with terminal Galα(1,6), the trisaccharide KM28 had excellent discrimination between active *L. major* infection and heterologous controls. Anti-Gal titres against this NGP were also increased in cured patients, which may indicate that this NGP would have utility as a biomarker for cure; it is likely that despite

healed lesions, there are very low levels of parasite persistence which can result in reactivation or recurrence after apparent cure [299]. A glycovaccine based on a Galα(1,6) glycotope gave partial protection against an experimental *L. major* infection, and with the results presented in this Chapter, it appears that antibodies against this epitope likely have a role in natural infection [122].
Galα(1,6)Galα(1,3)Gal*f*β-R is based on the structure of *L. major* GIPL-3, which actually has additional Manα at the reducing end. Further development of this NGP type to extend the glycan to include the mannose residues could improve recognition even further.

Changing the second glycan in KM9's Galα(1,3)Galβ from β-galactopyranose to β-galactofuranose, as in KM27, gave much improved recognition by anti-Gal in *L. major* infection. The glycans of *L. major* GIPL-2 have the terminal structure of Galα(1,3)Gal*f*β(1,3)Manα, and the furanose in the second position appears important for recognition. There is not much difference in the discriminatory power between the disaccharide KM27 and the trisaccharide KM30, despite higher anti-Gal titres binding to the latter. The third glycan in the sequence may not be contributing much in terms of specificity of the antibody, and in fact, reduces the sensitivity of assay due to an increase in titres detected in controls. Interestingly, the significant increase of titres in both active *L. major* and cured sera that was detected by KM17 (Galα(1,3)Galα-BSA), indicates that having a Galα in the second position is at least immunogenic as Galβ, despite this structure not reported in *L. major* GIPLs (although it could of course be present on an alternative glycoconjugate).

Based on these results, the combination of galactopyranose and galactofuranose improves detection of anti-Gal more than the extension of the glycan structure from di- to trisaccharide. A combined diagnostic with KM27 (Galα(1,3)Gal*f*β-BSA) and KM28 (Galα(1,6)Galα(1,3)Gal*f*β-BSA) has excellent potential to detect anti-Gal during *L. major* infection, with minimal false positives. The dual antigen assays in Section 4.2.1.9 indicate that the anti-Gal binding to each of these NGPs are distinct populations, and the combination will maximise antibody capture.

Unfortunately, no NGP used in this thesis allowed identification of *L. tropica* patients; anti-Gal titres in the 15 *L. tropica* patients available for this study were indistinguishable from healthy controls using three αGal NGPs. In Chapter 3 and 5, I present evidence that αGal may be expressed by *L. tropica* cells, but at very low levels. This may explain the lack of reactivity of *L. tropica* sera to these NGPs, particularly as only three structures were available to test with these patients (and two of them are very similar to each other). It is likely the NGPs based on *L. major* GIPLs will be failing to detect anti-Gal in *L. tropica* samples, due to low affinity of *L. tropica* sera for *L. major* antigens. Of course, the small sample size here does not allow for definitive conclusions to be drawn, and a much larger cohort is required for investigation.

Some points to consider relating to this dataset remain. The data here somewhat differ to that shown by Al Salem *et al.* (2014), although the overall trend was similar (one NGP detected significantly higher titres in cured patients). This is likely explained by the variation in reagents used as both antigen and antibodies were different, due to discontinuation of the originals from suppliers. Additionally, Al Salem assayed the samples shortly after collection, whereas I accessed them years later. Degradation through long term storage could explain the dampened response seen here, and the lack of distinction between the control (KM15, cysteine-BSA) antigen and the galactosylated NGPs. An important consideration for the results in Figure 4.1 is the demographic differences between the groups. *L. major* infection was fairly evenly distributed across several nationalities, but the cured group was dominated by patients from India (14/31) and the heterologous group dominated by Saudi patients (21/29). As prior exposure to *L. major* will differ due to regional endemicities, antibody titres will also likely differ depending on nationality [81]. It is possible that the differences detected here are at least partly a result of selection bias.

Two NGP panels were utilised in screening Bolivian patient samples, with limited success. Parasite species in this cohort was not confirmed, but likely can be

attributed to *L. braziliensis*, based on epidemiological data for the region. *L. braziliensis* parasites have Type-II GIPLs, like *L. major*, and therefore a predominance of αGalactosylated surface glycolipids. NGPs that are useful in *L. major* diagnosis may therefore also have utility in *L. braziliensis* detection. The first panel, however, gave a combined AUC of 0.74 which indicates potential, but CL patients could not be accurately discriminated from controls. The follow up panel using NGPs based on *L. major* GIPLs (KM27, KM28 and KM30) was more successful but had very low specificity, likely due to the presence of non-*L. braziliensis* infected samples in this cohort. Further investigation should focus on the KM27/KM30 NGPs, as the Galα(1,3)Gal*f*β glycans detected higher titres in active tegumentary leishmaniasis, whereas the Galα(1,6) KM28 did not. However, the small sample size and high variation within each group could be masking true differences, so a larger cohort may improve discrimination.

L. infantum surface GIPLs do not have a predominance of αGal, unlike *L. major* or *L. braziliensis*, and are more similar to *L. tropica* GIPLs in glycosylation. However, patients with VL *L. infantum* infection did demonstrate higher titres against the KM27/KM28/KM30 panel, which were designed based on *L. major* GIPLs. An important caveat remains however; reactivity of sera in *L. infantum* patients (CL or VL, active or cured) was also significantly higher against the BME control. This cannot be attributed to a batch effect (the same stock was used for all assays with all cohorts and stored in aliquots at -80 °C until use) or a technical issue (all reagents, plates and equipment was identical). Furthermore, pooled serum positive and negative controls on each plate did not reflect this unusual pattern; *L. major* and *L. tropica* positive sera always showed minimal reactivity to BME, as did the healthy control pools. Finally, samples of all types were included on each plate so that they would all be subject to identical conditions, and the high titres are consistently detected only in *L. infantum* positive samples. In case this was due to excessive concentrations of reagents, I performed a separate assay with much lower antibody and NGP concentrations, and the trend was identical (data not shown). Therefore, I must conclude that there is an unusual, and unexplained cross

reactivity of *L. infantum* sera against some part of the NGP, potentially the BSA component. Therefore, based on the results shown in this Chapter, it is not possible draw conclusions on specificity of anti-Gal titres in *L. infantum* infection.

Reassuringly, the reported cross-reactivity between antibodies that bind blood type B antigens and pathogen αGalactosylated surface molecules was not detected in this analysis [204]. It should be noted that there are very few individuals with AB type blood in the 2017 KSA cohort, but this is reflective of the population; 3.8% of the Saudi population are Type AB [300]. Patients with Chagas infection reportedly demonstrate significant increases in anti-Gal titres, compared to healthy controls [301]. This potential cross-reactivity would confound the use of an antibody diagnostic in certain regions, if the biomarker is not sufficiently specific for *Leishmania*. Differential anti-Gal titres against the NGPs used in this chapter was not detected between patients with Chagas co-infection, *vs* patients without Chagas. These two important barriers to an anti-Gal RDT are not an issue with this antigen set, for the patients tested.

4.3.1.3 Specificity of the repertoire of anti-Gal antibodies in Old World cutaneous leishmaniasis

The results of inhibition experiments showed an interesting relationship between the glycan used and the sera type. While galactose (both αGal and βGal) showed similar levels of inhibition across all sera types, αMan was particularly effective at reducing *L. tropica* sera binding to all NGPs. *L. major* sera was relatively unaffected, even at 0.5 M αMan. These results, taken together with the known mannosylation of *L. tropica* surface glycoconjugates, indicates that *L. tropica* mannose-containing antigens may be generating an immune response that is otherwise undetected by TLC or other methods. Alternatively, immunogenic mannose residues may be part of another type of glycoconjugates yet to be characterised. It must be noted that the conditions used in these CL-ELISAs resulted in very low levels of *L. tropica* binding even in the controls, with RLU <100 in almost all cases, and therefore these results may be exaggerating what is, in reality, a small effect. Healthy Saudi sera was also more susceptible to mannose interference in binding, when compared to

UK healthy controls. The degree of cross-reactivity hinted at through this experiment is surprising. The literature indicates that anti-Gal antibodies are highly specific to galactose in the alpha-configuration, but as binding to these NGPs can be inhibited by 0.1 M βGal, it is unclear how much of the binding detected in these assays can be attributed to these antibodies alone.

Taken together with the detection of polyclonal antibodies in the dual antigen assays, it is likely that the NGPs are binding a population of both specific and polyclonal antibodies. A second assay should be conducted, using antigen at a high enough concentration to allow detection of binding in controls, and therefore calculation of any change in binding levels in experimental wells.

However, questions of specificity and polyclonality remain. The degree of inhibition by βGal was unexpected, and indicates, at the very least, that the NGPs based on αGal-terminating structures may face issues of cross-reactivity with βGal and α-mannose containing structures. It is unfortunate as these glycans are frequently found in nature and are a common feature of microbial pathogens faced by the human immune system. However, the controls used in this cohort are representative of a number of other dermatological infections, and false positives were minimal using the KM27-KM30 set.

4.3.1.2 Anti-Gal titres during chemotherapeutic treatment of *L. major* infection

The 2017 collection had a large advantage over the earlier KSA cohort in that several patients had multiple samples allowing a longitudinal assessment of anti-Gal throughout treatment. However, as visits were not at consistent set time points (i.e. one month post-diagnosis, six months post-diagnosis) or strictly categorised into treatment types, it's unsurprising that there were no consistent differences across the time points. Another complication of this dataset is missing information regarding treatment; it's unclear where some patients were in their treatment cycle, i.e. were they still under antibiotic treatment when the sample was taken, or had they completed the course. Considering these caveats, I decided to categorise

the patients based on visit number, assuming that, as cured patients do not return to the clinic for further treatment, and treatment assignation follows a specific sequence, the 15 patients with three visits are similar enough to warrant investigation.

Anti-Gal titres have been noted to persist for months in CL infection, and years in VL infection, following successful treatment, the short duration between first and final visit is unlikely to be long enough to detect reduction in circulating antibodies. A more useful study would follow up patients beyond treatment conclusion, to understand further how anti-Gal titres correlate with active *vs* past infection. Similar analysis in *L. infantum* infection did detect a reduction in antibody titre following cure in visceral infections, however, the specificity of these antibodies is in doubt, and this requires more investigation.

4.3.1.4 Correlation with CRP, DNA, lesion number and antibody titres

Antibody-based tests suffer from issues of sensitivity and could fail to detect low titres [302]. Antibody level variation between patients is a result of several complex factors, and in this Chapter, I investigated three; parasite burden, lesion number and disease severity. Antibody titre has been shown to positively correlate with lesion number, in both Old and New World CL [302,303]. Conversely, Sousa-Atta (2002) detected an inverse relationship between IgE antibody levels and lesion number, in a cohort of patients from Brazil. CRP levels and lesion number can be considered measures of disease severity [304–307]. Cases where multiple lesions occur may reflect an inability of the immune response to control infection, or a more advanced state of disease progression. Multiple lesions would cause more tissue damage, and therefore immune stimulation, including circulating antibodies against *Leishmania*. I have used CRP detection as a proxy for inflammation as it is a general marker of tissue damage, and increased levels are detected in several infectious diseases including VL, although less well studied in CL [307,308]. CRP levels can also be a useful marker of treatment efficacy in VL; elevated CRP levels remain high for up to three months in VL infection, and higher levels indicate slower parasite clearance [308–310].

Parasite number (estimated from qPCR analysis by Yasser Al Raey, for *L. major* infected patients in the 2017 cohort) had weak positive correlation with anti-Gal titres, and this was only significant for KM30. Conventional diagnosis of CL relies on heavily microscopy, which has limited sensitivity particularly when parasite numbers are low. These results indicate that detection of anti-Gal is sensitive to even the lowest parasite burdens, a substantial improvement on existing diagnostic methods. Lesion number has no linear relationship with anti-Gal titre. This is potentially due to the tendency of *L. major* infection to result in single lesions. This is reflected in this cohort with the majority of cases showing 1 or 2 lesions (24 out of the 44 patients included in this analysis). While CRP levels are higher in *L. major* infected patients than controls, there was no correlation with any other disease characteristic. In the Bolivian cohort, I was also unable to detect any difference in anti-Gal titre between patients with cutaneous lesions, and those with the more advanced pathology of mucosal lesions, despite reported increases in antibody titres associated with disease progression in NWCL [303]. This relationship requires further investigation (the sample size was small), but, as with parasite number, anti-Gal titres are independent of general inflammatory responses.

Ridley & Ridley (1984) reported that antibody infiltration into lesions is increased when parasite numbers are low, and a localised, lesion immune response differing to systemic levels is common for many immune complexes/effectors in *Leishmania* infection. Systemic CRP levels were unaffected in BALB/c mice infected with *L. major* parasites [311], and similarly the assays used here, may be failing to detect a localised response as described by Ridley and Ridley (1984).

4.3.1.5 Concluding Remarks

I found that while tegumentary leishmaniasis patients from Bolivia, or with *L. major* infection from KSA recognised terminal Galα(1,3)Galβ(1,4) NGPs, CL patients with *L. tropica* infection did not. Furthermore, sera from *L. major* infected individuals showed reactivity with terminal Galα(1,6)Galβ. Patients with *L. infantum* only had

higher anti-Gal titres with visceral disease, although cross-reactivity to the control in these assays requires additional investigation.

In summary, I have shown that three αGal-terminating NGPs are excellent discriminators of *L. major* from *L. tropica* infection, but also of *L. major* infection from healthy individuals. With further development, there is potential for their use in New World settings, due to lack of cross-reactivity with anti-Chagas antibodies. Detection of seropositive patients is robust, despite low parasite and lesion numbers.

Chapter Five
Detection and partial characterisation of surface αGalactosylated antigens from Leishmania spp.

5.1 Introduction

The detection of αGal epitopes on the surface of *L. major* cells and other kinetoplastid parasites, has been widely reported in the literature and discussed in the introduction of this thesis (Section 1.11). However, as previously mentioned, no such epitope has been detected on the surface of *L. tropica* cells. This in itself is not especially noteworthy, except when considered alongside the reportedly high levels of anti-Gal detected in *L. tropica* patients [217].

In the context of the evolutionary role of serum anti-Gal antibodies as a major protector of humans and higher primates against infectious disease, it is unsurprising that a successful, human kinetoplastid pathogen would not express surface αGal residues [312,313]. It would be highly advantageous in terms of immune system evasion to have lost (or to otherwise lack) the expression of this well-recognised epitope. A recent study has shown that a αGal-based glycovaccines offers a degree of protection against *L. major* infection in αGal-KO mice, supporting previous hypotheses about the evolutionary advantage of anti-Gal acquisition [122,201,314]. There is a key difference in the life cycles of *L. major* and *L. tropica*; *L. tropica* infections are largely anthroponotic, that is, human-to-human transmission via the vector, whereas *L. major* is found in many animal species, as well as humans [49]. With this in mind, it is perhaps more likely that *L. tropica* will lack (or produce fewer of) the antigenic glycoconjugates that can lead to a robust protective immune response, whereas *L. major*, faced with less evolutionary pressure against αGal expression will continue to benefit from the (assumed) non-immune related functions of these glycans when infecting non-human mammals.

However, if this is the case, what is responsible for generating the anti-Gal in *L. tropica* patients? Antibody binding to αGal in *L. tropica* infection requires that the epitope be accessible to the immune system, although this does not necessarily mean it must be an external, surface structure, as cryptic epitopes can be exposed to the immune system on cell death and lysis. To understand the antibody

specificity of anti-Gal for *L. tropica*, it is necessary to localise and characterise the epitope that is recognised by anti-Gal.

In this chapter, I detail the methods used to attempt purification of anti-Gal antibodies from patient sera using a commercially available NGP. In addition, results are shown on the labelling of *in vitro* cultured *Leishmania* cells using *Griffonia simplicifolia* Lectin I isolectin B4 (IB4 lectin), which is specific for αGal residues [283,315].

5.2 Results

Localising the binding of anti-Gal to cultured *Leishmania* cell required purification of antibodies from infected sera. Affinity chromatography exploits the strength of binding between antibody-antigen pairs, excluding non-binding antibodies from the final eluate. However, as no resin for the purification of anti-Gal is commercially available, I attempted to make my own.

5.2.1 Anti-Gal purification from *L. major* infected sera

Historically, researchers purifying anti-Gal from sera have used Synsorb 115 resin, manufactured by Chembiomed, (Alberta, Canada), which has subsequently ceased trading. To address this lack of specific resin, I used a Protein G column to enrich for IgG antibodies, followed by either a bespoke column of αGal-BSA conjugated to resin, or nitrocellulose membrane coated in αGal-BSA.

5.2.1.1 Anti-Gal purification using Dextra-BSA column resulted in low yield

Initially, I trialled antibody purification from sera using a series of columns. The first was a Protein G column, selected for its high affinity to all human IgG subtypes, in order to acquire a sample of IgG at a known concentration. This IgG sample was then applied to a column made through conjugation of a commercial NGP to NHS-activated agarose, exploiting the primary amines on the BSA component of the NGP. The acquisition of synthetic glycan with an easily conjugatable linker was challenging. Whilst I had an array of structures to hand (Methods Section 2.4.1,

Table 2.1), I opted to use Dextra-BSA (Galα(1,3)Galβ(1,4)GlcNAc-BSA) in order to represent the classic "Galili" epitope, in hopes of capturing this important population of antibodies. Additionally, this glycan being commercially available through Dextra Labs would be more easily acquired than the bespoke NGPs synthesised by UTEP collaborators. However, on elution from the second column there was no detectable protein in the final, concentrated sample. Repeated attempts using longer incubation (i.e. 4 °C overnight) or repeated application of the sera flow through back on to the column, increased the yield marginally. This low yield is potentially due to the use of Dextra-BSA, rather than the unconjugated glycan originally intended. It was clear that some of the NGP had bound to the column (measured through a reduction in the before and after protein concentration), however possibly the column was too small (0.5 mL) to bind a large enough quantity of antibody. Additionally, I investigated whether the method of elution from the column could be optimised, using a 0.5 M D-galactose solution for competition elution as compared to low pH elution buffer. Neither option offered a significant improvement in yield. Due to the high costs associated with scaling up this method, I decided at this point to attempt an alternative as the yield was too low to be useful.

5.2.1.2 Purification of anti-Gal from *L. major* infected sera using glycan-coated nitrocellulose

Nitrocellulose strips were incubated with Dextra-BSA in solution, before incubation of the coated strips in diluted *L. major* infected sera. Antibody bound to the Dextra-BSA was eluted with low pH buffer (termed anti-Dextra antibody). All fractions of the final elution from the nitrocellulose strip were pooled and dialysed into PBS, reducing the total volume to around 50 µL. Protein concentration was assessed through BCA quantification. The fractions collected were the FT (unbound IgG) and the final elution. A sample of the whole sera was kept as a comparison, as was a sample of the diluted sera that was applied to the column. This method resulted in successful purification of anti-Dextra antibody, as confirmed through a number of SDS-PAGE, western blot and dot blot experiments (Figures 5.1-5.6).

Samples were loaded onto a 12.5% gel at 1.5 µg/lane, or for whole sera, at 1:1000 dilution. The expected banding pattern was clearly seen in the eluted sample, with bands with an apparent molecular mass on SDS-PAGE of 50 kDa and 25 kDa, which correspond to the heavy and light chains of human IgG, respectively [316] (Figure 5.1).

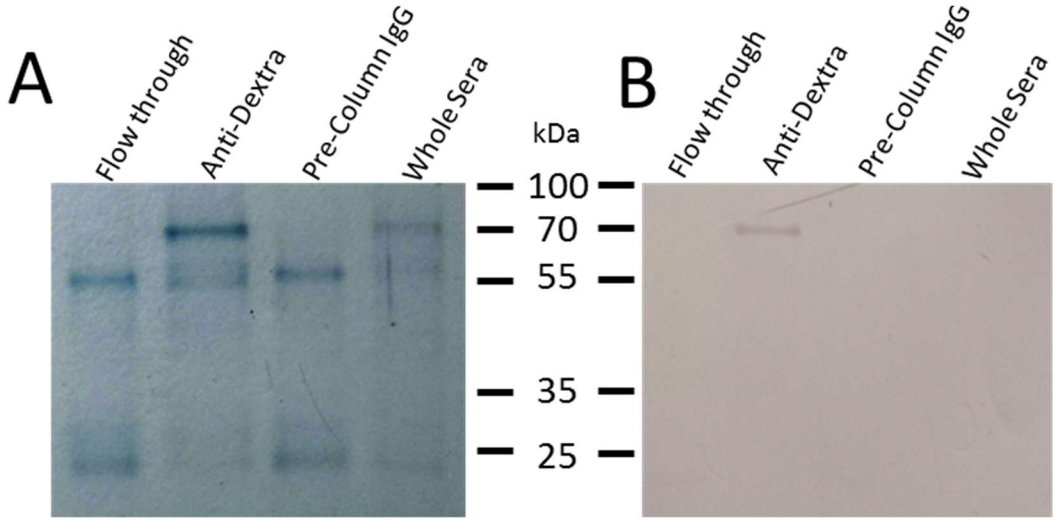

Figure 5.1. SDS-PAGE analysis of purified anti-Gal antibodies. A. Coomassie blue stained 12.5% protein gel showing IgG band pattern after elution. B, nigrosine nitrocellulose staining control after transfer and development. Flow through (unbound sera), anti-Dextra and Pre-Column IgG samples loaded at 1.5 µg/lane. Whole sera pooled from *L. major* positive patients was diluted 1:1000 before mixing with sample buffer**.**

This was confirmed through transfer to nitrocellulose and probing with Goat anti-Human IgG-HRP antibody. Signal was again clearly detected in the expected 50 kDa and 25 kDa pattern. (Figure 5.2).

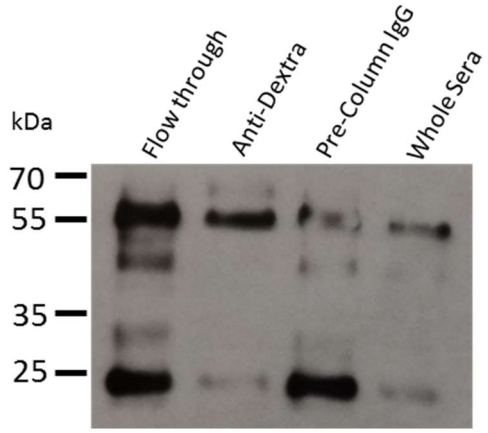

Figure 5.2. Recognition of purified anti-Gal from *L. major* positive sera by anti-IgG antibody. Nitrocellulose membrane with transferred proteins was incubated with HRP conjugated anti-Human IgG and processed for ECL development. Flow through (unbound sera), anti-Dextra and Pre-Column IgG samples loaded at 1.5 µg/lane. Whole sera pooled from *L. major* positive patients diluted 1:1000**.**

5.2.1.3 Galactosidase treatment of glycan, and glycan inhibition of purified antibody abolishes recognition by anti-Dextra

The next step was to confirm that the eluted antibody was specific for the αGal glycan structure, and not non-specific IgG contaminating the FT, or antibodies recognising the BSA component of the NGP.

Treatment with CBAG removes non-reducing terminal α(1,3/4/6)galactosyl residues [285]. Incubation of Dextra-BSA with CBAG removes the final glycan in the trisaccharide, leaving a Galβ terminating disaccharide, and rendering the glycan unrecognisable to anti-Gal antibodies (Figure 5.3A). To confirm that the eluted IgG recognised the Dextra-BSA glycan structure, a simple dot blot assay was performed (Figure 5.3B). 0.1 µg Dextra-BSA was incubated overnight with either CBAG or buffer, and spotted onto nitrocellulose, alongside BSA negative control. The membrane was incubated with 1 µg/mL anti-Dextra. Signal was detected in the untreated sample only, indicating that cleavage of the terminal Galα(1,3)-R abolished recognition by the purified antibody.

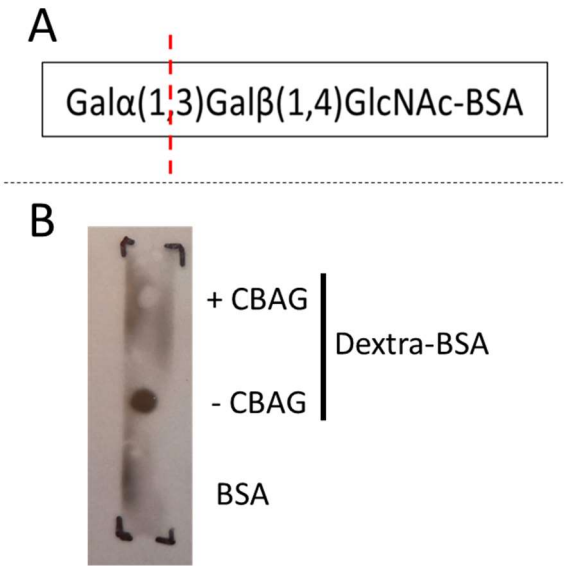

Figure 5.3. Dot blot shows treatment with CBAG blocks recognition of purified anti-Dextra antibody. A. Representation of cleavage site for CBAG on Dextra-BSA. B. Dot blot of enzyme treated and untreated Dextra-BSA spotted onto nitrocellulose (BSA was used as negative control). The membrane was probed with anti-Dextra antibody eluted from Dextra-column.

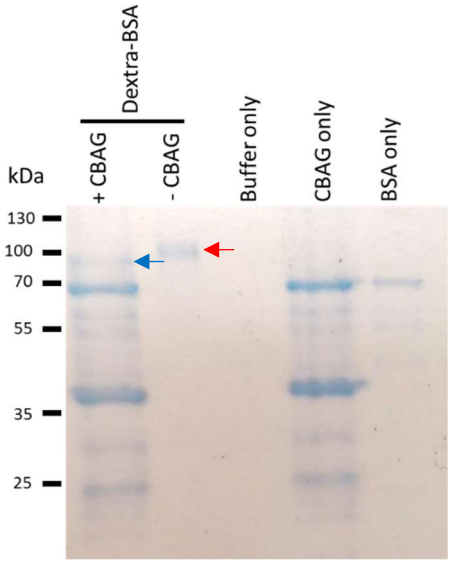

Figure 5.4. SDS-PAGE analysis of CBAG-treated Dextra-BSA. Coomassie blue staining of 12.5% agarose gel. The Dextra-BSA band (red arrow, ~88 kDa) migrates with a reduced apparent molecular mass after treatment with CBAG (blue arrow, ~83 kDa). The BSA carrier protein for the enzyme is visible in both CBAG lanes.

Following detection in a dot blot format, western blotting was used to confirm specificity more robustly, using both IB4-HRP lectin and the purified anti-Dextra antibody. Dextra-BSA was either mock-treated or incubated overnight with CBAG, and loaded on to a 12.5% polyacrylamide gel, alongside controls (BSA, CBAG alone and buffer alone). After the proteins were separated through electrophoresis, the gel was stained with Coomassie blue to confirm reduction in apparent molecular weight of the enzyme-treated glycan (Figure 5.4). The Mw shift is clear (comparing lane 1 and 2), where the band of untreated Dextra-BSA shifts from ~88 kDa to a band closer to 83 kDa. After Coomassie staining, the BSA carrier protein for the enzyme is distinctly visible in both enzyme-containing lanes.

A 12.5% polyacrylamide gel was loaded with CBAG-treated Dextra-BSA (0.1 µg/lane Dextra-BSA, 0.1 U/lane CBAG), untreated Dextra-BSA (0.1 µg/lane Dextra-BSA), CBAG only and Buffer only controls. The separated proteins were transferred to nitrocellulose and probed with either anti-Dextra (Figure 5.5A) or IB4-HRP (Figure 5.5B). Signal was detected only in lanes with untreated glycan, and not in lanes with treated glycan, or enzyme alone. Some recognition of BSA in the lanes with enzyme

was seen when incubated with anti-Dextra antibody, but this is most likely non-specific recognition due to the large amount of the BSA carrier in the enzyme sample (compare to Figure 5.4)

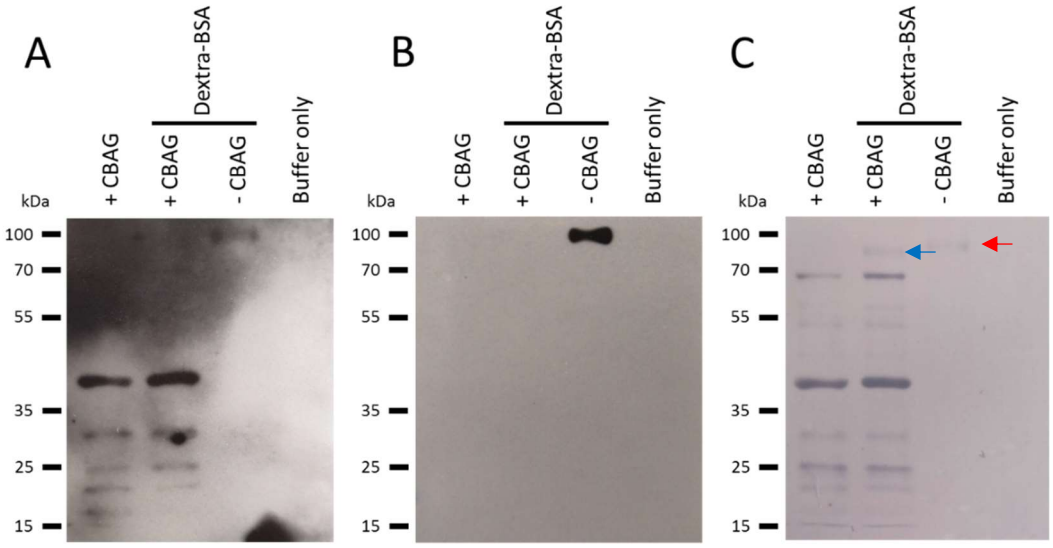

Figure 5.5. Recognition of Dextra-BSA by purified antibody and IB4-HRP lectin, following treatment with CBAG. A. Western blot showing specificity of anti-Dextra for αGal-terminating glycan. B. Lectin blot showing specificity of IB4-HRP for αGal-terminating glycan. Untreated Dextra-BSA band at ~88 kDa. C. Nitrocellulose membrane stained with Nigrosin. The Dextra-BSA band (red arrow, ~88 kDa) shows a reduced molecular mass after treatment with CBAG (blue arrow, ~83 kDa). The BSA carrier protein of the enzyme is also recognised by the purified antibody**.**

An experiment was performed to confirm the specificity of anti-Dextra through glycan inhibition. A 12.5% polyacrylamide gel was loaded with Dextra-BSA in four lanes. The proteins were then transferred to nitrocellulose and cut into four strips. IB4 lectin and anti-Dextra were each incubated with 0.5 M galactose for one hour, prior to incubation with the nitrocellulose strips. When the 0.5 M galactose was present, recognition of Dextra-BSA was inhibited completely for IB4 (Figure 5.6A) and reduced for anti-Dextra (Figure 5.6B), although the resolution for these films is poor due to high background signal for anti-Dextra.

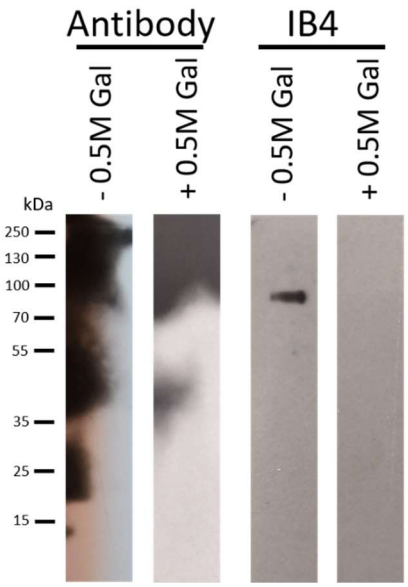

Figure 5.6. Inhibition of anti-Dextra and IB4-HRP recognition of Dextra-BSA, with 0.5 M D-galactose. SDS-PAGE of Dextra BSA loaded at 0.1 µg/lane and transferred to nitrocellulose membrane. Strips incubated with purified anti-Dextra antibody (Antibody) or IB4-HRP (IB4), preincubated with either 0.5 M D-Galactose (+) or buffer without D-galactose (-). Dextra-BSA migrates band at ~88 kDa.

Taken together, these results confirm the specificity of the purified anti-Dextra antibody for the trisaccharide (Galα(1,3)Galβ(1,4)GlcNAc-BSA).

5.2.2 Lectin fluorescence analysis of *Leishmania* promastigotes

An attempt to localise αGalactosylated epitopes on the surface of *Leishmania* parasites was made using anti-Gal antibodies. Methods were first validated using IB4 lectin, which is specific for αGal-terminating glycans, using *L. major* (as this species has known αGalactosylated surface lipids), before progression to *L. tropica* cells.

5.2.2.1 IB4-labelling of *L. major* promastigotes

L. major promastigotes were labelled with IB4-AF488, to localise the αGal-terminating residues during this life stage. The specificity of labelling was then confirmed through incubation with inhibitory glycan.

Initial difficulties in establishing this protocol required lengthy troubleshooting (summarised in Table 5.1). It was not clear if the problem lay in 1) high background/non-specific staining of the lectin masking true signal, 2) degradation or

other problem with the inhibitory glycan, or 3) technical error. When cells were fixed with PFA (either 1% or 4%) only, no stain was observed. This is possibly due to the epitopes (likely localised on the relatively short GIPLs) being inaccessible without a stronger method of fixation/permeabilisation. The addition of Triton-X was also unsuccessful, due to changes in cell morphology. However, when cells were fixed with 100% methanol (alone or following PFA fixation at 4%) bright fluorescence was visible throughout the parasite cytosol. Titration experiments allowed the selection of 5 μg/mL IB4-AF488 lectin as an acceptable level of signal, with minimal background green staining. While it was expected that the brightest stain would be localised to the cell surface, in promastigotes this was not the case, for reasons discussed below. Specificity was confirmed through the incubation of the lectin with 0.5 M of an inhibitory glycan, for one hour at 27°C (Figure 5.7, Table 5.2).

Table 5.1. Summary of conditions optimised during method development for the IB4-lectin stain of *L. major* promastigotes

Step	Conditions	Results
Washes	Presence of Tween	No difference
	Duration (5 x 1 min, 3 x 5 min, 1 hour, overnight)	3 x 5 minute optimal for minimal background
Buffer	PBS vs TBS	TBS optimal
	Salt concentration (0.1mM or 1mM)	1 mM
Fixation	Methanol, PFA, Triton X	Methanol only successful reagent
Block	Type	BSA and Human serum at 5% gave comparable bright stain. BSA selected for ease of use, reproducibility
	Incubation length (1 hour, 2 hours, overnight)	No difference, when block at 5%. With block at 1%, overnight was optimal.
	Concentration	1% sufficient for overnight, although gave lowest background.
	Presence of Glutaraldehyde	Inclusion during fixation had no influence on background level
Lectin	Concentration Range from 1- 20 ug/mL	5, 10 and 20 gave excellent stain, and 5 ug/mL and below showed complete inhibition.
	Incubation length (1 hr, 2 hr, 3 hr, overnight)	1 hour sufficient, similar results with 4C overnight.

Table 5.2. Summary of results testing inhibition of IB4 binding to *L. major* promastigotes by various glycans.

Glycan	Range Tested	Result
methyl-α-D-galactopyranoside	0.1 up to 1.5M	Some inhibition at 1M, but not complete.
galactose	0.1 up to 0.5M	Inhibition at 0.5M
methyl-β-D-galactose	0.1 up to 0.5M	No inhibition
melibiose	0.1 up to 0.5M	No inhibition
methyl-α-D-glucopyranoside	0.5M	No inhibition
methyl-α-D-mannopyranoside	0.5M	No inhibition

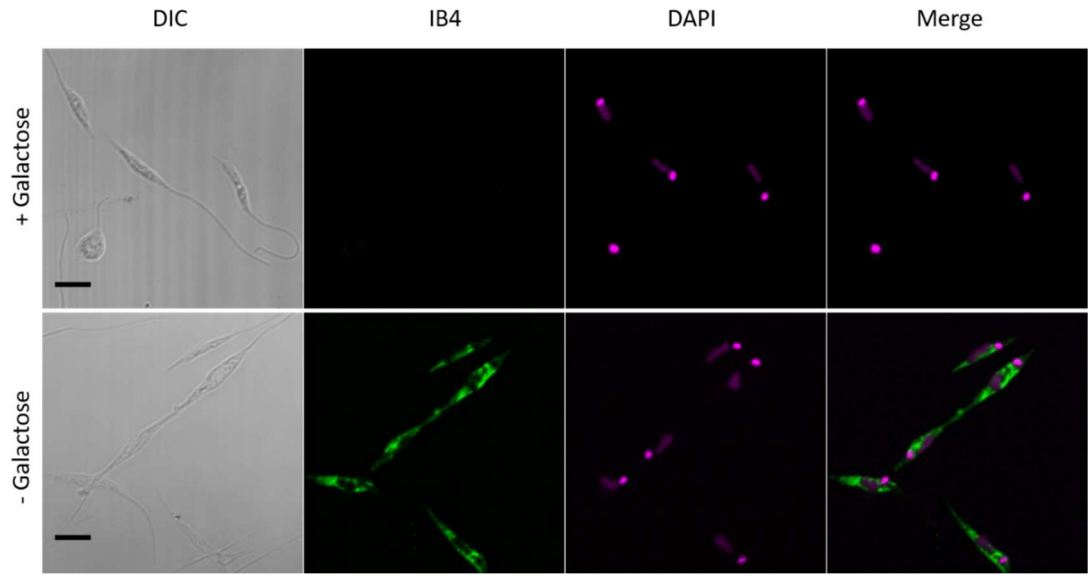

Figure 5.7. IB4 staining of *L. major* promastigotes is inhibited by 0.5 M D-galactose. Top Panel: IB4-AF488 lectin was pre-incubated with 0.5 M D-galactose. Bottom: IB4-488 without preincubation. Left to right: DIC, IB4, DAPI, merged fluorescence. Scale is 5 µM.

5.2.2.2 IB4-labelling of *L. tropica* promastigotes

L. tropica promastigotes cells showed a similar pattern of stain compared to *L. major* promastigotes. The level of fluorescence is considerably reduced in *L. tropica*, reflecting perhaps a lower amount of glycan on the parasite surface, or a low affinity/non-specific recognition. As this binding is inhibited by the presence of 0.5 M galactose, and to a lesser extent 0.5 M D-mannose, it may be a combination of these factors accounting for the reduced signal (Figure 5.8).

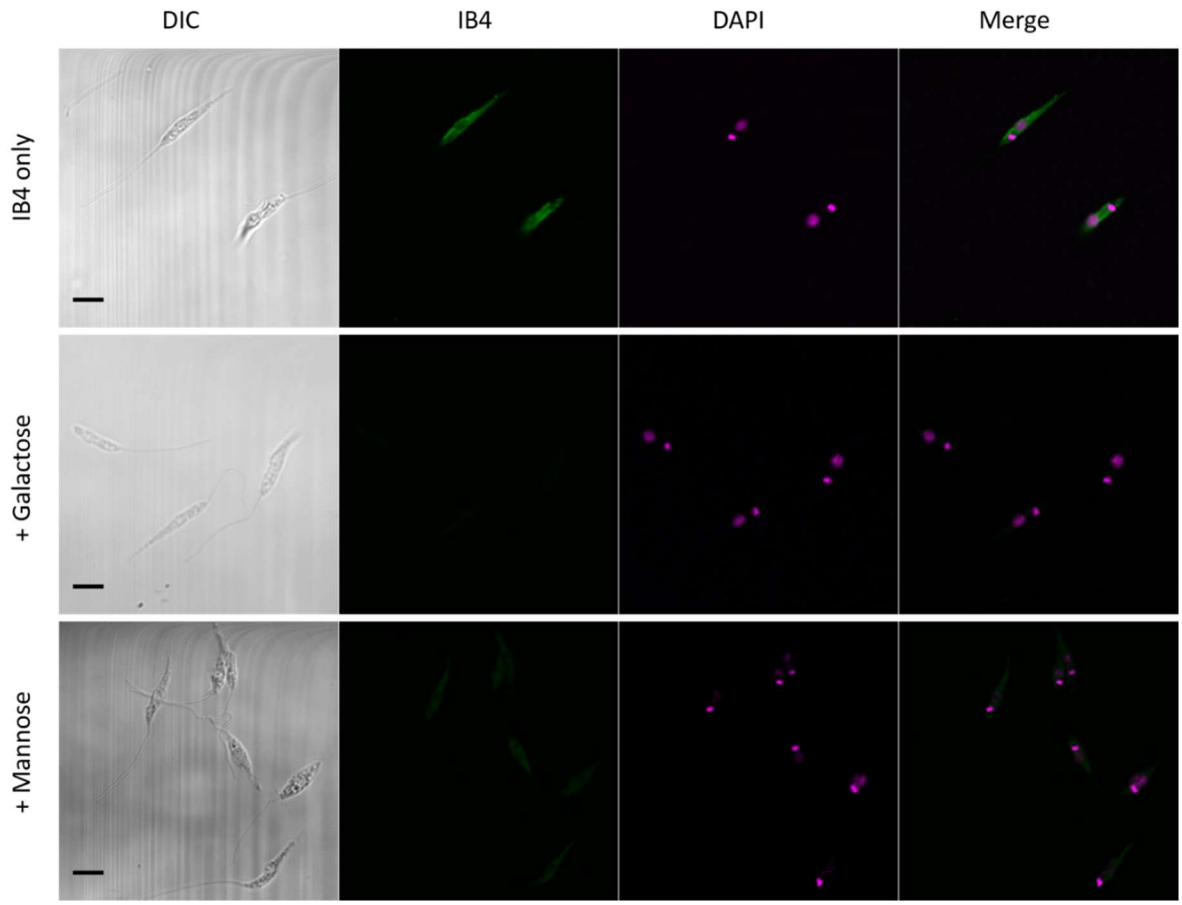

Figure 5.8. Pre-incubation with either galactose or mannose inhibits binding of IB4 lectin to *L. tropica* promastigotes. Top to bottom: uninhibited IB4-AF488, IB4-488 pre-incubated with 0.5M αgalactose or IB4-AF488 pre-incubated with 0.5M D-mannose. Left to right: DIC, IB4-AF488, DAPI, Merged fluorescence. Scale is 5 µM.

5.2.2.3 IB4-labelling of *L. major* amastigotes

While the GIPLs profile of *L. major* is reportedly invariant throughout the life cycle, other surface glycoconjugates are up or down regulated, reflecting their various, life stage-specific functions [235]. This may change availability of surface glycans for binding by antibodies at promastigote stages compared to amastigotes. Therefore, I extracted amastigotes from THP-1 cells, and labelled with IB4-AF488 to search for the location of αGalactosylated epitopes. Anti-paraflagellar rod (PFR) was used to confirm the cells were amastigotes (truncated flagellum as compared to promastigotes).

This protocol proved difficult due to the delicate touch required for extraction from infected macrophages. Increased addition of SDS gave a higher yield of extracted

parasites but resulted in degradation, malformation and death of the amastigotes. One experiment resulted in extraction and staining, and successful inhibition of IB4-AF488 through incubation with 0.5 M galactose (Figure 5.9).

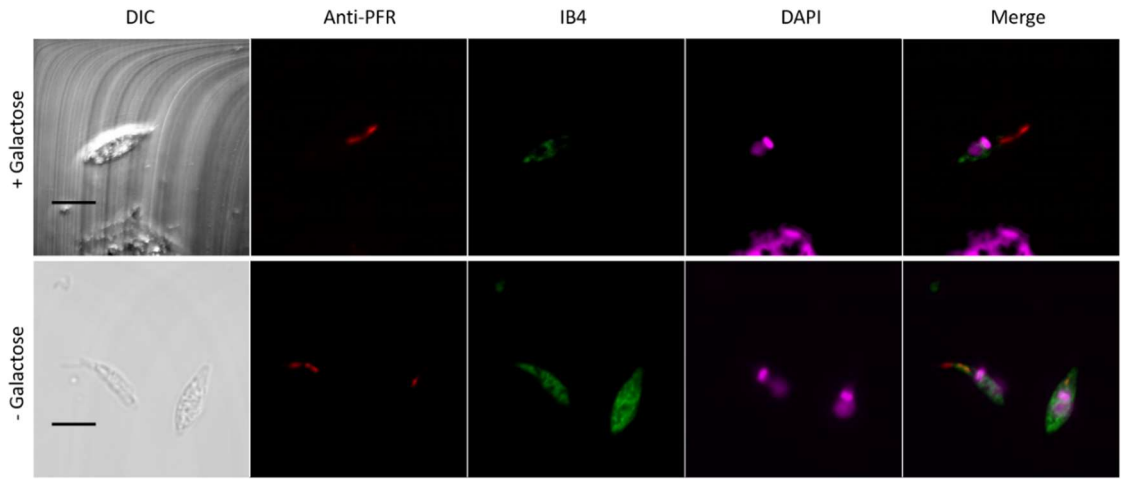

Figure 5.9. IB4-AF488 labelling of *L. major* amastigotes extracted from THP-1 cells. Top Panel: IB4-AF488 preincubated with 0.5M galactose. Bottom Panel: IB4-AF488 without preincubation. Left to right: DIC, anti-PFR. IB4-AF488, DAPI, merged fluorescence. Scale is 5 μM.

5.2.2.4 IB4-labelling of *L. major*-infected THP-1 cells

Due to difficulties extracting viable amastigotes for labelling, I subsequently focused on staining amastigotes *in situ*, without prior extraction from the THP-1 host cell. IB4 labelling of *L. major* amastigotes within human THP-1 cells showed bright surface stain of the intracellular parasites (Figure 5.10). There was also diffuse green staining with the cytoplasm of the THP-1 cells. It has been reported that N-glycosylated proteins from THP-1 cells could contain terminal galactosyl residues, but these are highly unlikely to be in the α-configuration, based on the structural analysis of these glycans and the lack of a human αGalactosyl-transferase that would be capable of producing such structures [317]. IB4 lectin is reportedly specific for terminal αGal residues, so is unlikely to be recognising other structures [315]. Inhibition experiments with promastigotes and various glycans show inhibition only through αGal. The high concentration required to stain the amastigotes may be resulting in non-specific stain and/or it may be that unbound lectin takes a long time to diffuse back out of the cell after incubation. However, neither the inclusion of Tween20 in the wash buffer, increasing the number and duration of washes had

any impact on the level of background staining. Therefore, it is possible that the diffuse green stain is a result of shed material from the parasites. Incubation of the IB4-AF488 lectin with 0.5 M galactose prior to application to the cells reduced the bright foci of fluorescence, but did not completely abolish all the diffuse, background stain.

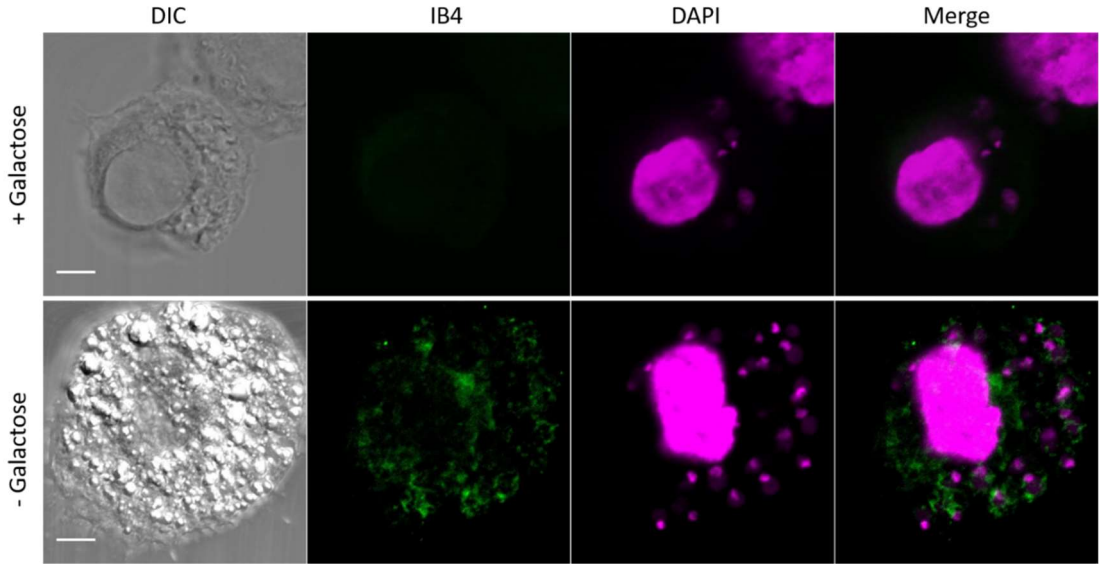

Figure 5.10. IB4 staining of THP-1 cells infected with *L. major* amastigotes. Top Panel: IB4-AF488 preincubated with 0.5M galactose. Bottom Panel: IB4-AF488 without preincubation. Left to right: DIC, IB4-AF488, DAPI, Merged fluorescence. Scale is 5 µM.

5.2.2.5 IB4-labelling of *L. tropica*-infected THP-1 cells with

Interestingly, IB4 did not seem to stain the amastigote surface of *L. tropica* parasites within THP-1 cells, despite apparent labelling in promastigote cells (Figure 5.11). All fluorescence in the green channel is not associated with the parasite surface (counterstained with anti-tubulin hybridoma). Label is the same regardless of the presence of 0.5 M galactose, which inhibits binding effectively in *L. major* infection.

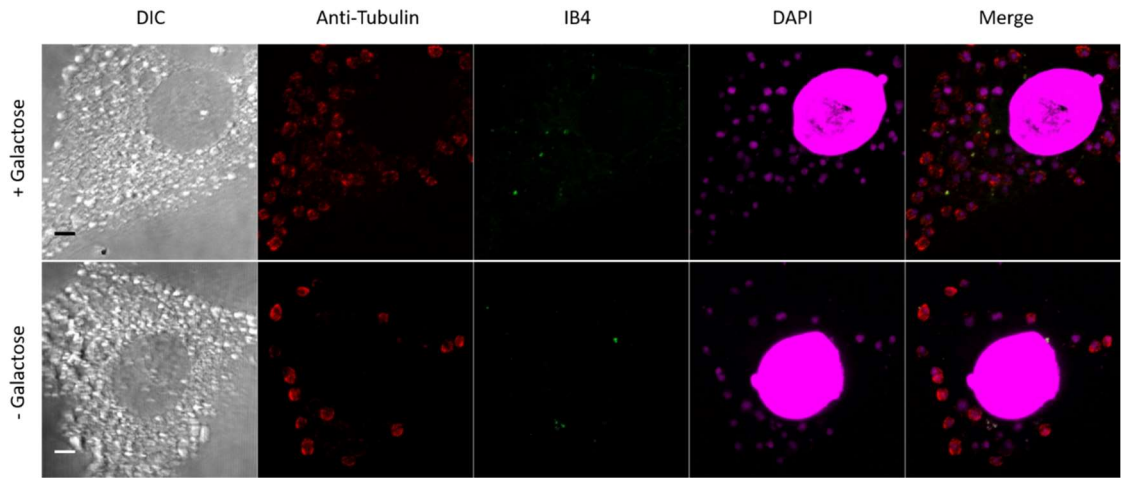

Figure 5.11. IB4 staining of THP-1 cells infected with *L. tropica* amastigotes. Top Panel: IB4-AF488 preincubated with 0.5M galactose. Bottom Panel: IB4-AF488 without preincubation. Left to right: DIC, anti-Tubulin, IB4-AF488, DAPI, Merged fluorescence. Scale is 5 μM

5.3 Discussion

Investigation of the immunogenicity of *L. tropica* glycolipids in Chapter 3 indicated that any αGal epitope must be located on an alternative glycoconjugate. While anti-Gal specificities for *L. major* have been studied Chapter 4, *L. tropica* sera did not show differential recognition of any of the three αGalactosylated NGPs used in the screen. Therefore, a different approach was required; the localisation and characterisation of the epitope in *L. tropica* cells.

In an attempt to identify the location of antigen expression in both *Leishmania* species, I have taken two main approaches. The first, to use a lectin to stain αGal at various parasite life stages, and the second, to use antibody purified directly from patient sera to localise αGal epitopes directly on the parasite surface. To study the localisation of αGal-structures, I have exploited a lectin derived from the seeds of the *Bandeira simplicifolia* (*Griffonia simplicifolia*), GSL I. GSL I is a family of glycoproteins of which there are two types of subunit, each with different glycan preferences [315]. GSL IB4 contains only the B type subunit, which is specific for terminal αGal residues.

L. major promastigotes are known to have a number of αGalactosylated GIPLs decorating the surface of the cell, and this was validated by staining of the

promastigotes with the lectin IB4. The fluorescence is clearly seen throughout the cytosol, although excluded from the nucleus and kinetoplast. All non-permeabilisation methods of fixation resulted in negative staining, as did live staining of cells with no fixation (not shown). The labelling by IB4 was inhibited by 0.5 M D-galactose and α-methyl-D-galactopyranoside, but not by β-methyl-D-galactopyranoside, D-mannose or D-glucose, emphasising the specificity of the lectin-glycan binding. Low level IB4 staining of *L. tropica* promastigotes was consistently observed. This was inhibited by prior incubation of the lectin with 0.5 M D-galactose and, to a lesser degree, 0.5 M D-mannose. *L. tropica* cells may be expressing αGal at low levels at this point in the life cycle, although the partial inhibition by incubation with mannose indicates that IB4 recognition of this epitope is perhaps lower affinity than would be expected.

It is unfortunate that non-permeabilisation methods of fixation did not allow IB4 labelling, as these images do not give a clear answer about the localisation of the αGal molecules. From this experiment, it looks likely that αGal residues are expressed on the amastigote surface, but it seems also detectable within the parasite cytosol, and shed within THP-1 cells. The percentage of *L. major* GIPLs that are expressed on the surface ranges from 15-84%, depending on the GIPL type [280]. Furthermore only 30% of *L. major* GIPLs quantified from whole cell lysate could be labelled at the cell surface [280]. A similar trend may be followed in *L. tropica* cells.

The most biologically relevant results in relation to anti-Gal production during a *Leishmania* infection, are in αGal localisation in amastigotes. After one successful extraction/labelling experiment using *L. major* infected THP-1, I was unable to replicate the amastigote extraction in order to further optimise the protocol, and so any images must be interpreted with caution. However, this experiment conforms with reported GIPL expression throughout *L. major* lifecycle, as the bright IB4 stain was completely inhibited on incubation of the lectin with 0.5 M D-galactose. I was unable to replicate this result using *L. tropica* amastigotes, and so I proceeded with labelling of amastigotes *in situ*.

Final experiments focussed on the labelling of *Leishmania* within the THP-1 host cell. Surprisingly, despite the additional complication of the intact human cell, this yielded the clearest IB4-AF488 labelling of the three life stages for *L. major*. In the presence of 0.5 M galactose, IB4-AF488 signal was almost completed inhibited, except in some case diffuse fluorescence remained at very low levels in some infected cells. It is likely that the diffuse staining material is shed from amastigotes, due to the noted exchange of parasite and host material, and it is reported that amastigote debris can result in stronger label signals by human sera than live amastigotes [31]. *L. tropica* infected THP-1 cells had very small amounts of IB4 stain, however it was not associated with amastigotes, and was uninhibited by glycan pre-incubation of the lectin. It is possible that this stain is the result of unbound lectin that is not removed by washes. The low level of recognition in the promastigote stage indicates that the method needs further optimisation for *L. tropica* cells due to the reduced level of αGal available for detection in this species.

The use of resin conjugated to an epitope of interest is an established method to obtain antibodies of a desired specificity. In this chapter I use Protein G resin to first purify IgG from sera, but the subsequent step required a different approach. The first approach was to attempt to make a column by conjugating an NGP to agarose beads. The commercially available NGP, Dextra-BSA), was the obvious first candidate for this protocol, as it was more easily sourced than the bespoke NGPs used elsewhere in this thesis (Chapter 4). The structure follows the classical Galili trisaccharide structure (Galα(1,3)Galβ(1,4)GlcNAc-R) where the R is linker-BSA.

I am confident, based on the work presented here, that I have successfully purified the anti-Dextra antibody of interest, due to its proven specificity for Dextra-BSA through both enzyme cleavage of the binding site and inhibition by galactose. Unfortunately, this came too late for use in immunofluorescent assays.

Aside from the localisation of the *L. tropica* αGal epitope, I hoped to use the purified antibody in a number of assays. Data showing the lytic potential of anti-Gal

antibodies from Chagasic serum hint at the protective role these antibodies may play in parasitic infection [318]. I had planned to incubate the parasites (both species) with anti-Dextra antibody, and monitor survival and agglutination. I am particularly interested in the *in vitro* binding of anti-Dextra to *L. tropica* parasites, to further understand the relationship between *L. tropica* infection and anti-Gal titres. Anti-Gal produced on immunisation of mice with Galα(1,6)Galβ has the ability to lyse *L. major* metacyclics [122]. No such investigation has been conducted with *L. tropica* cells, and would be an exciting prospect for further work.

Data shown in Chapter 4 indicates that there are multiple anti-Gal antibodies circulating in *L. major* infected sera. This presents the possibility that by using alternative glycans to purify antibodies from sera, I could obtain information about the relative abundance of the varying specificities. Furthermore, with the potential use of anti-Gal as a marker for treatment efficacy (as with Chagasic anti-Gal), the changing profile of anti-Gal during chemotherapy could inform the development of a robust method for monitoring treatment outcome.

Chapter Six
Discussion

Natural anti-Gal, antibodies that recognise terminal αGalactosyl residues, are the most abundant IgG antibodies in healthy adult humans [191]. Unique to humans and Old World apes, anti-Gal has been proposed as the major protective antibody following a catastrophic event during primate evolution around 30 million years ago, allowing the proliferation of individuals who had a mutated and therefore non-functional galactosyl transferase gene (α1,3GT) [203]. This gene is essential for the formation of saccharides terminating in αGal residues, and its silencing means no such epitopes are formed in human cells. As a result, antibodies against αGal are not selected out as self-reactive clones, and therefore can proliferate in response to xenoantigens from multiple pathogens [319].

In parasitic infection, anti-Gal has been implicated in protection from clinical malaria caused by *P. falciparum* [262]. High titres are detected in response to *P. vivax* infection, suggesting an additional role in disease caused by this species [263]. *T. cruzi*, the causative agent of Chagas disease, has heavily galactosylated surface mucins which elicit a strong immune response during human infection, and a glycan vaccine exploiting this response shows promising results in mice [271]. Levels of Chagasic anti-Gal can be exploited in monitoring response to treatment, as a sensitive marker of the presence of parasites [320].

Antibodies against αGalactosyl present an intriguing possibility for a *Leishmania* diagnostic that exploits their natural specificity. Diagnostic protocols vary, but typically require human expertise to identify parasites, or laboratory infrastructure and considerable resources for molecular approaches (elegantly reviewed by [3]). As global patterns of disease are changing through increased migration and human displacement throughout the Middle East and Europe, tools for rapid screening are sorely needed. Furthermore, in endemic settings where cases of CL are typically sporadic, active surveillance in rural clinics will be improved through the advent of rapid, easy-to-read tests that do not require the prohibitive costs of travel to specialist clinics. Early case detection has myriad benefits, including minimising the spread of the disease through rapid control, and the correct assignation of

treatment, avoiding complications and distress through inaccurate diagnoses [152]. An antibody-based diagnostic, with a simple interface and a short time to generate a result, has the potential to revolutionise the current state of CL diagnostics, much as RDTs have transformed malaria diagnosis.

The αGalactosylation of surface glycolipids (GIPLs) in *L. major* is described in the literature, as is the apparent lack of similar galactosylation in *L. tropica*. Anti-Gal antibodies have been detected in sera from patients infected with either *L. major* or *L. tropica* species; however the presence of αGalactosyl residues have only been identified for *L. major* GIPLs, whereas for *L. tropica* αGalactosylated surface glycoconjugates have not yet been detected [217]. In this thesis, I was able to corroborate previous work done Schneider *et al*. (1995), which showed that *L. tropica* promastigotes only express Type-I GIPLs, despite recognition of IB4 lectin (specific for terminal αGalactose) on the whole parasite surface in immunofluorescent assays (Chapter 5). *L. major* immunofluorescent labelling by IB4 was consistent throughout all stages, from promastigote to amastigote, fitting the reported pattern of GIPL expression. This suggests that αGalactosylation of another surface glycoconjugates may be taking place in *L. tropica*, most likely linked to glycoproteins. In fact, preliminary IB4 blotting on *L. tropica* protein fractions showed recognition of low molecular weight components after fractionation on SDS-PAGE (Yuk-Chien L., and Acosta-Serrano A, unpublished). Interestingly, TLC-immunostainings (Chapter 3) showed that unlike the excellent recognition of *L. major* GIPLs by sera from infected patients, *L. tropica* glycolipid extracts were poorly recognised by the same sera, suggesting a lack for diagnostic potential. Furthermore, *L. major* sera was shown to bind a single glycolipid species in *L. tropica* extract but, unfortunately, I was unable to confidently identify this band using LC-MS due to insufficient material. On the other hand, *L. tropica* sera was universally unreactive against glycolipid extract from either parasite species; a surprising result that points to an alternative source of any anti-Gal detected in previous studies. More biochemical work is needed to identify and structurally characterise αGalactosylated glycoconjugates expressed by *L. tropica* parasites. This

is necessary for to better design NGPs that will specifically discriminate *L. tropica* from *L. major* infections. This glycolipid analysis confirms the immunogenicity of *L. major* GIPL-2 and GIPL-3 in sera from *L. major*-infected patients only; no recognition of these molecules is detected in healthy sera. The specificity of the anti-Gal produced during *L. major* infection is key to designing a diagnostic based on this antibody; natural anti-Gal is ubiquitous in healthy adults, but Chapter 3 confirms that it has low affinity for *Leishmania* glycotopes.

The unexpected pattern of anti-Gal titres in *L. tropica* serum samples demonstrated by Al-Salem *et al.* (2014) was the inspiration for this thesis, but I was unable to replicate those results in Chapter 4.Both the antigen (Galα(1,3)Galβ(1,4)GlcNAc-R, Vector Labs) and secondary antibody used in that study are no longer available, which could explain some of the discrepancy. Nevertheless, I was able to screen a panel of NGPs that have excellent potential as biomarkers of *L. major* infection, which could be used in conjunction with microscopy to rapidly determine which infections are *L. major* (and therefore more likely to resolve without treatment).

L. major anti-Gal constitutes at least two separate populations, although there are likely more still undetected. In Chapter 4, two glycotopes have the most potential as biomarkers for *L. major* infection; Galα(1,6)Galα(1,3)Gal*f*β-R and Galα(1,3)Gal*f*β-R. Based on the *L. major* GIPLs, demonstrated in Chapter 3 to have excellent reactivity with *L. major* sera, a combination of these two structures has the potential to capture two distinct antibody populations. Confirming the pattern demonstrated with native GIPLs, antibodies binding these glycans are not found in sera from *L. tropica* patients, or in healthy adults.

Antibodies against Galα(1,6)Galα(1,3)Gal*f*β, (GIPL-3) were detected at significantly higher levels in patients with apparently healed lesions. Reactivation of CL is reported decades after clinical cure, indicating that parasites can persist at asymptomatic levels [299,321]. Antibody biomarkers of infection have potential utility in detecting such occult infections, as demonstrated in Chagas disease [320]. With

further investigation, KM28 may be another such marker. Unfortunately, the time scale for the longitudinal samples from patients with *L. major* infection collected for this study did not allow detection of antibody titre reduction in response to treatment, but a longer-term collection would allow such monitoring, and validation of this proposal.

With hindsight, I could have implemented a target product profile (TPP) prior to the design and synthesis of the update panel of biomarkers. A TPP is a critical evaluation of the optimal and minimal parameters for the eventual diagnostic, and is often used in diagnostic development [322–324]. This process would have focused my interpretation of the results and given a framework for assessment of a successful biomarker. The TPP for a point-of-care diagnostic for cutaneous leishmaniasis would give parameters for sensitivity and specificity, as well as target population (for example active surveillance of at-risk populations, or passive surveillance of individuals presenting at a clinic), required sample type and volume (such as serum or whole blood) and the expertise or training required for staff performing such tests. Such a report would be an asset in the further development of these NGPs into a viable and useful diagnostic test.

Looking ahead

With more time, I would investigate the mystery glycolipid band extracted from *L. tropica* cells and recognised by sera from *L. major* infected sera. The limitation so far has been extracting enough material for LC-MS or NMR analysis. With more time and resources, I would focus on characterising this band, with larger scale extraction. The antibody purified in Chapter 5 could also be used in TLC immuno-overlays, as could an additional panel of lectins with specificity for different glycans (e.g. Concavalin A which bind α-D-Mannose). These methods could indirectly characterise the antigenic glycans in this band.

The lack of immunogenic glycolipids detected in TLC overlays points to an alternative source of anti-Gal other than GIPLs. Preliminary work in this area detected low molecular weight proteins using IB4, although further experiments are

needed to confirm this. Treatment of protein lysate with coffee bean αGalactosidase (to remove terminal αGal residues) and PNGaseF (to remove N-linked saccharides from protein) followed by SDS-PAGE/Western blots, alongside incubation with sera/lectins using inhibitory glycans would be my immediate priorities. If *L. tropica* glycoproteins have a novel αGal-terminating oligosaccharide, this could be exploited alongside the NGPs used in this thesis, for the development of a *L. major*/*L. tropica* RDT with utility in areas of overlapping endemicity.

One unfortunately truncated aspect of this thesis is in the purification of anti-Gal from sera. The lack of a commercially available resin for affinity chromatography presented a challenge, although I am confident that I managed to acquire a small volume of anti-Gal through my second approach, using NGP-coated nitrocellulose. It's possible that more anti-Gal could be purified using a different glycotope, such as KM28 Galα(1,6)- or KM27 Galα(1,3)-, titres against which were excellent at discriminating *L. major* sera from healthy controls. The expense of synthesising these non-commercial NGPs meant I opted first to use the NGP available from Dextra Laboratories. Anti-Gal recognising this glycan was detected in high levels by Al-Salem *et al*. (2014), although as discussed above, the suppliers differed and therefore the linkage between the glycan and BSA component likely does too. One final method I did not try, was to biotinylate the BSA portion of the NGP, and use a streptavidin-sepharose column to capture it. This may have been successful, although more expensive, and time limitations meant I did not attempt it.

Lytic anti-Gal against *T. cruzi* is likely an important component of protection from, and control of, the infection, and I would have liked to investigate any similar properties of *L. major* anti-Gal. The preliminary success of the anti-*L. major* vaccine demonstrated by Iniguez *et al*. (2017), and their demonstration of complement-independent lysis of metacyclics by sera of immunised mice, indicates there may be similar potential in human anti-Gal. While the protocol for amastigote extraction was variable, with further fine-tuning, enough cells could be produced to

understand the protective potential throughout the life cycle of *L. major* within the mammalian host.

An unexplored aspect of αGal expression by *Leishmania* is the identification of the genes responsible for galactopyranose incorporation into glycoconjugates. No galactopyranosyl transferases have been incriminated in *Leishmania* as essential for GIPL synthesis. Galactofuranosyl transferases have been identified in the *L. major* genome, although all are linked to the biosynthesis of LPG and not GIPLs [325]. One approach would be to follow a methodology similar to that used to study galactosyl transferases in ticks [326]. Cabezas-Cruz *et al*. (2018) transfected human cells with candidate tick genes and used immunofluorescence to detect αGal expression. With the advent of efficient CRISPR cas9 genome editing in *Leishmania* spp., there is new potential for investigation of likely candidates coupled with the immunofluorescent methods optimised in this thesis; the knock down of genes responsible for GIPL αGalactosylation would abolish the IB4 labelling demonstrated in Chapter 5 [327,328].

In Chapter 4, I discuss the perplexing cross-reactivity of *L. infantum* sera with the control NGP. Further investigation was clearly warranted, but due to the limited amount of sera available I was forced to end this section unanswered. I would very much like to have solved this mystery. Natural antibodies against dietary proteins (such as BSA) is common, and could explain some of the cross-reactivity, although why this would be so elevated in *L. infantum* positive sera only is unclear [329]. One approach would be to pre-absorb sera with BSA, to remove any cross-reacting antibodies against this component of the NGP. A wider screen of this cohort with NGPs with different carrier protein would also help understand the relative importance of the protein and glycan portions, however, the costs associated with this are prohibitive. Deeper investigation of anti-Gal specificities in all sera pools could have come through the use of glycan microarrays, such as those available through the Imperial College Carbohydrate Microarray Facility. Additionally, for *L. tropica*, where the epitope is completely unknown, this approach could help to narrow the focus into a smaller subset of likely structures.

In summary, this thesis identifies excellent candidates for further development into a diagnostic capable of discriminating between two important causative species of Old World CL. With additional investigation, these NGPs may have utility in certain New World CL diagnoses, although *L. infantum* diagnosis is unsuited to this approach due to an unusual, and unexplained, cross-reactivity to the carrier.

Chapter Seven
Supplementary Tables

4.2.1.1 Serum levels of anti-Gal antibodies are higher in active *L. major* infected samples, compared to cured and non-CL samples from the 2013 collection

Supplementary Table 1. One-Way ANOVA results for nine NGPs, used to screen three groups of patient sera from the 2013 KSA collection. Active L. major (n = 17), cured leishmania (n = 31) and heterologous controls (n = 29). Degrees of freedom for the ANOVA results are marked [a]. A Welch adjustment is denoted by [w] for two NGPs, with associated degrees for freedom [b] and [c]. *P*-values of < 0.05 indicate a significant difference between patient groups and were followed with post-hoc tests.

NGP	*F*	*p* value
KM1	2.954 [a]	0.058
KM3	5.070 [a]	0.009*
KM5	0.004 [a]	0.996
KM8	2.451 [a]	0.093
KM9	3.681 [a]	0.030*
KM15	0.005 [a]	0.995
KM17	4.688 [a]	0.012*
KM11	3.690 [w,b]	0.032*
KM12	0.684 [w,c]	0.510

[w] Welch adjusted ANOVA
Degrees of freedom [a] 2,74; [b] 2,47.7; [c] 2,46.0
* Significance p < 0.05

Supplementary Table 2. Logistic regression predicting likelihood of being *L. major* positive (2013 cohort) based on antibody titres against 9 NGPs. ROC curves presented in Figure 2. * = p ≤ 0.05. ** = p ≤ 0.01, *** = p ≤ 0.001, **** = p < 0.0005, ns = p > 0.05.

NGP	B	S.E.	Wald	df	*p* value	Odds Ratio	95% C.I. for Odds Ratio	
							Lower	Upper
KM1	0.751	0.424	3.132	1	ns	2.119	0.922	4.867
KM3	3.497	1.521	5.283	1	*	33.013	1.674	651.203
KM5	-1.310	1.092	1.438	1	ns	0.270	0.032	2.295
KM8	-1.595	0.822	3.764	1	ns	0.203	0.040	1.016
KM9	-0.379	0.656	0.334	1	ns	0.685	0.189	2.476
KM11	0.162	0.567	0.081	1	ns	1.175	0.387	3.569
KM12	-0.407	0.574	0.504	1	ns	0.665	0.216	2.049
KM15	-0.913	0.918	0.990	1	ns	0.401	0.066	2.425
KM17	0.736	1.041	0.500	1	ns	2.088	0.272	16.056
Constant	-2.075	1.314	2.495	1	ns	0.126		

4.2.1.4 Anti-Gal detection in pools of sera samples from the 2017 collection

Supplementary Table 3. Independent Samples Kruskal Wallis results for comparison of pooled sera from healthy controls (UK or KSA patients), or active infection (*L. tropica* and *L. major* from KSA 2017 cohort), using KM27, KM28, KM30 and BME. Mean ranks for each serum type listed in Supplementary Table 4. Post-hoc pairwise comparisons listed in Table 3. **** = $p < 0.0005$, ns = $p > 0.05$.

NGP	χ^2	DF	*p* value
KM27	25.464	3	****
KM28	25.643	3	****
KM30	25.994	3	****
BME	0.408	3	ns

Supplementary Table 4. Kruskal Wallis calculated mean rank scores for pooled sera from healthy controls (UK or KSA patients), or active infection (*L. tropica* and *L. major,* from the 2017 cohort), using KM27, KM28 and KM30. Mean ranks are only calculated for NGPs with a p-value of < 0.05 for the Kruskal Wallis test (see Supplementary Table 3). Post-hoc pairwise comparisons of mean rank scores listed in Table 3.

Sera Type	KM27	KM28	KM30
L. tropica	15.2	13.6	18.0
L. major	36.5	36.5	36.5
UK	17.3	17.6	15.6
KSA	14.1	15.4	12.9

4.2.1.5 Anti-Gal detection with an updated panel of NGPs is increased in active *L. major* infection, but not *L. tropica*

Supplementary Table 5. Kruskal Wallis H test results for serum anti-Gal titres in individual patient serum samples from active *L. major* infection (either 2017 or 2013 collection cohorts), active *L. tropica* infection, post-infection (Cured) and heterologous (non-CL controls) against four NGPs (KM27, KM28, KM30 and BME). Mean rank scores reported in Supplementary Table 6. ** = $p \leq 0.01$, **** = $p < 0.0005$**.**

NGP	χ^2	DF	*p* value
KM27	85.838	4	****
KM28	63.068	4	****
KM30	87.124	4	****
BME	13.259	4	**

Supplementary Table 6. Mean Ranks scores for patient serum samples from active *L. major* infection (either 2017 or 2013 collection cohorts), active *L. tropica* infection, post-infection (Cured) and heterologous (non-CL controls) against four NGPs (KM27, KM28, KM30 and BME). Antibody titres were measured in individual patient serum samples from active *L. major* infection (either 2017 or 2013 collection cohorts), active *L. tropica* infection, post-infection (Cured) and heterologous (non-CL controls). Post-hoc pairwise comparisons of mean rank scores listed in Table 4**.**

Sera Type	KM27	KM28	KM30	BME
L. tropica	26.5	20.4	21.25	56.4
L. major 2017	103.4	95.29	103.79	85.17
L. major 2013	88.42	91.25	89.69	66.23
Cured	67.28	73.96	58.42	80.56
Heterologous	23.72	36.16	28.7	54.64

4.2.1.6 Three αGal NGPs have diagnostic potential for *L. major* but not *L. tropica* infection in KSA

Supplementary Table 7. Binomial logistic regression models for *L. major* infection prediction using either Combined (heterologous and cured) controls or Heterologous only controls, using KM27, KM28, KM30 and BME. Each row is a separate model. All NGPs is the model when data for all four NGPs is combined into a single analysis (Row 1). The model for each NGP is also presented individually in Rows 2-5. Details of each model are presented in Supplementary Tables 8 and 9. * = $p \leq 0.05$, ** = $p \leq 0.01$, **** = $p < 0.0005$**.**

NGP	Combined Controls			Heterologous only		
	X^2	DF	*p* value	X^2	DF	*p* value
All NGPs	90.998	4	****	99.498	4	****
KM27	62.004	1	****	84.769	1	****
KM28	45.903	1	****	52.438	1	****
KM30	88.097	1	****	81.542	1	****
BME	4.303	1	*	9.163	1	**

Supplementary Table 8. Detailed Binomial logistic regression models (Supplementary Table 7) for *L. major* infection predication using Heterologous only controls, using KM27, KM28, KM30 and BME. Each row is a separate model. The model for each NGP is presented individually in Rows 1-4. All NGPs is the model when data for all four NGPs ((KM27, KM28, KM30 and BME) is combined into a single analysis (Row 5).

NGP	Variable	B	S.E.	Wald	df	*p* value	Odds Ratio	95% CI for Odds Ratio	
								Lower	Upper
KM27	KM27	0.017	0.004	21.035	1	0.000	1.017	1.010	1.025
	Constant	-2.313	0.636	13.230	1	0.000	0.099		
KM28	KM28	0.009	0.002	15.107	1	0.000	1.009	1.004	1.013
	Constant	-0.944	0.477	3.922	1	0.048	0.389		
KM30	KM30	0.007	0.002	21.941	1	0.000	1.007	1.004	1.010
	Constant	-1.924	0.569	11.415	1	0.001	0.146		
BME	BME	0.028	0.011	6.911	1	0.009	1.028	1.007	1.050
	Constant	0.608	0.386	2.483	1	0.115	1.837		
Combined	KM27	0.012	0.005	6.094	1	0.014	1.012	1.002	1.022
	KM28	0.002	0.003	0.517	1	0.472	1.002	0.996	1.009
	KM30	0.004	0.002	4.964	1	0.026	1.004	1.001	1.008
	BME	-0.021	0.019	1.143	1	0.285	0.980	0.944	1.017
	Constant	-3.231	1.013	10.165	1	0.001	0.040		

Supplementary Table 9. Detailed Binomial logistic regression models (Supplementary Table 7) for *L. major* infection predication using all controls (Heterologous and cured) combined, using KM27, KM28, KM30 and BME. Each row is a separate model. The model for each NGP is presented individually in Rows 1-4. All NGPs is the model when data for all four NGPs (KM27, KM28, KM30 and BME) is combined into a single analysis (Row 5).

NGP	Variable	B	S.E.	Wald	df	*p* value	Odds Ratio	95% CI for Odds Ratio	
								Lower	Upper
KM27	KM27	0.005	0.001	27.166	1	0.000	1.005	1.003	1.007
	Constant	-1.111	0.348	10.172	1	0.001	0.329		
KM28	KM28	0.003	0.001	23.010	1	0.000	1.003	1.002	1.005
	Constant	-0.644	0.303	4.528	1	0.033	0.525		
KM30	KM30	0.004	0.001	33.910	1	0.000	1.004	1.002	1.005
	Constant	-1.599	0.378	17.898	1	0.000	0.202		
BME	BME	0.012	0.006	3.860	1	0.049	1.012	1.000	1.025
	Constant	0.401	0.293	1.880	1	0.170	1.494		
Combined	KM27	0.001	0.001	0.311	1	0.577	1.001	0.998	1.004
	KM28	0.001	0.001	0.537	1	0.464	1.001	0.999	1.003
	KM30	0.003	0.001	15.177	1	0.000	1.003	1.002	1.005
	BME	-0.008	0.008	1.085	1	0.297	0.992	0.976	1.007
	Constant	-1.622	0.472	11.810	1	0.001	0.198		

Supplementary Table 10. Binomial logistic regression models for *L. tropica* infection predication using either Combined (heterologous and cured) controls or Heterologous only controls, using KM27, KM28, KM30 and BME. Each row is a separate model. All NGPs is the model when data for significant, individual NGPs is combined into a single analysis [BME is not included] (Row 1). The model for each NGP is also presented individually in Rows 2-5. nd = not done. * = p ≤ 0.05, *** = p ≤ 0.001, **** = p < 0.0005, ns = p > 0.05**.**

NGP	Combined Controls			Heterologous only		
	X^2	DF	*p* value	X^2	DF	*p* value
All NGPs	22.986	3	****	nd		
KM27	6.77	1	***	0.03	1	ns
KM28	15.466	1	****	4.127	1	*
KM30	12.163	1	****	3.433	1	ns
BME	1.147	1	ns	0.002	1	ns

Supplementary Table 111. Detailed Binomial logistic regression models (Supplementary Table 10) for *L. tropica* infection predication using all controls (Heterologous and cured) combined, using KM27, KM28, KM30 and BME. Each row is a separate model. The model for each NGP is also presented individually in Rows 1-4. Combined NGPs is the model when data for three NGPS (KM27, KM28 and KM30) is combined into a single analysis (Row 5).

NGP	Variable	B	S.E.	Wald	df	*p* value	Odds Ratio	95% CI for Odds Ratio	
								Lower	Upper
KM27	KM27	-0.007	0.003	3.985	1.000	0.046	0.993	0.987	1.000
	Constant	-0.327	0.455	0.517	1.000	0.472	0.721		
KM28	KM28	-0.010	0.004	7.533	1.000	0.006	0.990	0.982	0.997
	Constant	0.207	0.472	0.192	1.000	0.661	1.230		
KM30	KM30	-0.010	0.005	4.066	1.000	0.044	0.990	0.981	1.000
	Constant	-0.101	0.485	0.043	1.000	0.835	0.904		
BME	BME	-0.013	0.013	1.057	1.000	0.304	0.987	0.962	1.012
	Constant	-0.786	0.480	2.684	1.000	0.101	0.455		
Combined	KM27	0.016	0.008	3.972	1.000	0.046	1.017	1.000	1.033
	KM28	-0.014	0.006	6.250	1.000	0.012	0.986	0.975	0.997
	KM30	-0.015	0.008	3.836	1.000	0.050	0.985	0.971	1.000
	Constant	0.419	0.612	0.468	1.000	0.494	1.520		

Supplementary Table 122. Detailed Binomial logistic regression models (Supplementary Table 10) for *L. tropica* infection predication using Heterologous controls only using KM27, KM28, KM30 and BME. Each row is a separate model. The model for each NGP is presented individually in Rows 1-4. No combined analysis was performed, as only one NGP was significant alone.

NGP	Variable	B	S.E.	Wald	df	*p* value	Odds Ratio	95% CI for Odds Ratio	
								Lower	Upper
KM27	KM27	0.001	0.005	0.030	1.000	0.863	1.001	0.991	1.011
	Constant	-0.546	0.553	0.975	1.000	0.323	0.579		
KM28	KM28	-0.007	0.004	3.321	1.000	0.068	0.993	0.986	1.001
	Constant	0.249	0.487	0.261	1.000	0.609	1.282		
KM30	KM30	-0.006	0.004	1.693	1.000	0.193	0.994	0.986	1.003
	Constant	0.003	0.474	0.000	1.000	0.995	1.003		
BME	BME	-0.001	0.015	0.002	1.000	0.968	0.999	0.970	1.030
	Constant	-0.453	0.542	0.697	1.000	0.404	0.636		

4.2.1.10.1 Serum CRP levels are increased in CL infection

Supplementary Table 133. Kruskal Wallis calculated mean rank scores for CRP levels in individual serum samples. CRP was measured in individual patient serum samples from active L. major infection (n = 37), Cured patients (n=7) and heterologous controls (n = 17)**.**

Sera Type	Mean Rank
L. major 2017	33.89
Cured	39.07
Heterologous	21.38

4.2.2.1 Anti-Gal titres in individual Bolivian sera are highest in ML/MCL patients

Supplementary Table 14. Kruskal Wallis H Test statistics for comparison of anti-Gal titres in Bolivian Patient Samples for three NGPs (KM3, KM24 and Dextra-BSA). Mean rank scores reported in Supplementary Table 16. * = $p \leq 0.05$**.**

NGP	χ^2	DF	*p* value
KM3	8.132	2	*
KM24	8.074	2	*
Dextra-BSA	7.525	2	*

Supplementary Table 154. Mean Rank scores for comparison of anti-Gal titres in Bolivian Patient Samples for three NGPs (KM3, KM24 and Dextra-BSA). Post-hoc pairwise comparisons of mean rank scores listed in Table 13.

Sera Type	Dextra-BSA	KM24	KM3
CL	49.09	48.12	45.75
ML/MCL	53.00	54.60	56.75
Control	35.69	35.67	36.58

4.2.2.4 Two panels of αGal NGPs have moderate diagnostic potential for Bolivian leishmaniasis

Supplementary Table 165. Logistic regression analysis of anti-Gal titres in Bolivian patient sera, against two panels of NGPs. Panel A = initial NGP panel (KM3, KM24, Dextra-BSA). Infected patients (n= 42), control patients (n = 36). Combined analysis includes all three NGPs. Panel B = second NGP panel (KM27, KM28, KM30 and BME). Infected patients (n = 21), control patients (n = 21). Combined analysis includes only the NGPs with significant individual models (KM27, KM28, KM30).

	NGP	χ^2	DF	*p* value
A	Dextra-BSA	9.23	1	0.002
	KM24	8.256	1	0.004
	KM3	11.532	1	0.001
	Combined	16.331	3	0.001
B	KM27	6.532	1	0.011
	KM28	4.501	1	0.034
	KM30	14.235	1	0.000
	BME	0.771	1	0.380
	Combined	14.28	3	0.003

Supplementary Table 17. Detailed Binomial logistic regression models (Supplementary Table 16A) for Bolivian patient serum samples combined, using Dextra-BSA, KM24 and KM3. Each row is a separate model. The model for each NGP is presented individually in Rows 1-3. Combined is the model when data for the three NGPS (Dextra-BSA, KM24 and KM3) is combined into a single analysis (Row 4).

NGP	Variable	B	S.E.	Wald	df	*p* value	Odds Ratio	95% CI of Odds Ratio	
								Lower	Upper
Dextra-BSA	Dextra	0.000	0.000	8.118	1	0.004	1.000	1.000	1.000
	Constant	-0.522	0.370	1.992	1	0.158	0.593		
KM24	KM24	0.000	0.000	7.464	1	0.006	1.000	1.000	1.000
	Constant	-0.956	0.521	3.361	1	0.067	0.385		
KM3	KM3	0.000	0.000	8.013	1	0.005	1.000	1.000	1.000
	Constant	-0.474	0.344	1.907	1	0.167	0.622		
Combined	Dextra-BSA	0.000	0.000	1.219	1	0.270	1.000	1.000	1.000
	KM24	0.000	0.000	0.040	1	0.841	1.000	1.000	1.000
	KM3	0.000	0.000	5.440	1	0.020	1.000	1.000	1.000
	Constant	-0.944	0.630	2.245	1	0.134	0.389		

Supplementary Table 186. Detailed Binomial logistic regression models (Supplementary Table 16B) for Bolivian patient serum samples combined, using KM27, KM28, KM30 and BME. Each row is a separate model. The model for each NGP is presented individually in Rows 1-4. Combined is the model when data for the three NGPS (KM27, KM28, KM30) is combined into a single analysis (Row 4).

NGP	Variable	B	S.E.	Wald	df	*p* value	Odds Ratio	95% CI of Odds Ratio	
								Lower	Upper
KM27	KM27	0.007	0.003	4.305	1	0.038	1.007	1.000	1.013
	Constant	-0.772	0.456	2.871	1	0.090	0.462		
KM28	KM28	0.002	0.001	2.822	1	0.093	1.002	1.000	1.004
	Constant	-0.486	0.399	1.479	1	0.224	0.615		
KM30	KM30	0.013	0.005	7.132	1	0.008	1.013	1.003	1.022
	Constant	-1.719	0.665	6.677	1	0.010	0.179		
BME	BME	-0.007	0.008	0.728	1	0.393	0.993	0.978	1.009
	Constant	0.280	0.448	0.392	1	0.531	1.324		
Combined	KM27	-0.001	0.005	0.025	1	0.875	0.999	0.990	1.009
	KM28	0.000	0.001	0.027	1	0.871	1.000	0.998	1.002
	KM30	0.013	0.007	3.911	1	0.048	1.013	1.000	1.026
	Constant	-1.717	0.664	6.690	1	0.010	0.180		

4.2.2.5 Anti-Gal levels are increased in serum samples from patients with active VL caused by *L. infantum* (Spanish cohort)

Supplementary Table 197. Independent Samples Kruskal Wallis results for comparison of individual Spanish sera from healthy controls (Endemic Control), active infection (VL or CL), cured infection (VL or CL) and asymptomatically infected patients. * = p ≤ 0.05, ** = p ≤ 0.01, *** = p ≤ 0.001, **** = p < 0.0005, ns = p > 0.05.

NGP	χ^2	DF	*p* value
KM27	44.519	5	****
KM28	28.636	5	****
KM30	50.531	5	****
BME	98.203	5	****

Chapter Eight
References

1. Zink, A. *et al.* Leishmaniasis in Ancient Egypt and Upper Nubia. *Emerg. Infect. Dis.* **12**, 12891–12897 (2006).
2. Steverding, D. The history of leishmaniasis. *Parasit. Vectors* **10**, 82 (2017).
3. Akhoundi, M. *et al.* Leishmania infections: Molecular targets and diagnosis. *Mol. Aspects Med.* **57**, 1–29 (2017).
4. Alvar, J., Yactayo, S. & Bern, C. Leishmaniasis and poverty. *Trends Parasitol.* **22**, 552–557 (2006).
5. Pigott, D. M. *et al.* Global distribution maps of the Leishmaniases. *Elife* **2014**, e35671 (2014).
6. Alvar, J. *et al.* Leishmaniasis worldwide and global estimates of its incidence. *PLoS One* **7**, e35671 (2012).
7. Shaw, J. The leishmaniases-survival and expansion in a changing world. A mini-review. *Mem Inst Oswaldo Cruz, Rio Janeiro* **102**, 541–547 (2007).
8. Dujardin, J.-C. Risk factors in the spread of leishmaniases: towards integrated monitoring? *Trends Parasitol.* **22**, 4–6 (2006).
9. Berry, I. & Berrang-Ford, L. Leishmaniasis, conflict, and political terror: A spatio-temporal analysis. *Soc. Sci. Med.* **167**, 140–149 (2016).
10. World Health Organisation. *Status of endemicitiy of CL worldwide 2016*. (2016).
11. Jones, K. E. *et al.* Global trends in emerging infectious diseases. *Nature* **451**, 990–993 (2008).
12. Reithinger, R. *Global burden of cutaneous leishmaniasis*. *The Lancet Infectious Diseases* **16**, (2016).
13. Jacobson, R. L. Leishmaniasis in an era of conflict in the Middle East. *Vector borne zoonotic Dis.* **11**, 247–258 (2011).
14. Abubakar, A. *et al.* Visceral Leishmaniasis Outbreak in South Sudan 2009–2012: Epidemiological Assessment and Impact of a Multisectoral Response. *PLoS Negl. Trop. Dis.* **8**, e2720 (2014).
15. WHO. Control of the leishmaniases. *WHO Tech. Rep. Ser.* 22–26 (2010).
16. Gossage, S. M., Rogers, M. E. & Bates, P. A. Two separate growth phases during the development of Leishmania in sand flies: implications for understanding the life cycle. *Int. J. Parasitol.* **33**, 1027–34 (2003).
17. Lainson, R. & Shaw, J. J. Evolution, Classification and Geographical Distribution. in *The Leishmaniases in Biology and Medicine* (1987).
18. Sereno, D. Leishmania (Mundinia) spp.: from description to emergence as new human and animal Leishmania pathogens. *New microbes new Infect.* **30**, 100540 (2019).
19. Espinosa, O. A., Serrano, M. G., Camargo, E. P., Teixeira, M. M. G. & Shaw, J. J. An appraisal of the taxonomy and nomenclature of trypanosomatids presently classified as Leishmania and Endotrypanum. *Parasitology* **145**, 430–442 (2018).
20. Serafim, T. D. *et al.* Sequential blood meals promote Leishmania replication and reverse metacyclogenesis augmenting vector infectivity. *Nat. Microbiol.* **3**, 548–555 (2018).
21. Ready, P. D. Biology of phlebotomine sand flies as vectors of disease agents. *Annu. Rev. Entomol.* **58**, 227–250 (2013).
22. Kamhawi, S. Phlebotomine sand flies and Leishmania parasites: friends or

foes? *Trends Parasitol.* **22**, 439–45 (2006).
23. Ashford, R. W. Leishmaniasis reservoirs and their significance in control. *Clin. Dermatol.* **14**, 523–532 (1996).
24. Saravia, N. G. *et al.* Epidemiologic, genetic, and clinical associations among phenotypically distinct populations of Leishmania (Viannia) in Colombia. *Am. J. Trop. Med. Hyg.* **59**, 86–94 (1998).
25. Abdeladhim, M., Kamhawi, S. & Valenzuela, J. G. What's behind a sand fly bite? The profound effect of sand fly saliva on host hemostasis, inflammation and immunity. *Infect. Genet. Evol.* **28**, 691–703 (2014).
26. Belkaid, Y. *et al.* Development of a natural model of cutaneous leishmaniasis: powerful effects of vector saliva and saliva preexposure on the long-term outcome of Leishmania major infection in the mouse ear dermis. *J. Exp. Med.* **188**, 1941–1953 (1998).
27. Oliveira, F., de Carvalho, A. M. & de Oliveira, C. I. Sand-fly saliva-Leishmania-man: The trigger trio. *Front. Immunol.* **4**, 1–8 (2013).
28. Titus, R. G. & Ribeiro, J. M. Salivary gland lysates from the sand fly Lutzomyia longipalpis enhance Leishmania infectivity. *Science (80-.).* **239**, 1306–1308 (1988).
29. Kaye, P. & Scott, P. Leishmaniasis: complexity at the host–pathogen interface. *Nat. Rev. Microbiol.* **9**, 604–615 (2011).
30. Ridley, D. S. & Ridley, M. J. The evolution of the lesion in cutaneous leishmaniasis. *J. Pathol.* **141**, 83–96 (1983).
31. Ridley, M. & Ridley, D. Cutaneous leishmaniasis: immune complex formation and necrosis in the acute phase. *Br. J. Exp. Pathol.* **65**, 327–336 (1984).
32. Guerin, P. J. *et al.* Visceral leishmaniasis: current status of control, diagnosis, and treatment, and a proposed research and development agenda. *Lancet Infect. Dis.* **2**, 494–501 (2002).
33. Chappuis, F. *et al.* Visceral leishmaniasis: What are the needs for diagnosis, treatment and control? *Nat. Rev. Microbiol.* **5**, 873–882 (2007).
34. Pérez-Cabezas, B. *et al.* Understanding Resistance vs. Susceptibility in Visceral Leishmaniasis Using Mouse Models of Leishmania infantum Infection. *Front. Cell. Infect. Microbiol.* **9**, 30 (2019).
35. Desjeux, P. The increase in risk factors for leishmaniasis worldwide. *Trans. R. Soc. Trop. Med. Hyg.* **95**, 239–243 (2001).
36. Ready, P. D. Epidemiology of visceral leishmaniasis. *Clin. Epidemiol.* **6**, 147 (2014).
37. Barral, A. *et al.* Leishmaniasis in Bahia, Brazil: evidence that Leishmania amazonensis produces a wide spectrum of clinical disease. *Am. J. Trop. Med. Hyg.* **44**, 536–546 (1991).
38. Sacks, D. L. *et al.* Indian kala-azar caused by Leishmania tropica. *Lancet* **345**, 959–961 (1995).
39. Al-Salem, W. S., Herricks, J. R. & Hotez, P. J. A review of visceral leishmaniasis during the conflict in South Sudan and the consequences for East African countries. *Parasit. Vectors* **9**, 460 (2016).
40. WHO. *Weekly epidemiological record*. (2017).
41. García, A. L. *et al.* Leishmaniases in Bolivia: Comprehensive Review and Current Status. The American journal of tropical medicine and hygiene. *Am. J.*

Trop. Med. Hyg **80**, 704–711 (2009).
42. Dowlati, Y. Cutaneous leishmaniasis: clinical aspect. *Clin. Dermatol.* **14**, 425–31 (2007).
43. Herwaldt, B. L. Leishmaniasis. *Lancet* **354**, 1191–1200 (1999).
44. Barral, A. *et al.* Lymphadenopathy as the first sign of human cutaneous infection by Leishmania braziliensis. *Am. J. Trop. Med. Hyg.* **53**, 256–259 (1995).
45. McMahon-Pratt, D. & Alexander, J. Does the Leishmania major paradigm of pathogenesis and protection hold for New World cutaneous leishmaniases or the visceral disease? *Immunol. Rev.* **201**, 206–224 (2004).
46. Tripathi, P., Singh, V. & Naik, S. Immune response to leishmania: Paradox rather than paradigm. *FEMS Immunol. Med. Microbiol.* **51**, 229–242 (2007).
47. Bailey, M. S. & Lockwood, D. N. J. Cutaneous leishmaniasis. *Clin. Dermatol.* **25**, 203–211 (2007).
48. Weigle, K. & Saravia, N. G. Natural history, clinical evolution, and the host-parasite interaction in new world cutaneous leishmaniasis. *Clin. Dermatol.* **14**, 433–450 (1996).
49. Reithinger, R. *et al.* Cutaneous leishmaniasis. *Lancet Infect. Dis.* **7**, 581–596 (2007).
50. Agostoni, C. *et al.* Mediterranean leishmaniasis in HIV-infected patients: Epidemiological, clinical, and diagnostic features of 22 cases. *Infection* **26**, 93–99 (1998).
51. Alvar, J. *et al.* The relationship between leishmaniasis and AIDS: The second 10 years. *Clin. Microbiol. Rev.* **21**, 334–359 (2008).
52. Ngouateu, O. B. *et al.* Clinical features and epidemiology of cutaneous leishmaniasis and Leishmania major/HIV co-infection in Cameroon: results of a large cross-sectional study. *Trans. R. Soc. Trop. Med. Hyg.* **106**, 137–142 (2012).
53. Al-Qadhi, B. N., Musa, I. S. & Al-Mulla Hummadi, Y. M. K. Comparative immune study on cutaneous leishmaniasis patients with single and multiple sores. *J. Parasit. Dis.* **39**, 361–370 (2015).
54. Sirdar, M. K. *et al.* Epidemiology and incidence of leishmaniasis in Jazan region, Saudi Arabia (2007-2015): An overview. *J. Entomol. Zool. Stud.* **6**, 859–864 (2018).
55. Desjeux, P. Leishmaniasis: Current situation and new perspectives. *Comp. Immunol. Microbiol. Infect. Dis.* **27**, 305–318 (2004).
56. Pearson, R. D. & de Queiroz Sousa, A. Clinical Spectrum of Leishmaniasis. *Clin. Infect. Dis.* **22**, 1–13 (1996).
57. Desjeux, P. Leishmaniasis: Public health aspects and control. *Clin. Dermatol.* **14**, 417–423 (1996).
58. Shirian, S., Oryan, A., Hatam, G. R. & Daneshbod, Y. Three Leishmania / L. species – L. infantum , L. major , L. tropica – as causative agents of mucosal leishmaniasis in Iran. *Pathog. Glob. Health* **107**, 267–272 (2013).
59. Kevric, I., Cappel, M. & Keeling, J. H. New World and Old World Leishmania Infections: A Practical Review. *Dermatol. Clin.* **33**, 579–593 (2015).
60. Antonio, L. de F. *et al.* Effect of secondary infection on epithelialisation and total healing of cutaneous leishmaniasis lesions. *Mem. Inst. Oswaldo Cruz*

112, 640–646 (2017).
61. Sadeghian, G., Ziaei, H., Bidabadi, L. S. & Baghbaderani, A. Z. Decreased effect of glucantime in cutaneous leishmaniasis complicated with secondary bacterial infection. *Indian J. Dermatol.* **56**, 37–9 (2011).
62. Alawieh, A. *et al.* Revisiting leishmaniasis in the time of war: The Syrian conflict and the Lebanese outbreak. *Int. J. Infect. Dis.* **29**, 115–119 (2014).
63. Al-Salem, W. S. *et al.* Cutaneous Leishmaniasis and Conflict in Syria. *Emerg. Infect. Dis.* **22**, 931–933 (2016).
64. Aronson, N. *et al.* Cutaneous Leishmaniasis in U.S. Military Personnel - Southwest/Central Asia, 2002-2003. *Morb. Mortal. Wkly. Rep.* **17**, 4–9 (2003).
65. Mansueto, P., Seidita, A., Vitale, G. & Cascio, A. Leishmaniasis in travelers: A literature review. *Travel Med. Infect. Dis.* **12**, 563–581 (2014).
66. Weina, P. J., Neafie, R. C., Wortmann, G., Polhemus, M. & Aronson, N. E. Old world leishmaniasis: an emerging infection among deployed US military and civilian workers. *Clin. Infect. Dis.* **39**, 1674–1680 (2004).
67. Bailey, F. *et al.* A new perspective on cutaneous leishmaniasis—Implications for global prevalence and burden of disease estimates. *PLoS Negl. Trop. Dis.* **11**, e0005739 (2017).
68. Markle, W. & Makhoul, K. Cutaneous Leishmaniasis: Recognition and Treatment. *Am. Fam. Phiyician* **69**, 1455–1460 (2004).
69. Reithinger, R., Aadil, K., Kolaczinski, J., Mohsen, M. & Hami, S. Social impact of leishmaniasis Afghanistan. *Emerg. Infect. Dis.* **11**, 634–636 (2005).
70. Refai, W. F. *et al.* Cutaneous leishmaniasis in Sri Lanka: effect on quality of life. *Int. J. Dermatol.* **57**, 1442–1446 (2018).
71. Yanik, M., Gurel, M. S., Simsek, Z. & Kati, M. The psychological impact of cutaneous leishmaniasis. *Clin. Exp. Dermatol.* **29**, 464–467 (2004).
72. Khatami, A. *et al.* Lived Experiences of Patients Suffering from Acute Old World Cutaneous Leishmaniasis: A Qualitative Content Analysis Study from Iran. *J. Arthropod. Borne. Dis.* **12**, 180–195 (2018).
73. Mondragon-Shem, K. & Acosta-Serrano, A. Cutaneous Leishmaniasis: The Truth about the 'Flesh-Eating Disease' in Syria. *Trends Parasitol.* **32**, 432–435 (2016).
74. Al-Kamel, M. A. Impact of leishmaniasis in women: a practical review with an update on my ISD-supported initiative to combat leishmaniasis in Yemen (ELYP). *Int. J. Women's Dermatology* **2**, 93–101 (2016).
75. Kassi, M., Kassi, M., Afghan, A. K., Rehman, R. & Kasi, P. M. Marring leishmaniasis: The stigmatization and the impact of cutaneous leishmaniasis in Pakistan and Afghanistan. *PLoS Negl. Trop. Dis.* **2**, 1–3 (2008).
76. Abuzaid, A. A. *et al.* Cutaneous Leishmaniasis in Saudi Arabia: A Comprehensive Overview. *Vector Borne Zoonotic Dis.* **17**, 673–684 (2017).
77. Al-Orainey, I. O. *et al.* Visceral Leishmaniasis in Gizan, Saudi Arabia. *Ann. Saudi Med.* **14**, (1994).
78. Salam, N., Al-Shaqha, W. M. & Azzi, A. Leishmaniasis in the Middle East: Incidence and Epidemiology. *PLoS Negl. Trop. Dis.* **8**, 1–8 (2014).
79. WHO. Cutaneous Leishmaniasis in KSA. 1–30 (2010).
80. Zakai, H. A. Cutaneous Leishmaniasis (CL) in Saudi Arabia: Current Status. *J. Adv. Lab. Res. Biol.* **5**, (2014).

81. Al-Tawfiq, J. & Abukhamsin, A. Cutaneous leishmaniasis: A 46-year study of the epidemiology and clinical features in Saudi Arabia (1956-2002). *Int. J. Infect. Dis.* **8**, 244–250 (2004).
82. Saliba, M. *et al.* Cutaneous leishmaniasis: an evolving disease with ancient roots. *Int. J. Dermatol.* **58**, 834–843 (2019).
83. Eroglu, F., Uzun, S. & Koltas, I. S. Comparison of Clinical Samples and Methods in Chronic Cutaneous Leishmaniasis. *Am. J. Trop. Med. Hyg.* **91**, 895–900 (2014).
84. Al-Salem, W. S. *et al.* Old World cutaneous leishmaniasis treatment response varies depending on parasite species, geographical location and development of secondary infection. *Parasites and Vectors* **12**, 1–9 (2019).
85. Haouas, N., Amer, O., Ishankyty, A., Alazmi, A. & Ishankyty, I. Profile and geographical distribution of reported cutaneous leishmaniasis cases in Northwestern Saudi Arabia, from 2010 to 2013. *Asian Pac. J. Trop. Med.* **8**, 287–291 (2015).
86. Amin, T. T., Al-Mohammed, H. I., Kaliyadan, F. & Mohammed, B. S. Cutaneous leishmaniasis in Al Hassa, Saudi Arabia: Epidemiological trends from 2000 to 2010. *Asian Pac. J. Trop. Med.* **6**, 667–672 (2013).
87. Haouas, N. *et al.* Cutaneous leishmaniasis in northwestern Saudi Arabia: identification of sand fly fauna and parasites. *Parasit. Vectors* **10**, 544 (2017).
88. Ready, P. D. Leishmaniasis emergence in Europe. *Euro Serveillance* **15**, 1–11 (2010).
89. Alvar, J. Leishmaniasis and AIDS co-infection: The Spanish example. *Parasitol. Today* **10**, (1994).
90. Desjeux, P. & Alvar, J. Leishmania/HIV co-infections: epidemiology in Europe. *Ann. Trop. Med. Parasitol.* **97**, 3–15 (2013).
91. Lindoso, J. A. L., Cunha, M. A., Queiroz, I. T. & Moreira, C. H. V. Leishmaniasis-HIV coinfection: current challenges. *HIV. AIDS. (Auckl).* **8**, 147–156 (2016).
92. Herrador, Z. *et al.* Epidemiological Changes in Leishmaniasis in Spain According to Hospitalization-Based Records, 1997–2011: Raising Awareness towards Leishmaniasis in Non-HIV Patients. *PLoS Negl. Trop. Dis.* **9**, e0003594 (2015).
93. Aguado, M. *et al.* Outbreak of Cutaneous Leishmaniasis in Fuenlabrada, Madrid. *Actas Dermosifiliogr.* **104**, 334–342 (2013).
94. Carrillo, E., Moreno, J. & Cruz, I. What is responsible for a large and unusual outbreak of leishmaniasis in Madrid? *Forum Sci. Soc.* **29**, (2013).
95. da Paixão Sevá, S. *et al.* Efficacies of prevention and control measures applied during an outbreak in Southwest Madrid, Spain. *PLoS One* **12**, e0186372 (2017).
96. González, E., Molina, R. & Jiménez, M. Rabbit trypanosome detection in Phlebotomus perniciosus sand flies from the leishmaniasis outbreak in Madrid, Spain. *Acta Trop.* **187**, 201–206 (2018).
97. PAHO & WHO. *Leishmaniasis Report #7. Epidemiological Report of the Americas*. (2017).
98. Monge-Maillo, B. & López-Vélez, R. Therapeutic Options for Old World Cutaneous Leishmaniasis and New World Cutaneous and Mucocutaneous Leishmaniasis. *Drugs* **73**, 1889–1920 (2013).

99. Harhay, M. O., Olliaro, P. L., Lamounier Costa, D., Henrique, C. & Costa, N. Urban parasitology: visceral leishmaniasis in Brazil. *Trends Parasitol.* **27**, (2011).
100. Goto, H., Angelo, J. & Lindoso, L. Current diagnosis and treatment of cutaneous and mucocutaneous leishmaniasis. *Expert Rev. Anti. Infect. Ther.* **8**, 419–433 (2014).
101. PAHO & WHO. *Bolivia; Cutaneous and mucosal Leishmaniasis 2017*. (2018).
102. Eid, D. *et al.* Risk factors for cutaneous leishmaniasis in the rainforest of Bolivia: a cross-sectional study. *Trop. Med. Health* **46**, 9 (2018).
103. Al-Salem, W. S. Epidemiological Characterization and Control of Old World Cutaneous Leishmaniasis in the Kingdom of Saudi Arabia. (University of Liverpool, 2015).
104. Ashford, D. A. *et al.* Studies on control of visceral leishmaniasis: impact of dog control on canine and human visceral leishmaniasis in Jacobina, Bahia, Brazil. *Am. J. Trop. Med. Hyg* **59**, 53–57 (1998).
105. Ribeiro, R. R. *et al.* Canine Leishmaniasis: An Overview of the Current Status and Strategies for Control. *Biomed Res. Int.* **2018**, 1–12 (2018).
106. Courtenay, O., Quinnell, R. J., Garcez, L. M., Shaw, J. J. & Dye, C. Infectiousness in a Cohort of Brazilian Dogs: Why Culling Fails to Control Visceral Leishmaniasis in Areas of High Transmission. *J. Infect. Dis.* **186**, 1314–1320 (2002).
107. Gradoni, L., Gramiccia, M., Mancianti, F. & Pieri, S. Studies on canine leishmaniasis control. 2. Effectiveness of control measures against canine leishmaniasis in the Isle of Elba, Italy. *Trans. R. Soc. Trop. Med. Hyg.* **82**, 568–571
108. Coleman, M. *et al.* DDT-based indoor residual spraying suboptimal for visceral leishmaniasis elimination in India. *PNAS* **112**, 8573–8578 (2009).
109. Kumar, V. *et al.* A report on the indoor residual spraying (IRS) in the control of Phlebotomus argentipes, the vector of visceral leishmaniasis in Bihar (India): an initiative towards total elimination targeting 2015 (Series-1). *J Vector Borne Dis* **46**, 225–229 (2009).
110. Chowdhury, R. *et al.* The Indian and Nepalese programmes of indoor residual spraying for the elimination of visceral leishmaniasis: performance and effectiveness. *Ann. Trop. Med. Parasitol.* **105**, 31–35 (2011).
111. Dinesh, D. S. *et al.* Insecticide Susceptibility of Phlebotomus argentipes in Visceral Leishmaniasis Endemic Districts in India and Nepal. *PLoS Negl. Trop. Dis.* **4**, e859 (2010).
112. Reithinger, R., Mohsen, M. & Leslie, T. Risk Factors for Anthroponotic Cutaneous Leishmaniasis at the Household Level in Kabul, Afghanistan. *PLoS Negl. Trop. Dis.* **4**, e639 (2010).
113. Reithinger, R. *et al.* Anthroponotic cutaneous leishmaniasis, Kabul, Afghanistan. *Emerg. Infect. Dis.* **9**, 727–9 (2003).
114. Bern, C. *et al.* Factors associated with visceral leishmaniasis in nepal: bed-net use is strongly protective. *Am. J. Trop. Med. Hyg* **63**, 184–188 (2000).
115. González, U. *et al.* Vector and reservoir control for preventing leishmaniasis. *Cochrane Database Syst. Rev.* **2015**, (2015).
116. Khamesipour, A. *et al.* Leishmanization: Use of an old method for evaluation

of candidate vaccines against leishmaniasis. *Vaccine* **23**, 3642–3648 (2005).
117. Nadim, A., Javadian, E. & Mohebali, M. The experience of leishmanization in the Islamic Republic of Iran. *East. Mediterr. Heal. J.* **3**, 284–289 (1997).
118. Dunning, N. Leishmania vaccines: from leishmanization to the era of DNA technology. *Biosci. Horizons* **2**, (2009).
119. Kedzierski, L., Zhu, Y. & Handman, E. Leishmania vaccines : progress and problems. *Parasitology* **133**, 87–112 (2006).
120. Ghorbani, M. & Farhoudi, R. Leishmaniasis in human: drug or vaccine therapy. *Drug Des. Devel. Ther.* 12–25 (2018). doi:10.2147/DDDT.S146521
121. Kumar, R. & Engwerda, C. Vaccines to prevent leishmaniasis. *Clin. Transl. Immunol.* **3**, (2014).
122. Iniguez, E. *et al.* An α-Gal-containing neoglycoprotein-based vaccine partially protects against murine cutaneous leishmaniasis caused by Leishmania major. *PLoS Negl. Trop. Dis.* **11**, e0006039 (2017).
123. Joshi, A. *et al.* Can visceral leishmaniasis be eliminated from Asia? *J Vector Borne Dis* **45**, 105–111 (2008).
124. Hodiamont, C. J. *et al.* Species-directed therapy for leishmaniasis in returning travellers: a comprehensive guide. *PLoS Negl. Trop. Dis.* **8**, e2832 (2014).
125. Asilian, A. *et al.* A randomized, placebo-controlled trial of a two-week regimen of aminosidine (paromomycin) ointment for treatment of cutaneous leishmaniasis in Iran. *Am. J. Trop. Med. Hyg.* **53**, 648–651 (1995).
126. Salah, A. B. *et al.* A randomized, placebo-controlled trial in Tunisia treating cutaneous leishmaniasis with paromomycin ointment. *Am. J. Trop. Med. Hyg.* **53**, 162–166 (1995).
127. Singh, N., Kumar, M. & Singh, R. K. Leishmaniasis: Current status of available drugs and new potential drug targets. *Asian Pac. J. Trop. Med.* **5**, 485–497 (2012).
128. Ponte-Sucre, A. *et al.* Drug resistance and treatment failure in leishmaniasis: A 21st century challenge. *PLoS Negl. Trop. Dis.* **11**, e0006052 (2017).
129. Murray, H. W., Berman, J. D., Davies, C. R. & Saravia, N. G. Advances in leishmaniasis. *Lancet* **366**, 1561–1577 (2005).
130. Minodier, P. & Parola, P. Cutaneous leishmaniasis treatment. *Travel Med. Infect. Dis.* **5**, 150–158 (2007).
131. Bourreau, E. *et al.* Presence of Leishmania RNA Virus 1 in Leishmania guyanensis Increases the Risk of First-Line Treatment Failure and Symptomatic Relapse. *J. Infect. Dis.* **213**, 105–111 (2016).
132. Kumar Sinha, P. & Bhattacharya, S. Single-dose liposomal amphotericin B: an eff ective treatment for visceral leishmaniasis. *Lancet Glob. Heal.* **2**, e7–e8 (2014).
133. Sundar, S. *et al.* Single-Dose Liposomal Amphotericin B in the Treatment of Visceral Leishmaniasis in India: A Multicenter Study. *Clin. Infect. Dis.* **37**, 800–804 (2003).
134. Mondal, D. *et al.* Efficacy and safety of single-dose liposomal amphotericin B for visceral leishmaniasis in a rural public hospital in Bangladesh: a feasibility study. *Lancet Glob. Heal.* **2**, e51–e57 (2014).
135. Velez, I. *et al.* Efficacy of Miltefosine for the Treatment of American Cutaneous Leishmaniasis. *Am. J. Trop. Med. Hyg.* **83**, 351–356 (2010).

136. Sundar, S., Jha, T. K., Thakur, C. P., Bhattacharya, S. K. & Rai, M. Oral miltefosine for the treatment of Indian visceral leishmaniasis. *Trans. R. Soc. Trop. Med. Hyg.* **100**, 26–33 (2006).
137. Sundar, S. & Olliaro, P. L. Miltefosine in the treatment of leishmaniasis: Clinical evidence for informed clinical risk management. *Ther. Clin. Risk Manag.* **3**, 733–740 (2007).
138. Soto, J. *et al. Treatment of Bolivian Mucosal Leishmaniasis with Miltefosine*. (2007).
139. Kim, D. H., Chung, H. J., Bleys, J. & Ghohestani, R. F. Is paromomycin an effective and safe treatment against cutaneous leishmaniasis? A meta-analysis of 14 randomized controlled trials. *PLoS Negl. Trop. Dis.* **3**, (2009).
140. Tiuman, T. S., Santos, A. O., Ueda-Nakamura, T., Filho, B. P. D. & Nakamura, C. V. Recent advances in leishmaniasis treatment. *Int. J. Infect. Dis.* **15**, (2011).
141. Al-Jaser, M. H. Treatment trends of cutaneous leishmaniasis in Saudi Arabia. *Saudi Med. J.* **26**, 1220–4 (2005).
142. Mosleh, I. M. *et al.* Efficacy of a weekly cryotherapy regimen to treat Leishmania major cutaneous leishmaniasis. *J. Am. Acad. Dermatol.* **58**, 617–624 (2008).
143. Farajzadeh, S. *et al.* Evaluation of the efficacy of intralesional Glucantime plus niosomal zinc sulphate in comparison with intralesional Glucantime plus cryotherapy in the treatment of acute cutaneous leishmaniasis, a randomized clinical trial. *J. Parasit. Dis.* **42**, 616–620 (2018).
144. Al-Qubati, Y., Janniger, E. J. & Schwartz, R. A. Cutaneous leishmaniasis: cryosurgery using carbon dioxide slush in a resource-poor country. *Int. J. Dermatol.* **51**, 1217–1220 (2012).
145. Johansen, M. B., Jemec, G. B. E. & Fabricius, S. Effective treatment with photodynamic therapy of cutaneous leishmaniasis: A case report. *Dermatol. Ther.* **32**, e13022 (2019).
146. Reithinger, R. *et al.* Efficacy of Thermotherapy to Treat Cutaneous Leishmaniasis Caused by Leishmania tropica in Kabul, Afghanistan: A Randomized, Controlled Trials. *Clin. Infect. Dis.* **40**, 1148–55 (2005).
147. Refai, W. F. *et al.* Efficacy, Safety and Cost-Effectiveness of Thermotherapy in the Treatment of Leishmania donovani-Induced Cutaneous Leishmaniasis: A Randomized Controlled Clinical Trial. *Am. J. Trop. Med. Hyg* **97**, 1120–1126 (2017).
148. Cardona-Arias, J. A., Vélez, I. D. & López-Carvajal, L. Efficacy of Thermotherapy to Treat Cutaneous Leishmaniasis: A Meta-Analysis of Controlled Clinical Trials. *PLoS One* **10**, e0122569 (2015).
149. Ramdas, S. Cruel disease, cruel medicine: Self-treatment of cutaneous leishmaniasis with harmful chemical substances in Suriname. *Soc. Sci. Med.* **75**, 1097–1105 (2012).
150. Kebede, N. *et al.* Community knowledge, attitude and practice towards cutaneous leishmaniasis endemic area Ochello, Gamo Gofa Zone, South Ethiopia. *Asian Pac. J. Trop. Biomed.* **6**, 562–567 (2016).
151. Sarkari, B., Qasem, A. & Shafaf, M. R. Knowledge, attitude, and practices related to cutaneous leishmaniasis in an endemic focus of cutaneous leishmaniasis, Southern Iran. *Asian Pac. J. Trop. Biomed.* **4**, 566–569 (2014).

152. Swain, S. K., Behera, I. C., Sahu, M. C. & Panda, M. Isolated cutaneous leishmaniasis over face – A diagnostic dilemma. *Alexandria J. Med.* **52**, 343–346 (2016).
153. Alam, E., Abbas, O., Moukarbel, R. & Khalifeh, I. Cutaneous Leishmaniasis: An Overlooked Etiology of Midfacial Destructive Lesions. *PLoS Negl. Trop. Dis.* **10**, e0004426 (2016).
154. Handler, M. Z., Patel, P. A., Kapila, R., Al-Qubati, Y. & Schwartz, R. A. Cutaneous and mucocutaneous leishmaniasis: Differential diagnosis, diagnosis, histopathology, and management. *J. Am. Acad. Dermatol.* **73**, 911–926 (2015).
155. Saab, J. *et al.* Cutaneous leishmaniasis mimicking inflammatory and neoplastic processes: A clinical, histopathological and molecular study of 57 cases. *J. Cutan. Pathol.* **39**, 251–262 (2012).
156. De Vries, H. J. C., Reedijk, S. H. & Schallig, H. D. F. H. Cutaneous Leishmaniasis: Recent Developments in Diagnosis and Management. *Am. J. Clin. Dermatol.* **16**, 99–109 (2015).
157. WHO. *Recognizing neglected tropical diseases through changes on the skin: a training guide for front-line health workers*. (2018).
158. Vega-López, F. Diagnosis of cutaneous leishmaniasis. *Curr. Opin. Infect. Dis.* **16**, 97–101 (2003).
159. Sundar, S., Rai, M., Shyam Sundar and M. Rai & Kala-Azar. Laboratory Diagnosis of Visceral Leishmaniasis. *Clin. Diagn. Lab. Immunol.* **9**, 951–958 (2002).
160. Bensoussan, E., Nasereddin, A., Jonas, F., Schnur, L. F. & Jaffe, C. L. Comparison of PCR Assays for Diagnosis of Cutaneous Leishmaniasis. *J. Clin. Microbiol.* **44**, 1435–1439 (2006).
161. Aviles, H., Belli, A., Armijos, R., Monroy, F. P. & Harris, E. PCR detection and identification of Leishmania parasites in clinical specimens in Ecuador: a comparison with classical diagnostic methods. *J. Parasitol.* **85**, 181–7 (1999).
162. Faber, W. R. *et al.* Value of diagnostic techniques for cutaneous leishmaniasis. *J. Am. Acad. Dermatol.* **49**, 70–74 (2003).
163. Saab, M., El Hage, H., Charafeddine, K., Habib, R. H. & Khalifeh, I. Diagnosis of cutaneous leishmaniasis: Why punch when you can scrape? *Am. J. Trop. Med. Hyg.* **92**, 518–522 (2015).
164. Adams, E. R. *et al.* Development and Evaluation of a Novel Loop-Mediated Isothermal Amplification Assay for Diagnosis of Cutaneous and Visceral Leishmaniasis. *J. Clin. Microbiol.* **56**, (2018).
165. Khan, M. G. M. *et al.* Diagnostic accuracy of loop-mediated isothermal amplification (LAMP) for detection of Leishmania DNA in buffy coat from visceral leishmaniasis patients. *Parasit. Vectors* **5**, 280 (2012).
166. Mukhtar, M. *et al.* Sensitive and less invasive confirmatory diagnosis of visceral leishmaniasis in Sudan using loop-mediated isothermal amplification (LAMP). *PLoS Negl. Trop. Dis.* **12**, e0006264 (2018).
167. Mikita, K. *et al.* The Direct Boil-LAMP method: A simple and rapid diagnostic method for cutaneous leishmaniasis. *Parasitol. Int.* **63**, 785–789 (2014).
168. Imai, K. *et al.* Non-invasive diagnosis of cutaneous leishmaniasis by the direct boil loop-mediated isothermal amplification method and MinION™ nanopore

sequencing. *Parasitol. Int.* **67**, 34–37 (2018).
169. WHO. *The Use of Visceral Leishmaniasis Rapid Diagnostic Tests*. (2008).
170. Kumar, R., Pai, K., Pathak, K. & Sundar, S. Enzyme-Linked Immunosorbent Assay for Recombinant K39 Antigen in Diagnosis and Prognosis of Indian Visceral Leishmaniasis. *Clin. Diagn. Lab. Immunol.* **8**, 1220–1224 (2001).
171. Varani, S. *et al.* Serological and molecular tools to diagnose visceral leishmaniasis: 2-years' experience of a single center in Northern Italy. *PLoS One* **12**, e0183699 (2017).
172. Barbosa-De-Deus, R. *et al.* Leishmania major-Like Antigen for Specific and Sensitive Serodiagnosis of Human and Canine Visceral Leishmaniasis. *Clin. Diagn. Lab. Immunol.* **9**, 1361–1366 (2002).
173. Ryan, J. R. *et al.* Enzyme-Linked Immunosorbent Assay Based on Soluble Promastigote Antigen Detects Immunoglobulin M (IgM) and IgG Antibodies in Sera from Cases of Visceral and Cutaneous Leishmaniasis. *J. Clin. Microbiol.* **40**, 1037–1043 (2002).
174. Guimarães, M. C., Celeste, B. J. & Franco, E. L. Diagnostic performance indices for immunofluorescent tests and enzyme immunoassays of leishmaniasis sera from northern and north-eastern Brazil. *Bull. World Health Organ.* **68**, 39–43 (1990).
175. Yildiz Zeyrek, F. & Korkmaz, M. Serodiagnosis of Anthroponotic Cutaneous Leishmaniasis (ACL) Caused by Leishmania tropica in Sanliurfa Province, Turkey, Where ACL Is Highly Endemic. *Clin. VACCINE Immunol.* **14**, 1409–1415 (2007).
176. Rohoušová, I. *et al.* Serological Evaluation of Cutaneous Leishmania tropica Infection in Northern Israel. *Am. J. Trop. Med. Hyg* **98**, 139–141 (2018).
177. Schallig, H. D. F. H. *et al.* Evaluation of point of care tests for the diagnosis of cutaneous leishmaniasis in Suriname. doi:10.1186/s12879-018-3634-3
178. De Silva, G. *et al.* Efficacy of a new rapid diagnostic test kit to diagnose Sri Lankan cutaneous leishmaniasis caused by Leishmania donovani. *PLoS One* **12**, e0187024 (2017).
179. Bennis, I. *et al.* Accuracy of a Rapid Diagnostic Test Based on Antigen Detection for the Diagnosis of Cutaneous Leishmaniasis in Patients with Suggestive Skin Lesions in Morocco. *Am. J. Trop. Med. Hyg.* **99**, 716–722 (2018).
180. Vink, M. M. T. *et al.* Evaluation of point-of-care tests for cutaneous leishmaniasis diagnosis in Kabul, Afghanistan. *EBioMedicine* **37**, 453–460 (2018).
181. Aerts, C. *et al.* Cost Effectiveness of New Diagnostic Tools for Cutaneous Leishmaniasis in Afghanistan. *Appl. Health Econ. Health Policy* **17**, 213–230 (2019).
182. Du, R. *et al.* Old World Cutaneous Leishmaniasis and Refugee Crises in the Middle East and North Africa. *PLoS Negl. Trop. Dis.* **10**, e0004545 (2016).
183. Safadi, D. El *et al.* Cutaneous leishmaniasis in north Lebanon: re-emergence of an important neglected tropical disease. *Trans R Soc Trop Med Hyg* **00**, 1–6 (2019).
184. Kanani, K. *et al.* Cutaneous leishmaniasis among Syrian refugees in Jordan. *Acta Trop.* **194**, 169–171 (2019).

185. Soltani, S., Foroutan, M., Hezarian, M., Afshari, H. & Kahvaz, M. S. Cutaneous leishmaniasis: an epidemiological study in southwest of Iran. *J. Parasit. Dis.* **43**, 190–197 (2019).
186. Eroglu, F. & Ozgoztasi, O. The increase in neglected cutaneous leishmaniasis in Gaziantep province of Turkey after mass human migration. *Acta Trop.* **192**, 138–143 (2019).
187. Özbilgin, A. *et al.* The current clinical and geographical situation of cutaneous leishmaniasis based on species identification in Turkey. *Acta Trop.* **190**, 59–67 (2019).
188. Özkeklikç, A., Karakus, M., Özbel, Y. & Töz, S. The new situation of cutaneous leishmaniasis after Syrian civil war in Gaziantep city, Southeastern region of Turkey. *Acta Trop.* **166**, 35–38 (2017).
189. Isenring, E., Fehr, J., Gültekin, N. & Schlagenhauf, P. Infectious disease profiles of Syrian and Eritrean migrants presenting in Europe: A systematic review. *Travel Med. Infect. Dis.* **25**, 65–76 (2018).
190. Söbirk, S. K., Inghammar, M., Collin, M. & Davidsson, L. Imported leishmaniasis in Sweden 1993–2016. *Epidemiol. Infect.* **146**, 1267–1274 (2017).
191. Galili, U., Rachmilewitz, E. A., Peleg, A. & Flechner, I. A unique natural human IgG antibody with anti-alpha-Gal specificity. *J. Exp. Med.* **160**, 1519–1531 (1984).
192. Ravindranath, M. H. & Muthugounder, S. Human Anti-A-Galactosyl Antibodies. in *Autoantibodies* 285–291 (Elsevier Inc., 2007).
193. Hamanova, M., Chmelikova, M., Nentwich, I., Thon, V. & Lokaj, J. Anti-Gal IgM, IgA and IgG natural antibodies in childhood. *Immunol. Lett.* **164**, 40–43 (2015).
194. Galili, U. The natural anti-Gal antibody, the B-like antigen, and human red cell aging. *Blood Cells* **14**, (1988).
195. Mañez, R. *et al.* Removal of bowel aerobic gram-negative bacteria is more effective than immunosuppression with cyclophosphamide and steroids to decrease natural α-Galactosyl IgG antibodies. *Xenotransplantation* **8**, 15–23 (2001).
196. Böer, U. *et al.* Antibody formation towards porcine tissue in patients implanted with crosslinked heart valves is directed to antigenic tissue proteins and αGal epitopes and is reduced in healthy vegetarian subjects. *Xenotransplantation* **24**, e12288 (2017).
197. Anraku, K. *et al.* The design and synthesis of an α-Gal trisaccharide epitope that provides a highly specific anti-Gal immune response. *Org. Biomol. Chem.* **15**, 2979–2992 (2017).
198. Agostino, M., Sandrin, M. S., Thompson, P. E., Yuriev, E. & Ramsland, P. A. In silico analysis of antibody-carbohydrate interactions and its application to xenoreactive antibodies. *Mol. Immunol.* **47**, 233–246 (2009).
199. Milland, J. *et al.* Carbohydrate residues downstream of the terminal Gala(1,3)Gal epitope modulate the specificity of xenoreactive antibodies. *Immunol. Cell Biol.* **85**, 623–632 (2007).
200. Agostino, M., Sandrin, M. S., Thompson, P. E., Yuriev, E. & Ramsland, P. A. Identification of preferred carbohydrate binding modes in xenoreactive

antibodies by combining conformational filters and binding site maps. *Glycobiology* **20**, 724–735 (2010).
201. Galili, U., Clark, M. R., Shohet, S. B., Buehler, J. & Macher, B. A. Evolutionary relationship between the natural anti-Gal antibody and the Gal alpha 1,3Gal epitope in primates. *Proc. Natl. Acad. Sci. U. S. A.* **84**, 1369–73 (1987).
202. Galili, U. Discovery of the natural anti-Gal antibody and its past and future relevance to medicine. *Xenotransplantation* **20**, (2013).
203. Galili, U. Evolution in primates by 'Catastrophic-selection' interplay between enveloped virus epidemics, mutated genes of enzymes synthesizing carbohydrate antigens, and natural anti-carbohydrate antibodies. *Am. J. Phys. Anthropol.* **168**, 352–363 (2018).
204. Galili, U. Xenotransplantation and ABO incompatible transplantation: The similarities they share. *Transfus. Apher. Sci.* **35**, (2006).
205. Galili, U. Anti-Gal Comprises Most of Anti-Blood Group B Antibodies: Landsteiner's B-Like Enigma. in *The Natural Anti-Gal Antibody As Foe Turned Friend In Medicine* 45–55 (Academic Press, 2018).
206. Galili, U., Ishida, H., Tanabe, K. & Toma, H. Anti-gal A/B, a novel anti-blood group antibody identified in recipients of ABO-incompatible kidney allografts. *Transplantation* **74**, (2002).
207. Cabezas-Cruz, A. *et al.* Effect of blood type on anti-α-Gal immunity and the incidence of infectious diseases. *Exp. Mol. Med.* **49**, 301 (2017).
208. Platt, J. L. A Perspective on Xenograft Rejection and Accommodation. *Immunol. Rev.* **141**, 127–149 (1994).
209. Xu, Y. *et al.* Removal of Anti-Porcine Natural Antibodies From Human and Nonhuman Primate Plasma in Vitro and in Vivo by a Galα1-3Galβ1-4Glc-x Immunoaffinity Column. *Transplantation* **65**, 172–179 (1998).
210. Lai, L. *et al.* Production of Knockout Pigs by Nuclear Transfer Cloning. *Science (80-.).* **295**, 1089–1092 (2002).
211. Sianturi, J. *et al.* Development of α-Gal-Antibody Conjugates to Increase Immune Response by Recruiting Natural Antibodies. *Angew. Chemie Int. Ed.* **58**, 4526–4530 (2019).
212. Abdel-Motal, U., Guay, H. M., Wigglesworth, K., Welsh, R. M. & Galili, U. Immunogenicity of Influenza Virus Vaccine Is Increased by Anti-Gal-Mediated Targeting to Antigen-Presenting Cells. *J. Virol.* **81**, 9131–9141 (2007).
213. Abdel-Motal, U., Wang, S., Lu, S., Wigglesworth, K. & Galili, U. Increased Immunogenicity of Human Immunodeficiency Virus gp120 Engineered To Express Gal1-3Gal1-4GlcNAc-R Epitopes. *J. Virol.* **80**, 6943–6951 (2006).
214. Whalen, G. F., Sullivan, M., Piperdi, B., Wasseff, W. & Galili, U. Cancer immunotherapy by intratumoral injection of α-gal glycolipids. *Anticancer Res.* **32**, (2012).
215. Galili, U. Conversion of tumors into autologous vaccines by intratumoral injection of -gal glycolipids that induce anti-gal/-gal epitope interaction. *Clin. Dev. Immunol.* **2011**, (2011).
216. Tanemura, M. *et al.* Cancer immunotherapy for pancreatic cancer utilizing α-gal epitope/natural anti-Gal antibody reaction. *World J. Gastroenterol.* **21**, 11396–11410 (2015).
217. Al-Salem, W. S. *et al.* Detection of high levels of anti-α-galactosyl antibodies

in sera of patients with Old World cutaneous leishmaniasis: a possible tool for diagnosis and biomarker for cure in an elimination setting. *Parasitology* **141**, 1898–1903 (2014).
218. Avila, J. L., Rojas, M. & Garcia, L. Persistence of Elevated Levels of Galactosyl-Alpha(1-3)Galactose Antibodies in Sera From Patients Cured of Visceral Leishmaniasis. *J. Clin. Microbiol.* **26**, 1842–1847 (1988).
219. Avila, J. L., Rojas, M. & Towbin, H. Serological activity against galactosyl-alpha(1-3)galactose in sera from patients with several kinetoplastida infections. *J. Clin. Microbiol.* **26**, 126–32 (1988).
220. Towbin, H. *et al.* Circulating antibodies to mouse laminin in Chagas disease, American cutaneous leishmaniasis, and normal individuals recognize terminal galactosyl(alpha 1-3)-galactose epitopes. *J. Exp. Med.* **166**, 419–432 (1987).
221. Pearse, M. J. *et al.* Anti-gal antibody-mediated allograft rejection in α1,3-galactosyltransferase gene knockout mice: A model of delayed xenograft rejection. *Transplantation* **66**, 748–754 (1998).
222. Ferguson, M. A. J. The structure, biosynthesis and functions of glycosylphosphatidylinositol anchors, and the contributions of trypanosome research. *J. Cell Sci.* **112**, 2799–2809 (1999).
223. Ilgoutz, S. C. & McConville, M. J. Function and assembly of the Leishmania surface coat. *Int. J. Parasitol.* **31**, 899–908 (2001).
224. Ilg, T. Lipophosphoglycan of the protozoan parasite Leishmania: stage- and species-specific importance for colonization of the sandfly vector, transmission and virulence to mammals. *Med. Microbiol. Immunol.* **190**, 13–17 (2001).
225. Ilg, T. Proteophosphoglycans of Leishmania. *Parasitol. Today* **16**, 489–497 (2000).
226. McConville, M. J. & Ferguson, M. A. J. The structure, biosynthesis and function of glycosylated phosphatidylinositols in the parasitic protozoa and higher eukaryotes. *Biochem. J.* **294**, 305–324 (1993).
227. Moody, S. F., Handman, E., McConville, M. J. & Bacic, A. The structure of Leishmania major amastigote lipophosphoglycan. *J. Biol. Chem.* **268**, 18457–66 (1993).
228. McConville, M. J. & Blackwell, J. M. Developmental changes in the glycosylated phosphatidylinositols of Leishmania donovani. *J. Biol. Chem.* **266**, 15170–15179 (1991).
229. Avila, J. L. & Rojas, M. A galactosyl (alpha1-3) mannose epitope on phospholipids of Leishmania mexicana and L. braziliensis is recognized by trypanosomatid-infected human sera. *J. Clin. Microbiol.* **28**, 1530–1537 (1990).
230. Schneider, P., Schnur, L. F., Jaffe, C. L., Ferguson, M. A. J. & McConville, M. J. Glycoinositol-phospholipid profiles of four serotypically distinct Old World Leishmania strains. *Biochem. J.* **304**, 603–9 (1994).
231. Assis, R. R., Ibraim, I. C., Noronha, F. S., Turco, S. J. & Soares, R. P. Glycoinositolphospholipids from Leishmania braziliensis and L. infantum: Modulation of Innate Immune System and Variations in Carbohydrate Structure. *PLoS Negl. Trop. Dis.* **6**, e1543 (2012).
232. Yoneyama, K. A. G., Tanaka, A. K., Silveira, T. G. V, Takahashi, H. K. & Straus,

A. H. Characterization of Leishmania (Viannia) braziliensis membrane microdomains, and their role in macrophage infectivity. *J. Lipid Res.* **47**, 2171–2178 (2006).
233. Descoteaux, A. & Turco, S. J. Glycoconjugates in Leishmania infectivity. *Biochim. Biophys. Acta - Mol. Basis Dis.* **1455**, 341–352 (1999).
234. Cabezas, Y. *et al.* Leishmania cell wall as a potent target for antiparasitic drugs. A focus on the glycoconjugates. *Org. Biomol. Chem.* **13**, (2015).
235. Schneider, P., Rosat, J. P., Ransijn, A., Ferguson, M. A. J. & McConville, M. J. Characterization of glycoinositol phospholipids in the amastigote stage of the protozoan parasite Leishmania major. *Biochem. J.* **295**, 555–64 (1993).
236. de Assis, R. R., Ibraim, I. C., Nogueira, P. M., Soares, R. P. & Turco, S. J. Glycoconjugates in New World species of Leishmania: Polymorphisms in lipophosphoglycan and glycoinositolphospholipids and interaction with hosts. *Biochim. Biophys. Acta* **1820**, 1354–1365 (2012).
237. McConville, M. J., Homans, S. W. W., Thomas-Oates, J. E. E., Dell, A. & Bacic, A. Structures of the glycoinositolphospholipids from Leishmania major. A family of novel galactofuranose-containing glycolipids. *J. Biol. Chem.* **265**, 7385–94 (1990).
238. McConville, M. J., Thomas-Oates, J. E., Ferguson, M. A. J. & Homans, S. W. Structure of the lipophosphoglycan from Leishmania major. *J. Biol. Chem.* **265**, 19611–23 (1990).
239. McConville, M. J. & Bacic, A. A family of glycoinositol phospholipids from Leishmania major. *J. Biol. Chem.* **264**, 757–766 (1989).
240. Stanaway, J. D. & ROth, G. The Burden of Chagas Disease: Estimates and Challenges. *Glob. Heart* **10**, 139–144 (2015).
241. Schmunis, G. A. Prevention of Transfusional Trypanosoma cruzi Infection in Latin America. *Memórias do Inst. Oswaldo Cruz* **94**, 93–101 (1999).
242. Wendel, S. Transfusion transmitted Chagas disease: Is it really under control? *Acta Trop.* **115**, 28–34 (2010).
243. Grinnage-Pulley, T., Scott, B. & Petersen, C. A. A Mother's Gift: Congenital Transmission of Trypanosoma and Leishmania Species. *PLOS Pathog.* **12**, e1005302 (2016).
244. Sasagawa, S. *et al.* Mother to Child Transmission of Chagas Disease in El Salvador. *Am. J. Trop. Med. Hyg.* **93**, 326–333 (2015).
245. Coura, J. R. The main sceneries of chagas disease transmission. The vectors, blood and oral transmissions - A comprehensive review. *Memórias do Inst. Oswaldo Cruz* **110**, 277–282 (2015).
246. Andrade, D. V, Gollob, K. J. & Dutra, W. O. Acute Chagas Disease: New Global Challenges for an Old Neglected Disease. *PLoS Negl. Trop. Dis.* **8**, (2014).
247. Malik, L. H., Singh, G. D. & Amsterdam, E. A. Chagas Heart Disease: An Update. *Am. J. Med.* **128**, 1251.e7-1251.e9 (2015).
248. Acosta-Serrano, A., Almeida, I. C., Freitas-Junior, L. H., Yoshida, N. & Schenkman, S. The mucin-like glycoprotein super-family of Trypanosoma cruzi: Structure and biological roles. *Mol. Biochem. Parasitol.* **114**, 143–150 (2001).
249. Almeida, I. C., Gazzinelli, R. T., Ferguson, M. A. J. & Travassos, L. R. Trypanosoma cruzi mucins: potential functions of a complex structure.

Memórias do Inst. Oswaldo Cruz **94**, 173–6 (1999).
250. Soares, R. P. *et al.* Intraspecies variation in Trypanosoma cruzi GPI-mucins: biological activities and differential expression of α-galactosyl residues. *Am. J. Trop. Med. Hyg.* **87**, 87–96 (2012).
251. Avila, J. L., Rojas, M. & Velazquez-Avila, G. Characterization of a natural human antibody with anti- galactosyl(alpha 1-2)galactose specificity that is present at high titers in chronic Trypanosoma cruzi infection. *Am. J. Trop. Med. Hyg.* **47**, 413–421 (1992).
252. Avila, J. L., Rojas, M. & Galili, U. Immunogenic Gal alpha 1-3Gal carbohydrate epitopes are present on pathogenic American Trypanosoma and Leishmania. *J. Immunol.* **142**, 2828–34 (1989).
253. Almeida, I. C., Milani, S. R., Gorin, P. A. & Travassos, L. R. Complement-mediated lysis of Trypanosoma cruzi trypomastigotes by human anti-alpha-galctosyl antibodies. *J. Immunol.* **146**, 2394–2400 (1991).
254. Almeida, I. C., Ferguson, M. A. J., Schenkman, S. & Travassos, L. R. Lytic anti-α-galactosyl antibodies from patients with chronic Chagas' disease recognize novel O-linked oligosaccharides on mucin-like glycosyl-phosphatidylinositol-anchored glycoproteins of Trypanosoma cruzi. *Biochem. J.* **304**, 793–802 (1994).
255. Gazzinelli, R. T. Natural anti-Gal antibodies prevent, rather than cause, autoimmunity in human Chagas' disease. *Res. Immunol.* **142**, 164–7 (1991).
256. Gorin, A. J. & Travassos, L. R. Complement-mediated lysis of Trypanosoma cruzi trypomastigotes by human anti-alpha-galactosyl antibodies. *J. Immunol.* **146**, 2394–2400 (1991).
257. Pereira-Chioccola, V. L. *et al.* Mucin-like molecules form a negatively charged coat that protects Trypanosoma cruzi trypomastigotes from killing by human anti-alpha-galactosyl antibodies. *J. Cell Sci.* **113**, 1299–1307 (2000).
258. Almeida, I. C., Ferguson, M. A., Schenkman, S. & Travassos, L. R. GPI-anchored glycoconjugates from Trypanosoma cruzi trypomastigotes are recognized by lytic anti-alpha-galactosyl antibodies isolated from patients with chronic Chagas' disease. *Brazilian J. Med. Biol. Res.* **27**, (1994).
259. Torrico, F. *et al.* Treatment of adult chronic indeterminate Chagas disease with benznidazole and three E1224 dosing regimens: a proof-of-concept, randomised, placebo-controlled trial. *Lancet Infect. Dis.* **18**, 419–430 (2018).
260. Schocker, N. S. *et al.* Synthesis of Galα(1,3)Galβ(1,4)GlcNAcα-, Galβ(1,4)GlcNAcα-, and GlcNAcα-containing neoglycoproteins and their immunological evaluation in the context of Chagas disease. *Glycobiology* **26**, 39–50 (2016).
261. Ortega-Rodriguez, U. *et al.* Purification of Glycosylphosphatidylinositol-Anchored Mucins from Trypanosoma cruzi Trypomastigotes and Synthesis of α-Gal-Containing Neoglycoproteins: Application as Biomarkers for Reliable Diagnosis and Early Assessment of Chemotherapeutic Outcomes of C. in *T. cruzi Infection* 287–308 (Humana Press, New York, NY, 2019). doi:10.1007/978-1-4939-9148-8_22
262. Ravindran, B., Satapathy, A. K. & Das, M. K. Naturally-occurring anti-a-galactosyl antibodies in human Plasmodium falciparum infections -a possible role for autoantibodies in malaria. *Immunol. Lett.* **19**, 137–141 (1988).

263. Coelho, Z. B. A. *et al.* Preliminary assessment of anti-α-Gal IgG and IgM levels in patients with patent Plasmodium vivax infection. *Mem Inst Oswaldo Cruz* **114**, 1–3 (2019).
264. Ramasamy, R. & Reese, R. T. A role for carbohydrate moieties in the immune rsponse to malaria. *J Immunol* **134**, 1952–1955 (1985).
265. Yilmaz, B. *et al.* Gut microbiota elicits a protective immune response against malaria transmission. *Cell* **159**, 1277–1289 (2014).
266. Ramasamy, R. & Field, M. C. Terminal galactosylation of glycoconjugates in Plasmodium falciparum asexual blood stages and Trypanosoma brucei bloodstream trypomastigotes. *Exp. Parasitol.* **130**, 314–320 (2012).
267. Soares, M. P. & Yilmaz, B. Microbiota Control of Malaria Transmission. *Trends Parasitol.* **32**, 120–130 (2016).
268. Ngwa, C. J. & Pradel, G. Coming soon: probiotics-based malaria vaccines. *Cell* **31**, (2015).
269. Cabezas-Cruz, A. & de la Fuente, J. Immunity to α-Gal: Toward a Single-Antigen Pan-Vaccine To Control Major Infectious Diseases. *ACS Cent. Sci.* **3**, 1140–1142 (2017).
270. Cabezas-Cruz, A. & de la Fuente, J. Immunity to α-Gal: The Opportunity for Malaria and Tuberculosis Control. *Front. Immunol.* **8**, 1733 (2017).
271. Portillo, S. *et al.* A prophylactic α-Gal-based glycovaccine effectively protects against murine acute Chagas disease. *npj Vaccines* **4**, 13 (2019).
272. Schonian, G. *et al.* PCR diagnosis and characterization of Leishmania in local and imported clinical samples. *Diagn. Microbiol. Infect. Dis.* **47**, 349–358 (2003).
273. Tsuchiya, S. *et al.* Establishment and characterization of a human acute monocytic leukemia cell line (THP-1). *Int. J. Cancer* **26**, 171–176 (1980).
274. Ashmus, R. A. *et al.* Potential use of synthetic α-galactosyl-containing glycotopes of the parasite Trypanosoma cruzi as diagnostic antigens for Chagas disease. *Org. Biomol. Chem.* **11**, 5579–83 (2013).
275. Subramaniam, K. S. *et al.* Anti-α-Gal antibodies detected by novel neoglycoproteins as a diagnostic tool for Old World cutaneous leishmaniasis caused by Leishmania major. *Parasitology* **145**, 1758–1764 (2018).
276. Greenhouse, S. W. & Geisser, S. On methods in the analysis of profile data. *Psychometrika* **24**, 95–112 (1959).
277. Tabachnick, B. G. & Fidell, L. S. *Using multivariate statistics*. (Pearson, 2014).
278. Box, G. E. P. & Tidwell, P. W. Transformation of the Independent Variables. *Technometrics* **4**, 531–550 (1962).
279. Avila, J. L., Rojas, M. & Acosta-Serrano, A. Glycoinositol phospholipids from American Leishmania and Trypanosoma spp.: Partial characterization of the glycan cores and the human humoral immune response to them. *J. Clin. Microbiol.* **29**, 2305–2312 (1991).
280. McConville, M. J. & Bacic, A. The glycoinositolphospholipid profiles of two Leishmania major strains that differ in lipophosphoglycan expression. *Mol. Biochem. Parasitol.* **38**, 57–62 (1990).
281. Laitinen, L. Griffonia simplicifolia lectins bind specifically to endothelial cells and some epithelial cells in mouse tissues. *Histochem. J.* **19**, 225–234 (1987).
282. Lin, S. S., Parker, W., Everett, M. L. & Platt, J. Differential recognition by

proteins of α-galactosyl residues on endothelial cell surfaces. *Glycobiology* **8**, 433–443 (1998).
283. Kirkeby, S. & Moe, D. Lectin interactions with α-galactosylated xenoantigens. *Xenotransplantation* **9**, (2002).
284. Zufferey, R. *et al.* Ether Phospholipids and Glycosylinositolphospholipids Are Not Required for Amastigote Virulence or for Inhibition of Macrophage Activation by Leishmania major. *J. Biol. Chem.* **278**, 44708–44718 (2003).
285. Zhu, A. *et al.* Characterization of Recombinant α-Galactosidase for Use in Seroconversion from Blood Group B to O of Human Erythrocytes. *Arch. Biochem. Biophys.* **327**, 324–329 (1996).
286. Zhu, A. *et al.* High-Level Expression and Purification of Coffee Bean alpha-Galactosidase Produced in the Yeast Pichia pastoris. *Arch. Biochem. Biophys.* **324**, 65–70 (1995).
287. Luo, Y., Wen, J., Luo, C., Cummings, R. D. & Cooper, D. K. C. Pig xenogeneic antigen modification with green coffee bean α-galactosidase. *Xenotransplantation* **6**, 238–248 (1999).
288. Zhong, R. *et al.* Improvement in human decay accelerating factor transgenic porcine kidney xenograft rejection with intravenous administration of GAS914, a polymeric form of αGAL. *Transplantation* **75**, (2003).
289. Souto-Padron, T., Almeida, I. C., de Souza, W. & Travassos, L. R. Distribution of alpha-galactosyl-containing epitopes on Trypanosoma cruzi trypomastigote and amastigote forms from infected Vero cells detected by Chagasic antibodies. *J. Eukaryot. Microbiol.* **41**, 47–54 (1994).
290. de Souza, L. M. B., Thomaz Soccol, V., Petterle, R. R., Bates, M. D. & Bates, P. A. Analysis of Leishmania mimetic neoglycoproteins for the cutaneous leishmaniasis diagnosis. *Parasitology* **145**, 1938–1948 (2018).
291. Galili, U. Anti-Gal in Humans and Its Antigen the α-Gal Epitope. in *The Natural Anti-Gal Antibody As Foe Turned Friend In Medicine* 3–22 (Elsevier, 2018). doi:10.1016/B978-0-12-813362-0.00001-4
292. Hanfland, P. *et al.* Structure elucidation of blood group B-like and I-active ceramide eicosa- and pentacosa-saccharides from rabbit erythrocyte membranes by combined gas chromatography-mass spectrometry; electron-impact and fast-atom-bombardment mass spectrometry; and two-dimensional correlated, relayed-coherence transfer, and nuclear overhauser effect 500-MHz 1H-N.m.r. spectroscopy. *Carbohydr. Res.* **178**, 1–21 (1988).
293. Adolfo, G. *et al.* Comparison of cutaneous leishmaniasis due to Leishmania (Viannia) braziliensis and L. (V.) guyanensis in Brazil: Therapeutic response to meglumine antimonate. *Am. J. Trop. Med. Hyg* **65**, 456–465 (2001).
294. Frey, A., Di Canzio, J. & Zurakowski, D. A statistically defined endpoint titer determination method for immunoassays. *J. Immunol. Methods* **221**, 35–41 (1998).
295. Scott, A. J., Hosmer, D. W. & Lemeshow, S. Applied Logistic Regression. *Biometrics* **47**, 1632 (2013).
296. Satapathy, A. K. & Ravindran, B. Naturally occurring α-galactosyl antibodies in human sera display polyreactivity. *Immunol. Lett.* **69**, 347–351 (1999).
297. Ansar, W. & Ghosh, S. C-reactive protein and the biology of disease. *Immunol. Res.* **56**, 131–142 (2013).

298. Bretaaa, A., Avila, J. L., Contreras-Bretaaa, M. & Tapia, F. J. American Leishmania Spp. and Trypanosoma cruzi: Galactosyla(l-3)Galactose Epitope Localization by Colloidal Gold lmmunocytochemistry and Lectin Cytochemistry. *Exp. Parasitol.* **14**, 27–37 (1992).
299. Wortmann, G. W., Aronson, N. E., Miller, R. S., Blazes, D. & Oster, C. N. Cutaneous Leishmaniasis following Local Trauma. *Clin. Infect. Dis.* **31**, 199–202 (2001).
300. Sarhan, M., Saleh, K. & Bin Dajem, S. M. Distribution of ABO blood groups and rhesus factor in Southwest Saudi Arabia Micronucleus test View project Physical Inorganic Chemistry View project. *Saudi Med. J.* **30**, 116–119 (2009).
301. Pappas, M. G. *et al.* Evaluation of promastigote and amastigote antigens in the indirect fluorescent antibody test for American Cutaneous Leishmaniasis. *Am. J. Trap. Med. Hyg* **32**, 1260–1267 (1983).
302. Mosleh, I. M., Saliba, E. K., Bisharat, Z., Oumeish, O. Y. & Bitar, W. Serodiagnosis of cutaneous leishmaniasis in Jordan using indirect fluorescent antibody test and the enzyme-linked immunosorbent assay. *Acta Trop.* **59**, 163 (1995).
303. Roffi, J., Dedet, J.-P., Desjeux, P. & Garre, M.-T. Detection of circulating antibodies in cutaneous leishmaniasis by enzyme-linked immunosorbent assay (ELISA). *Am. J.* **29**, 183–189 (1980).
304. Hurt, N. *et al.* Evaluation of C-reactive protein and haptoglobin as malaria episode markers in an area of high transmission in Africa. *Trans. R. Soc. Trop. Med. Hyg.* **88**, 182–186 (1994).
305. Paul, R. *et al.* Study of C reactive protein as a prognostic marker in malaria from Eastern India. *Adv. Biomed. Res.* **1**, 41 (2012).
306. Kip, A. E. *et al.* Systematic review of biomarkers to monitor therapeutic response in leishmaniasis. *Antimicrob. Agents Chemother.* **59**, 1–14 (2015).
307. Gasim, S., Theander, T. G. & ElHassan, A. M. High levels of C-reactive protein in the peripheral blood during visceral leishmaniasis predict subsequent development of post kala-azar dermal leishmaniasis. *Acta Trop.* **75**, 35–38 (2000).
308. Wasunna, K. M. *et al.* Acute phase protein concentrations predict parasite clearance rate during therapy for visceral leishmaniasis. *Trans. R. Soc. Trop. Med. Hyg.* **89**, 678–681 (1995).
309. Ansari, N. A., Sharma, P. & Salotra, P. Circulating nitric oxide and C-reactive protein levels in Indian kala azar patients: Correlation with clinical outcome. *Clin. Immunol.* **122**, 343–348 (2007).
310. Singh, U. K., Patwari, A. K., Kumar Sinha, R. & Kumar, R. Prognostic Value of Serum C-reactive Protein in Kala-azar. *J. Trop. Pediatr.* **45**, (1999).
311. Fanemati, S., Nahrevanian, H., Haniloo, A. & Farahmand, M. Investigation on nitric oxide and C-reactive protein involvement in antileishmanial effects of artemisinin and glucantim on cutaneous leishmaniasis. *Adv. Stud. Biol.* **5**, 27–36 (2013).
312. Galili, U. Evolution and pathophysiology of the human natural anti-alpha-galactosyl IgG (anti-Gal) antibody. *Springer Semin. Immunopathol.* **15**, (1993).
313. Galili, U. Natural anti-carbohydrate antibodies contributing to evolutionary survival of primates in viral epidemics? *Glycobiology* **26**, 1140–1150 (2016).

314. Galili, U., Shohet, S. B. B., Kobrin, E., Stults, C. L. L. M. & Macher, B. A. A. Man, apes, and Old World monkeys differ from other mammals in the expression of alpha-galactosyl epitopes on nucleated cells. *J. Biol. Chem.* **263**, 17755–17762 (1988).
315. Kirkeby, S. & Moe, D. Binding of Griffonia simplicifolia 1 isolectin B4 (GS1 B4) to alpha-galactose antigens. *Immunol. Cell Biol.* **79**, 121–127 (2001).
316. Vidarsson, G., Dekkers, G. & Rispens, T. IgG subclasses and allotypes: From structure to effector functions. *Front. Immunol.* **5**, 1–17 (2014).
317. Delannoy, C. P. *et al.* Glycosylation Changes Triggered by the Differentiation of Monocytic THP-1 Cell Line into Macrophages. *J. Proteome Res.* **16**, 156–169 (2017).
318. Gazzinelli, R. T., Pereira, M. E., Romanha, A., Gazzinelli, G. & Brener, Z. Direct lysis of Trypanosoma cruzi: a novel effector mechanism of protection mediated by human anti-gal antibodies. *Parasite Immunol.* **13**, 345–356 (1991).
319. Galili, U. Anti-Gal: An abundant human natural antibody of multiple pathogeneses and clinical benefits. *Immunology* **140**, 1–11 (2013).
320. Izquierdo, L. *et al.* Evaluation of a chemiluminescent enzyme-linked immunosorbent assay for the diagnosis of Trypanosoma cruzi infection in a nonendemic setting. *Memórias do Inst. Oswaldo Cruz* **108**, 928–31 (2013).
321. Chinel, L. V., Walton, B. C. & y Eguia, O. E. Onset of espundia after many years of occult infection with Leishmania braziliensis. *Am. J. Trop. Med. Hyg.* **22**, 696–698 (1973).
322. Porrás, A. I. *et al.* Target product profile (TPP) for chagas disease point-of-care diagnosis and assessment of response to treatment. *PLoS Negl. Trop. Dis.* **9**, (2015).
323. FIND & WHO. *Target product profile for a test to identify susceptibility/resistance of gonorrhoea to antibiotics to facilitate antibiotic stewardship*. (2014).
324. FIND & WHO. *Target product profile for a rapid, low-cost diagnostic to distinguish gonorrhoea from Chlamydia infection at primary care*. (2014).
325. Zhang, K., Barron, T., Turco, S. J. & Beverley, S. M. The LPG1 gene family of Leishmania major. *Mol. Biochem. Parasitol.* **136**, 11–23 (2004).
326. Cabezas-Cruz, A. *et al.* Tick galactosyltransferases are involved in α-Gal synthesis and play a role during Anaplasma phagocytophilum infection and Ixodes scapularis tick vector development. *Sci. Rep.* **8**, 14224 (2018).
327. Sollelis, L. *et al.* First efficient CRISPR-Cas9-mediated genome editing in Leishmania parasites. *Cell. Microbiol.* **17**, 1405–1412 (2015).
328. Beneke, T. *et al.* A CRISPR Cas9 high-throughput genome editing toolkit for kinetoplastids. *R. Soc. Open Sci.* **4**, 170095 (2017).
329. Hilger, C. *et al.* Differential binding of IgG and IgA antibodies to antigenic determinants of bovine serum albumin. *Clin. Exp. Immunol.* **123**, 387–94 (2001).